Multiscale analysis of ancient ceramic by engineering methods in materials science : case studies of Dacian vessel, Roman amphorae and traditional products

Laura Teodorescu

I.O.S.U.D. UNIVERSITATEA DIN PITEŞTI
Şcoala Doctorală Interdisciplinară
Domeniul de doctorat: Ingineria Materialelor

Multiscale analysis of ancient ceramic by engineering methods in materials science

- Teză de doctorat -

Conducători de doctorat
Prof. Univ. Dr. Ing. Mărioara ABRUDEANU
Prof. Univ.Dr. Rémy CHAPOULIE

Doctorand
Ing. Laura TEODORESCU

Pitești
2022

I.O.S.U.D. UNIVERSITATEA DIN PITEŞTI
Şcoala Doctorală Interdisciplinară
Domeniul de doctorat: Ingineria Materialelor

UNIVERSITÉ BORDEAUX MONTAIGNE
École Doctorale Montaigne Humanités (ED 480)

Analyse multiéchelle de la céramique ancienne par des méthodes d'ingénierie en science des matériaux. Études de cas sur les céramiques daciennes, des amphores romaines et des productions traditionnelles

- Thèse de Doctorat -

Sous la direction de :
Prof. Univ. Dr. Ing. Mărioara ABRUDEANU
Prof. Univ.Dr. Rémy CHAPOULIE

Présentée et soutenue par :
Ing. Laura TEODORESCU
le 11/05/2022

Pitești
2022

I.O.S.U.D. UNIVERSITATEA DIN PITEŞTI
AND
UNIVERSITÉ BORDEAUX MONTAIGNE

THESIS presented by:

Laura TEODORESCU

Defense on: 11/05/2022

Multiscale analysis of ancient ceramic by engineering methods in materials science

Case studies of Dacian vessel, Roman amphorae and traditional products

Domain: Materials Science

THESIS led by:

Mme. **ABRUDEANU Mărioara**	Professor, University of Piteşti
M. **CHAPOULIE Rémy**	Professor, University Bordeaux Montaigne

JURY MEMBERS :

M. **Marian ENĂCHESCU**	Director of CSUD Piteşti University
M. **Ion CIUCĂ**	Professor at Politehnica Bucharest University
Mme. **Simona RANERI**	Researcher at Dep. of Earth Sciences, University of Pisa
M. **Mohammadamin EMAMI**	Professor at Art University of Isfahan
M. **Cătălin Marian DUCU**	Professor at Piteşti University
M. **Rémy CHAPOULIE**	Professor at Bordeaux Montaigne University
Mme. **Mărioara ABRUDEANU**	Professor at Piteşti University

Acknowledgements

For sure, the work of this thesis could not have been done, or realized until today, without the help and support of many people, that I would like to thank them, with apologies in advance for any potential omissions.

First of all, I would like to express all my sincere gratitude to Professor Mrs. Mărioara Abrudeanu that offered me this opportunity to develop myself professionally, by working on this beautiful research topic on ceramic materials. Thank you very much for all your guidance, your availability, your advices and all your support, that you have offered me during my PhD study.

I would like to express my grateful appreciation to Mr. Professor Rémy Chapoulie, for having welcomed me in the laboratory of IRAMAT-CRP2A (nowadays under the name Archéosciences Bordeaux UMR 6034), and for his kind attention during all my work. Thank you for your belief in me, for providing a lot of help and support, for your time spent in the proofreading of my work and all the opportunities you gave me for meeting new people.

I have a lot of appreciation to express to Nadia Cantin, for giving me the chance to work with her. Thank you for believing in me, for helping me and being there during my hard times. For all your patience that you have offered all these years, for teaching me starting from zero, for our meetings every Thursday (that I cherish them deeply) and for helping me to become a better me.

I would also like to express my appreciation to Ayed Ben Amara, for taking me under his guidance as well. Thank you for all your advices during my work and in general, your precious help and time, for the kindness that you have showed me, for looking after me and for giving me confidence when I needed the most.

To Professor Cătălin Ducu, I also express my sincere gratitude for giving me the possibility to be his employed in the laboratory CRC&D-Auto in Pitesti, which allowed me the financial support throughout my years of study. Thank you for all your kind advices, for the understanding that you have showed towards me and for your assistance during these years of scientific work and collaboration.

Of course, all my gratitude to the directors of Romanian Museums Mr. Cornel Popescu (Director of County Museum of Argeş) and Mr. Claudiu Aurel Tulugea (Director of "Aurelian Sacerdoțeanu" Vâlcea County Museum), for providing the first ceramic samples that were studied in the project of this thesis.

I wish to express my thankfulness to Valentine Roux, Constantin Augustus Bărbulescu, Dragoş Măndescu, Carol Terteci, Yolande Marion and Francis Tassaux for allowing me to

add and to study the ceramic sherds in the framework of the thesis and to better understand, by our discussions and meetings the archaeological contexts.

I would also like to thank all the members of laboratory of Archéosciences Bordeaux UMR 6034 (UBM-CNRS-UB; ancient IRAMAT-CRP2A, UMR 5060 Université Bordeaux Montaigne – CNRS) for their warm welcome during my stay in Bordeaux. Thanks to Stéphan Dubernet, Yannick Lefrais, Brigitte Spiteri, Pierre Selva and Francois-Xavier Le Bourdonnec for the trainings in different characterization techniques, for their guidance and availability.

A big mention where I would like to express my appreciation to the old and new PhD students from Archéosciences Bordeaux, which we shared so many beautiful moments at office and outside, moments that I will always remember. All my warm thoughts of friendship goes to Ninon, Estelle, Emmie, JB, Camille, Sri, Carol, Marie-Claire, Brice, Juliette, Arthur, Océane, Hortense, Dantes, Tifannie, Alexandre, Pierre and to Nicolas, which he had patience and willingness to help me with the statistical part in my research.

I would like to express all my gratitude to my former professor from licence and master, Mr. Professor Sorin Ciucă, from University Politehnica of Bucharest, that since 2014 till nowadays, he guided me, believed in me and helped me to outgrow myself. Thank you for all your advices and for giving me the chance to study abroad.

Not to forget to mention CRC&D-Auto Pitesti team for their kindness towards me and their willingness to help me when I needed it during my work.

I can never thank enough my family who, despite the miles that separated us, have always been present and for their encouragements. A special mention goes to my parents, for their belief in me, for raising my moral when I needed the most and for their support to pursue my own path.

To Manouel, thank you for encouraging me, for believing in me, for your patience and for making me laugh, even in my hardest moments. Thank you for helping me to grow into the person I am today.

To my good friends since highschool (and a little less) Sabina, Lucia, Răzvan, Robert and Cristina, for always welcoming me home with open arms, for encouraging me no matter the situation and for helping me unconditionally.

Finally, I would like to express my gratitude to all who I may have forgotten to mention and contributed to the achievement of this study.

CONTENTS

ABBREVIATIONS LIST

CL - Cathodoluminescence

ICP-MS - Inductively Coupled Plasma - Mass Spectrometry

LD – Limit Detection

ND - Not Detected

OM - Optical Microscopy

p-XRF - Portable X-Ray Spectrometry Fluorescence

RC - Red Clay sediment

RSD - Relative Standard Deviation

SD - Standard Deviation

SEM–BSE - Scanning Electron Microscopy - Back-Scattered Electrons

SEM-EDX - Scanning Electron Microscopy - Energy Dispersive X-ray Spectroscopy

XRD - X-Ray Diffraction

XRF - X-Ray spectrometry Fluorescence

YC - Yellow Clay sediment

LIST OF FIGURES

LIST OF TABLES

PUBLICATIONS LIST

ISI-listed journal articles:

1. **Teodorescu, Laura**, Ben Amara, A., Cantin, N., Chapoulie, R., Ducu, C., Ciucă, S., Tulugea, C., Terteci, C., Abrudeanu, M., 2021. "Characterization of Archaeological Artefacts Using Methods Specific to Materials Science: The Case Study of Dacian Ceramics from 2nd c. BC to 1st c. AD." Materials 14, 3908. https://doi.org/10.3390/ma14143908 (Impact Score : 3.623)

2. **Teodorescu, Laura**, Cantin, N., Ben Amara, A., Chapoulie, R., Roux, V., 2022. "Mineralogical transformations due to salt whitening agent in modern Hebron ceramics". Journal of Archaeological Science: Reports 41, 103303. https://doi.org/10.1016/j.jasrep.2021.103303 (Impact Score : 1.67)

Sum of Impact Score achieved : 5.29

Volume publications / Conferences presented at the international level

1. **Teodorescu, Laura**, Chapoulie R., Ben Amara A., Ducu M. C., Ciucă S., Tulugea C.A, Bărbulescu A.C., Terteci C.C., Abrudeanu M., *Ancient ceramics from the Ocnița archaeological site: an archaeometric study,* Romanian Academy of Technical Sciences (ASTR) 15th edition of the Conference "Day of the Romanian Academy of Technical Sciences, Zoom platform, 26-27 November, 2020

2. **Teodorescu, Laura**, *The Characterisation of Geto-Dacian Pottery Using Scientific Techniques*, International Conference 7th PhD Students Day of the Federation of Archaeological Sciences of Bordeaux, 14 May, 2019

ABSTRACT

The project of the thesis was made between the University of Pitesti and University Bordeaux Montaigne, making possible in obtaining a double PhD diploma in materials science and in physics of archeomaterials. This study was carried out under the direction of Professor Mrs. Mărioara Abrudeanu (Professor at University of Pitesti) and Professor Mr. Rémy Chapoulie (Professor at University Bordeaux Montaigne). The thesis research was focused on three case studies, thus each of them has benefited different financial support:

- Characterisation of heritage materials using material engineering techniques, from archaeological excavations at south of Carpathians – a collaboration between Argeş County Museum, "Aurelian Sacerdoțeanu" Vâlcea County Museum and University of Pitesti. The research funded by a doctoral grant from University of Pitesti and an ERASMUS mobility support between University of Pitesti and University Bordeaux Montaigne.
- A case study of the diffusion of Istrian olive oil amphorae workshops to the Danube provinces in the Roman period – research based on a previous program of a collaboration between Ausonius and IRAMAT - CRP2A. The work on this thesis is part of the continuation concerning the questions of circulation and diffusion of amphorae towards the Danube areas. The research has been funded by a grant obtained from the Institut Français de Roumanie (IFR) - Bucarest and a LabEx Science Archeologiques de Bordeaux grant (ANR-10-LABX-52).
- Mineralogical transformations due to salt whitening agent in Hebron ceramics – This research is part of the project "Traditional knowledge of the Hebron's potters and Heritage Resilience (Palestinian Territories)" in collaboration with the archaeologist V. Roux (Préhistoire et Technologie, UMR 7055, CNRS, University of Paris Nanterre), which will allow to discover the challenges of an ethnographic corpus with ceramic traditions, making possible to test our interpretive methods in archaeometry.

During the three years of research (2019-2021), I was employed as a scientific research assistant at the Regional Research and Development Centre for Innovative Materials, Processes and Products for the Automotive Industry (CRC&D-Auto), at University of Pitesti, under the guidance of Prof. Conf. Cătălin Ducu.

Most of the investigations presented in this thesis have been carried out in the laboratory of "Centre de Recherche en Physique Appliquée à l'Archéologie de l'Institut de Recherche sur les Archéomatériaux" (IRAMAT-CRP2A, UMR 5060 Université Bordeaux Montaigne – CNRS), known today under the name of Archéosciences Bordeaux UMR 6034 (UBM-CNRS-UB), Bordeaux, France.

The manuscript of this thesis is divided in **six chapters.**

The **first chapter** of the thesis provides a general introduction with two aspects: the archaeometric interdisciplinary research and the ceramic material. It will underline the complexity of a ceramic body, starting with the mineralogical composition of the raw material, the shaping and modelling process, the firing conditions, the surface decorations and their use. In addition, it will present some scientific methods and analyses that are commonly used nowadays, for providing information of the material heritage. Thus, it will put into evidence the fact that a strong cooperation between different specialists in this field is extremely important.

The second chapter focuses on the sampling preparations and the methods employed during this work. Each analysis demands a different type of preparation of the studied sample. Furthermore the investigations were adopted in order to understand the physico-chemical changes in the ceramic bodies and their final shape. Each used technique contains a brief presentation regarding their fundamentals and their information provided when applied to the ceramic. The experimental devices and the conditions that have been used in this thesis research will be presented as well.

The third chapter presents the case study of Dacian ceramics. The aim of this research was to explore the relation between the ceramic composition and the manufacturing process. For that, we characterized chemical and mineralogical potteries selected in archaeological context, curated in museums (from Argeş County Museum and from Vâlcea County Museum). Therefore a multi-analytical approach was implemented, in order to formulate hypotheses about the nature of the raw materials employed and as well for the heat treatments applied.

Firstly, image data obtained by petrographic analysis of potsherds will be presented. The analyses will reveal insights of the mineralogical composition of the clay sediment, used in the manufacture of the ceramic body. The images will then be correlated with the images obtained by cathodoluminescence. This method brings other type of data related to the chemical nature of the clay and inclusions, and can very often easily help in the differentiation process, such as in petrography.

A second aspect will focus on X-ray diffraction to identify the mineral content of the ceramic sherds. To confirm the presence of certain minerals and phases, these results will be compared with petrographic data. Finally, the last aspect will focus on the scanning electron microscopy (SEM) coupled with energy dispersive X-ray spectrometry (EDXS) analysis, providing information about the chemical composition and details about the microtexture of the ceramics.

The **chapter four** aims to develop an analytical methodology of portable X-ray Fluorescence, in order to provide answers regarding the questioning of Istrian oil amphorae diffusion. Beyond the methodological approach, the archaeological objective was to study the export of the amphorae Dressel 6B from the initial production Center (Loron, in present Croatia) to other sites following the Danube region. Using the p-XRF setup, the measurements test of

cleaned and soft polished amphorae fragments made possible to create a compositional database by using a non-destructive method and to complete and to broaden the vision of archaeologists and historians interested in the circulation routes and trades of the territory of ancient societies, reaching the southern part of Romania. The statistical approach made possible to answer to the question regarding the provenance and origin of the amphorae.

The fifth chapter will highlight the complexity of the research of ceramic materials. To underline better the physico-chemical changes that can occur into a ceramic body, a case study on Hebron potteries was chosen, showing the effects and the influence of salt (NaCl) on the colour and in the chemical composition, especially in Ca-rich ceramic bodies. To carry out this particular research, raw clay materials and sherds from modern pottery made in Hebron were collected. In addition, for enlarging our understanding of the observed phenomena in a ceramic body, eighteen experimental bricks have been manufactured in the laboratory of IRAMAT-CRP2A (Bordeaux). Mineralogy (petrography, XRD), chemistry (SEM-EDX) and colour analyses were carried out on raw clay materials, pot sherds and experimental (lab-made) bricks. SEM imagery offered the possibility to monitor the evolution of the mineralogical transformations, notably the pore system when increasing the firing temperature and changing the salt content.

The last chapter, **chapter six**, presents the general conclusions deduced from the results of the research carried out, highlighting the diversity in studying ceramic material, especially with archaeological fragments with invasive or non-invasive methods and the perspective for future projects. Original contributions concern the design and implementation of the experimental methodology and future prospects for further research in this area.

INTRODUCTION

Ceramic artefacts are among the most studied objects by archaeologists, as they can be found in vast quantities in most archaeological sites, dating from the Neolithic period to the present day (Tite, 2008). Thus, the analysis of these findings has been essential for the archaeological understanding of a site, area and time period. Analytical techniques that have been successfully developed in the field of material science are extensively applied to the study of ancient artefacts in archaeology and art, providing information regarding the composition and structure of the material employed (Montana et al., 2011; Sciau and Goudeau, 2015).

To obtain the needed data, a multi-level approach is required to analyze the materials. The areas to be examined must be chosen according to objectives. An appropriate selection of techniques allows the study of the composition and structure of specific components.

Several methods are specially applied to study different types of pottery from the past.

One of the main subjects of this thesis is the identification and fine characterisation of ceramics produced in Romania during the Dacian period, using the methods and techniques of engineering sciences. This research requires the mastery of methods and, above all, the definition of an adequate methodology for each type of ceramic according to the archaeological issue.

The complexity of studying the ceramic materials will be put into evidence, as well in providing information regarding of the use of raw materials, the manufacturing process, the firing conditions and the provenance of the objects.

Thus, the thesis encompasses **two important aims** such as:

1. Creating a suitable methodological approach in the study of Dacian potteries and to promote their study since archaeometry is a field in continuous development in Romania.
2. Answering to the question: which analytical technical methods of materials science can provide an answer to different archaeological questions?

In order to respond to these challenges, to explore the applicability of traditional and innovative techniques, and creating a constructive methodology in the analysis of the ceramics, during this thesis research, we established our methodology starting with a case study of Dacian ceramic from Ocnița-Buridava, and other two defined corpuses with a problematic clearly exposed:

- One case concerns the diffusion of Adriatic oil amphorae in the Danube region in Roman times,
- The other case deals with a particular ceramic manufacturing process in Palestine today. This case aims to understand the role of salt as a bleaching agent and to better understand the transformations of the ceramic material during its manufacture.

This implementation allowed us to know more about ceramics and to apply the right methods and methodology to study ceramics from Romania, whose archaeological issues were less well defined but whose study is so promising.

CHAPTER I

CURRENT STATE OF ARCHAEOMATERIALS RESEARCH

Summary

This chapter will highlight the importance of studying and being aware of the cultural heritage in order to understand better the historical events and the ancient cultures. It will start with an introduction on the ceramic material, particularly with the mineralogical composition of the raw materials, the shaping and modeling process, the firing process and the surface treatments and decorations. After, a summary regarding the techniques applied for the investigation and characterisation of the ceramics artefacts will be presented as well with the objective of the thesis followed by the experimental plan.

In the last part of the XXth century, a scientific discipline emerged, broadly defined as the application of physical, chemical, biological, geological or mathematical principles and methods for the characterization of archaeological objects and materials related to cultural heritage. The term widely used for this discipline is "Archaeometry", which has been used since the founding of the international research journal "Archaeometry" in 1958 in Oxford, England. Archaeometry is largely used as an alternative term for "Archaeological Science" or "Science in Archeology" (Artioli, 2010).

The archaeological materials discovered from excavations, in terms of their attributions, can be grouped into artifacts, structures and articles associated with human activities (Renfrew and Bahn, 2016).

Artifacts are objects made or modified by man at a specific time and place. They can provide various evidence of how the ancient population incorporated different types of materials into everyday life, as well as the techniques used in their manufacture. Their analysis requires an interaction between specialists such as archaeologists, curators, art historians and scientists from different fields.

The ceramic artifacts have been studied from various points of view: mineralogical and chemical aspects, artistic, aesthetic and use. In particular, a lot of archaeological research has been devoted to the study of the chemical and mineral composition of ancient pottery to identify, origin, raw material and manufacturing process, dating, and to gain a perspective on human history and culture (Stefan and Mazare, 2001).

The study of artefacts requires the integration of a multitude of sciences, in particular physics, chemistry and materials science (**Fig.1**), known also as archaeometric methods.

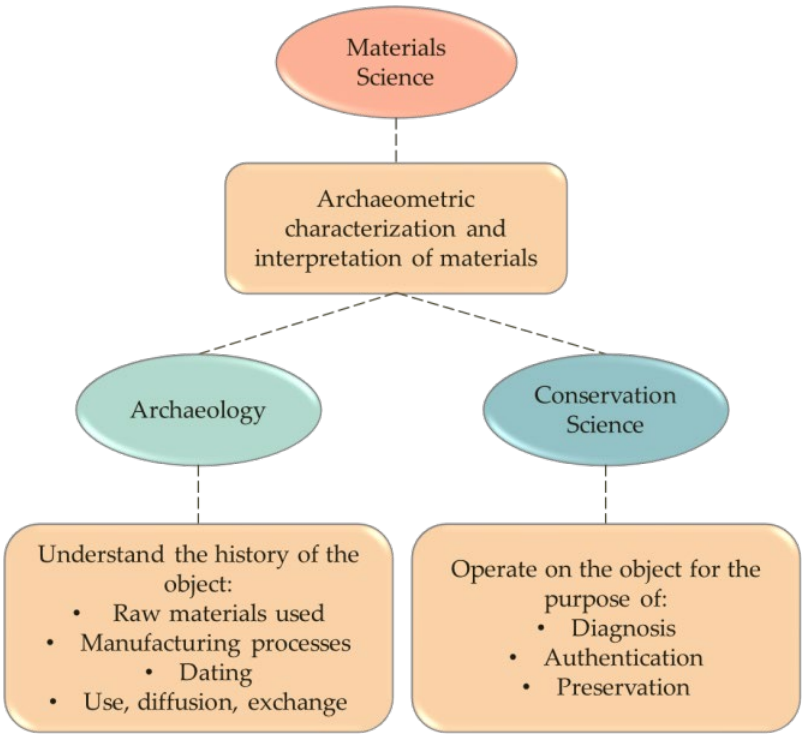

Fig. 1 Fields of application of archaeometric analyzes (modified after Artioli, 2010)

It is important to emphasize that every analytical technique provides advantages as well as constrains, so a wide knowledge of the techniques available is necessary to take advantage of the full spectrum of modern analytical tools (Edwards and Vandenabeele, 2016).

I.1 Ceramic archeomaterials

Among the archaeological discoveries, ceramics, and in general ceramic artifacts are the most studied objects by the community of archaeologists, people of art and science related to this field (Sciau and Goudeau, 2015). The oldest pottery (a statuette called Venus from the Western Dolni, discovered in the Czech Republic) dates to the approx. 25th century BC, but the ceramic vessel technology had independent origins in East Asia around the 12th century BC, which indicates that pottery was a well-known activity at that time (Vandiver et al., 1989; Bougard, 2011).

In the study of ceramics, the most important aspects are:

- Identification of the raw materials used (as well as their geological origin)
- Shaping process
- Firing conditions

- Glazing and coloring (if present)
- Chronology
- Field of use

I.1.1 Raw materials

Ceramic products are mainly made of clay sediments, a material found in abundance anywhere in the world (generally from a clay sediment or a soil), accessible to obtain. Of course, clay sediments differ from a compositional point of view depending on the geological aspects of geographical areas, which has led to an extraordinary diversity of ceramic products. The differences are not only limited to the mineralogical composition, but they are also reflected in the plasticity, colour, and temperature of firing.
An essential component of clays mixtures are the non-plastic materials, known as well under the name of tempers, (e.g. inclusions, additives). These are natural or added to the clay mixture in order to obtain a paste with good functional and drying properties, which during firing gains toughness and strength (Goffer, 2007; Rapp, 2009).
When choosing clay for pottery, the primary condition is to ensure that the clay is sufficiently plastic to be molded, but that is drying shrinkage is not very good, since it can create cracks. Thus a balance between the clay mineral and the contents of **non-plastic inclusions** (tempers) is required (Tite, 1999).
The temper materials can be divided in two main groups: mineral and organic materials (cut grass and straw, broken shells and bones, plant sap, etc.)(Velde and Druc, 1999; Tsetlin, 2003). Thus there is a wide variety of tempers, but the commonest ones for archaeological ceramics are: quartz sand, shells, crushed rock (limestone, sandstone) and grog. Furthermore, besides the variety of the tempers which the potter can use, the cultural influences must also be taken into account. For example, the presence of the raw materials depends on the local environment and the technical ability of the potter to collect and process them, but also its perception in making the clay a suitable material for the pottery. The choice of the non-plastic materials and the shaping method can have some cultural meaning or can express some aspects of an group identity or social status (Tite, 2008). Thus, the identification of the mineral inclusions allows in some cases to identify the origin of raw materials.

I.1.2 Characteristics of the clay sediments

Clay is broadly defined as a fine-granular soil material. The clays are formed due to alteration though aging and weathering of primary rocks such as: granite, feldspar, mica and quartz (Ricci, 2016; Kumari and Mohan, 2021).
Thanks to their small size (inf. 2 μm) and sheet structure, the clays minerals become plastic when mixed with a limited amount of water, due to a molecular film of water surrounding the clay particles, but become hard, brittle and non–plastic upon drying or firing. The clay

minerals are hydrous aluminum phyllosilicates with minor amounts of impurities (such as potassium, sodium, calcium, magnesium and iron) and are represented by two-dimensional sheets: tetrahedral (SiO_4) and octahedral (Al_2O_3) (**Fig. 2**) (Stan, 2017).

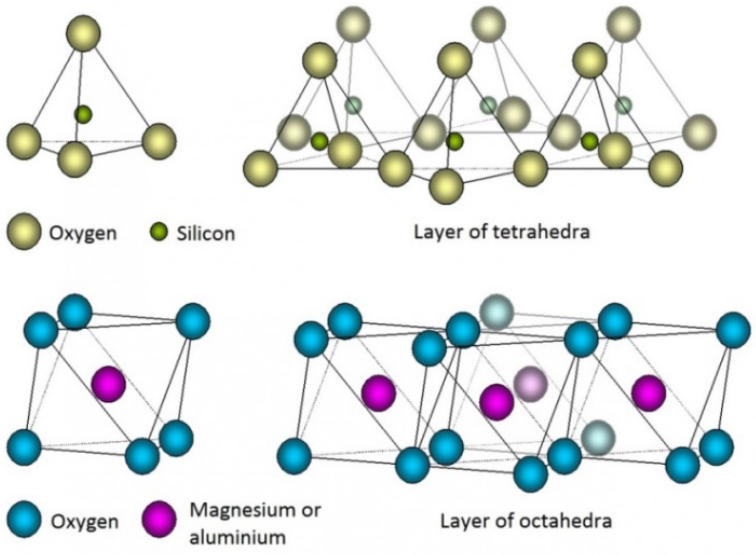

Fig. 2 Tetrahedral and octahedral structures of phyllosilicates (Jordán, 2014)

Furthermore, there are three main groups of clay minerals. The first main group is the *kaolinite group*, which have a neutral structure ($Al_2SiO_2(OH)_4$), being the most common group. The second group is *the illite group,* where illite is the most common clay mineral. It is formed due to the decomposition of some micas and feldspars. The last group is represented by *smectite*s (or montmorillonites), including bentonite and vermiculite. The last group is formed by alteration of Ca- and Mg- rich igneous mafic rocks. However, it exhibits weak binding to cations (e.g. Na+, Ca2+) and results in a high shrinkage, or swelling, effect (Dias et al., 2014).

I.1.3 Shaping and modeling process

Regarding the modeling technique of ceramic vessels, it has known a continuous development depending on the social and technological context. In the beginning, pottery was an individual activity, at most family, but over time, due to technological development, knowledge, and finally the requirements for this type of product, there were workshops and even small factories that have moved to the mass production of ceramics (Roux, 2019). Thus, several techniques were identified:

- pinching modeling (**Fig. 3**), by which the pot was made of a lump of clay, or of several attached fragments; the pots had a different thickness of the walls, the shapes were simple
- coiling from clay rolls, starting from the base, and continuing until the finish of the upper lip; a variant of this technique was the construction of the pots by superimposing clay rings, obtaining a various size and shape for the pots
- pressing into a pattern or basket
- throwing the clay on a hand-wheel pottery, process that allowed to obtain much more different and elaborate shapes, the walls of the pots were thinner and uniform
- molding in patterns, which gives high precision of wall's thickness, and a good surface finish (Griffiths, 1999).
-

https://nas.edu.au/product/intuitive-handbuilding-in-clay-3/

https://www.thesprucecrafts.com/how-to-center-clay-potters-

Fig. 3 Illustration of shaping and modelling process

I.1.4 Firing process

One of the most important steps in the production technology of a ceramic body is the firing process. At this stage the clay minerals are forming the pots, reaching at new phases (crystallized or vitreous) and giving new physical properties to the object (Sciau and Goudeau, 2015). The changes start to develop in some clays around 550 – 600°C and the ceramic which does not reach at this temperature during firing, will eventually break when immersed in water (Orton et al., 1993).

There are two types of firing procedures, such as the open firing and the kiln firing. The open firing (knows also as clump or bonfire firing) doesn't have a permanent structure and firing in a closed and fixed structure, such as a kiln (Gosselain, 1992).
During the firing process as the temperature starts to increase above 100°C, there are three successive chemical reactions: the oxidation (100°C - 400°C), the dehydration (450°C - 600°C) and the incipient vitrification (between 600°C - 700°C) (Goffer, 2007).
During heating the clay minerals and the tempers go through different chemical and structural modifications, which gives the final properties of the finished product (Riccardi et al., 1999). Thus, the new mineral phases formed (e.g. gehlenite, diopside, wollastonite, etc.) and with the presence (or not) of the carbonates and clay minerals can indicate the firing temperature which the ceramic body was under (**Fig. 4**) (Trindade et al., 2009; Montana et al., 2011; El Ouahabi et al., 2015).

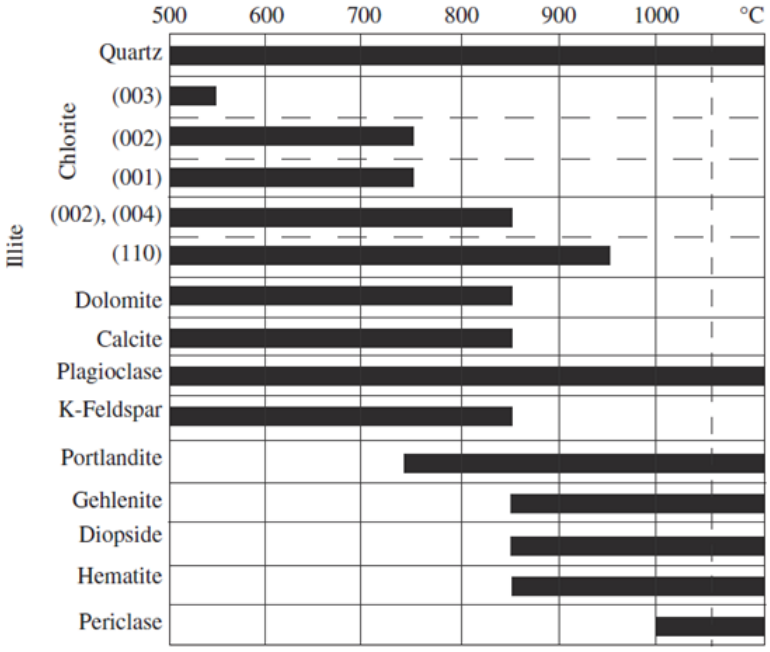

Fig. 4 Stability of minerals in Ca-rich clay under oxidizing conditions (Maggetti et al., 2011)

The transformation of clay into ceramics, with changes in crystalline structure, takes place at temperatures and different holding period; these two parameters together with the type of firing atmosphere: oxidizing or reducing characterize the firing process (**Fig. 5**)(Breuer, 2012). In addition, the firing atmosphere has a significant effect on the structure of the fired ceramic body.

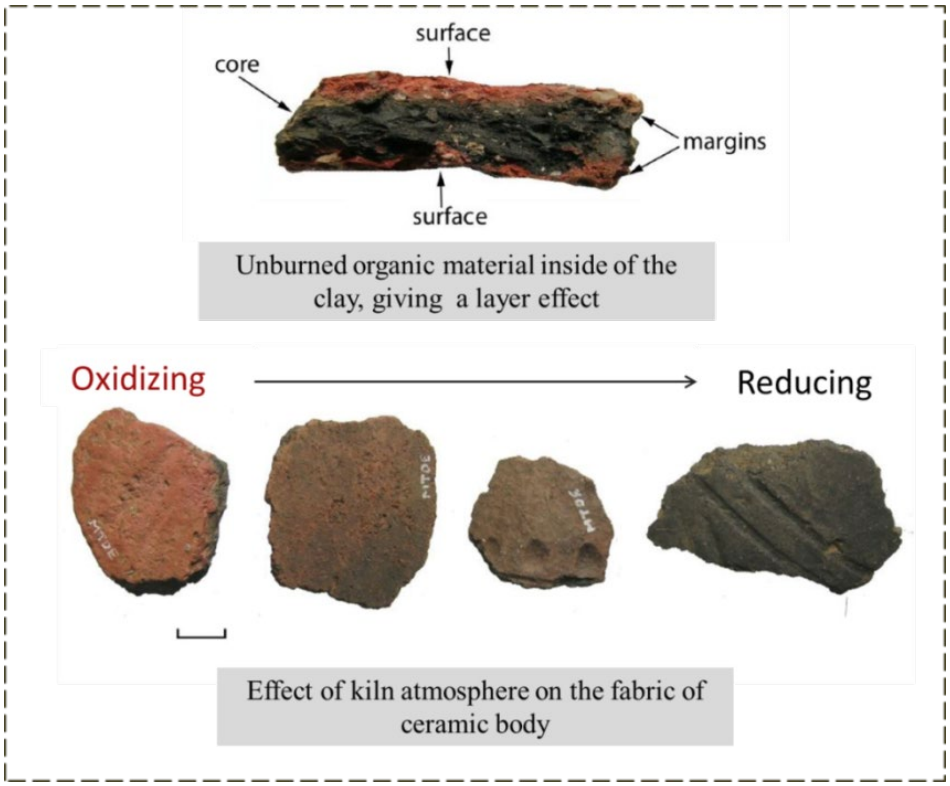

Fig. 5 Illustration regarding the firing effects on a ceramic material (Leahy and Geake, 2019)

For example, the red (or buff) pottery indicates an oxidizing atmosphere, while the black (or grey) pottery indicates either a reducing atmosphere, either an insufficient firing time for the organic material inside of the clay to burn out (Orton et al., 1993; Tite, 2008).

I.1.5 Surface treatments and decoration

In generally the objective of most potters is the aesthetic appearance of the pottery. Thus, either due to aesthetic or cultic reasons, man resorted to the decoration of ceramic vessels, using various techniques: enamel, glazing, polishing, painting, smoothing, surface displacement (penetration or addition), slip decorating, glazes and even gilding (Schindelholz, 2001; Pacheco et al., 2015; Beauvoit et al., 2019).
In addition to the aesthetic aspect, they gave to the vessels, the enamel contributed to the increase of the impermeability of the vessel walls, to the increase of the resistance in time (Breuer, 2012). Also, surface treatments were used for important reasons as well, such as

waterproofing the surface of storage and cooking vessels. The surface decorations are often specific to cultural communities or civilizations, allowing for temporal-spatial identification.

I.1.6 Fields of application

Uses of ceramic pots range from utility vessels for storage, for food preparation (e.g., soaking, grinding), cooking vessels (e.g., boiling, frying) for food or drink to vessels of a socio-political and ritual nature. The first step in the investigation of the use of certain ceramic vessels is a careful assessment of the archaeological contexts (i.e., houses, tombs, religious structures such as temples and altars) in which they were found. Then the dimensions and shape of the vessels must be considered, as they give an indication of the capacity, stability, ease of handling and removal of the contents.
Similarly, the nature of surface decoration provides an indication of their potential role in socio-political and ritual contexts (Tite, 2008).

I.1.7 Types of ceramic materials

Usually the pottery is mainly divided in two types: the vitrified ware and the non-vitrified ware (Carter and Norton, 2007). In addition, depending on the chemical composition of the raw material, the temper, the firing conditions, and the destination of the ceramic product, different typologies have been established (Tite, 2008). They are as follows:
Coarse earthenware, a ceramic material with high porosity, obtained from common clay, with the addition of non-plastic raw materials as tempers, fired at usual temperatures of 500-900°C. This category includes terracotta (Terra Cotta in Italian means burnt earth), bricks and tiles.
Earthenware made of clay with a high content of quartz and feldspar, with a content of 5-10% limestone. They are ceramics with lower strengths. They become impermeable after the firing process (which takes place at temperatures of 1000-1200 °C) and the objects are glazed. This category also includes faience.
Stoneware, a hard and compact material with a coarse structure, burned at temperatures above 1200°C. To increase their strength, they were covered with glass powder and reheated, a phenomenon that causes an interaction between the enamel and the body of the ceramic, creating a glassy surface. The colours of this pottery varied from gray to brown, but could also be green, as in the case of Chinese pottery called celadon.
Porcelains are made of hard kaolin paste, white clay without impurities, which by burning at temperatures above 1400°C become white-translucent. They were first made in ancient China. Later, due to the increasing demand for this type of product, in the medieval period also appeared the European porcelain which was a porcelain from soft paste (Tite, 2008). The body of the vessel was made of a mixture of quartz, alkaline products and clay, and in some cases, limestone was added for bleaching.

I.2 Techniques for investigation and characterisation of ceramic artifacts

Archaeometry refers to each application that uses physico-chemical characterization methods to understand the nature and changes over time of art and archaeological materials.
The object under investigation must necessarily be a physical material, either artistic or archaeological, and no matter how unclear or debatable the origin of the object, regardless of its size or complexity, the object is related to human activity.
Therefore, understanding the nature of the object is to discover not only the physico-chemical nature, but to reveal the human process that produced it, the social context. For this purpose, archaeometry uses all available techniques and methods, developed in the most diverse and specialized scientific disciplines (Tykot, 2004).
The bridge between ancient ceramics and materials science and engineering (defined as an interdisciplinary field focused on the discovery and design of new materials), would seem that it doesn't exist. However, the basis of materials science involves the study of the microstructure, crystallographic phases and defects of materials in relation to their properties, which can be applied directly to heritage materials (Sciau and Goudeau, 2015).
After defining the questions, the decisions specifically involved in the archaeometric analysis of the archaeological materials are:

- sample's preparation
- selection of analysis techniques and methods
- duration and cost of investigations
- interpretation of results and drawing conclusions

Several principles are needed to understand the operations and limitations of available analytical techniques. Most analytical techniques use a sample to investigate the material of interest, whether it is a natural mineral, or a synthetic compound, present in different states: liquid, gaseous, solid, amorphous, and crystalline (Greene and Moore, 2010; Tian, 2016).
Thus there are different ways to analyse the ceramic bodies. For example some **methods for elemental analysis** employed for the ceramic characterisations are: Inductively Coupled Plasma Mass Spectrometry (IPC-MS), Energy Dispersive X-ray Spectroscopy (EDX/EDS) and X-Ray Fluorescence spectroscopy (XRF). These methods are broadly used in order to determinate the major and minor elements in the ceramic matrix.
The chemical analyses for major, minor and trace elements help in grouping together the pottery made from the same raw material. They can also enable to distinguish the groups by studying the ceramic bodies made from different raw materials. Since there is a variability in the chemical composition of the different sources, for provenance studies the analysis needs to be performed on a large number of samples, which are then grouped together using statistical methods (Tite, 2008).

However, in this thesis it was used another way to determine a ceramic provenance by comparing discovered ceramic samples from different places with other ceramics coming from a certain production site, as reference group (see Chapter IV- The Case Study Of Istrian Olive Oil Amphorae Workshop To The Danube Provinces In The Roman Period) (Maritan, 2004; Ricci, 2016).
The chemical and mineralogical composition of the minerals present in the ceramic matrix also makes it possible to determine characteristics such as firing conditions and raw materials used, to characterize a certain workshop with regard to time and origin and to examine the manufacturing technology. Knowledge of the manufacturing process helps to reconstruct the technical history of ancient potters and assesses their ability to produce and craft specialization as well as cultural exchange (Ricci, 2016).
The field of **ethnoarchaeology** (see Chapter V - The Action Of Salt In The Manufacturing Process In Hebron's Ceramic) is defined as a sub-discipline of archaeology combined with anthropology, offering in a comprehensive way a direct observation of the manufacture, form, use and meaning of the artifacts made by people. Thus, with the help of ethnographic methods, improves the interpretation of archaeological data by providing more information and explanations (Stiles, 1977; Cantin and Mayor, 2018).
Most of the times, these studies are more focused on the determination of the firing conditions than the forming methods, making possible to estimate the original firing temperature with the help of the detection of different mineralogical phases.
The ceramic mineralogy is usually investigated with the help of optical microscope (OM – petrographic analysis), X-Ray Diffraction (XRD), Scanning Electron Microscope with Energy-Dispersive X-ray Spectroscopy (SEM-EDX), thermogravimetric analysis (TGA/DSG), Fourier-Transform InfraRed spectroscopy (FT-IR) and Raman spectroscopy. The effects of the firing conditions can be also analysed and observed on the morphology and microstructure of the final product. These features are examined using SEM, petrographic microscopy and porosity analysis (Shepard, 1985; Duminuco et al., 1998; Cultrone et al., 2001; Maritan et al., 2006; Ricci, 2016).

I.3 Specific objectives of the thesis

As mentioned before, archaeometry is a field in continuous development in Romania. Thus, the objectives of the thesis work are:

- Characterization of the artifacts by using specific materials engineering techniques
- Establishing the composition of the ceramic objects, their structure and to associate their manufacturing technologies used.

At the beginning, the research was focused in answering to the questions regarding the choice (or selection) of the raw materials and the manufacturing technique of the ancient Dacian potters and to create a first archaeometric database regarding the area of Buridava. Since the

corpus was limited, a second case study was added regarding the provenance of ceramic vessels, the amphorae Dressel 6B from Istria. The case study is focused in developing the analytical methodology for amphorae analysis, using a portable XRF.
Beyond the methodological approach, the archaeological objective was to study the export of the amphoras Dressel 6B from the initial production Center (Loron) to other sites following the Danube region.

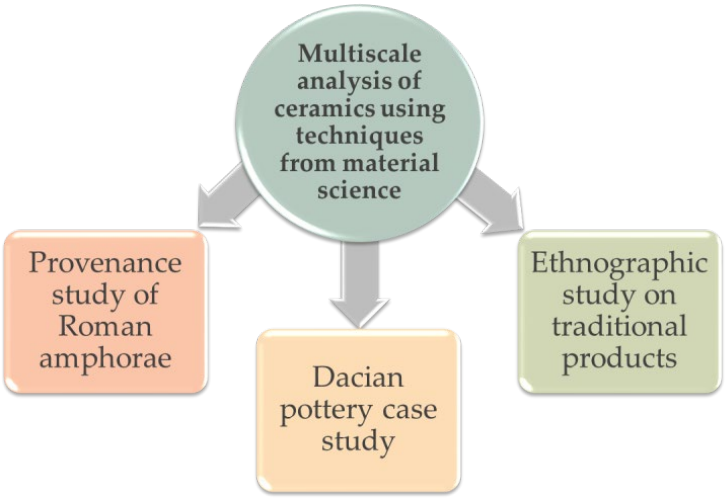

Fig. 6 Plan of the research thesis

In the end, in order to formulate a suitable methodology for understanding the complexity of the ceramic material, a last case was added is based on an ethnographic study (**Fig 6**). This last case concerns modern ceramic production. It is based on an ethnographic study; the aim of our research was to develop a multi-approach methodology in order to answer to the questions of the archaeologist, such as: how salt is influencing the colour of a ceramic body? What kind of physico-chemical changes occur in the ceramic bodies from Hebron? In order to widen our knowledge, eighteen experimental bricks have been manufactured in the laboratory, varying the percentage of salt and the firing temperatures.

I.4 Experimental research plan

After the preliminary steps, the ceramics were analyzed with a variety of methods available in the laboratory. The choice of the methods used depended on the specific problematic or question, of each series of corpus samples.

The defined milestones for the experimental program were chosen in order to obtain the desired information of the ceramic (**Fig. 7** Multi-scale analysis employed for this thesis research and their sample preparation), such as:

- the measurement of colour
- the study of texture
- the analysis of the various components of the ceramics
- the study of the mineralogical changes during firing, inside of a ceramic body.

The principle of the devices will be briefly presented in the following chapter, as well with the corresponding experimental parameters (since are always the same). The study of the texture of the ceramic bodies will be carried out mainly on polished sections.

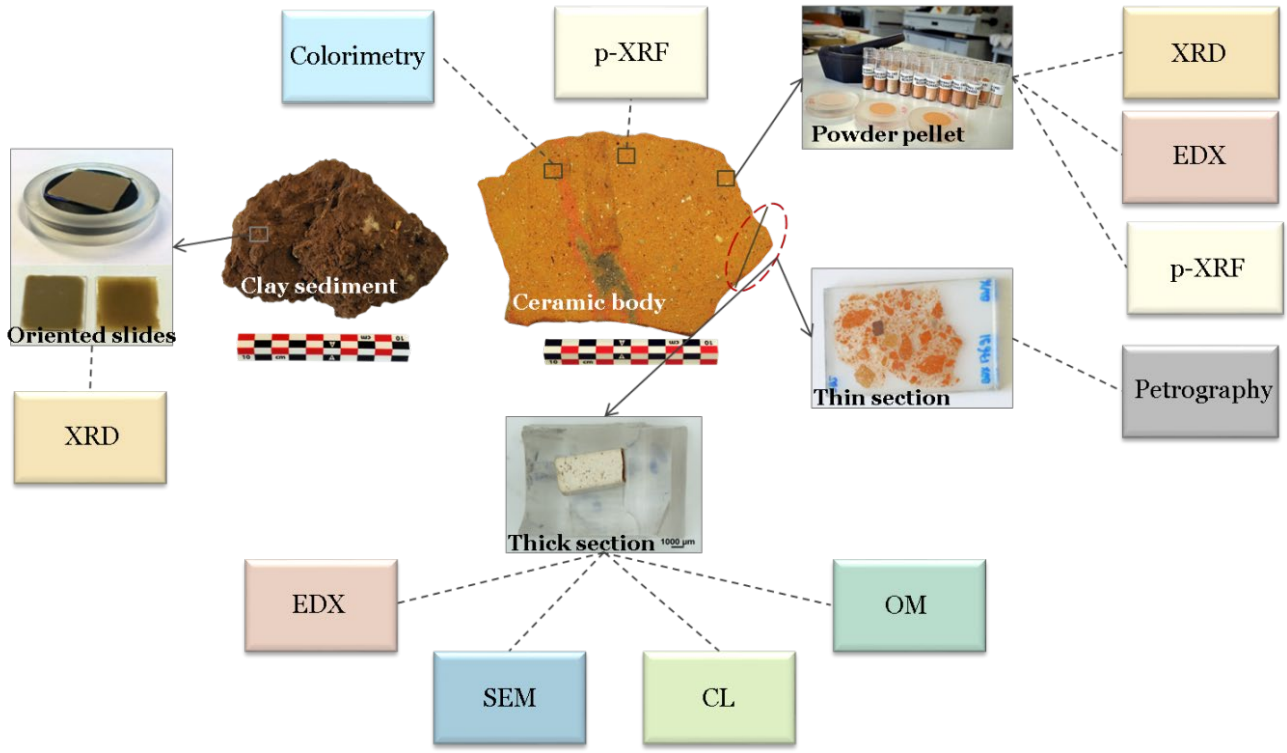

Fig. 7 Multi-scale analysis employed for this thesis research and their sample preparation

(Note that to facilitate the reading of the experimental results, they will be briefly presented in each chapter in the used methods)

CHAPTER II

A MULTI-SCALE ANALYTICAL APPROACH

Summary

This chapter focuses on the sample preparation and on the analysis techniques used. It should be taken into account that specific sample preparations are required for different analyzes. Therefore, a summary of the types of preparation of samples used for this research is presented, followed by the analytical techniques used and the information that these techniques can provide when used in ceramic material analysis. In addition, details on the setups and conditions are provided after each description of the device.

II.1 Sample strategy and preparation

As generally indicated in the previous chapter (see Chapter I – Ceramic archeomaterials) the field of ceramic studies is wide and complex, allowing to obtain information about: a certain territory and its geo-sources, the production technology, the morphological-style evolution of the ceramic bodies, and the socio-economics dynamics related to the exchange (or trading) of goods. Thus, for responding to these different problematics, generally three conditions must be considered in order to proceed for sampling:

- conclusion of the archaeological study of the territory and / or the archaeological site and completion of the morphological-stylistic analysis of the ceramic collection,
- formulation and implementation of the archaeometric research questions,
- choosing the experimental procedure (Gliozzo, 2020).

In addition, for suitable sampling criteria it should be taken into account the following conditions:

- the sample collection to be *representative*, linked to chronology, raw material and the manufacturing technologies used
- another requirement should ensure the *functionality* of the sampling strategy. For example, sampling should always remain flexible enough in allowing the research to be expanded if new questions can appear in the analysis process.
- the last prerequisite for a sampling strategy is that the *suitability* between the types of samples taken and the analytical techniques used, should be taken into account. These techniques can be **non-destructive**, **micro-destructive**, or **destructive** (Gliozzo, 2020).

Furthermore, the sample preparation is one of the most important points in order to obtain a quality data. A first aspect is to focus on the zone of the interest which will be after analyzed. A second aspect is to be aware that some analysis methods require different shape of sample.
Most of the preparation of the samples is divided in two types: the "thick" samples which are used for reflection observations and the "thin" samples; which are used for the transmission observations (Tian, 2016).
Before studying any sample in the laboratory, a reference number has to be assigned. This consisted in the case of Bordeaux laboratory, of attributing a reference starting by BDX (BorDeauX) prefix and followed by an inventory number. The samples were then photographed in order to preserve, in the form of an image, the state of the object at the time of its entry into the laboratory. As mentioned above, it should be considered that in order to accede to different analysis, different sample preparations are needed.
For instance, **the thick sections** are suited to study the texture of the ceramic body and to specify the chemical composition, thanks to the use of SEM-EDX (Scanning Electron Microscope with Energy Dispersive X-Ray Spectroscopy), CL (CathodoLuminescence) and OM (Optical Microscopy).
For petrography analysis, **thin sections** are needed, since the polarized light should cross the section in order to determinate the mineralogical composition due to the optical properties of the minerals.
As sherds are generally heterogeneous, powder can be prepared. Then, the **powder pellets** are produced in order to face the heterogeneity of the samples by homogenizing them after grinding them, and setting them as pellets for p-XRF and SEM-EDX measurements. In addition, **the oriented slides** prepared for the clay minerals, allow the precise identification of the clay minerals by XRD.
All the preparations used for this research thesis are presented in **Fig. 7**.

II.1.1 Thick sections

The preparation of the thick sections has few steps, starting with cutting the ceramic fragment. The ceramic body is fixed on the cutting table and is cut using a diamond abrasive disk. The sections perpendicular to the sample surface were cut with an ATM Brilliant device, at 2000 rpm. The samples are cleaned, dried and put into a Teflon mould. Then they are embedded in a two-component resin, ARALDITE A/B, in the ratio of 100 g resin to 30 g hardener. The used resin is transparent and hardens at room temperature below 24 hours. A pre-polished of the ceramic body was made using a 35 µm (P400) and 26 µm (P600) abrasive discs until a uniform surface is obtained. The polishing is carried out on a 6 µm disc using liquid polycrystalline diamond lubricant. Samples prepared at this level can be used for cathodoluminescence analysis.

Subsequently, polishing is continued with 3 µm and 1 µm liquid polycrystalline diamond lubricant to obtain the ideal surface for observing the samples by SEM-EDX for providing surface morphology and chemical information.

II.1.2 Thin sections

Accessing the microscopic observation of a ceramic fragment requires making a very thin section of 30 µm to allow light to pass through (most minerals are not translucent). One of the most important steps is to select an appropriate area of the sample to be prepared. Thickness is controlled by the polarizing microscope on the most common and easily identifiable minerals in ceramics, such as quartz or plagioclase. At the correct thickness, quartz polarization tones range in the gray band from white to black; if the section is too thick, these sections have yellowish tones analyzed in polarized light (Beaux et al., 2011).
After demolding step from the anterior paragraph (see 2.1 Thick sample), the samples are glued to glass slides using an epoxy resin (Brotlab Hillquist Hille glue HQ 340 G). After gluing, drying is carried out on a heated press at 45° C. Then, after drying, the blade and the resin assembly is cut with a saw to a thickness of approximately 2.3 mm. The blades are then polished to the desired thickness (30 µm); one part is made with a bench grinder and the last two with an automatic polisher (Presi Tissediam 200 µm diamond grid), then finished with silicon carbide polish. The slides are finally polished with disks and felts of decreasing granulometry (6 µm, 3 µm, 1 µm).

II.1.3 Powder pellets

The chemical analysis of shards and clays is carried out on powdered pellets in order to avoid the problems of heterogeneity specific to ceramic material. The samples must therefore be preliminarily reduced to powder and homogenized. Pre-grinding is carried out manually with a hammer and then a fine grinding is carried out on an automated tungsten carbide mill (Retsch S 100). Each sample is ground for 5 minutes at a speed of 400 rpm, resulting in a homogeneous powder. The clays are also ground using the same protocol.
When using sample powder, pellets were obtained using the Carver 4350 L pelletizer, from 95% powder mixed with 5% Hoecht C wax. It is necessary that all pellets have a flat and homogeneous surface and that their thickness is constant in order to ensure the reproducibility of the analysis.

II.1.4 Oriented slides

In order to identify clay minerals, it is necessary to separate the clay fraction (mostly constituted by the clay minerals) from the coarse particles and carbonates (Adriaens, 2015).

The process consists first in eliminating the carbonates without attacking the clay phases. The attack method consists in using a weak acid solution with a buffer at pH 5, because at this pH value it is assumed that the crystal lattice of clays is not attacked. Once the destruction of the carbonates is done, it is necessary to wash the clay residue in order to remove residual acid and calcium ions. For preparing the attack solution, 82 g of sodium acetate [$C_2H_3O_2Na.3H_2O$] was weighed into a 1L beaker and diluted in 950 mL distilled water. After, about 20 mL of glacial acetic acid [$C_2H_4O_2$] was added to adjust the pH to 5. In the end of the reaction, the washing is carried out by using distilled water and centrifugation.

The oriented slides were submitted to heat treatments in order to dehydrate certain phases (halloysite) and to close the interfoliar space of the expending minerals (smectites and vermiculites):

- closing the vermiculite layers at 350° C (displacement from 14.4 to 10 Å),
- closing the smectite layers (displacement from 15 Å to 10 – 9.8 Å),
- closing the kaolinite layers at 550° C (peak 7 Å disappearing).

The drying of the slide was done at room temperature. Then, the ethylene glycol saturation was performed on the same slide, using the method on vapor phase (the oriented slide was placed in a desiccator, containing a tank of ethylene glycol in its lower par, and which vacuum was applied, pumping for 45 minutes). Then heating treatments (at 350° C and 550° C) were performed in an electric oven.

The analysis of the clayey sediments was carried out by X-ray diffraction both on powder to identify the minerals and on oriented deposit to discriminate the clayey mineral species present. The results were obtained on oriented slides after treatment with ethylene-glycol, then successive heating at 350° C and 550° C according to Bouchet (Bouchet et al., 2000).

II.2 Analytical techniques

A main aspect in approaching the study of archaeological materials is the correct identification of the type of material under investigation, as the first step in interpreting how it was made, its field of use, its provenience and other cultural information related to the human society (Tite, 2008).

Thus, the methodological protocol used encompasses a multitude of analytical techniques to ensure representativeness and complementarity of responses.

II.2.1.1 Colorimetry

The definition of a colour is rather subjective and it depends on different criteria such as: the spectral sensitivity of the eye, the nature of the incident light and the surface condition of the

object (Nassau, 1998). The main purpose of colorimetry is to establish the relationship between visual perceptions and the physical characteristics of the objects.

The Munsell System analysis is one of the most common, used technic in order to characterize and differentiate the soils, by their typical or predominant colour of the sediment. In the Munsell System the colour perception can be defined by three variables: hue (labelled with a letter), value and chrome (both labelled with a number) (Cochrane, 2014).

The Munsell soil colour charts were developed in 1940's, consisting of 7 charts (hues 10R, 2.5YR, 5YR, 10YR, 2.5Y and 5Y) and a total of 196 colours (**Fig. 8**).

The colour chips are mounted on gray cover stock with apertures between the colours to facilitate comparison with the sample specimen (Miller, 1958). Even though the Munsell soil colour charts are an easy semi-quantitative analysis, it presents disadvantages as well, such as:

- the colour perception can vary from person to person,
- the colour chips do not fully cover the range of the natural soil colours,
- the printed colours cannot be accurately produced so the colour chips may differ between copies of the chart.

In the meantime, progress in colorimetry and colour measurements technology has been developed, leading to the apparition of the spectrophotometers (Kirillova et al., 2018).

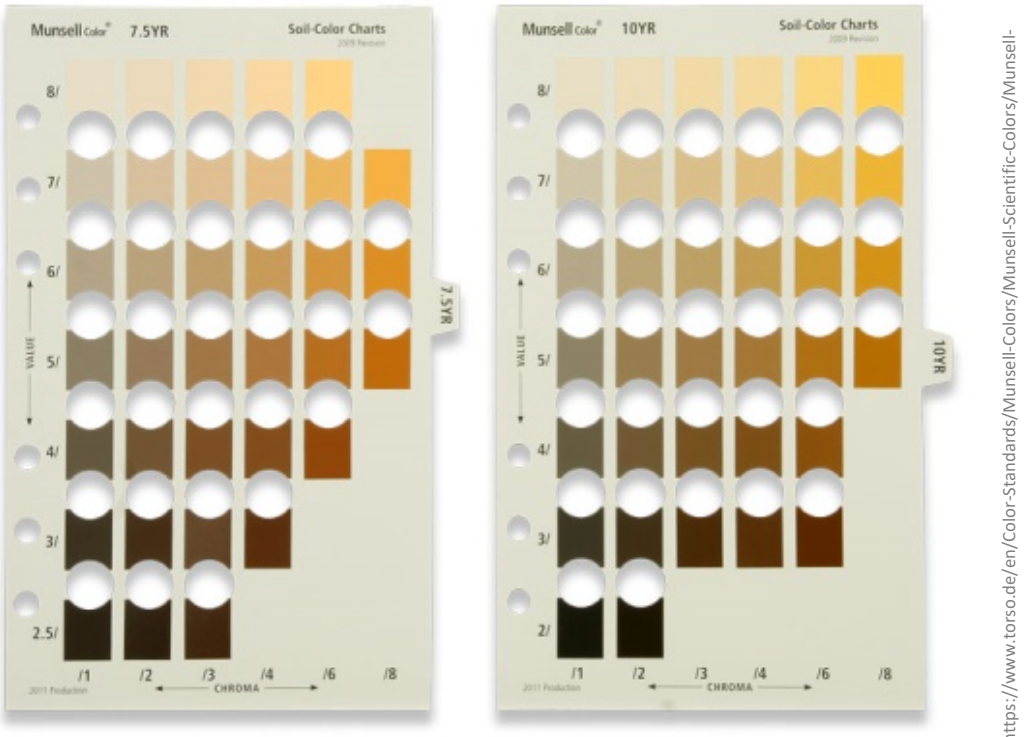

https://www.torso.de/en/Color-Standards/Munsell-Colors/Munsell-Scientific-Colors/Munsell-Soil-Color-YR-Kit:417.html

Fig. 8 Munsell soil colour charts, YR-kit

II.2.1.2 Colorimetric measurements

This method objectively quantifies the intensity of colour in dyed objects and is based on three independent parameters, hue, saturation and brightness (Dupont and Steen, 2004). These three parameters are applied in a three-dimensional vector space, in the RGB system (CIE 1931) based on monochromatic primaries. Then, these data are converted into a virtual primary system XYZ where Y represents the brightness.
This system makes it possible to represent any existing colour based on the three primary colours red, green and blue.
Today, is mainly used the L*a*b* colour space (**Fig. 9**)(CIELAB 1976) where L* is the variable of lightness and a* and b* are the chromacity bands which indicate the direction of the colours (Lajarte, 1979).

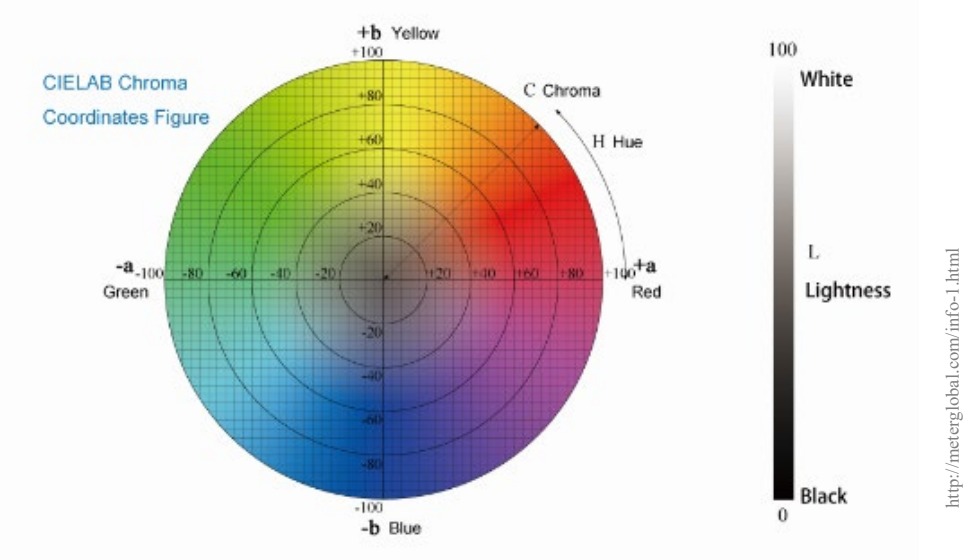

Fig. 9 System of CIELAB chroma

In the figure above it is shown that +a* indicates red colour, -a* green, +b* yellow, and -b* blue, while the middle is achromatic. In the study case of Hebron ceramics, the technique of colorimetry was used to identify the colour of the experimental samples, according to the heat treatments and percentage of salt in order to differentiate them.
The device used is a Konica Minolta Cm-2600D portable spectrophotometer (Fig. 10). The illuminator used is the D65 standard with an angle of 10 degrees. The calibration was performed on the reference black and white. SCI (spectral reflection included) and SCE (spectral reflection excluded) analyses are performed simultaneously.

The analysis is non-invasive because it does not require sampling.

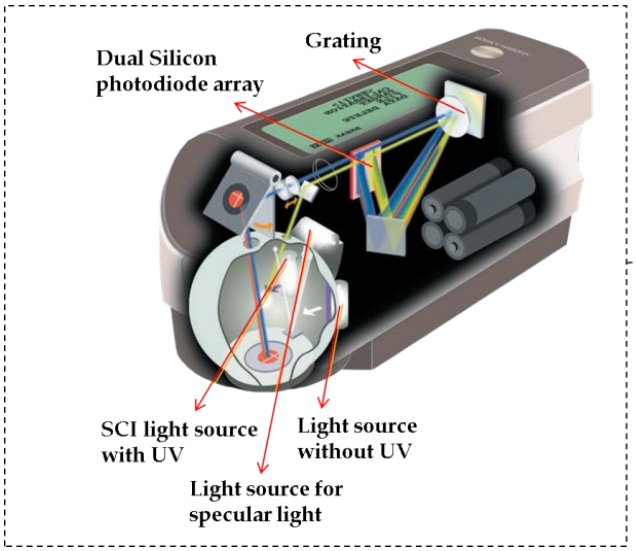

https://www.konicaminolta.com/instruments/download/catalog/color/pdf/cm2600d_catalog_eng.pdf

https://sensing.konicaminolta.us/us/products/cm-2600d-spectrophotometer/

Fig. 10 Schematic view of Konica Minolta Cm-2600D portable the device (right image); Spectrophotometer used in this thesis (left image)

II.2.2 Morphological and granulometric study

II.2.2.1 Optical Microscopy

The microscope is an optical instrument that magnifies the image of an object observed through a lens system. Microscopes can only magnify structures that are larger than the wavelength (light wave).The microscope forms visual, magnified, and inverted images of the object using a lens system, grouped in the lens and eyepiece (Price and Burton, 2011).

The optical microscope uses electromagnetic waves in the visible field. The light is transmitted along the optical axis of the instrument, through the sample, in these conditions obtaining a brightly illuminated visual field, in which the objects, to be seen, are distinguished on the light background either by their opacity or by their colour.

To make measurements, glass slides are used, on which scales are finely graduated, called micrometers, and which are auxiliary parts of the microscope (Levcovici et al., 2006).

II.2.2.2 Petrography

Petrography on thin sections (30 µm) was developed by geologists to identify rocks, sands and soils (Reedy, 2008), but it is also a valuable study for ceramologists (Quinn, 2013). It provides information on the nature of plastic inclusions naturally contained in the sediment employed by potters, but also on inclusions added (temper) by the potter. This method provides information on the nature of the raw materials used, their geological origin, but also on manufacturing techniques (Regert and Guerra, 2016).

Thus, the chemical analysis of the ceramic bodies is an advantage, as it allows making a group. In this study, the method was used to characterize the minerals and rocks present in the ceramic paste. Most of the minerals were identified, as well as their size, shape and grain size distribution.

A Leica DM2500 polarizing microscope was used with objectives from 2.5x to 40x. The support of petrography observation is a thin section created from a ceramic sample (**Fig**. **11**) is therefore a destructive analysis in relation to the objects.

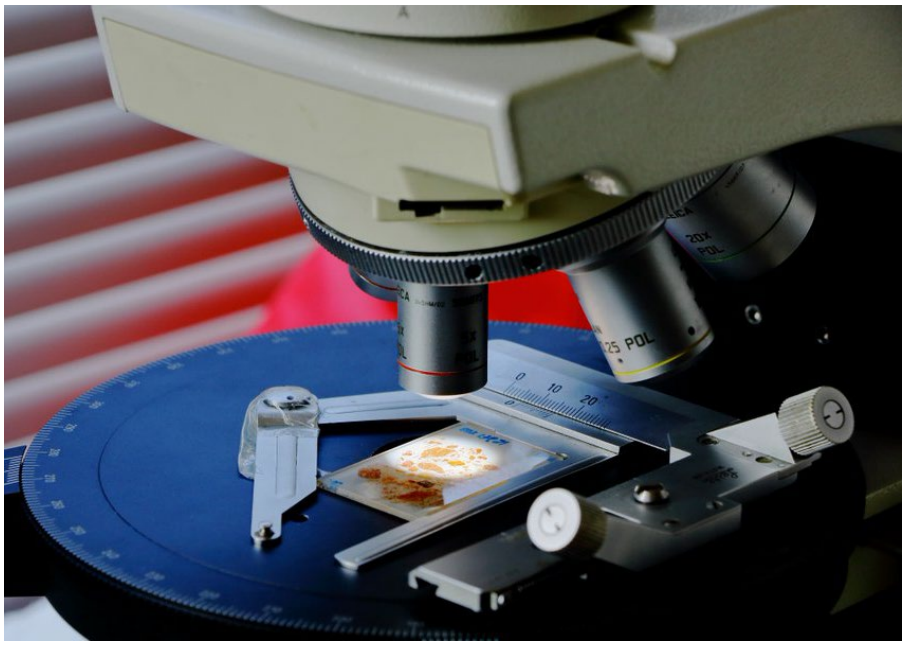

Fig. 11 Illustration of polarized microscope from IRAMAT-CRP2A (Photo credit J.B. Javel)

II.2.2.3 Cathodoluminescence

Cathodoluminescence, or the emission of photons in the visible wavelength range of the electromagnetic spectrum under cathode excitation, is a very practical method used to further study the ceramics (Chapoulie et al., 2016). The principle of this method is based on the acquisition and analysis of the image produced by the interaction between an electron beam and a material surface. When a solid is bombarded by an electron beam, it emits electrons and photons (**Fig. 12**). Among these photons some are produced by a phenomenon of luminescence in UV, IR and the visible (Barbin and Schvoerer, 1997; Chapoulie et al., 2005; Chapoulie and Daniel, 2007).
The colours taken by the minerals can be characteristic of them. However, the CL emission is a contribution of different emissions: those that come from the internal structure of the crystal and those that come from the presence of point defects such as chemical impurities or structural defects. These latter emissions would differentiate mineral types and eventually minerals of the same type according to their geological provenance.

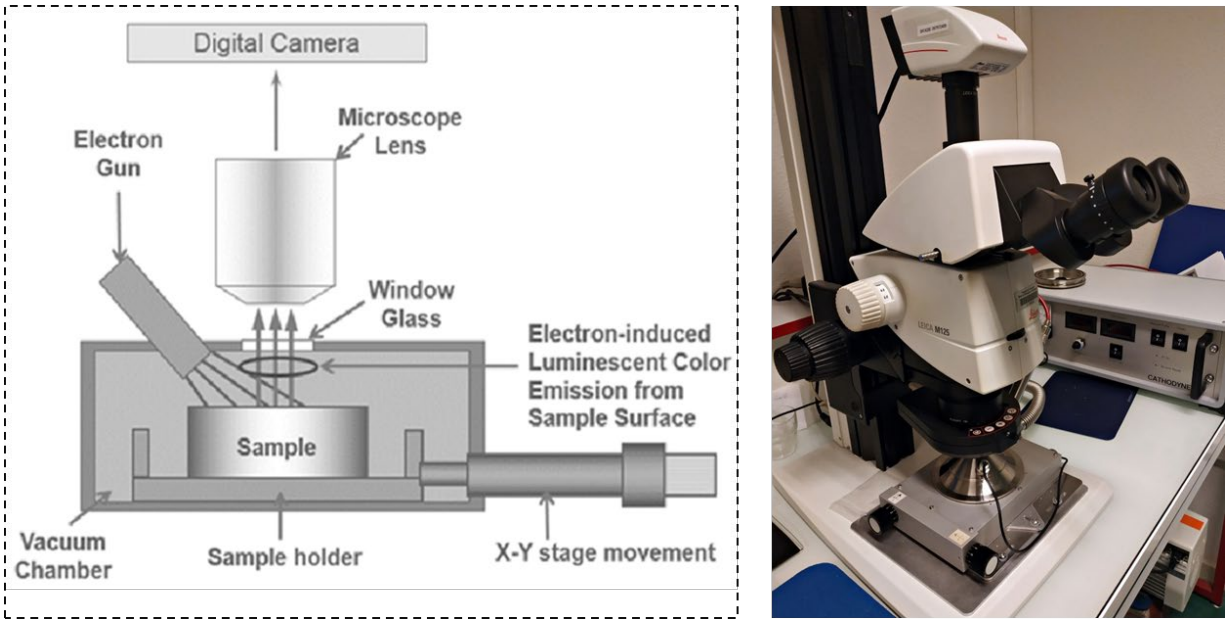

Fig. 12 Schematic view of cathodoluminescence microscope (Fan et al., 2017) (right image); Cathodoluminescence microscope used in this study (left image)(IRAMAT-CRP2A)

The cathodoluminescence allows making assumptions about the nature on the minerals. In order to clearly identify these minerals, SEM-EDX is essential. In addition, it provides data on the shape and size of inclusions, grain size/distribution and porosities.
For all the studies conducted in this thesis, updated Cathodyne OPEA instrument (Microvision Instruments, Evry, France) with a cold cathode cathodoluminescence system was used. The device is paired with a Leica M125 binocular lens and a Leica DFC4500 digital camera (Leica Microsystems, Wetzlar, Germany) to capture images (using LAS software) with an electron gun fixed and positioned at 45°.
The exposure time for the CL images is about 15 seconds with a tension of 15kV/10µA.

II.2.2.4 Scanning Electron Microscopy

The observation at the electron microscopy allows studying the texture of the ceramic body, using and electron beam to "illuminate" the sample and to obtain a magnified image.
The magnification is related to the wavelength that is associated with the electrons, depending on their energy, according to De Broglie's concept:

$$\lambda = 1.225/\sqrt{(E + 10^{-6} \times E^2)}$$

where λ is the wavelength and E the energy of the electrons.
The magnification in electron microscope can go up to 100 000 , but for the cultural heritage standard operations, a magnification of 20 000 is considered sufficient (Edwards and Vandenabeele, 2016). SEM imagery (JEOL - IT500 HR) facilitated the observations of the micro-texture of all our ceramic samples and more specifically the modern potsherds and briquettes in thick sections, and notably the progress of the mineral transformations upon firing.

II.2.2.5 Clay Granulometry

Granulometry is the study of the distribution of the elements of a rock according to their size (Foucault and Raoult, 2010). However, the same classification can be done for ceramics. The classes are defined in percent by a minimum and maximum diameter.
The granulometric study has been carried out in order to know the grain size distribution of the clay, from the raw material to the clay ready for molding. This method also allowed knowing the granulometric composition of the clay mixture and it can give hypotheses regarding the plasticity of the materials, based on the percentage of clay sediments.
The analysis performed in this thesis, was performed in the laboratory of PACEA (Université de Bordeaux), using a Horiba LA-950 device.

This method is based on the spatial distribution of light emitted by a laser beam and diffracted by the particles of the material analyzed, regarding the distribution, which is a function of particle size. The raw material was prepared before the measurements were taken. The samples were treated with oxygenated water (H_2O_2) and sodium hexametaphosphate ($Na_6O_{18}P_6$). The samples are diluted before pipetting to 300 ml and placed in the granulometer sampler. The results are presented by grain size classes, according to the classification proposed by Konert and Vandenberghe (Konert and Vandenberghe, 1997): coarse sands (2000-500 µm), fine sands (500-63 µm), coarse silts (63-16 µm), fine silts (16-7 µm) and clays (<7 µm) (**Fig. 13**).

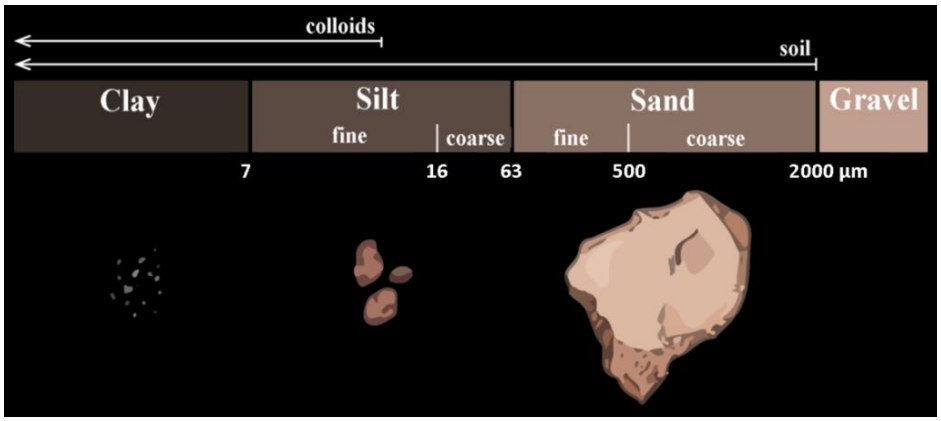

Modified after:
http://www.biogeochimie.fr/enseignement/geosciences/pedologie/chapitre_3_fr.html

Fig. 13 Soil particle size scales

II.2.3 Mineralogical and elemental composition analysis

II.2.3.1 X-Ray Diffraction analysis

The XRD allows the identification of crystalline phases in ceramics (indifferently natural inclusions, temper, clays) It is thus complementary to petrography as it can identify minerals. If you are interested in clay sediments, this method allows under certain conditions to identify clay minerals.

The analysis that is been carried out it's a destructive one, requiring the grinding of the samples to powder. The analysis involves an X-ray goniometer θ/θ, measuring the distances between the reticular planes of the crystals. For a specific incident beam, it will be obtained the reflections of wavelength λ, the angular value θ and the reticular planes of a distance d (according to the Bragg law) (**Fig. 14**)(Foucault and Raoult, 2010).

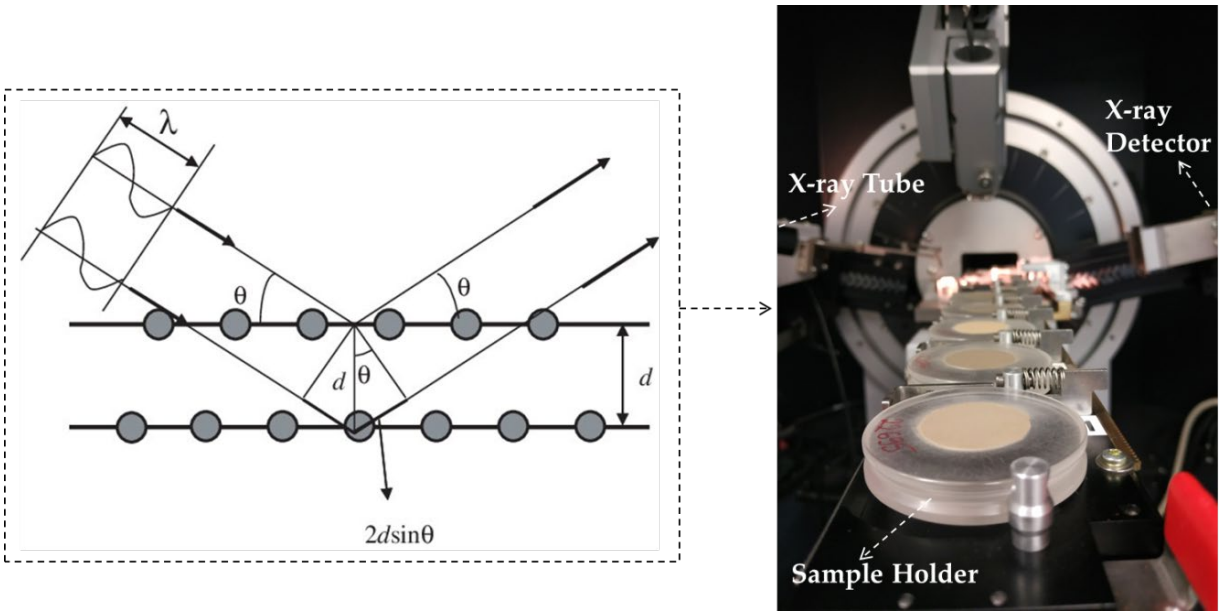

Fig. 14 Scheme of Bragg diffraction with crystalline lattice (Nakamura, 2021)(right image); X-ray diffraction instrument used in this study (left image)(IRAMAT-CRP2A)

The measurements for the studied ceramics were performed in the laboratory of IRAMAT-CRP2A using a diffractometer Bruker D8-Advance. The diffractometer uses CuKα radiations (ranging 3° to 60°), with a scan step size of 0.01° and an acquisition time/step of 1 s).
The qualitative analysis of the acquired diffractograms was performed with EVA software using the ICDD PDF - 2008 database.
A first attempt at relative quantification of the present phases was carried out by normalizing the intensities obtained to those of quartz. After it was proceeded to quantify the phases identified using EVA software, and we applied a treatment by Rietveld refinement, using TOPAS (Bruker) software.

II.2.3.2 Scanning Electron Microscopy with Energy Dispersive X-Ray spectroscopy

SEM-EDX allows an observation at high magnification and is a compositional analysis that makes possible the detection of the major and minor chemical elements (EDX). This method is based on applying a beam of accelerated electrons to the sample which excites the electrons of the atoms constituting the sample (Regert and Guerra, 2016).

This interaction gives a multitude of simultaneous emissions including backscattering electrons (chemical contrast), secondary electrons (topography) and X-rays which are characteristic of the elements present in the sample.
The backscattered electron intensity generated by electron can be correlated to the atomic number of the element within the sampling volume (**Fig. 15**). Therefore, qualitative information about the element can be revealed.

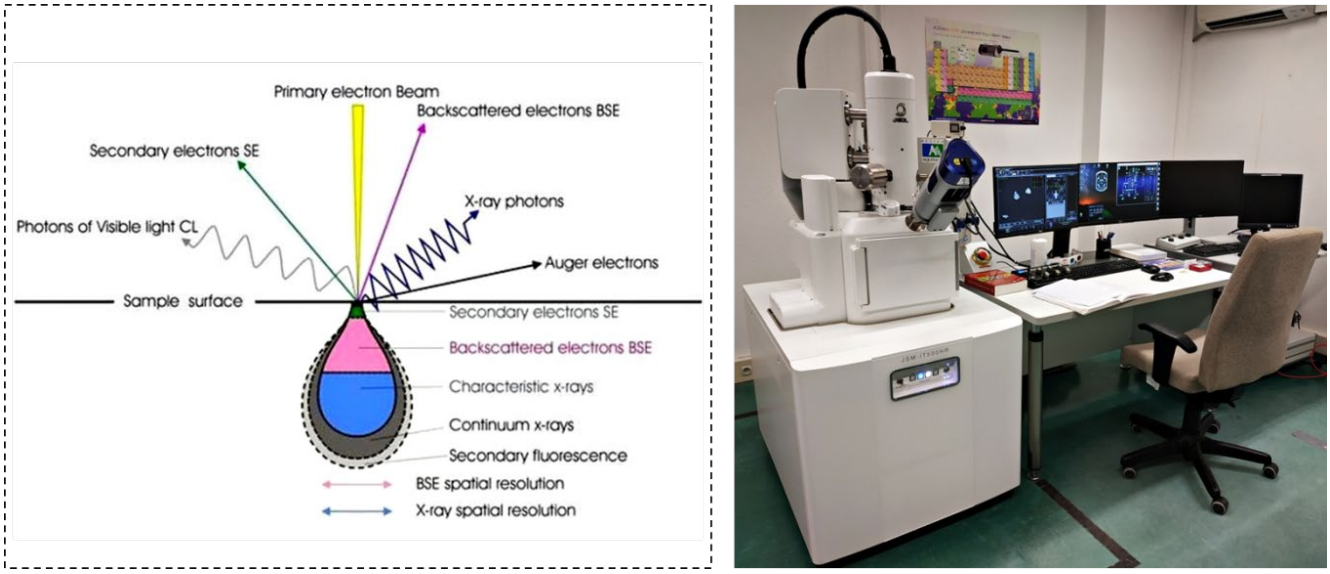

Fig. 15 Principle of SEM: electrons-matter interactions (Irigoyen Otamendi, 2016) (left image); SEM-EDX instrument (JEOL - IT500 HR) used for this research (right image) (IRAMAT-CRP2A)

The device was operated in Low Vacuum mode with a pressure of 30 Pa. The settings used for the samples analysis included an accelerating voltage of 20 kV, with a probe current from 10^{-10} to 5.10^{-9}A and about 4 000 000 counts per second, per spectrum.
The spectra acquisition (performed with a double EDX, Oxford Instruments UltimMax 100) was done on thick, polished sections of the ceramic bodies and on pressed powder pellets. Finally, the analysis was performed using Oxford Instruments AZtec NanoAnalysis.
The quantification of chemical composition was obtained from the average of four areas of 0.58 mm^2 each.
All results were expressed in wt% oxides (normalized to 100%), thus making it possible to quantify the major and minor elements (Na_2O, MgO, Al_2O_3, SiO_2, SO_3, K_2O, CaO, TiO_2 and Fe_2O_3), while Cl was expressed in simple wt%.

II.2.3.3 Portable X-ray Fluorescence Spectrometry

The XRF is based on the use of incident X rays to excite a sample and the measurement of X rays that come out of the sample.
The fluorescence emission, also called secondary X-rays, represents the "characteristic" spectrum of the atom, and it may be readily used to identify and quantify the chemical elements.
The calculated X-ray emission lines for all elements in the periodic table are an essential tool for the interpretation of all measured spectra (Artioli, 2010).
Thus, in the past years the portable XRF became a known technique having the advantage of the miniaturization of the device and the semiconductor detector technology.
The technique of the pXRF uses either a miniature X-ray tube or a sealed radioactive source to excite the sample with X-ray photons (**Fig. 16**) (Potts and West, 2008).

Modified after: https://openei.org/wiki/Hand-held_X-

https://www.olympus-ims.com/cs/vanta/accessories/

Fig. 16 Schematic diagram of portable XRF analyzer (left image); p-XRF instrument illustration (right image)

In our case, the p-XRF spectra was collected using a Vanta Olympus C Series instrument, which is equipped with a Rh anode, 40 kV X-ray tube and with a Si drift detector (SDD).

The equipment uses two different energy beams for quantifying the elements: one beam with 10 kV for the light elements (Mg, Al, Si, K, Ca, Ti, Mn) and one beam with 40 kV for the other detectable elements (Cr, Fe, Zn, Rb, Sr, Y, Zr).
The equipment proposed an internal calibration "GeoChem", algorithm in fundamental parameters. Even if different researchers don't agree with this method (Speakman and Shackley, 2013; Conrey et al., 2014), we will present a series of tests carried out in the laboratory on a known data set in order to improve the methodology. Then we will evaluate the necessity to correct or not this algorithm for the analysis of ceramic matrices.
The results presented in this study will be expressed as oxides percentage (MgO, Al_2O_3, SiO_2, K_2O, CaO, TiO_2, MnO, Fe_2O_3) and trace elements (Cr, Zn, Rb, Sr, Y, Zn) expressed in parts per million.

CHAPTER III

THE CASE STUDY OF DACIAN POTTERY

Foreword

This chapter deals with the main topic of this thesis, which is the identification and characterization of ceramics that were manufactured in Romania during La Tène period.
Since no similar studies have been carried out on the ceramics from Ocnița-Buridava site, this study will help to create a specific methodology that can serve as a starting point for future and new analysis of Dacian ceramics.
A detailed study of the first Dacian potteries which were analysed, is presented on the following pages.

III.1 Introduction

Before 1960, in Romania, the introduction of archaeometry in the study of ceramics was limited to simple analysis bulletins, with little or no interpretation.
Since 2000 methods of analysis and investigation have been diversified, and archaeometric studies have been increasingly involved in the analysis of artifacts.
Nowadays, archaeometry has become a necessity to be implemented in Romania, for at least two reasons:

- It completes the knowledge of human behavior in the historical past by revealing information invisible to the archaeologist,
- It makes an essential contribution in bringing local archaeological research to be known internationally (Opris, 2018).

In the past decade, the number of articles and studies regarding the Dacian pottery started to rise (e.g. Ionescu et al., 2007; Ionescu and Hoeck, 2011; Crandell et al., 2015; Ion et al., 2016; Giurgiu et al., 2017; Bugoi et al., 2019; Ignat et al., 2019; Fierascu et al., 2020; Drob et al., 2021), but definitely it doesn't cover the quantity of the artifacts discovered during all the archaeological campaigns (Cristescu, 2011).

History of ceramics in Romania

From literature, regarding the origins of Dacian potteries there are two hypotheses:

- the manufacture of the ceramics by Dacian people started to evolve from original and regional forms into new manufacturing techniques acquired from abroad;
- the local cultural background consisted in forming basic ceramic shapes, being in concordance with the foreign contemporary influences, for example from the Greek-roman world (Cristescu, 2011).

During the Neolithic period, different societies occupied what is nowadays the territory of Romania. As in the rest of Europe, in Romania the Late Neolithic Age begins in the 4th millennium BC. The Neolithic artworks were characterized mostly by decorations with abstract geometrical motifs, spirals and lines.

Fig. 17 Ceramic models from Neolithic period, in Romania; a) Idol figurine (Turdaș culture); b) Goddess figurine from Vidra (Boian culture); c) Sanctuary model (Gumelnița culture)

The earliest Neolithic culture, the "Criș-Starčevo culture", occupied most of Romania, produced numerous ceramic objects, but also zoomorphic and anthropomorphic figurines. After that, the cultures "Vinča-Turdaș", "Boian", "Vădastra", "Hamangia", "Gumelnița", and "Cernavodă" appeared in different areas at the same time (**Fig. 17**).

Chronologically, the Turdaș culture is the oldest of those listed and has covered parts of Transylvania, Banat and northern Oltenia since the 5th millennium BC, merging with elements from the Criș culture producing humanlike statuettes (Florea, 2017).

Such statues will be surpassed by those belonging to a culture of the 4th millennium, called Hamangia, after the dobrogean settlement of the same name. A particularly famous figurine, known as the Thinker of Hamangia (**Fig. 18**), portrays a thinking man seated on a little chair with his elbows on his knees. Due to its expressiveness, the statue is one of "the most emblematic works of Romanian art" (Ion et al., 2016; Florea, 2017).

http://www.istorie-pe-scurt.ro/ganditorul-de-la-hamangia-un-mister-in-varsta-de-8000-de-ani/

Fig. 18 The thinker of Hamangia with his pair (Hamangia culture statuettes, height 115 mm, width 75 mm)

Furthermore the highest stage of perfection of pottery was reached in the late Neolithic period, by the "Cucuteni culture" (a village in the district of Iasi, being widespread in Moldova, northeast Muntenia and southeast Transylvania), which produced polychrome vessels in various shapes. Later, in the Bronze Age, pottery began to change.

A few cultures began to develop on Romanian territory, going beyond the technical and aesthetic level, such as that of "Sighișoara-Wietenberg" (which occupied a vast territory covering present-day western Romania, northeastern Serbia and northwestern Bulgaria), "Verbicioara" and "Monteoru" (north of Danube and spread till the southern of Moldova) (Comsa and Szücs-Csillik, 2013; Bălan et al., 2016; Ion et al., 2016; Giurgiu et al., 2017).

Main aim and questions

The major objective of this research is to identify the chemical and mineralogical properties of ceramics and to establish the possibility in distinguishing the ceramics according to their manufacturing technique (Thér, 2020). These sets of analyses provide hypotheses about the nature, type of the raw materials used and the heat treatments applied.
The first analysis focuses on the petrographic examination (image-data) of the ceramic fragments, giving information regarding the mineralogical composition of the clay sediment. The images will then be correlated with images obtained by the cathodoluminescence method. The next aspect concentrates on X-ray diffraction to identify the mineralogical content of the ceramic vessels.
The results are then linked to petrographic observations to confirm the presence of specific minerals/phases. Lastly, the third aspect focuses on SEM-EDX analysis, giving information about the chemical composition of major and minor chemical elements and as well as information on the microtexture of the ceramics. The ceramic fragments found in the Southern Carpathians area have not been studied archaeometrically, which makes it possible to create a first database for future studies.
In the first years of the research in this thesis, a wide corpus of ceramics samples was provided for laboratory (or archaeometrical) studies, by the Museums of Argeș County Museum and from "Aurel Sacerdoțeanu" Vâlcea County Museum, dating from different time periods (**Fig. 19**).

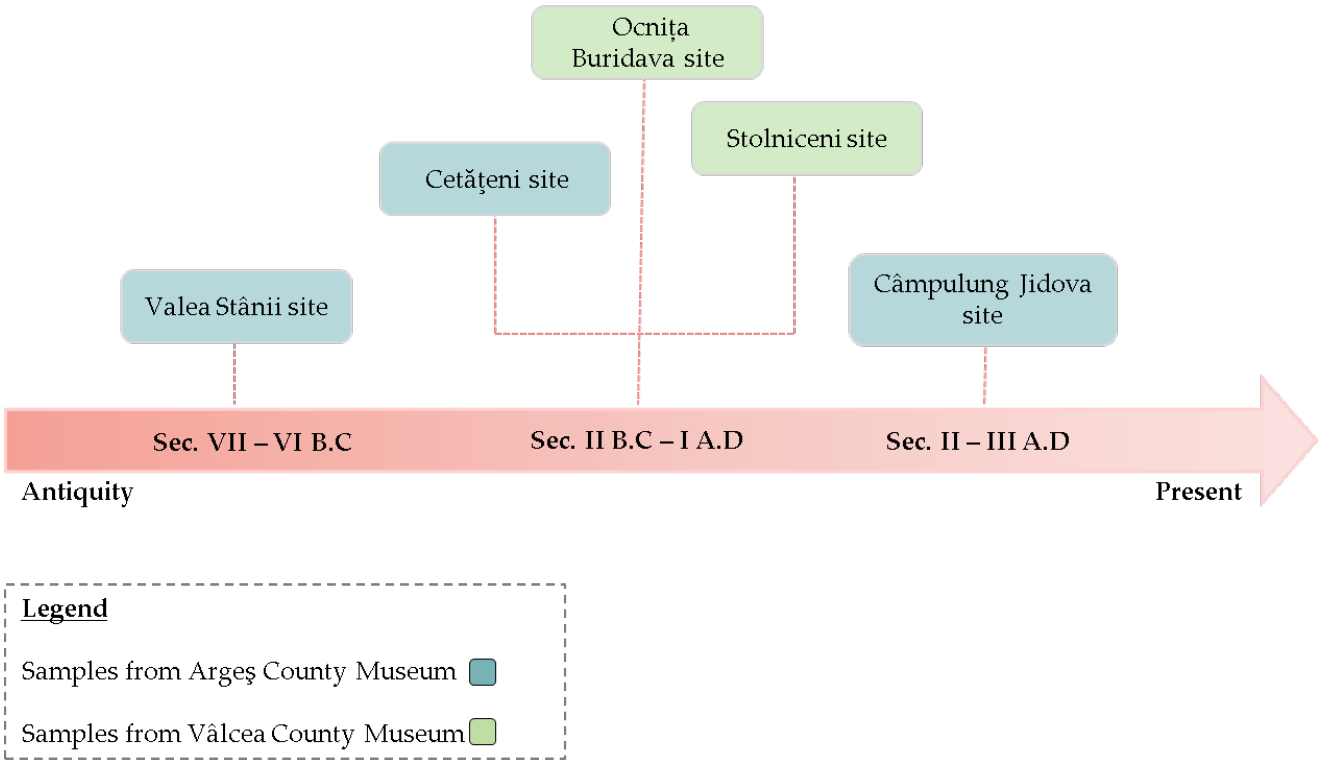

Fig. 19 Samples provided for archaeometrical study from Argeş County Museum and from Vâlcea County Museum

The first scientific studies were realized on selecting **five** representative samples, from the following ceramic sherds, given by the Argeş County Museum:

- 26 sherds, dating from the Roman period 2nd-3rd century AD, which were discovered in the archaeological layer excavated in the site of Câmpulung - Jidova. The ceramic fragments come from various common vessels (semi-fine pottery)(see Annex Figure 1A, Figure 2A).
- 7 sherds, dating from the 2nd Iron Age (Classic Geto-Dacian culture, IInd century BC - Ist century AD), being discovered without archaeological context, in the site of Cetățeni, Argeș county. The ceramic fragments come from different common vessels, represented by a pottery made of coarse clay with the addition of sand and mica. It is a type of pottery that is found in large quantities in any discovered Geto-Dacian site dating from the Second Iron Age (see Annex Figure 3A).
- and 11 sherds, dated by the archaeologist from the early Iron Age, belonging to the "Ferigile" cultural group. It is a pottery commonly found in the necropolises (see Annex Figure 4A).

However, since the archaeological questions were still under construction, our corpus of research was extended. Ceramic sherds from Ocnița-Buridava and Stolniceni, provided by "Aurel Sacerdoțeanu" Vâlcea County Museum were added to the corpus, enlarging the possibilities to develop new questions for the research.
Our main attention was focused on the Ocnița-Buridava site, since it was known as one of the most important Dacian fortified city at south of the Carpathians, the area being known by its richness in salt. The main aim was to discriminate and to show two types of ceramics manufacture, such as hand-made and wheel-made.

III.2 Archaeological context of Ocnița - Buridava

Modern Romania is located in Eastern Europe, to the north of the Balkan Peninsula and west to the Black sea. The history of Romania begins with the Neolithic Age (Berciu, 1967).
The Geto-Dacians are known to be the northern branch of the widespread Indo-European Thracians, settling between the Carpathian Mountains, the Danube River and the Black Sea (called in Latin Pontus Euxinus) since the late 2nd century BC (Crișan and Daicoviciu, 1969; Copoeru and Pop, 2013).

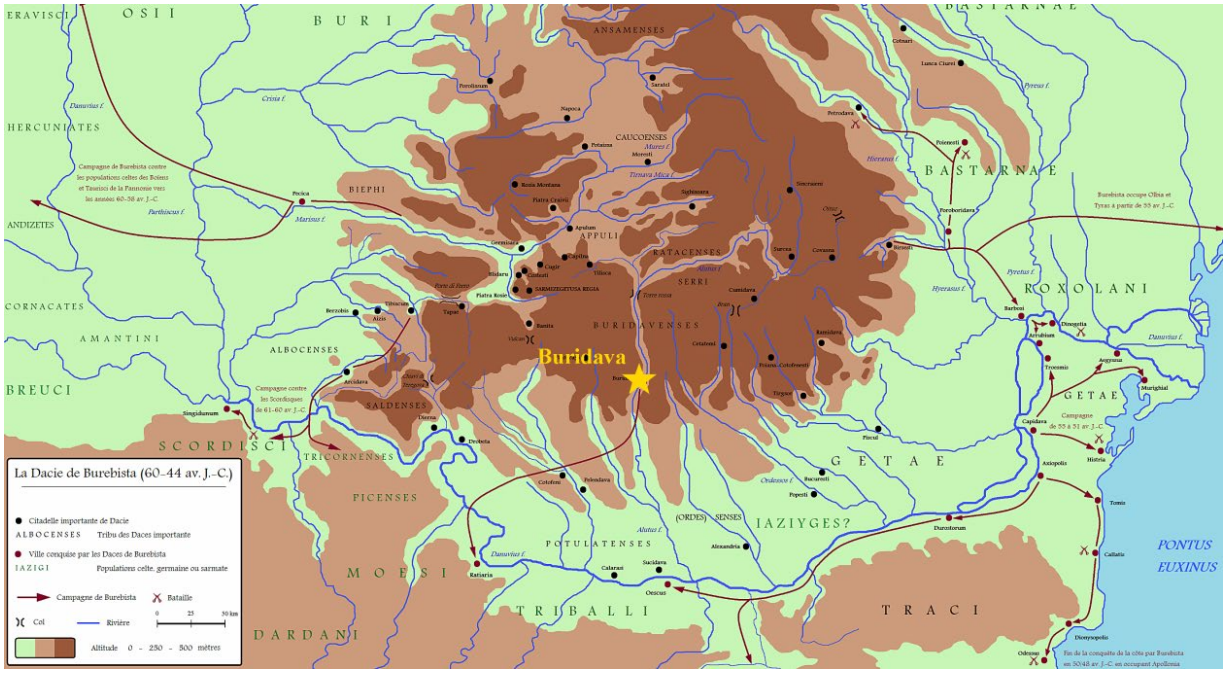

Modified after https://commons.wikimedia.org/wiki/File:Dacia_around

Fig. 20 Map of Dacia around 60 - 44 BC

One of the most interesting locations in Dacia was Buridava Dacică, being located in Vâlcea County, in Ocnița (many items of certain value discovered here were exhibited at the museum in Râmnicu Vâlcea).

The complex of Ocnița consists of three fortified citadels and a civil settlement, located on the right side of the Sărat brook and north of the Coşota River. (Iosifaru, 2011). Archaeological excavations revealed the importance of the Dacian settlement (**Fig. 20**) in the commercial trade with the Roman world, pointing to possible dynastic power center. The region has been known for its wealth in salt since prehistoric times. Numerous Roman artefacts, Latin inscriptions and the chronology assign Buridava a special status, as early as the 1st century BC (Berciu, 1967, 1981; Berciu and Iosifaru, 1980).

Although the Dacian settlement was of great importance to the region, after the Roman conquest the Dacian city began to lose its reputation (Crişan, 1993).

In 1973, as a result of excavations carried out by Dumitru Berciu's team (former Romanian historian and archaeologist, from the Institute of Archaeology in Bucharest), potsherds, glass and metal objects were discovered the area of Ocnița-Buridava archeological site (Iosifaru, 2011; Tuţulescu et al., 2012; Institutul Național al Patrimoniului - "Cronica cercetărilor arheologice campania 2016", 2016).

Based on a classification made by Crişan (Crişan and Daicoviciu, 1969), from a typological and chronological point of view, the Geto-Dacian pottery was classified into five phases, such as:

- the Proto-Dacian pottery, 6th-5th century BC,
- the Dacian pottery phase I, ancient, 5th-4th century BC,
- the Dacian pottery phase II, middle, 3rd-2nd century BC,
- the Dacian pottery phase III, classical, 100 BC-106 BC,
- and the Dacian pottery phase IV, late, after 106 AD
-

Ten different pottery fragments were selected for this research thesis (**Table 1**). These come from broken vessels, dating from the La Tène culture. The dating of the ceramics was carried out by the archaeologist, using typological and stratigraphic dating methods.

Five wheel-made vessels and five hand-made vessels were provided for investigation by the archaeologists **(Fig. 21, Fig. 22**).

They samples were sorted based on macroscopic observations (morphology and topography of the surface and fresh fractures), the colour of the ceramic body, the granulometry and the proportion of inclusions according to their manufacturing technique (Teodorescu et al., 2021).

Table 1 Context and detailed characteristics of the investigated ceramic vessels (YD - Year of Discovery, Tr.- Trench Number)

Technology group	Sample ID	Archaeological Context	Category	Object Type
Wheel-made	BDX 24414	YD. 1975, Tr. XXVE	Fine	Pitcher
	BDX 24415	YD. 1976, Tr. XXIX		Fruit bowl
	BDX 24416	YD. 1975, Tr. XXVF		Fruit bowl
	BDX 24417	YD. 1968, Tr. Xa		Bowl
	BDX 24418	YD. 1974, Tr. XXVD		Bowl
Hand-made	BDX 24419	YD. 1975, Tr. XXVF	Coarse	Bowl
	BDX 24420	YD. 1974, Tr. XXVD		Bowl
	BDX 24421	YD. 1968, Tr. Xa		Bowl
	BDX 24422	YD. 1974, Tr. XXVD		Bowl
	BDX 24423	YD. 1975, Tr. XXVF		Bowl

We indexed the samples in the laboratory, from BDX 24414 to BDX 24423. Two types of sampling were carried out for each ceramic fragment, for the preparation of the powder on the one hand and the thick and thin sections on the other hand.

Fig. 21 Fragments of wheel-made ceramics, donated by the Museum of Rm. Vâlcea "Aurelian Sacerdoțeanu", County Museum of History Vâlcea.

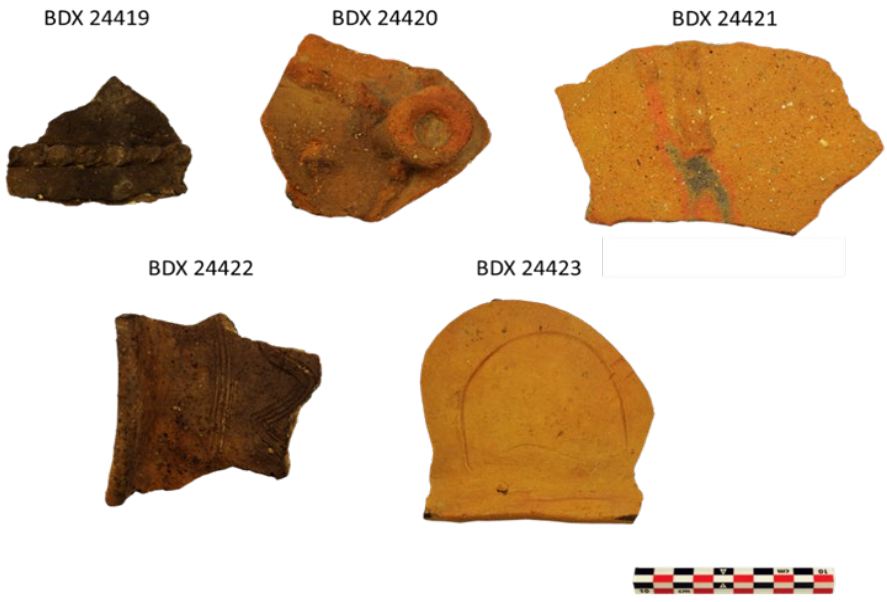

Fig. 22 Handmade ceramic fragments, donated by the museum in Rm. Vâlcea "Aurelian Sacerdoțeanu", County Museum of History Vâlcea.

III.3 Methodological strategy

Petrographic analysis (using OM optical microscopy) has been carried out to distinguish non-plastic inclusions in the ceramic paste, especially minerals and rocks (Foucault and Raoult, 2010; Regert and Guerra, 2016). Inclusions were identified, as well the shape and grain size distribution. Both, pore distribution and pore shape were also considered. Images were acquired in parallel and cross-polarized light. For the description of thin ceramic sections, F.J. Pettijohn's diagrams were used to evaluate the particle size distribution and pore shape (Pettijohn et al., 2012).

Cathodoluminescence (CL) provided an overall view of all ceramics. CL images obtained on large cross-sectional areas helped us to distinguish minerals and provide clues of the heat treatment applied.

The **XRD** measurements were performed on the ceramic powder to identify the minerals in the ceramic body, using TOPAS software for the quantification of mineral phases.

SEM imagery allowed the observation of the microtexture of the samples on polished thick sections and **SEM-EDX** provided a quantification of major and minor elements (Na_2O, MgO, Al_2O_3, SiO_2, SO_3, K_2O, CaO, TiO_2, MnO, and Fe_2O_3) obtained from the clay matrix and powder pellets. The chemical composition was quantified by averaging four areas of 0.58 mm^2 each, all results expressed in %wt of oxides.

The data was acquired in low-vacuum mode (20 Pa), giving results equivalent to those obtained in high-vacuum mode (Eméry, 2012). Standard corrections were applied using the software's built-in standard. The detection limit for most elements was about 0.1 wt%. In addition, the composition data was transformed into a log-ratio analysis and allowed to examine the interdependencies in the case of a multivariate dataset and to focus on the covariance and the correlation between the variables (Aitchison, 1982; Frerebeau et al., 2020).

All parameters used for this study have been presented previously with more detailed information (see Chapter II - Analytical techniques).

III.4 Results and discussion

III.4.1 Petrographic analysis

Firstly, ceramic microstructure information was obtained by polarizing microscope analysis, where petrographic observations were conducted on all 10 thin sections.
The petrographic analysis made possible to notice the grain size and the distribution of inclusions, allowing us to formulate first hypotheses about the manufacturing techniques. Microscopically, all ceramic bodies are mainly composed of feldspars, quartz, micas (muscovite and biotite), amphiboles and voids.
The wheel-made samples (BDX 24414 to BDX 24418) present a fine and compact matrix, being abundant in very fine inclusions, not exceeding 40 μm dimension (**Fig. 23**, a - b).
The non-plastic component size distribution displays a unimodal texture, assuming therefore that the raw clay material has been purified or specially selected by the potter.
The occurrence of the voids is reduced, revealing the compactness of the ceramic. Also the porosity observed at the microscope suggests a controlled and slow firing in specific kilns, where such a two-chamber kiln was found at "Dacia Buridava" (Anghel, 2002, 2011).
In return, hand-made samples contain also acid plutonic and metamorphic rocks. These have a coarse matrix, with inclusions up to about 2 mm in grain size (**Fig. 23**, c – d).
The porosity observed under the microscope is mainly represented by elongated voids and the size distribution of the inclusions presents a tri-modal texture. Usually, these voids are primary pores, which are dispersed randomly throughout the ceramic body. They occur during the moulding process, when thin layers of air and/or water are trapped between layers of clay. Then, after drying and firing the ceramic, the size of the primary pores increases (Ionescu et al., 2007).

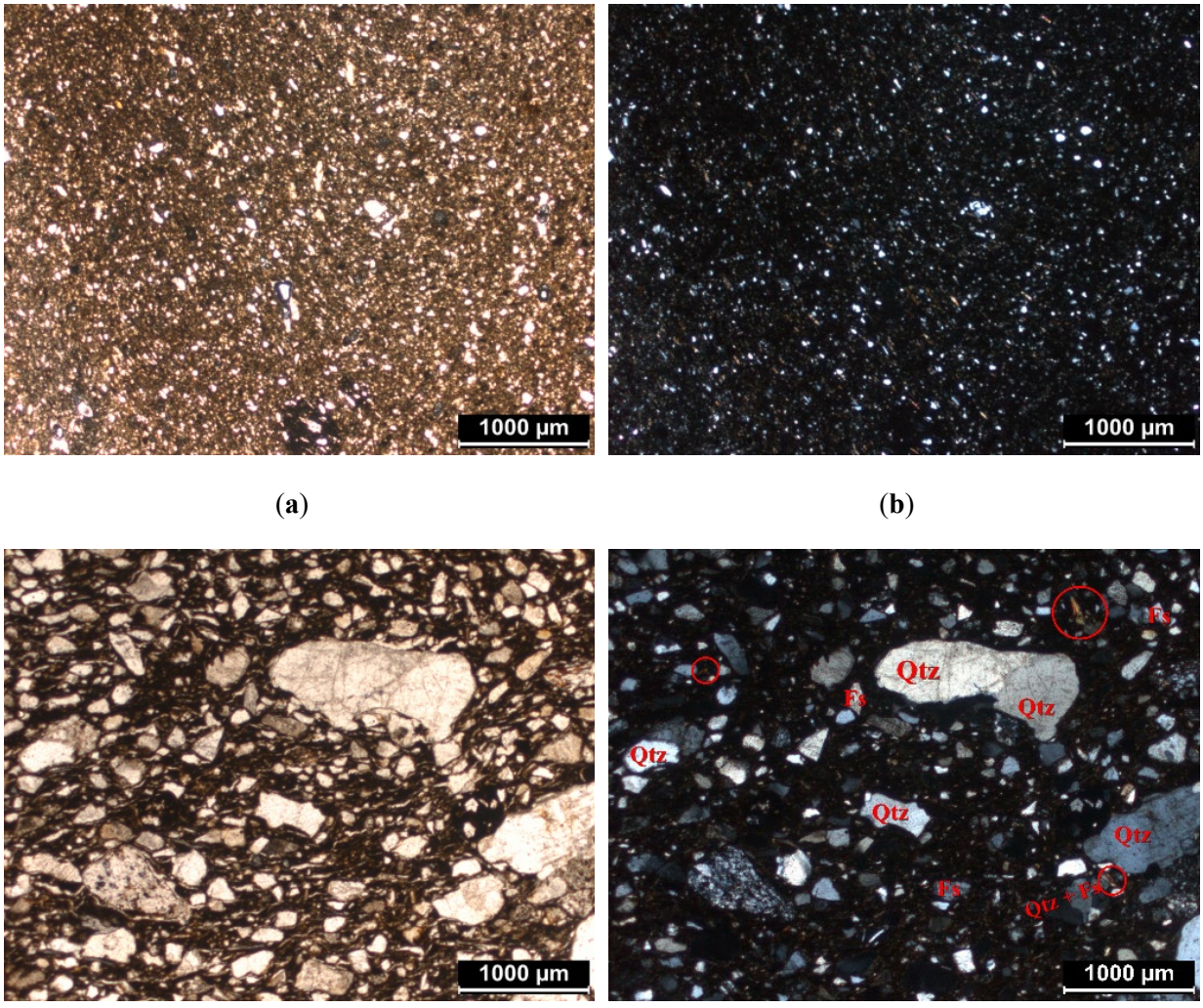

Fig. 23 Petrographic images: matrix from BDX 24418 ((**a**) plane-polarized light; (**b**) cross-polarized light); matrix from BDX 24419 ((**c**) plane-polarized light; (**d**) cross-polarized light). The identified minerals are mainly quartz (Q), altered feldspars (Fs) and mica (marked by red circle)

The difference in porosity typology between wheel-made and hand-made samples may be the result of the different moulding technique. **Fig. 23** presents images obtained with the polarizing microscope, revealing the difference between a very fine and a coarse matrix (at the same scale).

III.4.2 Cathodoluminescence imaging

With the help of cathodoluminescence, the first recorded results have allowed several hypotheses to be formulated concerning the nature of the minerals in the clay matrix.
For example, in the wheel-made samples, a homogeneous ceramic body with weakly luminescent yellow-green and blue inclusions was observed. As noticed in the petrographic analysis, the presence of very fine and few inclusions provided evidence suggesting the use of a purified clay for wheel-made manufacture, reflecting the potter's choice to obtain a plastic clay.
In the case of hand-made samples, the CL images (**Fig. 24**) revealed the presence of large angular inclusions (about 1 mm to 2 mm) dispersed in the matrix. Porosity was identified and observed in the CL images as dark green areas (due to resin impregnation).
As in the wheel-made samples, the main colours observed in the CL were a blue luminescent colour showing the presence of potassium feldspars, a yellow-green luminescence represented by plagioclase and a brown luminescent colour mixed with non-luminescent minerals representing quartz inclusions (**Fig. 24**) (Fonseca and Couto, 2017).
Considering that none of the samples showed inclusions with orange or red luminescence, inclusions, that are usually characterized as calcium carbonates (Piponnier et al., 1997), it allowed us to make first observations, such as that the clay used by potters is a Ca-poor clay.

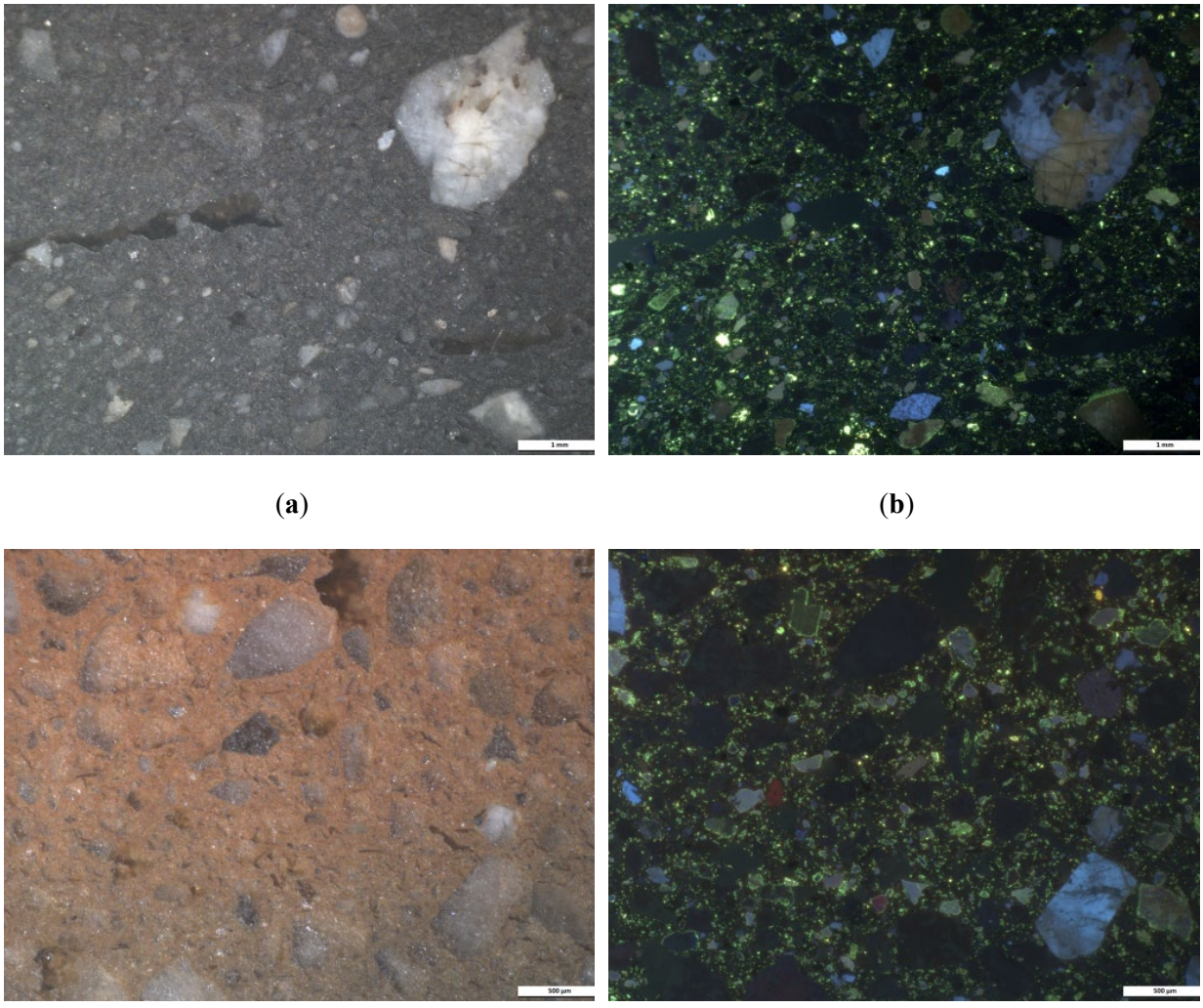

(**a**) (**b**)

(**c**) (**d**)

Fig. 24 Hand-made sherds observed in CL–imagery: BDX 24419 sample ((a) – white light reflectance; (b) cathodoluminescence emission); and BDX 24420 sample ((c) – white light reflectance; (d) cathodoluminescence emission)

III.4.3 XRD analysis

X-ray diffraction analysis revealed differences due to the deficiency or abundance of some mineralogical phases (**Table 2**).

Initially, we noticed some variability in each group of manufacturing techniques, which can be seen by the high standard deviation values. In addition, we observed mineralogical

differences between wheel-made and hand-made ceramics, in accordance with petrographic analyses.

Table 2 Mineralogical content (wt%) using X-ray diffraction analysis by Rietveld method. (SD: standard deviation). Hematite detected with a value of <1%

Technology group	Sample ID	Illite-Muscovite	Biotite	Quartz	Microcline	Orthoclase	Albite	Anorthite	Hornblende
Wheel-made	BDX 24414	22	3	36	6	5	18	9	1
	BDX 24415	11	4	35	20	1	35	14	3
	BDX 24416	11	3	32	16	5	32	14	5
	BDX 24417	31	8	23	9	5	23	12	5
	BDX 24418	21	7	29	17	1	29	11	4
Hand-made	BDX 24419	19	6	43	3	5	13	7	4
	BDX 24420	14	4	55	7	1	9	7	2
	BDX 24421	16	5	43	2	6	20	6	3
	BDX 24422	25	5	37	14	1	6	7	4
	BDX 24423	20	8	35	8	3	13	10	4

Muscovite/illite reflections were recorded in all samples, even though two of the wheel-made samples (BDX 24415 and BDX 24416) reported lower values than the rest (**Fig. 25**). The content of quartz is generally higher in handmade ceramics. Slightly higher values of microcline and anorthite were recorded in the wheel-made samples compared to the hand-made samples **(Table 2).**

It should be pointed out that illite-muscovite can be used as a thermal guideline. In previous investigations, Rodriguez-Navarro (Rodriguez-Navarro et al., 2003) described that the crystals of muscovite can undergo a noticeable change upon heating at temperatures over 350°C. In addition, the previous investigations showed that illite (muscovite) decomposes entirely at approximately 900°C (Bohor, 1963; Holakooei et al., 2014).

Moreover, the anorthite detected in all samples did not occur as a result of high-temperature transformation during the newly formed Ca phases, but more likely from its natural presence in the clay sediments, used for pottery manufacture. In conclusion, the firing temperature in all samples is quite low (below 900°C), which is consistent with their porosity features.

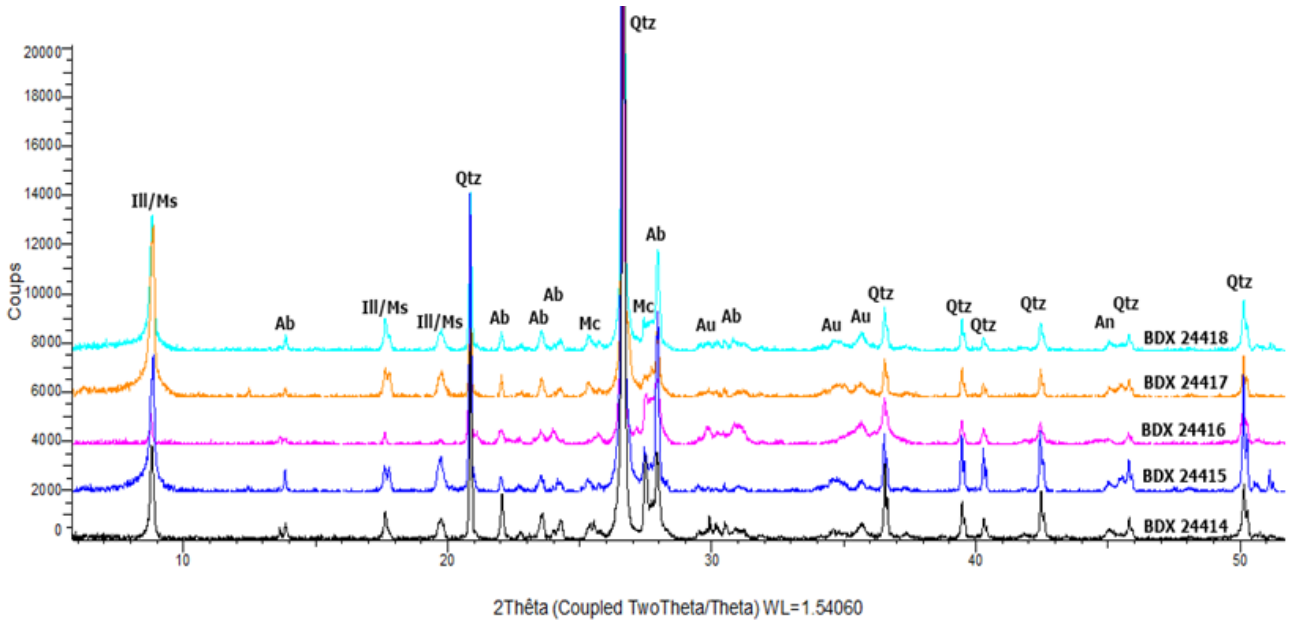

Fig. 25 X-ray diffractograms from samples BDX 24414 to BDX 24418, of Ocnița: Qtz - Quartz, Ill / Mus - Illite, muscovite, Ab - Albite, Mc - Microcline, Au - Augite, An – Anorthite (according to Kretz, 1983)

III.4.4 SEM-EDX analysis

SEM observations highlighted the microtexture of the ceramic sherds, wheel-made and hand-made. Additionally, SEM-EDX analyses were carried out ceramic powder pellets and thick sections.

The SEM images have outlined a compacted matrix and the presence of fine inclusions present in the wheel-made pots, confirming the observations made by petrography and cathodoluminescence. Moreover, in terms of the dimension of the inclusions, a clear difference corresponding to the two groups of manufacturing techniques was observed (**Fig. 26**).

Based on SEM-EDX, the values acquired for the powder pellets samples were expressed in percent oxides, choosing the average value of the spectrum.

The matrix of all samples shows the following composition: 58 - 70% SiO2, 16 - 21% Al_2O_3, 1 - 5% CaO, 6 - 8% Fe_2O_3, 3 - 4% K_2O and 1 - 4% MgO. A, it is confirmed that the clay imposes a dominant alumino-silicate matrix, and therefore a Ca-poor one, as indicated by petrography and CL.

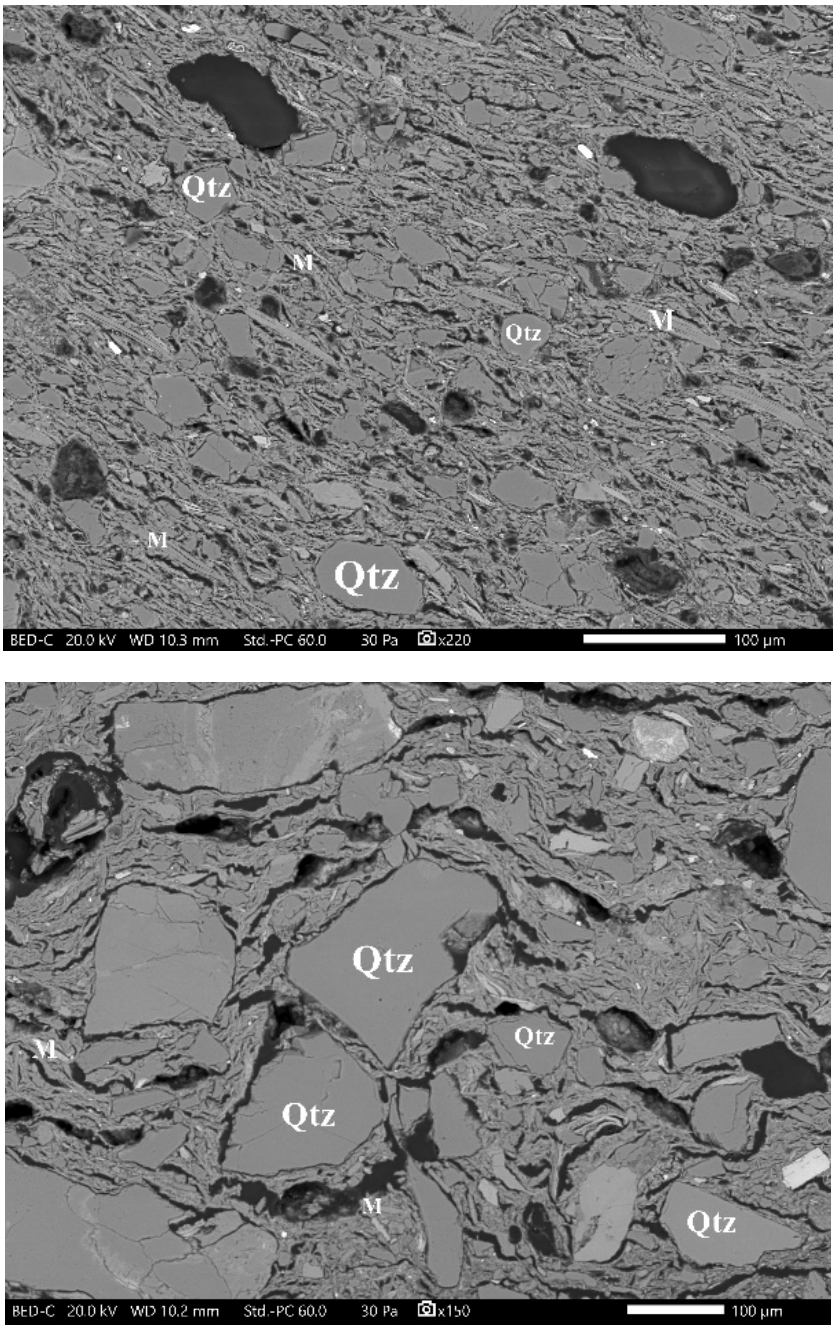

Fig. 26 SEM-BSE images displaying mica (M) and quartz (Qtz) inclusions, (**a**) sample BDX 24414 and (**b**) sample BDX 24421

The high calcium content (compared to the CaO content of hand-made ceramics) of wheel-made ceramics is probably related to the anorthite content.

Table 3 Chemical composition (wt%) of the ceramic fragments acquired by SEM-EDX (SD – standard deviations, number of measurements n = 4)

Technology group	Sample ID	Na_2O	MgO	Al_2O_3	SiO_2	P_2O_5	K_2O	CaO	TiO_2	MnO	Fe_2O_3
Wheel-made	BDX 24414	1.1	2.4	19.4	61.8	1.0	3.3	2.7	0.9	0.1	7.2
	BDX 24415	1.4	3.5	19.1	57.8	0.8	3.5	5.2	0.9	0.1	7.6
	BDX 24416	1.3	3.6	19.2	58.7	0.5	3.6	4.1	1.0	0.1	7.9
	BDX 24417	1.1	3.2	21.1	58.4	2.1	3.6	1.8	1.0	0.1	7.7
	BDX 24418	1.1	3.2	20.1	58.7	1.5	3.6	2.7	1.0	0.1	8.0
	Average	1.2	3.2	19.8	59.1	1.2	3.5	3.3	1.0	0.1	7.7
	SD	0.1	0.5	0.8	1.6	0.6	0.1	1.3	0.1	0.1	0.3
Hand-made	BDX 24419	1.7	1.4	17.4	67.1	1.5	2.5	1.6	0.7	0.2	5.9
	BDX 24420	1.6	1.4	17.4	67.1	1.6	2.5	1.6	0.7	0.2	6.0
	BDX 24421	1.5	1.7	15.7	69.7	0.7	2.6	1.2	0.8	0.1	6.1
	BDX 24422	0.9	1.8	18.5	64.3	1.4	3.5	1.3	0.8	0.2	7.1
	BDX 24423	1.6	1.9	17.7	66.2	0.8	2.7	1.5	0.8	0.1	6.6
	Average	1.5	1.6	17.3	66.9	1.2	2.8	1.4	0.8	0.2	6.3
	SD	0.3	0.2	1.0	1.9	0.4	0.4	0.2	0.1	0.1	0.5

Besides, it was observed that two chemical composition groups can be distinguished according to the content of Al_2O_3, SiO_2, CaO and MgO content (**Table 3**), corresponding to the manufacturing type groups. The group represented by wheel-made pottery is more abundant in MgO, Al_2O_3 and CaO contents, with a lower SiO_2 content.

To achieve a better overview of these two groups, binary diagrams were made using logarithmic ratios on Al_2O_3/SiO_2 - MgO/SiO_2 and CaO/SiO_2 - MgO/SiO_2 (**Fig. 27**).

The identified differences noted between the two groups by mineralogy and microtexture is confirmed by the chemical data. According to these results, it is very probable that the clay sediments used are quite different and selected to satisfy the requirements for each manufacturing technique (e.g. high presence of inclusions in hand-made ceramics).

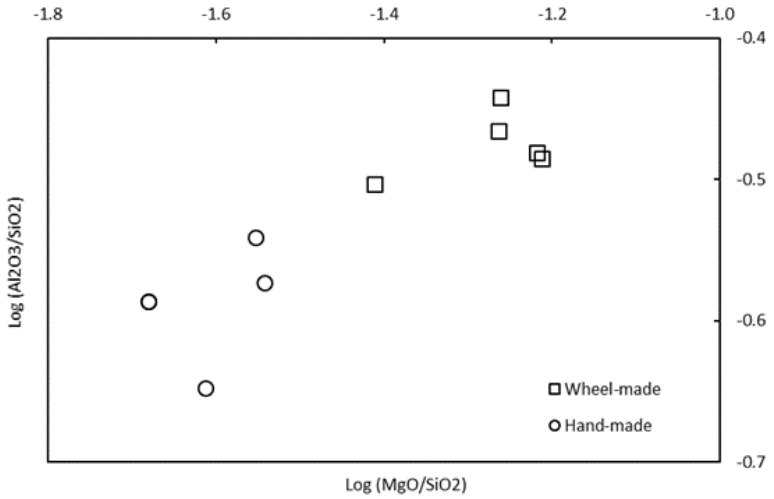

(**a**)

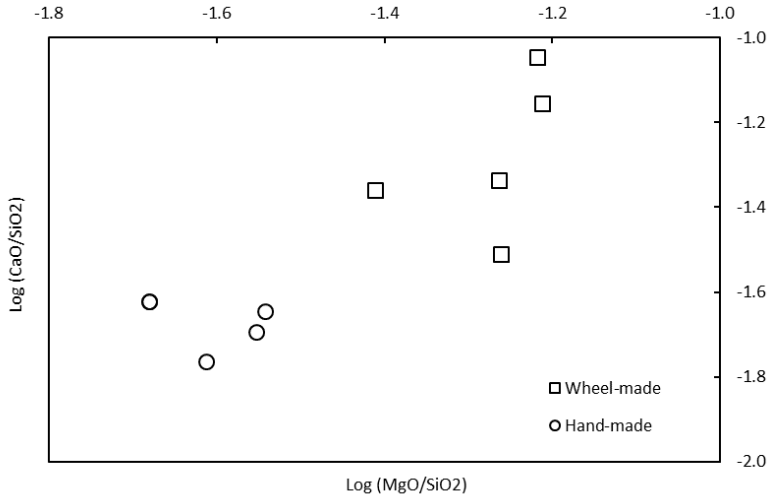

(**b**)

Fig. 27 Binary diagrams of ceramic fragments (circle shape - potsherds made by wheel; square shape - potsherds made by hand) expressed in log Al_2O_3/SiO_2 - log MgO/SiO_2 and log CaO/SiO_2 - log MgO/SiO_2. Samples hand-made BDX 24419 and BDX 24421 show very close values, so that their points overlap

III.5 Concluding remarks

Multi-scale analysis methods allowed differentiating two types of ceramic manufacture in ten Dacian vessels, excavated from the archaeological site of "Ocnița-Buridava", Romania.

In the manufacture of all pottery, non-calcareous clay sediments were used. We noticed a significant difference in grain size among the ceramic fragments, where the hand-made ones are coarser. Petrographic analysis, cathodoluminescence imaging and SEM revealed that the proportion of inclusions (mainly quartz, muscovite and albite) is relatively higher in this group.

The grain size distribution suggests that these tempers were initially present in the clay sediment, rather than added by the potter. The presence of these inclusions decreases the plasticity of the clays and gives a more convenient raw material for moulding handmade ceramics.

At this point of the study and from the reduced number of samples, we observed differences in texture, mineralogical and chemical compositions among the ceramics depending on their manufacturing technique. For example, for making wheel-made pottery, fine clay sediments were used (possibly obtained by removing a large part of the inclusions) and coarse clay sediments were selected for making hand-made pottery. Furthermore, for all ceramics, the firing temperature is generally under 900°C, being in accordance with their porosity aspect.

However, these initial investigations have generated archaeometric data that will enable the formation of an initial database for future comparisons when other additional data will be collected.

Open Access Article

Characterization of Archaeological Artefacts Using Methods Specific to Materials Science: The Case Study of Dacian Ceramics from 2nd c. BC to 1st c. AD

by Laura Teodorescu [1,2,*], Ayed Ben Amara [1], Nadia Cantin [1], Rémy Chapoulie [1], Cătălin Ducu [2], Sorin Ciucă [3], Claudiu Tulugea [4], Carol Terteci [4] and Mărioara Abrudeanu [2,5]

[1] Institut de Recherche sur les Archéomatériaux—Centre de Recherche en Physique Appliquée à L'archéologie, IRAMAT-CRP2A, UMR5060 CNRS—Université Bordeaux Montaigne, CEDEX 33607 Pessac, France

[2] Department of Materials Science and Engineering, University of Pitesti, 110040 Pitesti, Romania

[3] Department of Materials Science and Engineering, University Politehnica of Bucharest, 060042 Bucharest, Romania

[4] "Aurelian Sacerdoțeanu" Vâlcea County Museum, 240096 Râmnicu Vâlcea, Romania

[5] Department of Materials Science and Engineering, Technical Sciences Academy of Romania, 030167 Bucharest, Romania

[*] Author to whom correspondence should be addressed.

Academic Editor: Cornel Samoilă

Materials **2021**, *14*(14), 3908; https://doi.org/10.3390/ma14143908

Received: 7 June 2021 / Revised: 30 June 2021 / Accepted: 8 July 2021 / Published: 13 July 2021

(This article belongs to the Special Issue Collection of Papers in Material Science from Romania)

Abstract

Combined analysis methods such as optical microscopy (OM), cathodoluminescence (CL) microscopy, X-ray diffraction (XRD), and scanning electron microscopy–energy dispersive X-ray spectrometry (SEM–EDX) have made it possible to obtain the first physico-chemical data of Dacian potsherds, exhumed at the archeological site of Ocnița-Buridava, Romania; the samples were provided by the "Aurelian Sacerdoțeanu" County Museum Vâlcea, dating from the 2nd century BC to the 1st century AD. The mineralogical and petrographic analyses revealed two types of ceramic pastes, taking into account the granulometry of the inclusions and highlighting the choice of the potter for fabricating the ceramic either by wheel or by hand. All samples showed an abundance in quartz, mica (muscovite and biotite), and feldspars. These observations were confirmed by cathodoluminescence imagery, revealing heterogeneous pastes with varied granulometric distributions. The XRD patterns indicated the presence of the mineral phases, indicating a firing temperature below 900 °C. The wheel-made ceramics have a fine, compact matrix with very fine inclusions (<40 µm). On the other hand, the hand-made ceramics present a coarse matrix, with inclusions whose granulometry reaches approximately 2 mm. The difference between these two types of ceramics is also confirmed by the mineralogical and chemical analysis. The wheel-made potsherds are more abundant in MgO, Al_2O_3, and CaO contents. View Full-Text

Keywords: Dacian archaeological ceramic; materials science; mineralogy; petrography; cathodoluminescence; XRD; SEM–EDX

CHAPTER IV

THE CASE STUDY OF ISTRIAN OLIVE OIL AMPHORAE WORKSHOP TO THE DANUBE PROVINCES IN THE ROMAN PERIOD

Foreword

This chapter questions the presence of oil amphorae Dr 6B in the Danube region (with an extension to the far East area that corresponds to the Dacian culture area). Their similarity to Istrian amphorae is discussed through the analysis of their composition. In order to deal with this possible diffusion from the known Istrian workshops of Loron and Fažana we have used and implemented the portable XRF as an additional analytical technique in the thesis. The determination of pottery provenance is one of the most important contributions of archaeometry to archaeology (Tite, 2008). Its significance lies in the fact that the results of provenance studies provide information on distribution workshops, influence of cultures, trading routes and contacts between different sites (Kilikoglou et al., 1988). Thus, besides the advancements of hypothetical and theoretical perspectives of the archaeologists, a lot of traces are due to the geochemical analyses of ceramics (Frahm, 2018).

IV.1 Introduction

The study of amphorae on northern Adriatic during the Roman period awakened a special interest of different researches such as archaeologists, historians and archaeometers. The past of several decades of research on the production and consumption sites of Dressel 6B amphorae made possible nowadays to access to a wide database and bibliography. In Istria (nowadays Croatia) a general picture was drawn regarding the production and distribution of Dressel 6B from Fažana and Loron (Bulić, 2020; Cipriano, 2020; Machut et al., 2020; Marion and Tassaux, 2020; Szakmány, 2020).

Thus the research that will be presented in the following paragraphs was based on a previous program of collaboration between Ausonius and IRAMAT - CRP2A laboratories, allowing a continuation concerning the questions of circulation and diffusion of amphorae towards the

Danube areas by developing an analytical methodology of portable X-ray fluorescence to give answers to the question of the diffusion of Istrian oil amphorae.

IV.2 Archaeological background

The Dressel 6B amphorae originate from the second half of the 1st century BC, being designed for the transport of olive oil produced in the Adriatic area. Between the 1st and the 4th century AD, the workshop of Loron (located in the present Croatia) produced and commercialized amphorae of the Dressel 6B type (**Fig. 28**), which were used to distribute the Istrian olive oil in the Po Valley and the Danube provinces of the Roman Empire (Machut et al., 2020).

Fig. 28 Amphora Dressel 6B type (Machut, 2013)

The workshop of Loron was one of the major ones known for this region, operated continuously for four centuries under the leadership of wealthy owners, who left their mark through the numerous stamps applied to the amphorae.

At first, private possession of nobles from the senatorial aristocracy and close to the emperor, the workshop then became imperial property and continued to produce stamped amphorae until the end of the reign of Hadrian (138 A.D.); thereafter, the production of amphorae continued for two more centuries until the end of the 3rd century (perhaps until the beginning of the 4th century), but they were no longer stamped. Since 1994, Loron being noted as a great archaeological site, it has been excavated by a multidisciplinary French, Italian and Croatian team (Machut, 2013).

Until nowadays, intense research has made possible to establish a quite precise picture of the workshop's production and the commercial circuits through which the products were shipped. In general, the distribution of Loron amphorae corresponded to other Dressel 6B, whether Istrian or Italian. However, some nuances can be made with regard to the amphorae produced on the other side of the Adriatic.

First of all, the later ones disappeared shortly after 50 BC, while the Istrian ones continued to flourish (Machut et al., 2020). The map proposed in the **Fig. 29**, shows the places where the stamped amphorae were discovered in the eastern Europe. However, the marketing of Istrian oil continued beyond Hadrian period, as the two stamps of M. Aurelius Iustus on DR 6B were discovered.

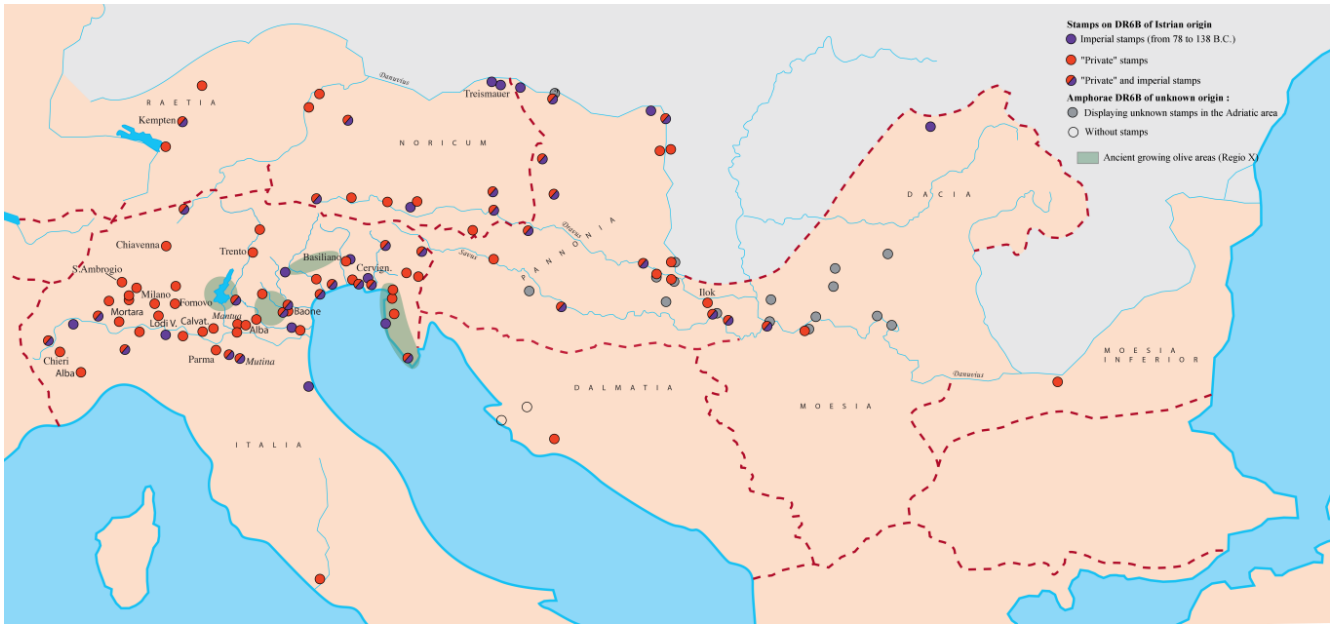

Fig. 29 Diffusion of Dr 6B Istrian oil amphorae. Modified after Y. Marion (Marion and Tassaux, 2020)

The first advantage of such a map is to observe the distribution of stamped amphorae of Istrian origin throughout the Roman Empire.

In the 1st century, the production was mainly dominated by the workshops of Fažana, in the south part of the peninsula, on the antic Pola's territory, and Loron, on the antic Parentium's territory (nowadays Poreč). At first, they were private domains, managed by the aristocratic families, but they both became part of the imperial domain during the reign of the Flavians (Machut et. al, 2015). The Dressel 6B amphorae produced at Loron are dated mainly by cross-referencing epigraphic data and the context of the distribution areas, rather than by stratigraphic data from the workshop excavation, where the amphorae uncovered were generally in a position of backfill.

As observed, the first owner of the workshop of Loron was Sisenna (Sisenna Statilius Taurus) and the amphorae manufactured under his rule had a high rim, hardly convex, and their production was between 10 B.C. till 30 B.C. Then, probably high-ranking personalities acquired the property: the stamps bring the name of MESCAE (unknown up to now) and next (**Fig. 30**) those of CRISPIN, CRISPINIL or CRISPINILLI, before 50 B.C. After, there are other private owners: AELI CRIS and Calvia Crispinilla; this one cede the ownership to the emperor Dominitian, probably in 81 A.D. Therefore, Loron is part of the imperial estate (as Fažana a few years earlier with Vespasian (emperor from 69 to 79 A.D.), and the name of the emperors from Dominitian to Hadrian is applied on the amphorae funnel shaped rim (Tassaux et al., 2001; Schindler, 2009).

Fig. 30 The signature of the Dr 6B amphorae from Loron: from private to imperial ownership (Marion and Tassaux, 2020)

After this general summary of the production of Dressel 6B and in particular those of Loron, we will focus to study their circulation through the distribution areas identified by the archaeological excavations. The actual situation of the amphorae found on the consumption sites allows delimiting with precision the area of diffusion of the Loron amphorae, which corresponds more or less to that of other Istrian amphora producers, and notably Fažana (Machut, 2013). The amphorae from Loron were therefore exported to two privileged areas of distribution: on the one hand, northern Italy with the Padanian plain, and on the other hand, the Alpine provinces (Rhetia and Noricum) and the Danubian provinces (especially Pannonia but also Mesia and Dacia) (Tassaux, 2004; Tassaux et al., 2010). The analysis of the stamp

distribution maps also allows us to reconstruct the major routes followed by the amphorae, which show a predominance of trans-Adriatic and fluvial maritime transport (Tassaux, 2001).
Thus, the relationship between Loron and Fažana in the trade routes presented a predominance of the later ones; the stamped amphorae outnumbered those of Loron at in most of the locations until the reign of the Antonines (138-18 A.D.). However, during the reign of Nerva (96-98 A.D.) the imperial amphorae of Loron outnumbered those of Fažana (Cipriano, 2009).

Main aims and questions

In the past 10 years a rise of portable XRF research on ceramics in archaeology has increased significantly (Menne et al., 2020). The main aim of this study is to clarify the reliability of p-XRF, by making the analysis without any special preparation and demonstrating the practicability of this device directly on field, without special preparation of the samples (since this is only possible by accesing a laboratory).
Furthermore, the obtained data will make it possible to complete and to broad the vision of archaeologists and historians interested in the circulation routes, trade and modes of appropriation of the territory of ancient societies, reaching until the south of Romania. In addition, this research focuses also in creating a database by using a non-destructive method for the identification of the amphora production with the help of a portable XRF.

IV.3 Analytical development and strategy

A number of different analytical techniques have been employed to characterize elemental chemical compositions of archaeological materials, such as X-Ray Fluorescence (XRF), Inductively Coupled Plasma-Mass Spectrometry (IPC-MS) and Instrumental Neutron Activation Analysis (INAA). However, as well as for other material characterization devices, it involves some constrains because of sampling preparation procedures, measurement conditions, calibration procedures and use of the correction factors that will improve the results (Sanjurjo-Sánchez et al., 2016).
Starting with 60's one of the most generally used analytical tool in the archeological applications, for determining (qualitatively and quantitatively) the chemical composition for a variety of archaeological and historical materials, was the XRF (X-Ray Fluorescence) spectrometry (Speakman et al., 2011). Since it became one of the most widely applied techniques in archaeology, the modernization of this method lead to the manufacture of portable instruments, allowing analyzing faster the elemental composition of archaeological material, in a non-destructive manner (Shackley, 2011; Frahm and Doonan, 2013).

For this reason it became an easily routine analysis to correlate ceramic productions and to confirm (or not) the identifications based mostly on macroscopic observations (Ceccarelli et al., 2016). Furthermore, Speakman (Speakman et al., 2011) noticed that there were no fundamental differences in the physics or capabilities between the portable XRF and the energy dispersive (XRF) instrument. The only major difference was the fact that the portable devices presented the deficiency in measuring the lower atomic weight elements, since no vacuum can be achieved.

Thus, in the last past years, a rise have been seen in published p-XRF-based studies on archaeological ceramics (Aimers et al., 2012; McCormick and Wells, 2014; Hunt and Speakman, 2015; Frahm et al., 2017). Increasingly ceramics have been studied using the p-XRF instrument, gaining in the past years a considerable attention in the archaeological community and having a rise in publications (Aimers et al., 2012; Frankel and Webb, 2012; Frahm, 2018). Thus the interest of the p-XRF in archaeometry is well recognized. First of all it allows an identification of the composition of materials (without damaging) for a wide range of chemical elements, with a high sensitivity. In addition, this technique combines a miniature X-Ray generator with an electrical cooled detector in a compact geometry. Taking advantage of a low weight, it allows performing analysis on field rapidly, with one day autonomy. This flexibility allows not only the characterisation of a large number of samples, but also in-situ measurements, when moving the artefacts to the laboratory is not possible (Calligaro et al., 2019).

Moreover, the advantage of this method in terms of its use in archaeology is that, for determining the chemical compositions, no sample or only a small part of the sample needs to be destroyed (to produce powder). In addition, it allows measurements to be made even when sampling is not possible.

The quality of the obtained results under these conditions such as obtaining valid results, by making the analysis directly on soft polished amphora samples (in order to remove any surface contamination) will be presented in the following paraghraphs (see IV.5)

IV.4 Archaeological materials

As presented in the first chapter, a selection of thirty-three samples (**Table 4**) by Yolande Marion (Associate researcher at the Ausonius Center - Bordeaux), was analyzed representing the Dr 6B amphora type. They were sampled from different sites in order to compare their compositions and estimate their origin production (Istria or not?) and to establish a trading route. The amphorae could have been circulating either by river either by land. Thus, a list with thirty three amphorae sampling was made, inclosing different locations: eighteen samples which were donated by the National Museum of Zagreb (Croatia), five samples from

Museum of Sisak (Croatia), two samples from Museum of Sirmium (Serbia) and eight samples from Viminacium Study Center (Serbia).

The sampled amphorae, few of them, according their stamp, were produced in Istria (in the atelier of Loron: Crispinill…, Calvia Crispinilla and IMP.AVG. GER– title of the emperor Domitian and in the atelier of Fažana: LAEK B and LESBI and another one TRAVL ET CRIS on the Tergeste's territory). The others were produced in North-Eastern Italy – APIC and, probably, COSTINI and L. TRE OPTA. The other stamps (OFF (Hedera?) Cl, DAP.AT.P.F, ANT. (Hedera?) MAERIS, M.MAESII, T. FLA. TALANI, COCCEIVSII, TI SECANDIDVS) are unknown in the Adriatic area.

It should be highlighted that this study presents an analytical method based on portable XRF measurements for the identification of amphorae provenance identification.

Part of these results which will be presented in the following research are part of Ausonius laboratory (UMR 5607 CNRS-UBM), represented by Francis Tassaux and Yolande Marion, who started a collaboration with IRAMAT-CRP2A in 2012, concretized by Pierre Machut dissertation research. This partnership led to a specific research program (with the support of the Cluster of Excellence "Laboratoire des Sciences Archeologiques de Bordeaux) named "Production and diffusion by amphorae from Roman Istria". Thus, the results obtained by Pierre Machut helped to discriminate better the production sites and it allowed making new hypothesis about the trading routes.

At this stage, the first results showed a significant difference in the composition of the amphorae between the beginning of the workshop's operation (senatorial period) and the imperial period. On the other hand, during the different reigns, it seems that the production was homogeneous (Machut, 2013), which indicates either the continuity of a supply of raw materials during this period or a certain expertise in production techniques, and even perhaps probably both hypotheses.

The analytical method chosen for our study was a portable X-ray Fluorescence (p-XRF), as it is the most suitable characterization method to determine a large number of sample compositions in a non-destructive way, and particularly suitable in our case due to the small size of the shards, collected from the museum.

Then statistical methods will enable to make group showing similarities between the different ceramic bodies. These groups and individual samples will be then compared to the reference archaeological group (in our case from Loron and Fažana).

Table 4 Sampling of amphorae Dr 6B, collected by Y. Marion, with their indexed number; *YD – Year of Discovery

Sample ID	Old ID	Discovery Place	YD.*	Conservation Locations	Stamp Name
BDX 25412	E1	Teutoburgium / Dalj	1912	National Museum of Zagreb	OFF (hedera) CL (hedera?)
BDX 25413	E2	Teutoburgium / Dalj	not specified	National Museum of Zagreb	DAP. AT. P. F
BDX 25414	E3	Teutoburgium / Dalj	1912	National Museum of Zagreb	OFF (hedera) CL (hedera?)
BDX 25415	E4	Siscia / Sisak	not specified	National Museum of Zagreb	ANT (hedera) MAERIS (?)
BDX 25416	E10	Siscia / Sisak, Kupa	1912	National Museum of Zagreb	CAL. CRISPIN[illae]
BDX 25417	E11	Siscia / Sisak, Kupa	not specified	National Museum of Zagreb	CAL. CRISPINI++++
BDX 25418	E12	Siscia / Sisak, Kupa	1913	National Museum of Zagreb	IMP. AVG[.] GER
BDX 25419	E13	Siscia / Sisak, Kupa	1913	National Museum of Zagreb	IMP. AVG. GER
BDX 25420	E14	Siscia / Sisak	not specified	National Museum of Zagreb	M. MAESII
BDX 25421	E15	Siscia / Sisak	not specified	National Museum of Zagreb	M. MAESII
BDX 25422	E16	Siscia / Sisak, Kupa	1913	National Museum of Zagreb	M. MAESII
BDX 25423	E17	Siscia / Sisak, Kupa	1913	National Museum of Zagreb	unreadable
BDX 25424	E18	Siscia / Sisak, Kupa	1912	National Museum of Zagreb	tR. AVL. ET. CRIS
BDX 25425	E19	Siscia/Teutoburgium	1912	National Museum of Zagreb	LAEKB
BDX 25426	E20	Siscia / Sisak	1912	National Museum of Zagreb	LESBI
BDX 25427	E21	Siscia / Sisak	1912	National Museum of Zagreb	LESBI
BDX 25428	E22	Siscia / Sisak	not specified	National Museum of Zagreb	COSTINI
BDX 25429	E23	Siscia / Sisak	not specified	National Museum of Zagreb	ANT (hedera) MAERIS
BDX 25431	E5	Siscia / Sisak	not specified	Sisak Museum	L. TR.E. OPTA
BDX 25432	E6	Siscia / Sisak	not specified	Sisak Museum	APIC
BDX 25433	E7	Siscia / Sisak	not specified	Sisak Museum	CRISPINIL++
BDX 25434	E8	Siscia / Sisak	not specified	Sisak Museum	without stamp
BDX 25435	E9	Siscia / Sisak	not specified	Sisak Museum	without stamp

BDX 25436	E24	Sirmium (Sremska Mitrovica)	not specified	Museum of Sirmium	OFF (hedera) DA
BDX 25437	E25	Sirmium (Sremska Mitrovica)	not specified	Museum of Sirmium	T. FLA. TALANI
BDX 25438	E26	PIR'83, G1-32 (Viminacium)	1983	Viminacium Study Center	[---]ALANI (hedera)
BDX 25439	E29	Viminacium	not specified	Viminacium Study Center	COCCEIVSII
BDX 25440	E30	V. G. (Viminacium)	2015	Viminacium Study Center	OFF (hedera) C--
BDX 25441	E32	Viminacium	2004	Viminacium Study Center	TI SECANDIDVS
BDX 25442	E34	Viminacium	not specified	Viminacium Study Center	without stamp
BDX 25443	E35	Viminacium	not specified	Viminacium Study Center	without stamp
BDX 25444	E36	Viminacium	not specified	Viminacium Study Center	without stamp
BDX 25445	E37	Viminacium	not specified	Viminacium Study Center	without stamp

IV.5 Results and discussion

IV.5.1 Development of the p-XRF

At the beginning of the year 2021, the laboratory IRAMAT-CRP2A acquired a new device for elemental analysis, a Vanta Olympus C Series p-XRF instrument.
Thus, the last past months of this thesis were dedicated in testing the new device and as well completing a database regarding the Loron and Fažana amphorae, responding to the archaeological questions.
As mentioned before (see Chapter II - Portable X-ray Fluorescence Spectrometry) the equipment proposed an internal calibration "GeoChem", algorithm in fundamental parameters. Even if different researchers suggest avoiding the use of the automatic calibration because it can give misleading results (Speakman and Shackley, 2013; Conrey et al., 2014), in our case we have tested the reliability of the p-XRF Vanta Olympus by making will a series of tests, carried out in the laboratory, on a known dataset (laboratory standards) in order to improve the methodology. Then we have evaluated the necessity to correct or not this algorithm for the analysis of ceramic matrices.
The analyses of ceramic materials, since they present a poor homogeneity, calibration test have been realized and parameters of measurements were tested, before the actual measurements.

IV.5.1.1 Standard samples for testing p-XRF Vanta

Each sample was analyzed on crossed sections (soft polished to 35 μm) on a test surface of 10 mm diameter. For very thin samples a collimation to 3 mm diameter beam spot was necessary to be used.
In addition, each sherd was fresh polished, in order to avoid any external pollution and to obtain a flat surface for better measurements.
It should be however noted that the XRF beam radiation normally has limited penetration, so the elements that are more abundant on the surface are predominantly detected, which can be noticeably different from the global composition of a sample (Ceccarelli et al., 2016).
When using sample powder, pellets were obtained using the Carver 4350 L pelletizer, from 95% powder mixed with 5% Hoecht C wax.
The accuracy of the results was estimated from measurements carried out on international standard SARM69 (MINTEK, certified) powder and as well on our internal laboratory standards represented by three different types of ceramic bodies, which were previously analyzed with ICP-AES method (in Caen laboratory), with various concentrations of major elements, expressed as oxides percentage (MgO, Al_2O_3, SiO_2, K_2O, CaO, TiO_2, MnO, Fe_2O_3) and trace elements (Ba, Sr, V, Zr, Rb, Y, Zn, Cr, Ni) expressed in parts per million:

- one very homogeneous earthenware (BDX 21063),
- one amphora with very few inclusions (BDX 16854),
- one Ethiopian ethnographic pottery with many inclusions homogeneously distributed (BDX 17729).

All the reference values of these used standards are represented in the **Table 5**.

Table 5 Reference values of three laboratory standards and one international standard. Major and minor elements are given in mass percentages and expressed as oxides; trace elements are given in parts per million normalized to 100% (<l.d. – inferior to limit of detection, n.d – not detected)

Sample ID	Type	SiO_2	Al_2O_3	Fe_2O_3	TiO_2	CaO	MgO	Na_2O	K_2O	MnO
BDX 21063	ICP-AES	70.75	26.32	0.78	0.38	0.61	0.22	<l.d.	0.88	0.01
BDX 16854	ICP-AES	60.46	15.37	7.04	0.93	9.8	2.38	1.04	2.81	0.18
BDX 17729	ICP-AES	65.78	18.14	10.61	1.04	0.58	0.87	<l.d.	2.44	0.35
SARM69	MINTEK	69.23	14.97	7.46	0.81	2.46	1.92	0.82	2.04	0.13

Sample ID	Type	Ba	Sr	V	Zr	Rb	Y	Zn	Cr	Ni
BDX 21063	ICP-AES	143	65	61	42	114	22	98	31	35
BDX 16854	ICP-AES	383	246	145	145	148	28	n.d	n.d	n.d
BDX 17729	ICP-AES	262	56	90	1171	112	115	n.d	n.d	n.d
SARM69	MINTEK	583	113	163	282	69	30	71	232	55

The first test of the device consisted in choosing a suitable methodology regarding the repeatability the precision and the accuracy of the measurements, while setting the influence of the acquisition time, and the collimator parameters on the results.
Furthermore, different tests have been made as well, in order to obtain a good correction factor for the dosed elements.

IV.5.1.2 Acquisition time, use of collimator and preparation of the samples

A first approach regarding the precision of measurement was selecting the acquisition time. Different tests have been made on section and powder pellets of the sample BDX 16854, with and without the collimator. The precision check was carried out by collecting three spectra at the same sample point with three measures in three different areas, changing only the time of acquisition: **30 s** (30 s at 10 kV and 30 s at 40 kV, making three minutes per sample), **60 s** (60 s at 10 kV and 60 s at 40 kV, reaching a total of six minutes per sample) and **120 s** (120 s at 10 kV and 120 s at 40 kV, making twelve minutes per sample).
The results were after compared to the dispersion for each time measurement, without using the collimator (**Table 6**). Even if the results with 120 s per beam present low errors, the difference and considering the protocol of three measured zones per sample, we have chosen a compromise acquisition time of 60 s per beam, which results in a total analysis time of 6 minutes per sample.
Nevertheless one of the perspectives could be to increase the acquisition time to improve the detection of the lightest elements (notably Mg) but also Cr.

In addition the error measured on pellets is more important than in sections. It should be noted that the grinding of the samples into powder is a time-consuming preparation and more destructive than surface analyses.
In our case study the destructive sampling was not appropriate. We prepared these two types of sample preparation (pellets vs thick sections) in order to compare, to evaluate the best conditions measurements for further analysis.
Since the archaeological amphorae samples that will be presented in this study present a small size, making impossible for obtaining powder pellets and since our data justifies the analysis on sections, in this study all the measurements will be made on soft polished sections. Furthermore, same measurements were made on the sample BDX 16854 on powder pellet and soft polished section, this time using the collimator (**Table 7**).

Table 6 Relative measurement error (%) for different acquisition times per beam (30 seconds, 60 seconds and 120 seconds). All measurements were made on the same area, without using a collimator

BDX 16854 - without collimator			**1 sigma**	
Element	**Type**	**% Error (30s)**	**% Error (60s)**	**% Error (120s)**
Si	pellet	0.4	0.3	0.2
	section	0.4	0.3	0.2
Al	pellet	1.0	0.7	0.5
	section	0.8	0.6	0.4
Fe	pellet	0.5	0.4	0.3
	section	0.4	0.3	0.2
Ti	pellet	4.4	3.2	2.1
	section	3.3	2.5	1.7
Ca	pellet	0.4	0.3	0.2
	section	0.3	0.2	0.2
Mg	pellet	17.1	11.1	8.1
	section	13.2	8.0	6.9
K	pellet	0.5	0.4	0.3
	section	0.5	0.3	0.2
Mn	pellet	3.3	2.4	1.7
	section	3.7	2.8	1.9
Sr	pellet	1.1	1.1	0.5
	section	0.8	0.8	0.4
Zr	pellet	1.6	1.6	0.8
	section	1.3	1.3	0.6
Rb	pellet	1.9	1.0	1.0
	section	1.3	1.3	0.7
Y	pellet	9.5	4.3	4.5
	section	6.1	3.2	3.3
Cr	pellet	14.1	12.0	6.3
	section	11.4	8.8	5.9
Zn	pellet	8.3	4.8	3.4
	section	4.8	3.2	2.2

Table 7 Relative measurements error (%) for different acquisition times per beam (30 seconds, 60 seconds and 120 seconds). All measurements were made on the same area, using the collimator

BDX 16854 - with collimator			**1 sigma**	
Element	**Type**	**% Error (30s)**	**% Error (60s)**	**% Error (120s)**
Si	pellet	0.4	0.3	0.2
	section	0.4	0.3	0.2
Al	pellet	0.9	0.7	0.5
	section	0.9	0.6	0.5
Fe	pellet	0.4	0.3	0.2
	section	0.5	0.3	0.2
Ti	pellet	3.4	2.3	1.7
	section	3.0	2.4	1.5
Ca	pellet	0.3	0.3	0.2
	section	0.4	0.3	0.2
Mg	pellet	-	15.2	7.4
	section	21.4	10.5	6.3
K	pellet	0.5	0.3	0.2
	section	0.5	0.3	0.2
Mn	pellet	2.5	1.7	1.3
	section	2.8	2.2	1.7
Sr	pellet	0.8	0.8	0.4
	section	1.1	0.8	0.4
Zr	pellet	1.2	1.2	0.7
	section	1.0	1.2	0.6
Rb	pellet	1.3	0.7	0.7
	section	1.2	0.6	0.6
Y	pellet	3.7	2.9	3.1
	section	4.4	2.7	2.9
Cr	pellet	12.1	10.3	7.4
	section	21.9	11.6	11
Zn	pellet	5.2	3.5	2.6
	section	3.8	2.5	2.2

As we can notice by comparing the two tables **Table 6** and **Table 7**, for sections (since in our research we will be focused on them) the differences in using or not the collimator are very low (see Annex Figure **5A**). Comparing the results for each dosed chemical element, we

observed that for most of them, at 60 s % error the differences are very low, where only few elements (Cr, Mn, Zn, Rb, Y, Zr) presented a slight difference while using the collimator (for example Zn – 3.5% error without collimator and 2.5% error with collimator on).
However, since using the collimator makes possible to analyze a wide area (which can include temper or natural inclusions), we decided to make the analysis without collimator and to use the collimator only when samples do not allow using this setting (due to their size limit). It should be underlined that the built-in camera of the device, was used at each measurement in order to avoid large inclusions and/or temper.

IV.5.1.3 Reproducibility

Before examining the chemical variability of the studied amphorae on the basis of p-XRF, analyses of the reproducibility of the method were assessed by replicate measurements of standard samples (in each case being normalized). The measurements on the sample BDX 16854, made by the p-XRF in the laboratory of IRAMAT-CRP2A and the measurements made by ICP-AES in Caen, allowed to make a first comparison between the obtained results and the expected results .
A number of analyses were made in order to identify and to equate a comparable analysis area and as well we conducted repeated measurements on the internal laboratory standards, BDX 16854 (24 measurements) being measured at each start and end of the session. Furthermore, the reproducibility varies according to the dose elements. The repeated measurements showed and acceptable precision for most of the elements, such as Al, Si, K, CaO, Ti Fe, Cr, Rb and Zr having a standard deviation of 12% or better.
Furthermore, in order to observe better the accuracy of the measurements (as mentioned before), measurements have been made as well for the sample BDX 17729 and BDX 21063 which corresponds to laboratory standards (**Table 8**).

Table 8 p-XRF data for the archaeological samples BDX 16854, BDX 17729, BDX 21063 and SARM69 showing the reproducibility of the measurements. Results are given in wt% for majors and ppm for minor and traces; (SD – standard deviation; RSD – Relative Standard deviation), normalized to 100%

SARM69 - Powder pellet (4 measurements)																	
	SiO_2	Al_2O_3	Fe_2O_3	TiO_2	CaO	MgO	K_2O	MnO	Sr	Zr	Rb	Y	Cr	Zn	Ni	V	Ba
Average	**69.3**	**16.7**	**6.4**	**0.7**	**2.6**	**2.2**	**1.8**	**0.1**	**102**	**254**	**57**	**29**	**250**	**66**	**51**	**118**	**516**
SD	±0.5	±0.8	±0.1	±0.1	±0.3	±0.2	±0.1	±0.1	±3	±7	±3	±1	±18	±4	±4	±82	±344
RSD %	1%	5%	1%	3%	12%	10%	2%	2%	3%	3%	5%	4%	7%	6%	8%	69%	67%
BDX 16854 - Section (24 measurements)																	
	SiO_2	Al_2O_3	Fe_2O_3	TiO_2	CaO	MgO	K_2O	MnO	Sr	Zr	Rb	Y	Cr	Zn	Ni	V	Ba
Average	**58.2**	**16.3**	**7.1**	**0.9**	**12.1**	**2.3**	**2.8**	**0.2**	**257**	**161**	**154**	**32**	**219**	**106**	**152**	**119**	**93**
SD	±0.8	±0.3	±0.2	±0.1	±1.1	±0.1	±0.1	±0.1	±3	±5	±5	±1	±19	±4	±10	±45	±135
RSD %	1%	2%	3%	3%	9%	4%	2%	44%	1%	3%	3%	2%	8%	4%	6%	38%	146%
BDX 17729 - Section (9 measurements)																	
	SiO_2	Al_2O_3	Fe_2O_3	TiO_2	CaO	MgO	K_2O	MnO	Sr	Zr	Rb	Y	Cr	Zn	Ni	V	Ba
Average	**65.9**	**19.2**	**10.1**	**1.0**	**0.5**	**1.1**	**1.8**	**0.3**	**47**	**1103**	**95**	**107**	**165**	**201**	**50**	**17**	**626**
SD	±0.3	±0.4	±0.5	±0.1	±0.1	±0.2	±0.1	±0.1	±1	±1	±1	±1	±1	±1	±1	±1	±1
RSD %	1%	2%	5%	6%	6%	16%	2%	8%	1%	1%	1%	1%	1%	1%	1%	1%	1%
BDX 21063 - Section (9 measurements)																	
	SiO_2	Al_2O_3	Fe_2O_3	TiO_2	CaO	MgO	K_2O	MnO	Sr	Zr	Rb	Y	Cr	Zn	Ni	V	Ba
Average	**69.2**	**28.2**	**0.8**	**0.4**	**0.4**	**0.1**	**0.7**	**0.1**	**56**	**54**	**107**	**19**	**27**	**117**	**46**	**69**	**866**
SD	±0.7	±1.0	±0.1	±0.1	±0.1	±0.1	±0.1	±0.1	±11	±2	±9	±5	±5	±27	±16	±27	±51
RSD %	1%	4%	12%	1%	5%	141%	9%	2%	20%	4%	9%	26%	±5.3	23%	34%	40%	6%

To decide if the measurements on soft polished surface are providing a suitable average of the chemical composition for the entire sample, the powder pellet made of the international standard SARM69 was as well measured. Four measurements were made in different days, measuring three times each area, using the collimator since due to the small size of the pellet. Using the present p-XRF setup, the test measurements on the ceramic sections demonstrated that three measurements are sufficient in order to draw accurate conclusions.

IV.5.1.4 Measurement accuracy

Even if the main interest of the use of this kind of equipment is to measure directly the sherds, it was necessary to test the results obtain with the p-XRF Vanta on powder pellets. In fact, the international ceramic reference (SARM69) is a powder (see **Annex Table 2A**). Thus to verify

and to estimate accuracy of p-XRF Vanta, SARM69, and BDX 16854 powder pellets were measured and compared to the references.

The same approach was then used on ceramic sections for all of the three internal laboratory standards: BDX 16854, BDX 17729 and BDX 21063. All the values have been normalized to 100% on the detected elements (**Table 9**).

As mentioned above (see **IV.5.1.1** Standard samples for testing p-XRF Vanta) the matrix of the three ceramic bodies differs from one to another starting with a sample with few inclusions (BDX 16854), another one with many inclusions homogeneously distributed (BDX 17729) and a very homogeneous earthenware (BDX 21063). Also, since the measurements were made directly on the surface, the XRF incident radiation has limited penetration, so the results obtained on fresh fractures can be significantly different in comparison to powder pellets (Killick, 2015; Ceccarelli et al., 2016)

Thus, the relative variation between the chemical contents on the presented ceramics differs as well because of the diversity of the analyzed matrix.

Table 9 Results obtained with Vanta Geochem in relation to the reference values on ceramic section. Major and minor elements are given in mass percentages and expressed as oxides; trace elements are given in parts per million normalized to 100% (n.d – not detected, RSD – Relative Standard Deviation)

BDX 16854			
Element	**Vanta Geochem**	**Reference**	**RSD%**
SiO_2	58.19	60.46	4
Al_2O_3	16.26	15.37	6
Fe_2O_3	7.14	7.04	1
TiO_2	0.89	0.93	5
CaO	12.1	9.8	23
MgO	2.33	2.38	2
K_2O	2.84	2.81	1
MnO	0.16	0.18	8
Sr	258	246	5
Zr	161	145	11
Rb	154	148	4
Y	32	28	13
Zn	106	n.d	n.d
Cr	219	n.d	n.d

BDX 17729			
Element	**Vanta Geochem**	**Reference**	**RSD%**
SiO_2	65.9	65.78	-
Al_2O_3	19.15	18.14	6
Fe_2O_3	10.1	10.61	5
TiO_2	0.96	1.04	7
CaO	0.52	0.58	11
MgO	1.08	0.87	24
K_2O	1.8	2.44	26
MnO	0.29	0.35	16
Sr	47	56	17
Zr	1103	1171	6
Rb	95	112	15
Y	107	115	7
Zn	201	n.d	n.d
Cr	165	n.d	n.d

BDX 21063			
Element	**Vanta Geochem**	**Reference**	**RSD%**
SiO_2	69.79	70.64	1
Al_2O_3	27.51	26.28	5
Fe_2O_3	0.73	0.78	6
TiO_2	0.41	0.38	8
CaO	0.44	0.60	27
MgO	0.16	0.22	27
K_2O	0.76	0.88	14
MnO	0.02	0.01	231
Sr	64	65	2
Zr	55	42	32
Rb	101	114	12
Y	15	33	54
Zn	137	103	33
Cr	24	88	73

The p-XRF has proven to be internally accurate since the difference in % regarding the obtained results and the reference has low values. However, it should be underlined that for a polished section the analyzed area [with collimator (3 mm diameter) or without collimator (10 mm diameter)] can include tempers or natural inclusions and is not wide enough to represent the whole sample.

IV.5.1.5 Geochem mode or factor correction (calibration) ?

Generally, there are three critical aspects of a calibration:

- to include all the elements of interest in the sample material,
- that has a dynamic range appropriate for the elemental concentration typical or expected in the sample material,
- that the certified reference materials or standards used to build the calibration have a similar matrix to the samples (Hunt and Speakman, 2015).

Correction factors were determined using eight internal standards (archaeological ceramics) analyzed previously in other French partners laboratory by ICP-AES (Caen) and WD-XRF (Lyon) covering the range of compositions generally expected from archaeological ceramics (**Table 10**)(see Annex Table 1A).

Table 10 General chemical composition representing the minimum and maximum values expected from archaeological ceramic bodies (major and minor elements are given in mass percentages and expressed as oxides; trace elements are given in parts per million (n.d. – not detected)

Element	SiO_2	Al_2O_3	Fe_2O_3	TiO_2	CaO	MgO	K_2O	MnO	Sr	Zr	Rb	Y	Cr	Zn	Ni	V	Ba
Min.	57,4	14,0	0,6	0,3	0,6	0,2	0,5	n.d.	30	27	31	15	40	27	33	42	84
Max.	73,7	25,8	10,4	1,2	17,0	2,3	3,4	0,5	342	966	204	116	133	111	71	142	541

Empirical calibration curves comparing intensities with concentrations can be used for the analysis of samples with limited variations of the matrix composition (Gazulla Barreda et al., 2016). In this study, the eight references materials (analyzed with ICP-AES and WDXRF) were measured in order to construct the calibration curves (see Annex **Table 1A**).

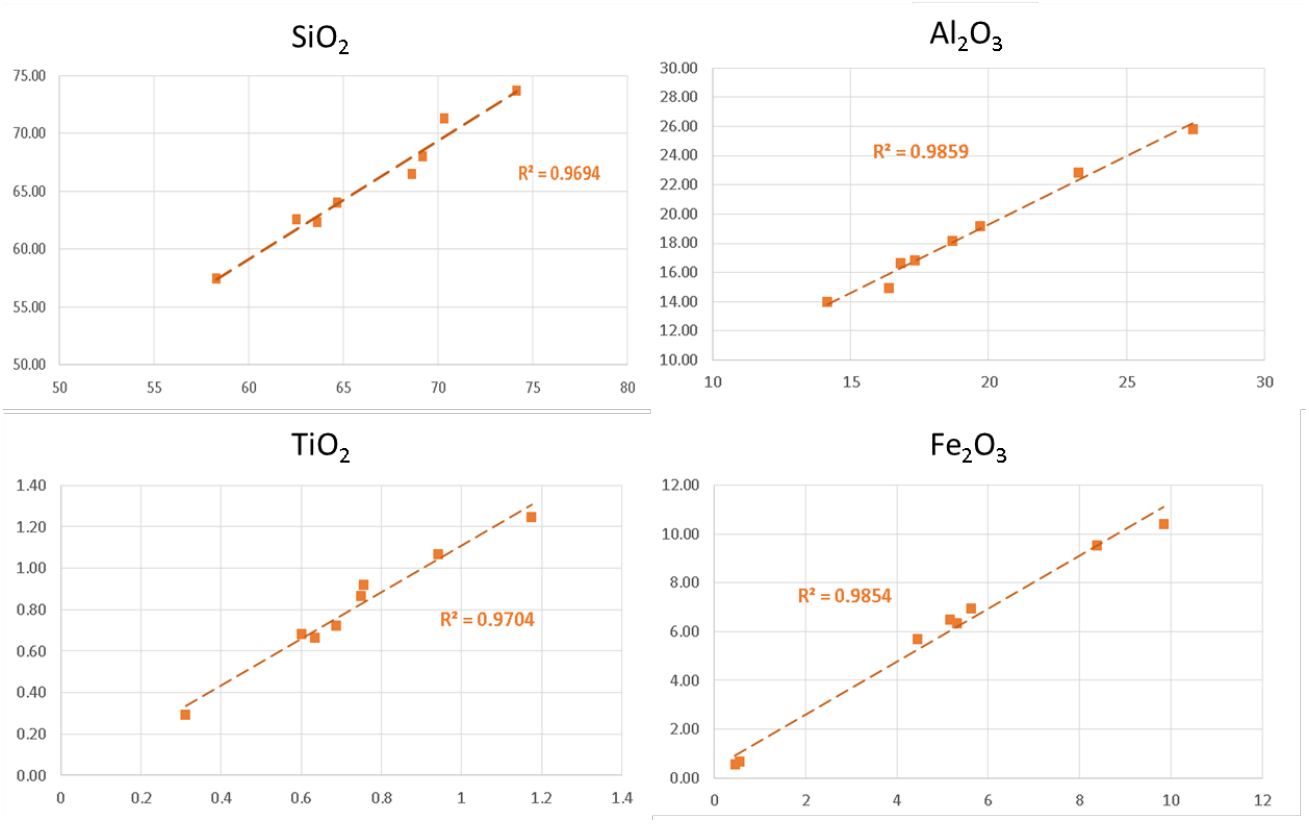

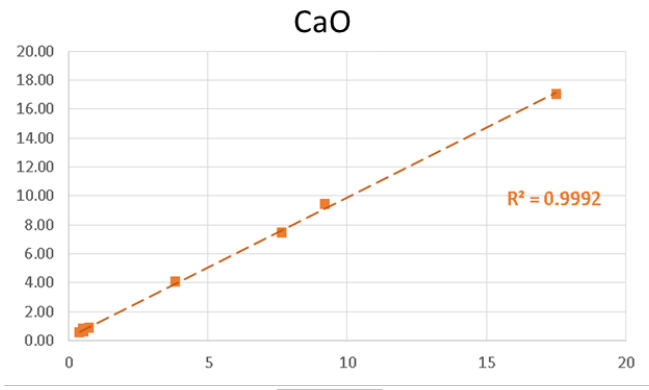
CaO
R² = 0.9992

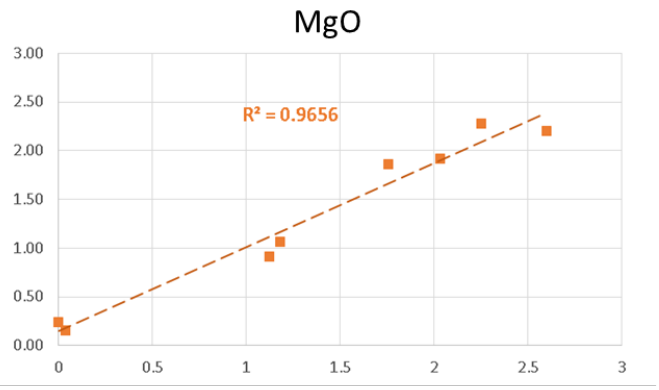
MgO
R² = 0.9656

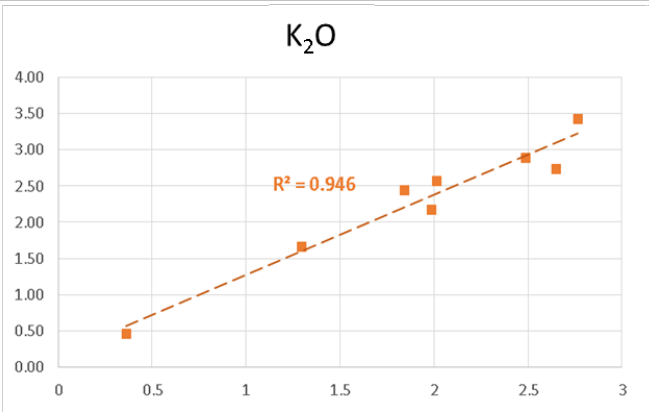
K2O
R² = 0.946

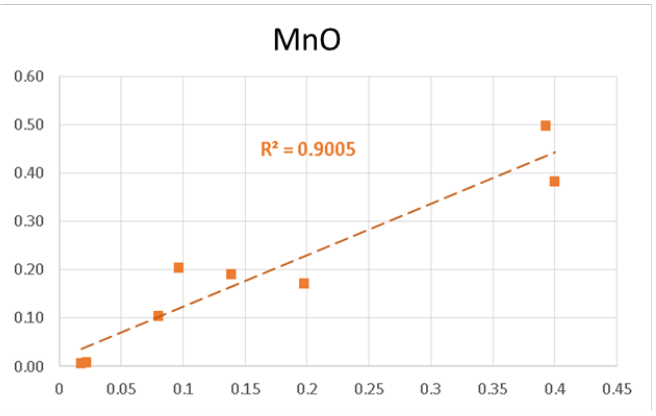
MnO
R² = 0.9005

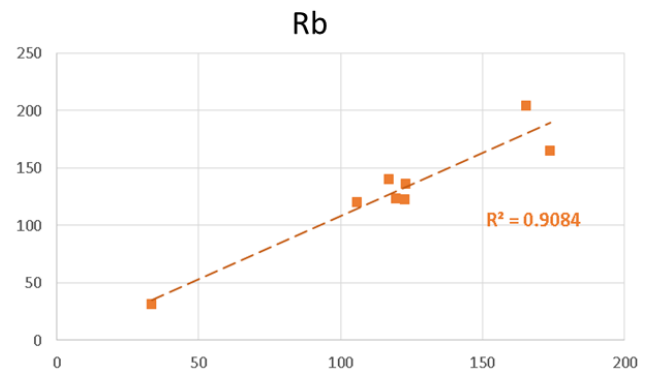
Rb
R² = 0.9084

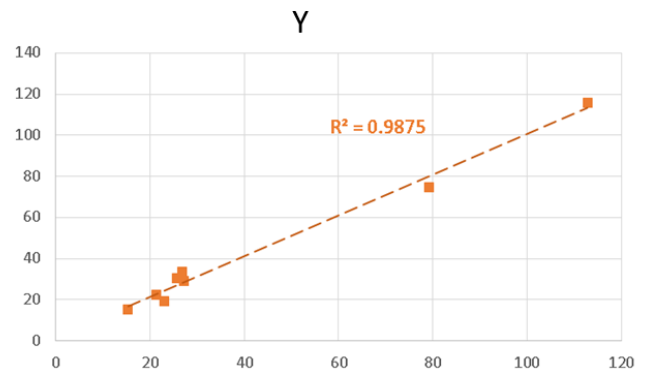
Y
R² = 0.9875

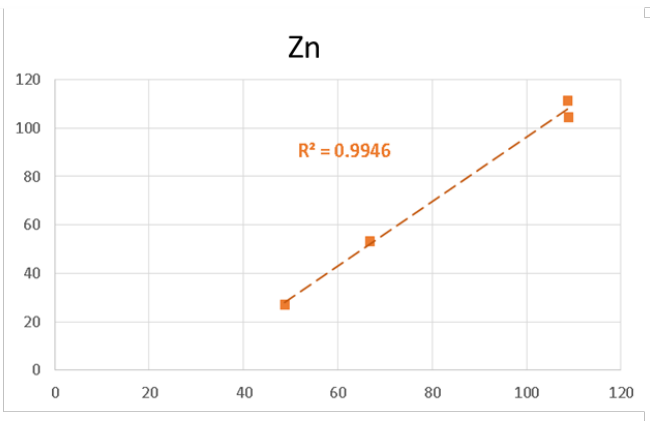
Zn
R² = 0.9946

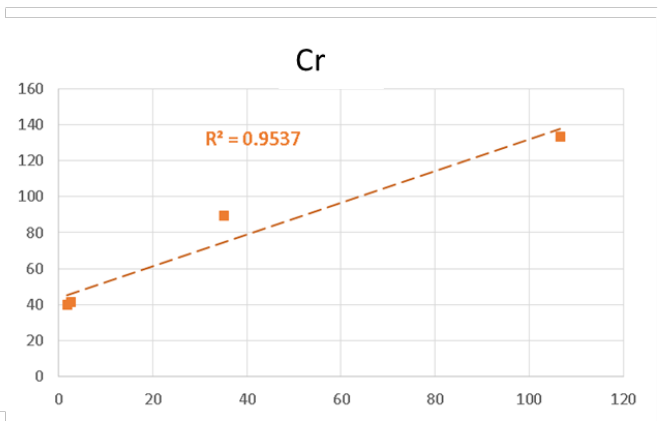
Cr
R² = 0.9537

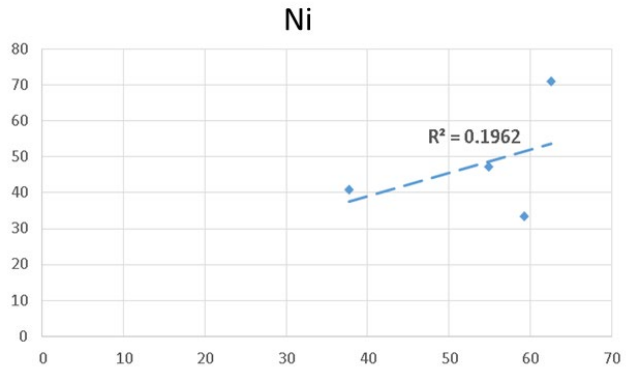

Fig. 31 Elemental scatterplots covering the range of values obtained from eight ceramic bodies samples, using p-XRF (x - axis) and lab based with ICP-AES and WDXRF (y – axis)

The p-XRF net peak area correlated with the quantitative ICP-AES and WDXRF data (**Fig. 31)** by using the Geochem mode. With his internal calibration, it is noticed a high degree of accuracy ($R^2 \geq 0.9$), apart from those to V, Ba and Ni which presented low accuracy. Thus, we decided for the analysis of the amphorae samplings, to not dose these chemical elements.

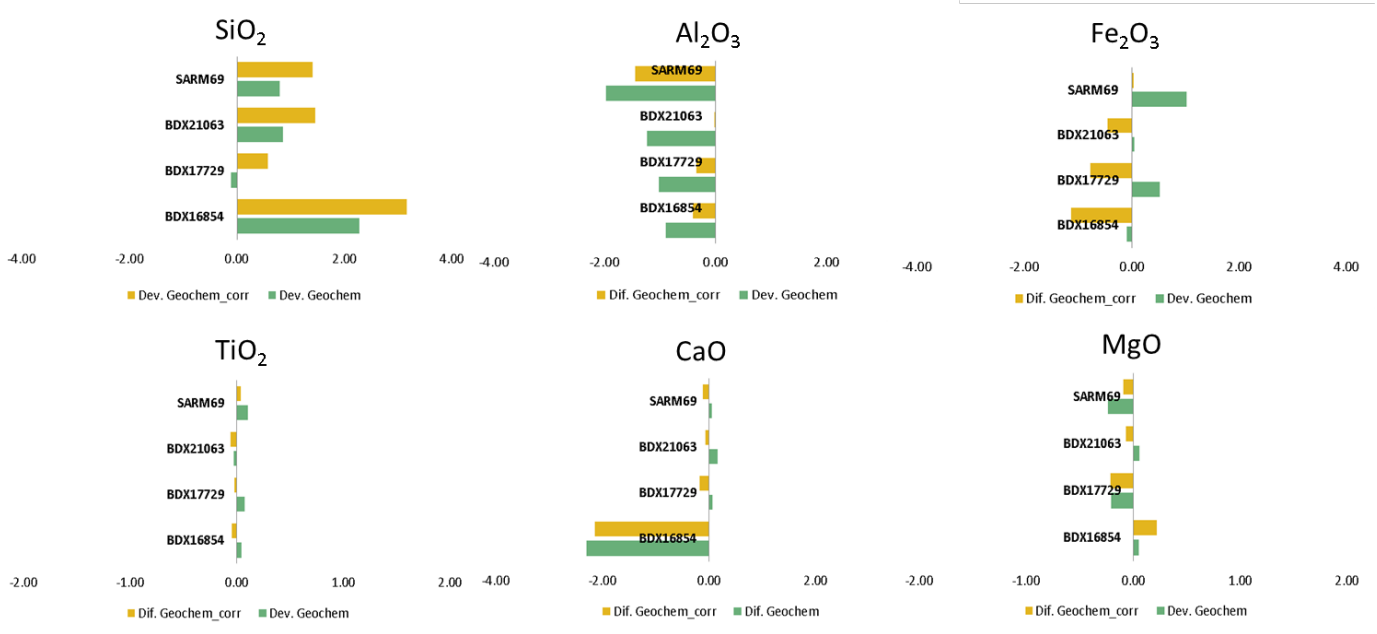

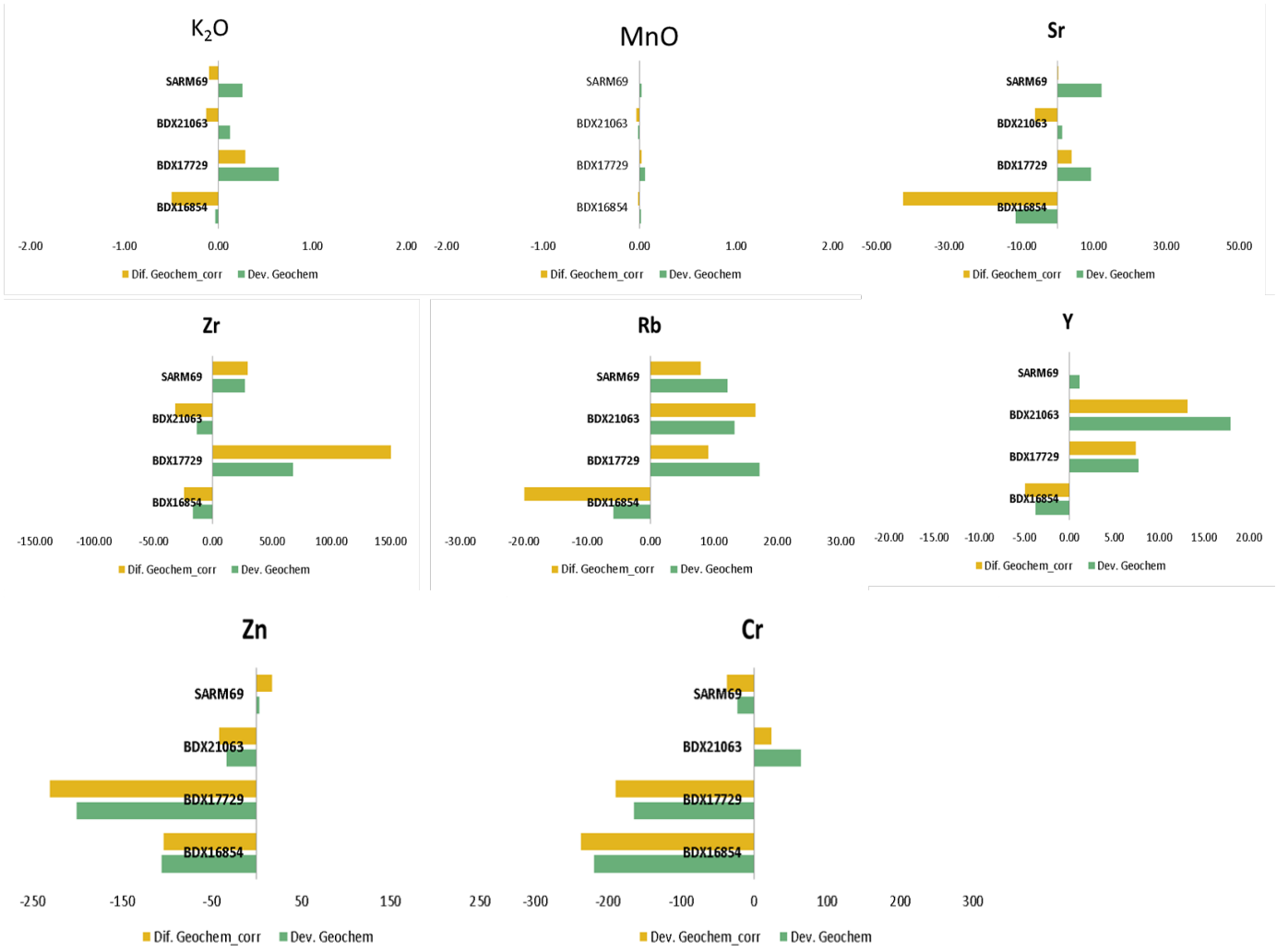

Fig. 32 Deviations between measurements, determined with four laboratory standards. Yellow colour represents the measurements obtained by the software Geochem, and the green colour represents the correction factor applied

In addition, **Fig. 32** indicates the precision of the p-XRF measurements of the element concentrations in the four laboratory standards (BDX 21063, BDX 17729, BDX 16854 and SARM 69), where the reference value corresponding to 0, yellow colour represent the measurements with the R^2 correction and green colour corresponds to the internal calibration Geochem measurements.

For observing better these differences between measurements (Geochem versus correction factor), in **Table 11** presented more detailed, the acquired data.

As mentioned in the upper paragraphs (see **IV.5.1** Standard samples for testing p-XRF Vanta), the internal calibration of the device "Geochem mode" is using fundamental parameters (FP) calibrated with standards.
The case of BDX 16854 (**Table 11**), which it is represented by an amphora with few inclusions, we can notice that for the chemical elements Si, Fe, Ti, Mg, K, Sr, Zr, Rb, Y, we obtained better values using the Geochem mode, instead of using the factor correction. Thus, we decided for the analysis of the archaeological samples to be under investigation by using the internal calibration of the p-XRF Vanta Olympus "Geochem".

Table 11 Deviations between measurements of Geochem (Dev.Geochem) and factor correction (Dev.Geochem_corr) compared to the reference value in percentage %. (For additional data, see Annex – Table 2A)(n.d. – not detected)

	Parameter	BDX16854 %	BDX17729 %	BDX21063 %	SARM69 %
SiO_2	Dev. Geochem	4	1	2	1
	Dev. Geochem_corr	5	1	3	2
Al_2O_3	Dev. Geochem	-6	-6	-8	-13
	Dev. Geochem_corr	-3	-2	-3	-10
Fe_2O_3	Dev. Geochem	-1	5	4	13
	Dev. Geochem_corr	-16	-7	-60	5
TiO_2	Dev. Geochem	5	7	7	13
	Dev. Geochem_corr	-5	-2	-15	1
CaO	Dev. Geochem	23	11	30	2
	Dev. Geochem_corr	-22	-29	-9	-5
MgO	Dev. Geochem	2	-24	63	12
	Dev. Geochem_corr	9	-24	-1	-5
K_2O	Dev. Geochem	1	26	19	-12
	Dev. Geochem_corr	-18	12	-9	-5
MnO	Dev. Geochem	8	16	-231	16
	Dev. Geochem_corr	-7	5	-537	-2
Sr	Dev. Geochem	-5	17	14	11
	Dev. Geochem_corr	17	7	4	1
Zr	Dev. Geochem	11	6	-28	10
	Dev. Geochem_corr	-16	13	-72	10
Rb	Dev. Geochem	-4	15	47	18
	Dev. Geochem_corr	-13	8	42	11
Y	Dev. Geochem	-13	7	44	4
	Dev. Geochem_corr	-18	6	40	1
Zn	Dev. Geochem	n.d	n.d	-14	5
	Dev. Geochem_corr	n.d	n.d	-16	25
Cr	Dev. Geochem	n.d	n.d	69	-10
	Dev. Geochem_corr	n.d	n.d	23	-16

IV.5.2 Archaeological results

The results obtained by the portable XRF made possible to make a first classification (**Table 12, Table 13**). It can be observed a wide range of variation of CaO (1%-17%), which makes difficult to make a classification after it.

Table 12 p-XRF data composition obtained from three measured zones per amphora sample. Major and minor elements are given in Wt % oxides; (SD – standard deviation, l.d – limit of detection), with three measured zone per sampling

Sample ID	Discovery Place	MgO	Al2O3	SiO2	K2O	CaO	TiO2	Fe2O3	MnO
BDX25412		**2.4**	**19.9**	**65.5**	**2.2**	**1.7**	**1**	**7**	**0.1**
SD	**Teutoburgium**	±0.1	±0.1	±0.1	±0.1	±0.1	±0.1	±0.1	±0.1
BDX25413		**1.7**	**14.1**	**59.6**	**1.4**	**16.5**	**0.9**	**5.5**	**0.1**
SD	**Teutoburgium**	±0.8	±0.2	±0.4	±0.1	±0.2	±0.1	±0.1	±0.1
BDX25414		**2.1**	**19.7**	**66**	**2.2**	**1.8**	**1.1**	**6.6**	**0.1**
SD	**Teutoburgium**	±0.1	±0.3	±0.3	±0.1	±0.1	±0.1	±0.1	±0.1
BDX25415		**2.7**	**16**	**59.1**	**2.8**	**11.6**	**0.7**	**6.8**	**0.1**
SD	**Siscia**	±0.1	±0.2	±0.4	±0.1	±0.5	±0.1	±0.8	±0.1
BDX25416		**2.4**	**17**	**63.7**	**2.8**	**7.3**	**0.8**	**5.8**	**0.1**
SD	**Siscia**	±0.1	±0.1	±0.1	±0.1	±0.2	±0.1	±0.1	±0.1
BDX25417		**2.9**	**14.9**	**56.3**	**2.7**	**14.9**	**0.8**	**7**	**0.3**
SD	**Siscia**	±0.3	±0.4	±0.5	±0.1	±0.9	±0.1	±0.3	±0.1
BDX25418		**2.7**	**17.7**	**58.3**	**2.8**	**9.7**	**0.9**	**7.4**	**0.1**
SD	**Siscia**	±0.1	±0.1	±0.7	±0.1	±0.4	±0.1	±0.4	±0.1
BDX25419		**2.5**	**17.4**	**60.8**	**2.9**	**7.8**	**0.9**	**7.3**	**0.1**
SD	**Siscia**	±0.3	±0.1	±0.3	±0.1	±0.1	±0.1	±0.1	±0.1
BDX25420		**2.5**	**17.5**	**58.8**	**2.9**	**9.6**	**0.9**	**7.5**	**0.1**
SD	**Siscia**	±0.3	±0.1	±0.8	±0.1	±0.6	±0.1	±0.2	±0.1
BDX25421		**1.2**	**17.5**	**61.4**	**2.6**	**8.4**	**0.9**	**7.5**	**0.1**
SD	**Siscia**	±0.1	±0.3	±0.4	±0.1	±0.4	±0.1	±0.1	±0.1
BDX25422		**2.3**	**15.8**	**60.1**	**2.6**	**11.2**	**0.9**	**6.9**	**0.1**
SD	**Siscia**	±0.2	±0.1	±0.1	±0.1	±0.1	±0.1	±0.1	±0.1
BDX25423		**2.2**	**15.7**	**60.4**	**2.4**	**10.1**	**1**	**7.7**	**0.1**
SD	**Siscia**	±0.6	±0.4	±0.4	±0.1	±0.2	±0.1	±0.6	±0.1
BDX25424		**1.9**	**15.4**	**61.6**	**2.7**	**11.2**	**0.8**	**6.3**	**0.1**
SD	**Siscia**	±0.2	±0.1	±0.3	±0.1	±0.3	±0.1	±0.1	±0.1
BDX25425		**3.3**	**15.9**	**61**	**2.3**	**9.2**	**0.9**	**7**	**0.1**
SD	**Siscia**	±0.9	±0.6	±0.9	±0.1	±0.2	±0.1	±0.1	±0.1
BDX25426		**2.2**	**15.6**	**62.6**	**2.6**	**10.1**	**0.8**	**5.9**	**0.1**
SD	**Siscia**	±0.1	±0.1	±0.2	±0.1	±0.1	±0.1	±0.1	±0.1

BDX25427		**2.1**	**16.3**	**61.6**	**2.7**	**10**	**0.8**	**6.3**	**0.1**
SD	**Siscia**	±0.1	±0.1	±0.5	±0.1	±0.4	±0.1	±0.2	±0.1
BDX25428		**4.1**	**16.2**	**58.8**	**2.4**	**10.6**	**0.7**	**6.7**	**0.1**
SD	**Siscia**	±0.7	±0.2	±0.9	±0.1	±0.9	±0.1	±0.1	±0.1
BDX25429		**2.5**	**16.9**	**60.4**	**2.6**	**10**	**0.9**	**6.3**	**0.1**
SD	**Siscia**	±0.6	±0.3	±0.8	±0.1	±0.2	±0.1	±0.2	±0.1
BDX25431		**3.3**	**18.3**	**54.7**	**2.7**	**13.3**	**0.7**	**6.7**	**0.1**
SD	**Siscia**	±0.1	±0.1	±0.8	±0.1	±0.3	±0.1	±0.4	±0.1
BDX25432		**1.9**	**17**	**58.9**	**2.2**	**11.9**	**0.8**	**6.9**	**0.1**
SD	**Siscia**	±0.6	±0.6	±1.2	±0.1	±1.0	±0.1	±0.2	±0.1
BDX25433		**2.3**	**18.8**	**65.3**	**1.6**	**4.4**	**0.9**	**6.5**	**0.1**
SD	**Siscia**	±0.1	±0.2	±0.5	±0.1	±0.1	±0.1	±0.1	±0.1
BDX25434		**2.1**	**16**	**64.1**	**2.6**	**6.5**	**0.8**	**7.5**	**0.1**
SD	**Siscia**	±0.1	±0.4	±0.5	±0.2	±0.1	±0.1	±1.2	±0.1
BDX25435		**3.4**	**16.4**	**55**	**2.6**	**14.7**	**0.6**	**6.8**	**0.2**
SD	**Siscia**	0.2	0.3	0.2	0.1	0.5	0.1	0.1	0.1
BDX25436		**2.2**	**20.9**	**65**	**2.7**	**1.2**	**1.1**	**6.7**	**0.1**
SD	**Sirmium**	±0.5	±0.7	±0.4	±0.1	±0.1	±0.1	±0.1	±0.1
BDX25437		**2.5**	**18.9**	**63.9**	**2.6**	**1.9**	**1**	**8.9**	**0.1**
SD	**Sirmium**	±0.4	±0.3	±0.5	±0.1	±0.2	±0.1	±0.1	±0.1
BDX25438		**2.2**	**19.9**	**66.4**	**2.5**	**1.3**	**1.1**	**6.3**	**0.1**
SD	**Viminacium**	±0.5	±0.1	±0.4	±0.1	±0.1	±0.1	±0.1	±0.1
BDX25439		**3.3**	**20.3**	**62.9**	**2.5**	**1.5**	**0.9**	**8.1**	**0.1**
SD	**Viminacium**	±0.3	±0.3	±.3	±0.1	±0.1	±0.1	±0.2	±0.1
BDX25440		**2.5**	**18.2**	**59.9**	**2.3**	**9.6**	**0.9**	**6.3**	**0.1**
SD	**Viminacium**	±0.7	±0.4	±0.7	±0.1	±0.9	±0.1	±0.1	±0.1
BDX25441		**3.2**	**19.3**	**62.1**	**2.5**	**3**	**1**	**8.4**	**0.1**
SD	**Viminacium**	±0.7	±0.3	±0.8	±0.1	±0.2	±0.1	±0.1	±0.1
BDX25442		**3.8**	**18.3**	**59.1**	**3.5**	**5.9**	**0.9**	**8.1**	**0.1**
SD	**Viminacium**	±0.2	±0.4	±0.4	±0.1	±0.3	±0.1	±0.3	±0.1
BDX25443		**1.7**	**16.5**	**71.4**	**1.8**	**0.9**	**0.8**	**6.7**	**n.d**
SD	**Viminacium**	±0.2	±0.1	±0.4	±0.1	±0.1	±0.1	±0.1	
BDX25444		**1**	**20.7**	**62.5**	**2**	**5.8**	**1.1**	**6.5**	**n.d.**
SD	**Viminacium**	±0.2	±0.5	±0.8	±0.1	±0.3	±0.1	±0.2	
BDX25445		**2**	**17.6**	**69.2**	**2.2**	**1.1**	**1.1**	**6.6**	**0.1**
SD	**Viminacium**	±0.2	±0.1	±0.4	±0.1	±0.1	±0.1	±0.2	±0.1

Table 13 p-XRF data composition obtained from three measured zones per amphora sample. Trace elements are given in ppm normalized to 100% (SD – standard deviation)

Sample ID	Discovery Place	Sr	Zr	Rb	Y	Zn	Cr
BDX25412	**Teutoburgium**	**163**	**325**	**153**	**48**	**159**	**240**
SD		±9	±38	±3	±2	±14	±32
BDX25413	**Teutoburgium**	**321**	**244**	**108**	**37**	**109**	**219**
SD		±2	±23	±3	±2	±10	±23
BDX25414	**Teutoburgium**	**162**	**300**	**152**	**53**	**153**	**174**
SD		±5	±4	±5	±4	±17	±15
BDX25415	**Siscia**	**239**	**158**	**113**	**28**	**120**	**167**
SD		±2	±3	±2	±1	±5	±13
BDX25416	**Siscia**	**166**	**168**	**123**	**31**	**115**	**189**
SD		±1	±3	±1	±1	±6	±17
BDX25417	**Siscia**	**282**	**149**	**129**	**30**	**118**	**181**
SD		±8	±1	±5	±2	±6	±16
BDX25418	**Siscia**	**246**	**159**	**177**	**27**	**132**	**237**
SD		±2	±1	±3	±1	±5	±6
BDX25419	**Siscia**	**191**	**168**	**233**	**17**	**134**	**237**
SD		±4	±1	±17	±4	±4	±13
BDX25420	**Siscia**	**269**	**170**	**299**	**11**	**107**	**236**
SD		±5	±4	±3	±2	±5	±24
BDX25421	**Siscia**	**300**	**190**	**211**	**34**	**128**	**252**
SD		±5	±7	±11	±7	±15	±36
BDX25422	**Siscia**	**248**	**169**	**144**	**32**	**126**	**198**
SD		±1	±1	±1	±2	±2	±1
BDX25423	**Siscia**	**258**	**193**	**154**	**37**	**147**	**163**
SD		±16	±10	±12	±10	±18	±31
BDX25424	**Siscia**	**208**	**167**	**127**	**31**	**112**	**189**
SD		±3	±5	±2	±1	±4	±20
BDX25425	**Siscia**	**246**	**219**	**134**	**42**	**135**	**225**
SD		±9	±2	±4	±3	±15	±52
BDX25426	**Siscia**	**190**	**142**	**103**	**25**	**101**	**155**
SD		±1	±2	±2	±2	±4	±9
BDX25427	**Siscia**	**198**	**175**	**117**	**31**	**111**	**200**
SD		±4	±1	±2	±1	±3	±14
BDX25428	**Siscia**	**323**	**138**	**196**	**21**	**109**	**119**
SD		±6	±7	±9	±6	±5	±9

BDX25429	**Siscia**	**264**	**164**	**125**	**30**	**123**	**149**
SD		±4	±13	±8	±6	±19	±58
BDX25431	**Siscia**	**405**	**119**	**112**	**30**	**114**	**161**
SD		±2	±3	±5	±2	±9	±17
BDX25432	**Siscia**	**474**	**179**	**147**	**37**	**157**	**116**
SD		±18	±5	±1	±1	±8	±37
BDX25433	**Siscia**	**70**	**237**	**74**	**34**	**77**	**216**
SD		±1	±7	±1	±2	±1	±16
BDX25434	**Siscia**	**249**	**168**	**121**	**31**	**299**	**184**
SD		±11	±11	±9	±1	±35	±22
BDX25435	**Siscia**	**437**	**124**	**116**	**26**	**133**	**165**
SD		10	2	3	2	4	16
BDX25436	**Sirmium**	**155**	**264**	**153**	**45**	**159**	**148**
SD		±10	±7	±11	±4	±19	±83
BDX25437	**Sirmium**	**146**	**269**	**170**	**48**	**173**	**164**
SD		±4	±7	±10	±6	±25	±40
BDX25438	**Viminacium**	**148**	**299**	**149**	**48**	**143**	**107**
SD		±3	±16	±2	±7	±11	±57
BDX25439	**Viminacium**	**148**	**265**	**159**	**45**	**166**	**161**
SD		±7	±21	±3	±6	±8	±113
BDX25440	**Viminacium**	**184**	**245**	**135**	**41**	**136**	**150**
SD		±9	±16	±7	±2	±14	±41
BDX25441	**Viminacium**	**176**	**237**	**168**	**49**	**174**	**175**
SD		±10	±6	±3	±6	±18	±82
BDX25442	**Viminacium**	**225**	**32**	**132**	**32**	**135**	**223**
SD		±2	±2	±1	±2	±2	±23
BDX25443	**Viminacium**	**98**	**165**	**85**	**22**	**74**	**149**
SD		±2	±4	±2	±1	±2	±20
BDX25444	**Viminacium**	**198**	**271**	**157**	**40**	**101**	**178**
SD		±3	±5	±2	±5	±7	±15
BDX25445	**Viminacium**	**169**	**232**	**134**	**34**	**86**	**152**
SD		±3	±5	±2	±5	±7	±15

For exploring the similarity (or dissimilarity) of the chemical composition, the analytical data should be evaluated using a suitable statistical approach. Some constrains have to be taken into account due to the nature of the pottery compositions. The variation of a specific element concentration within a series of pottery samples can be estimated, for example, by calculating the standard deviation of the measured values. However, in the case of natural variation of the trace elements, their concentrations are expected to show a log-normal distribution.

It should be highlighted the fact that the elements concentrations in a ceramic body, the element distribution (and concentration) are linked to one another. Some elements are linked because they are associated with the same mineral components, which can vary in the original clay, or that can be affected by post-depositional alteration (Hein, 2018). Thus, a log-ratio transformed data can be used for developing the dataset with a multivariate statistical method such as principal component analysis (PCA).

For this research the statistical analysis was performed via the R software (R Core Team, 2014). More specifically, it was the Principal Component Analysis (PCA) and the Mahalanobis distance. Therefore, to identify the patterns in these results, the multivariate statistical approach was implemented in order to examine graphically the grouping patterns of the amphorae samples, from a chemical composition point of view.

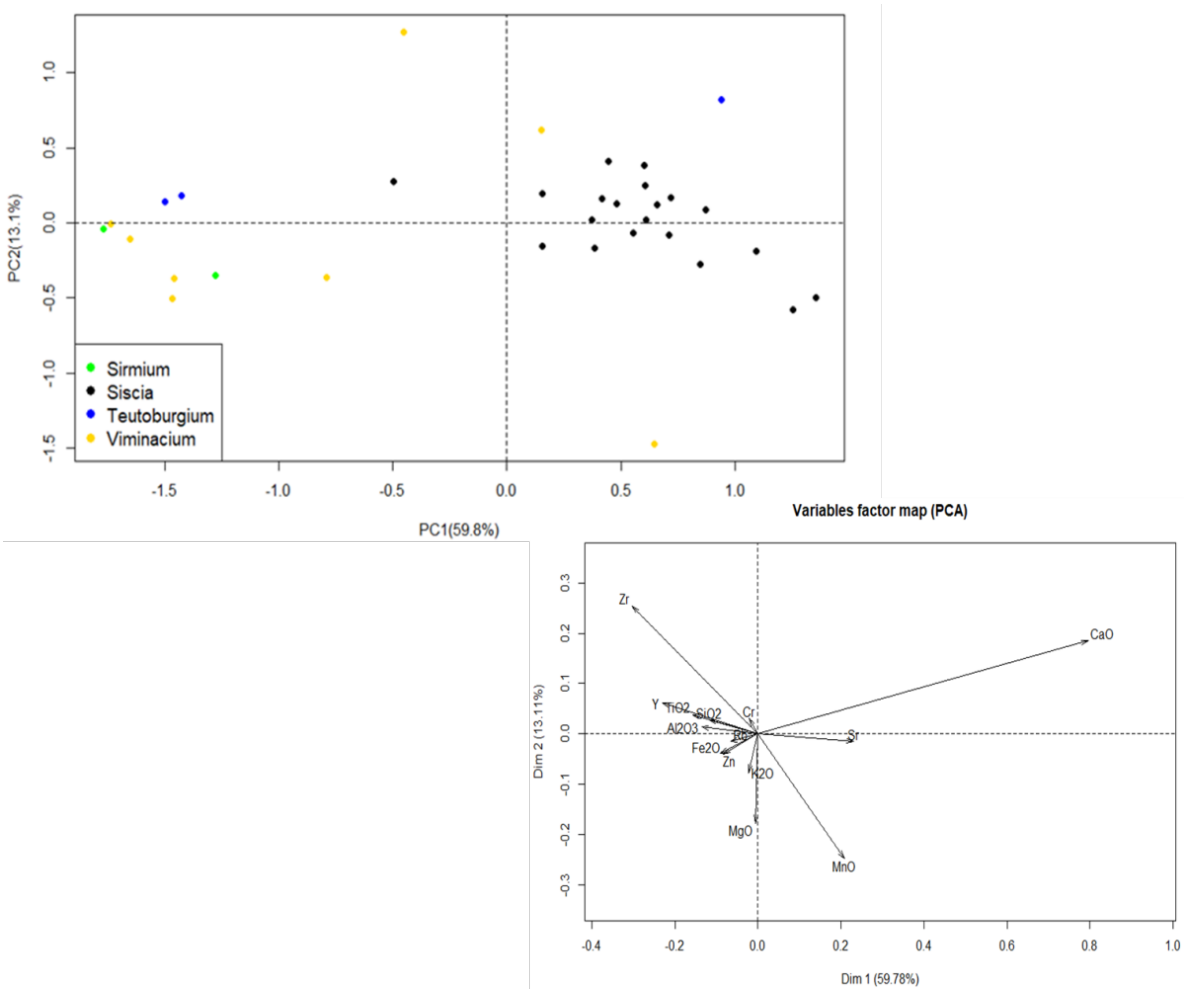

Fig. 33 Scatter-plot and multivariate diagram illustrating the obtained data measured by p-XRF, for each amphora sample

The distribution of the identified amphorae on the archaeological sites across the Danube region is illustrated in **Fig. 33**. The diagrams make it possible to highlight the elements with a very high differentiating power, such as CaO, Zr, MnO. It can be clearly observed that only the samples of Siscia can be used as an individual cluster (where the number of analyzed samples plays a big role), since the others are distributed randomly.
In addition, variations in CaO content could be related to the different natural presence of calcareous inclusions and affected by soil enrichment phenomena, and there is a probability that they also stem from the technological choices made by ancient potters (Machut et al., 2015).
In addition, in order to observe if the patterns emerge with the reference group, EDXRF data obtained from previous studies (Machut, 2013; Machut et al., 2017, 2020) from Loron and Fažana were added to the dataset.

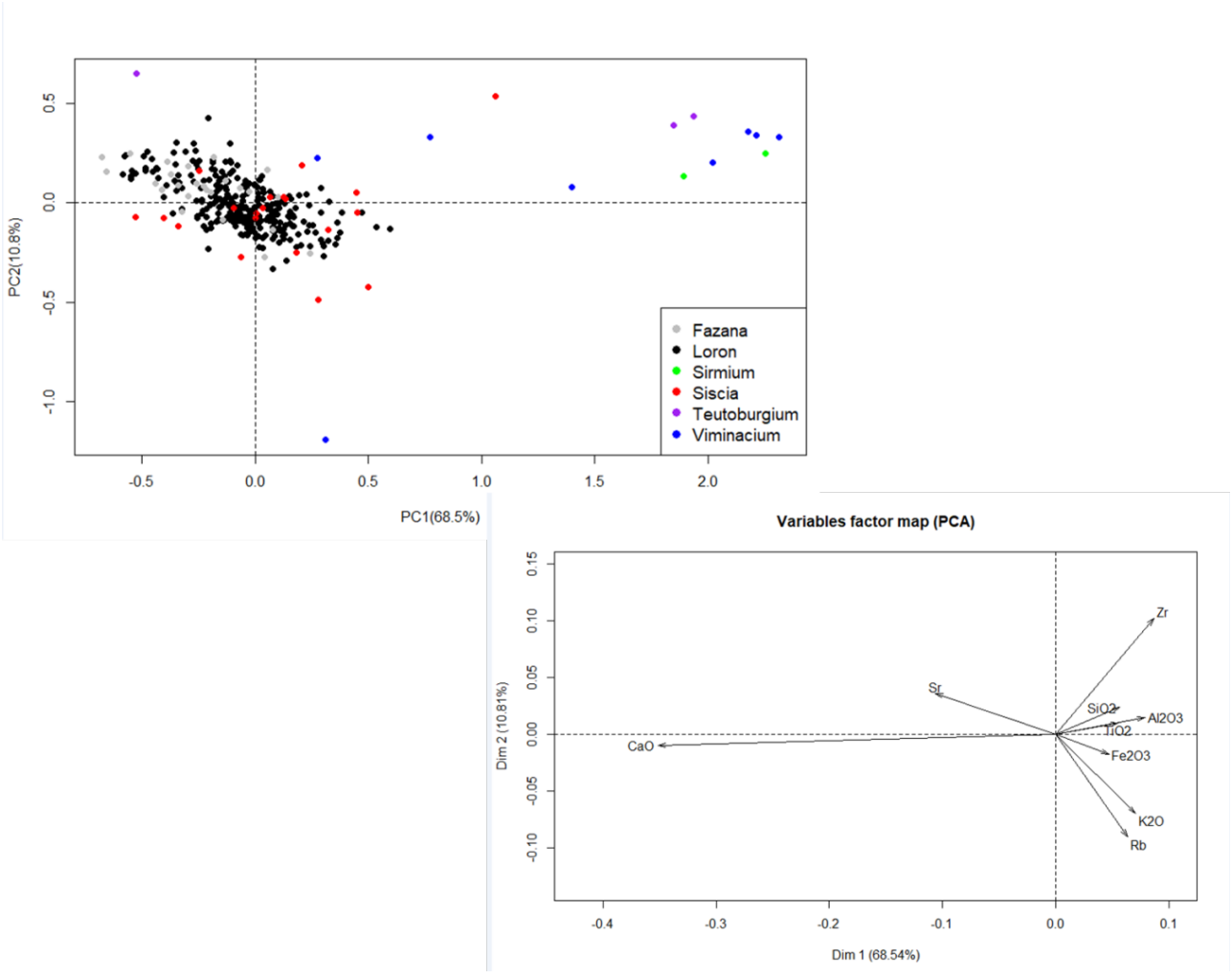

Fig. 34 Scatter-plot and multivariate diagram comparing the obtained data, from each archaeological site

It can be observed from the scatter-plot **Fig. 34** that the dataset which corresponds to the Siscia group is the only one which can be integrated with the dataset group from Loron and Fažana.

In addition, we applied an approach for considering the elements correlations in the use of the Mahalanobis distance for determining probabilities of the similarity of the compositional groups. This distance is a measure in accordance with a given sample to a group (it can only be calculated with reference to a particular group).

The squared Mahalanobis (d_i^2) distance between a case and a centroid of a group is defined as:

$$d_i^2 = (x_i - \overline{x})' S^{-1} (x_i - \overline{x})$$

(Baxter, 2001)

where S is the variance-covariance sampling matrix and $(x_i - \overline{x})$ is the vector of difference between the concentrations measured in one group and the concentrations measured in the other group.

It can be viewed as a generalization of Euclidean distance that allows for the correlation structure of a group.

The smaller d_i^2 is, the closer a case is to a group centroid. Thus calculating a Mahalanobis distance between a particular point and a given group centroid, will permit to indicate the probability that the group will include that point, or not (Bieber et al., 1976).

The search for outliers in geochemical studies is usually based on the Mahalanobis distance (MD), because the points in multivariate space being at larger distance than some predetermined values from the center of the data, are considered as outliers (Santos et al., 2013).

The first group used as a reference was the one representing the Loron corpus. The Mahalanobis distance (MD) was calculated for each sample and the samples with the distance higher than the critical value (3,70 value in our case) were excluded from the data set. In accordance with the MD, in **Table 14** all the samples were recorded as outliers, besides only one sample, BDX 25423.

Table 14 Calculated Mahalanobis distance between the archaeological reference group and each individual sample

Sample ID	Mahalanobis Distance
BDX25412	24,94
BDX25413	9,92
BDX25414	23,62
BDX25415	9,98
BDX25416	9,49
BDX25417	6,99
BDX25418	6,90
BDX25419	6,88
BDX25420	9,91
BDX25421	7,67
BDX25422	4,31
BDX25423	**2,70**
BDX25424	6,43
BDX25425	7,25
BDX25426	8,36
BDX25427	8,02
BDX25428	7,03

Sample ID	Mahalanobis Distance
BDX25429	6,99
BDX25431	13,09
BDX25432	10,06
BDX25433	20,73
BDX25434	9,43
BDX25435	12,56
BDX25436	25,74
BDX25437	18,04
BDX25438	26,06
BDX25439	22,25
BDX25440	15,39
BDX25441	15,44
BDX25442	32,09
BDX25443	20,78
BDX25444	20,98
BDX25445	19,81

The same approach was made using the Fažana corpus. However, in this case, all the samples were observed as outliers.

IV.6 Concluding remarks

The case study chosen aimed to develop an analytical methodology for amphorae analysis using a portable XRF. Beyond the methodological approach, the archaeological objective was to study the export of the amphoras Dressel 6B from the initial production Center (Loron) to other sites following the Danube region.

Using the p-XRF setup, the measurements test of cleaned and soft polished with silicon carbide on amphora fragments (in order to eliminate any surface contamination) made possible to select a suitable protocol for our analysis and where three measurements allowed us to distinguish individual fragments.

Furthermore, the idea of measuring directly on gently polished fractures of amphorae was to show the accuracy of the results without preparation needed of the ceramic bodies and to observe the efficacy of the portable XRF in when taken directly on field by the archaeologist.
In our case, since the amphorae samples differed in size (weight and height), so we were obliged to use the collimator for some of them.
The used protocol was one measurement per area, making an average of three zones, with 60 seconds measurement time per beam, making in total 6 minutes of analysis per sample.
The **Table 8** indicated the precision of the pXRF measurements of particular element concentrations in four individual samples (BDX 16854, BDX 17729, BDX 20163 and SARM69), which were analyzed in at least three different spots. Measurements of the elements such as: Mg, Al, Si, K, Ti, Fe and Mn appear to provide sufficient precision for distinguishing different samples. In other cases, such as: Ca, Cr, Sr, Zn the precision could be affected by high concentrations of a particular element determined in specific spots, that can be related to the presence of inclusions (Hein et al., 2021).
The statistical approach made possible to answer to the question regarding the provenance of the amphora bodies. Only one sample (BDX 25423) out of thirty-three, could correspond to the Loron production. However, it should be taken into account that in order to obtain a better visualization of the groups, more amphora samples are needed.
Altogether, the present case study shows that p-XRF can be a powerful tool for preliminary analytical approach in the case of amphorae samplings and can provide an initial classification based on elemental composition, helping to refine and prioritize the sample selection.
Nevertheless, it should be underlined the fact that in order to have a better view of the data and to link better all these information, additional analysis and measurements should be taken into account such as petrography, XRD and SEM-EDX.

CHAPTER V

THE ACTION OF SALT IN THE MANUFACTURING PROCESS IN HEBRON'S CERAMIC

Foreword

In general, ceramic analyzes usually aim to reconstruct the production processes from the selection of raw materials to the firing of the vessel (Cantin and Mayor, 2018). As noticed sometimes the ceramic analyzes are not necessarily informative about the origin of the raw material, as clayey can go through different treatments, as well for the firing process and conditions from the finished products (Arnold et al., 1991; Livingstone Smith, 2001). This last case study will put into evidence the fact that the comparison between the data obtained from observing the modern pottery practices (and the data from laboratory analysis) will permit to better understand the past behavior (Cantin and Mayor, 2018). The used strategy in this chapter can be referred to by the term ethno-archaeometry, a term first proposed in the early 1990's (Gosselain, 1992), but increasingly used since the beginning of the 21st century (Buxeda i Garrigós et al., 2003; Cau Ontiveros et al., 2015). Thus combining two approaches ethnoarchaeology and archaeometry will permit to understand better the complexity of the ceramic body and to help in the interpretation of compositions, identified in the laboratory.

V.1 Introduction

The productions of ceramics have experienced a wide evolution during time. The potters improved in a way their techniques of fabrication of the vessels, and in another way from an esthetic/artistic approach. One of the most interesting thematic is the way potters chose in whitening their pottery by using/adding either table salt, either sea water. The use of salt to obtain white pottery, in the form of salted clay (salted water or added salt), is noted in Mesopotamia and can still currently be found in a diversity of countries, from Central America to the Indian subcontinent (Rye, 1976; von der Crone and Maggetti, 1998).

The goal of this particular research is to examine the effect of NaCl on ceramic colours and also the effect of salt in clays (a flocculant or deflocculant?). The addition of salt to pottery is a custom that has been noted in several pottery communities, where the use of salt is specifically meant to whiten the pottery.

To carry out these investigations and to further characterize the physicochemical properties induced by the presence of salt, raw clay materials and pot sherds from modern Hebron production were collected. Laboratory experimental bricks were manufactured using two clay sediments: one with low CaO content (<10%) and one with higher CaO content (20-25%). Different proportions of NaCl (from none to 5%) were added to the clay pastes which were fired at different temperatures.
Mineralogy (petrography, XRD), chemistry (SEM-EDX) and colour analyses were carried out on raw clay materials, pot sherds and experimental bricks (lab-made). SEM imagery offered the possibility to monitor the evolution of the mineralogical transformations and see the pore system evolving with increasing firing temperature and salt content. In order to decide if the salt is reacting as a flocculant or deflocculant agent, tests have been made in the laboratory (IRAMAT-CRP2A). The test was made on both type of raw materials (yellow clay and red clay).

V.1.1 Role of salt in ceramics

Salt has long been used by potters in various forms because they knew the different effects produced on their ceramics, especially a whitening effect (Brooks et al., 1974). The question of the physico-chemical properties induced by the presence of salt continue to intrigue, as several scientific studies have been conducted to better understand the effect of halite in ceramic production, from an analytical point of view. For example, Rye (1976) highlighted conspicuous cubic voids in thin sections, which were interpreted as pseudomorphs of salt crystals. The effects produced during firing by the presence of sodium chloride in a Ca-rich ceramic body (obtained from a carbonate-rich clayey material) are numerous and wide-ranging (Combès and Louis, 1967; Bearat et al., 1989)
In various studies, it has been pointed out that the use of salt in addition to raw clay material prevents the hydration of the CaO grains after firing (Rye, 1976). The presence of chlorides, such NaCl, also accelerates and participates in the dissociation reaction of calcite. The resultant decarbonation of the $CaCO_3$ increases the porosity of the paste (Bearat, 1990a). Furthermore, salt can be considered as a discoloration agent in ceramic pastes produced from these carbonate-rich (Dufournier, 1982). Finally, the use of salt can also cause a partial disappearance of potassium in Ca-rich pastes during firing (Fabbri and Fiori, 1985). According to previous works, it was observed that the maximum addition of salt to the clay material was 5% (Rye, 1976). As for the firing temperature range, Fabbri and Fiori (1985) noticed that with 2% of salt addition, crystalline phases such as gehlenite and diopside start to appear at 700°C. In addition, Bearat (Bearat et al., 1989) specified that the alkalin chlorures will typically start to volatize with the addition of NaCl at temperatures of 700°C -750°C.
In this study, a multi-approach methodology is used to better understand the effects of salt in terms of whitening and physico-chemical changes in the ceramic body. Furthermore,

elaborated experimental bricks were manufactured by varying the salt content and the firing temperatures, with the same raw materials as those used by the Hebron potters for their production (Teodorescu et al., 2022).

V.1.2 The effect of salt in clays: a flocculant or a deflocculant agent?

Another problematic considered was the behavior of salt in contact with the moistened clay.
In the case of the clays that are suspended in water, the alkalies tend to hold the clay in suspension, obtaining a dispersive mass state, called the state of deflocculation. However, the salts and the acids tend to coagulate and to dispatch the material, leaving a clear liquid, above the precipitated matter (Bleininger, 1915).
Usually the flocculation process involves three main steps: destabilization of the suspended fine particles, the floc formation and growth (developments of the aggregates by particle – particle collision) and the floc degradation (the mechanical breakage of the aggregates) (Hogg, 2000). Furthermore, the clay dispersion is influenced by the attractive and repulsive forces in the electrical double layer at the surface of charged colloids.
The equilibrium between these forces is determinate by different parameters such as the exchange between cations and ions strength of the soil solution (Chorom and Rengasamy, 1995).
In addition, the clays come in the form of particles of less than 2 μm, which it serves as "glue" for larger elements. Thus, clays form the mineral colloidal fraction of the soil and give the soil its physico-chemical properties.
Depending on the desired porosity of the pots, since clay materials have a tendency to a flocculating effect, it can often produce a high porous paste, which can easily result in an unwanted cracking of the ceramic during drying and firing. In order to solve this problem, the potters have been trying to access to a deflocculation effect, where it enables to make clay paste with low water content, thus lowering the shrinkage problem as well.
Montana (Montana, 2016) presented that in order to overcome the problem of flocculation, potters from Sicilia added salt to freshwater during the preparation of the clay paste (or using seawater) in order to avoid the flocculation of the calcium-rich clay present in that area.
The clay is mainly composed by a heterogeneous collection of coarse and fine mineral particles, varying in gravity, size and shape. By adding alkaline compounds, the amount of water required is highly decreased as well as the effect of the drying shrinkage (Bleininger, 1915). In 1982, Worrall (Worrall, 1982) explained in details the process, remaining until today a main reference. He highlighted the fact that the "balancing cations" are associated with negatively-charged particles of Ca^{2+}, Mg^{2+}, Na^{+} and K^{+} ions, but in the same time these ions are exchanged rapidly by others. Also, for natural clay, the main exchangeable ion is Ca^{2+}, where in the beginning the suspension of this clay is flocculated. In order to deflocculate, it must be added NaCl (or KCl), which contains these cations. Therefore, the

choice of deflocculant for a good dispersion depends of the type of the exchangeable cations (Worrall, 1982).

Main aims and questions

Thus, "salted potteries" of Hebron study have two important aims. A first aim is to characterize the physical-chemical properties induced by the presence of salt in the ceramic and to understand the consequences of the addition of the salt on the ceramic properties: the colour (effect), the porosity and the chemical composition, and in the microtexture of the material. For that, it was necessary to analyze the composition of the used raw materials (such as the granulometry, the mineralogical composition and the chemical elements). A second aim is to highlight the relationship between the raw clay compositions, firing temperature, porosity, colorimetry, through the analysis of results obtained using techniques for characterization of materials. Knowing this links between them, it will help understanding better the physico-chemical changes inside the clay ceramic and it may bring new point of view in the archaeometry field.
The methodological protocol involved a multitude of analytical techniques to ensure a complementarity to provide the right answer.

V.2 Materials

V.2.1 Ethnographic context: Hebron's potters workshops

An ethnographic survey was recently conducted in Hebron (Palestinian territories) by Valentine Roux (French Director of Research at the CNRS, member of the Prehistory and Technology Laboratory UMR 7055). She observed and described the potters traditions using salt as an adjuvant in the making process. Hebron potters explain the addition of salt in the clay paste for a whitening effect. She described the Hebron's ceramic tradition meaning the manufacturing process shared by the potters, the variety between the workshops and the finished products. In addition, V. Roux observed the same effect of whitening of water jars in the Jodhpur region (India). The potters from India are using directly salted clay, adding sawdust and crushed granite or gravel. In the end, they will obtain a white jar with high porosity. Apparently, the secret of the potters to obtain a jar that keeps water fresh is to prepare a paste, which is porous and permeable, so that the water will percolate through the clay walls (Roux, 2015).
In her study, she found that potters used four raw materials for producing utilitarian vessels: yellow clay sediment (noted as YC), red clay sediment (terra rossa) (noted as RC), sand and salt (**Fig. 35**). The volumic proportion used in the preparation between yellow clay and red

clay is 2/3 part for 1/3. The sand is 1/6 of the total volume. The potters believe that the addition of the red clay, gives more plasticity to the mixture in order to prevent the clay from shrinking too fast while drying and to avoid the accidents during the firing process. The clay material and sand are brought by truck. The cost of the clay material is limited to the cost of the transportation, the clay material coming from construction sites and given for free. The yellow clay is brought from construction sites located in the region of Hebron.
There are two types of yellow clay: high quality yellow clay under the form of solid blocks and low quality yellow clay containing impurities. The purer the yellow clay is, the more expensive. The red clay is brought from the neighboring lands (the type of agricultural soil). It comes also by truck from construction sites. The sand is extracted from local mountains. Adding sand is said to be necessary for the vessels not to crack during the firing process. In addition, the potters are using tires as fuel for the firing process.

Fig. 35 Raw materials: yellow and red clay sediments and sand (left image); wedging the clay with a pug mill (right image). At this stage the salt is added to the clay material (photographs by V. Roux)

The salt it is taken from the shops. The use of salt is said to date since the seventies. The potters from Hebron explained that the use of salt will enable them to get homogeneous white potteries. This is a "story" transmitted within families knowing however that in the forties salt was already used as observed on pots from Tel el-Sultan camp dated from 1948. Since then the Hebron potters would put salt in their clay and their potteries are white.
In the case where we studied, sand and salt are mixed with the clay. It's been said by potters that 0,5% of salt is added. For each batch of clay, the potters add, while the clay is on the

press, a small handful of salt. Salt is added for the pots to be white and for the clay to "better behave". This is also at stage when more sand can be added, but it only happens if the sand has been added in insufficient quantity in the mixing tank. The potters become aware of it at the firing stage, when too many jars have crack problems. In this case, the sand is sieved with a 1 mm mesh and added to the clay when put on the press for wedging. The potter adds one big handful of sand, followed by a small handful of salt (Roux, 2018).

Fig. 36 Modern potsherds collected by V. Roux, representing the "pink" sherds (image on left – BDX 22971) and "white" sherds (image on right – BDX 22969)

V.2.2 Samples preparation

In this study, the samples consist in four modern potsherds and four raw materials (which are used by the Hebron potters in their manufacture), collected in Hebron.
The modern sherds were selected by visual aspects, representing two types of ceramic bodies: a white and a pink ceramic sherd (**Fig. 36**). The raw clay materials included yellow (YC) and red (RC) clayey sediments. To these, sand was then added as a temper along with salt for achieving a whitening effect (**Table 15**).

Table 15 Description the different studied samples

Sample ID	Type	Description
BDX 22964	clay	Red clay, used by Hebron's potters
BDX 22965	clay	Yellow clay, used by Hebron's potters
BDX 22966	clay	Mixed clay (yellow clay and red clay)
BDX 22967	clay	Prepared clay ready for potters use
BDX 22968	adjuvant	Common salt, from Hebron region
BDX 22969	ceramic	White sherd nr.1
BDX 22970	ceramic	White sherd nr.2
BDX 22971	ceramic	Pink sherd nr.1
BDX 22972	ceramic	Pink sherd nr.2
BDX 22978	sediment	Red sand, used as temper by Hebron's potter

In addition, for enlarging our understanding of the whitening effect and the parameters involved in the mechanism of the firing process, eighteen experimental samples were prepared, using the same clays used by Hebron's potters (**Table 16**). These samples were placed on an aluminium container and allowed to air-dry at room temperature for 48 hours. Each of them was composed of 20 g of clay sediment (previously desegregated), to which salt was added in different proportions: 0%, 2% and 5% of total clay by weight. Due to the absorption effect, the red sediment was mixed with 10 ml of water, and the yellow sediment, with 15 ml.

To facilitate observations in multiple of firing conditions, the experimental samples were fired in an electric kiln (the electric kiln being easier to run and more accessible in the laboratory) at 750°C, 900°C and 1000°C (according to previous works, see V.1.1 Role of salt in ceramics), in an oxidizing atmosphere. The temperature was ramped up to a heating rate of 100°C/h, with a soaking time of three hours and cooling at room temperature (**Fig. 41**).

Table 16 Procedure for the preparation of the 18 experimental bricks

Salt NaCl	Clay type	Firing Temperature (°C)	Sample ID Name
0 %	YC	750	YC 0% 750°C
		900	YC 0% 900°C
		1000	YC 0% 1000 °C
	RC	750	RC 0% 750°C
		900	RC 0% 900°C
		1000	RC 0% 1000 °C
2 %	YC	750	YC 2% 750°C
		900	YC 2% 900°C
		1000	YC 2% 1000 °C
	RC	750	RC 2% 750°C
		900	RC 2% 900°C
		1000	RC 2% 1000 °C
5 %	YC	750	YC 5% 750°C
		900	YC 5% 900°C
		1000	YC 5% 1000 °C
	RC	750	RC 5% 750°C
		900	RC 5% 900°C
		1000	RC 5% 1000 °C

V.3 Methodological strategy

The methodological protocol encompasses a multitude of analytical techniques (petrography, cathodoluminescence, SEM-EDX, XRD, colorimetry) to ensure representativeness and complementarity of observations (**Fig. 37**).

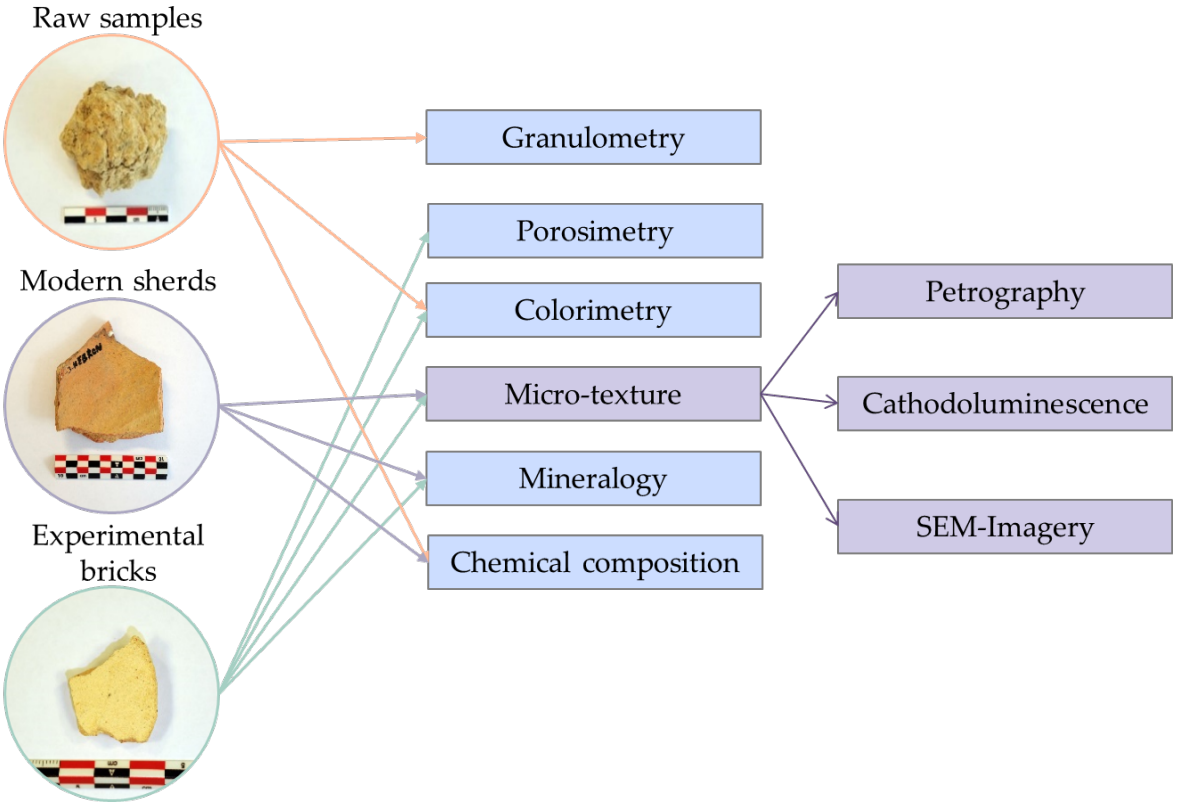

Fig. 37 Chart of the analytical strategy employed for the study of raw materials, modern ceramics and experimental bricks

Before analyzing the potsherds and the experimental bricks, the **grain size** distribution of the raw materials was first measured using a Laser Diffraction particle size analyser (Horiba LA-950) device in order to characterize their properties and evaluate clay plasticity. The raw material-samples were treated with oxygenated water and sodium hexametaphosphate. They were diluted before pipetting to 300 ml, and placed in the grain size sampler.

The **colour of the ceramic bodies** was studied and monitored using a Konica Minolta CM-2600D portable spectrophotometer (360-740 nm) with a spectral resolution of 10 nm and a diameter analytical area of 10 mm. The standard illuminator was D65 using CIE 1964 10°

standard observer. The calibration was performed with a black and white reference set to SCI (spectral reflection included) mode.

Cathodoluminescence (CL) was then utilized to provide data on the shape and size of inclusions, grain size/distribution and pore spaces in polished section of the fired samples.

The XRD measurements were made on powder samples to identify the mineral constituents of both raw materials and fired briquettes and for the orientation of deposits to discriminate the clay mineral species. In addition, a Rietveld refinement was applied by using TOPAS software, to quantify the mineral phases. For analyzing clay minerals on oriented slides, it was first necessary to eliminate the carbonates without attacking the clay phases. For this, a weak acid solution with a buffer at pH 5 was used. The oriented slides were then submitted to ethylene glycol and heat treatments (at 350°C and 550°C) according to Bouchet et al. (2000).

SEM imagery (JEOL - IT500 HR) facilitated the observations of the micro-texture of the modern potsherds and briquettes in thick sections, as well as the progress of the mineral transformations upon firing. The acquisition of the spectra (**SEM-EDX**) was done on thick polished sections of the ceramic bodies and on pressed pellets obtained from the powder of the samples. All results were expressed in wt% oxides (normalized to 100%), making possible to quantify the major and minor elements (Na_2O, MgO, Al_2O_3, SiO_2, SO_3, K_2O, CaO, TiO_2 and Fe_2O_3), while Cl was expressed in simple wt%.

V.4 Results and discussion – raw materials

V.4.1 Colorimetry on raw materials

The colour of the materials was determined by visual observation using the Munsell Soil Colour chart code. The two clays used by the potters show clearly distinct colours. The name used for describing the colours in the Munsell code is different from the one used by the potters. The red clay is classified as "brown" (7.5 YR 4/4) and the yellow clay as "pale brown" (2.5Y 8/3). The mixture of the two clay sediments appears as "light yellow brown" (10YR 6/4).

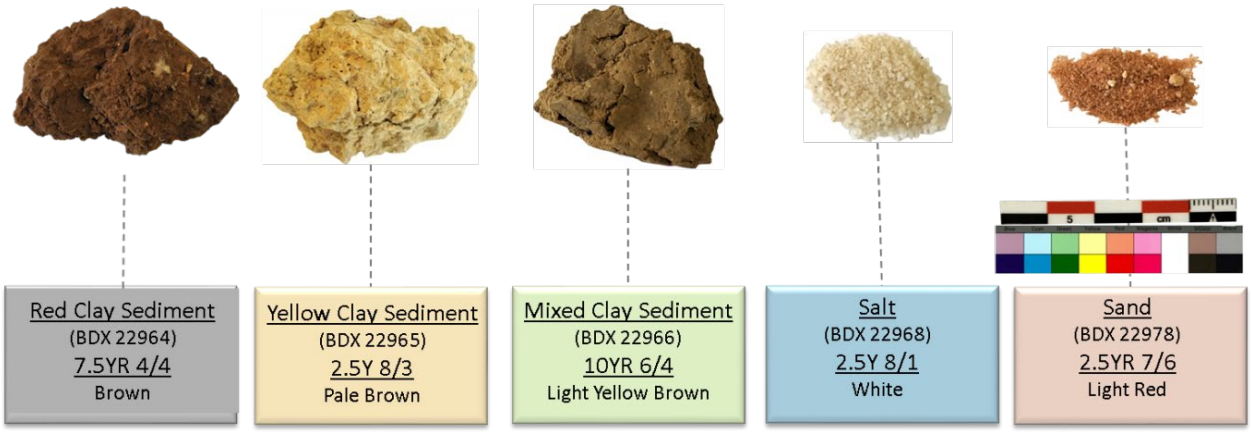

Fig. 38 Raw materials used by the potters for the production of Palestinian vessels

Furthermore, the sand used as a degreasing agent has a "red" hue, being in concordance with the Munsell code terminology as "light red" (2.5YR 7/6) **(Fig. 38**).

V.4.2 Mineralogical and chemical characterisation of raw materials

Initial measurements regarding grain size in the raw materials were obtained using laser-particle size analyser. The yellow clay sediment has a higher concentration of particles smaller than 7 µm compared to the red clay sediment (**Table 17**). Furthermore, approximately 26% of the particles in the red clay sediment are larger than 16 µm and are distributed between coarse silt (17%) and fine sand (9%). In contrast, the yellow clay sediment is mainly composed of particles smaller than 16 µm, ranging from fine silt (37%) to clay particles (58%). The sand used as temper consists of 75% fine sand and 16% coarse sand. Regarding the salt, it contains approximately 79% coarse particles, with sizes between 16 and 500 µm.

Table 17 Grain size distribution of raw materials of Hebron

Sample	% coarse sand (2000-500 µm)	% fine sand (500-63 µm)	% coarse silt (63-16 µm)	% fine silt (16-7 µm)	Clay (<7 µm)
Red Clay Sediment (RC)	0	9	17	27	46
Yellow Clay Sediment (YC)	0	1	4	37	58
Salt	0	41	28	21	11
Sand temper	16	75	2	3	4

X-ray diffraction analysis showed that the two clay sediments used by the Hebron potters have a similar mineralogical composition, mainly composed of clay minerals, calcite, quartz, iron oxides (for RC) and iron hydroxides (for YC), potassium feldspars and plagioclases. However, YC is richer in potassium feldspar and calcite. Finally, the analysis of the oriented slides allows the precise identification of the clay minerals detected during the powder analysis. The yellow clay sediment consists of a large proportion of kaolinite, a smaller proportion of a mineral inter-stratified around 11.3 Å (Illite/Vermiculite), illite and a small proportion of chlorite. The RC sediment has a similar clay mineral composition but the proportions differ. The proportion of kaolinite is lower in this sediment and the ratio of the others minerals (I/V, Ch, I) are therefore higher, giving this raw clay material more plasticity.
The chemical analysis by SEM-EDX indicates that the both clayey sediments are rich in calcium (**Table** 18), the yellow sediment being more calcium-rich with 23% CaO. The potassium content is also higher (3.5% K_2O), which may be related to the presence of the orthoclases detected by X-Ray diffraction. Iron and magnesium contents are relatively similar between the two clayey sediments. Therefore, the colour difference between the two clays it is not related to differences in iron content, but rather to its crystallographic form: hematite for the red clay sediment and goethite for the yellow clay sediment according to XRD results. The salt has a high Cl and Na_2O content, which is specific for halite. The sand used consists mainly of silica (95%). It contains clay minerals, detected by XRD, as impurities.

Table 18 Chemical composition (wt%) obtained by SEM-EDX on powder pellets for raw materials (SD – standard deviation, ld –limit of detection)

		Na_2O	**MgO**	**Al_2O_3**	**SiO_2**	**SO_3**	**Cl**	**K_2O**	**CaO**	**TiO_2**	**Fe_2O_3**
Raw Materials	Sand	0.1	0.2	1.9	95	0.2	<dl	<dl	1.2	0.5	0.9
	SD	0.1	0.1	0.1	0.3	0.1			0.1	0.1	0.1
	Salt	46.2	0.1	0.2	0.7	1.8	49.2	0.2	1.6	<ld	0.2
	SD	0.1	0.1	0.1	0.1	0.2	0.1	0.1	0.1		0.1
	YC	0.2	2.3	18.7	42.6	0.2	<ld	3.5	23.3	0.8	8.3
	SD	0.1	0.1	0.3	0.7	0.1		0.1	0.5	0.1	0.7
	RC	0.4	2.2	18.5	57.3	0.1	<ld	1.5	8.9	1.4	9.8
	SD	0.1	0.1	0.1	0.1	0.1		0.1	0.2	0.1	0.1

V.4.3 Salt: a flocculant or deflocculant agent?

In order to decide if the salt is reacting as a flocculant or deflocculant agent; tests have been made on both yellow clay and red clay, where 10 g (after sieving at 2 mm) was mixed with 200 ml of distilled water and dispersed in a glass beaker. Three samples were compared: one beaker with 0% of salt, one beaker with 2% of salt and one beaker with 5% of salt, corresponding to the amounts used for our laboratory-made samples.
The results were recorded every 30 minutes in order to observe the evolution of the solution (clarity, particles deposition) (**Fig. 39**).

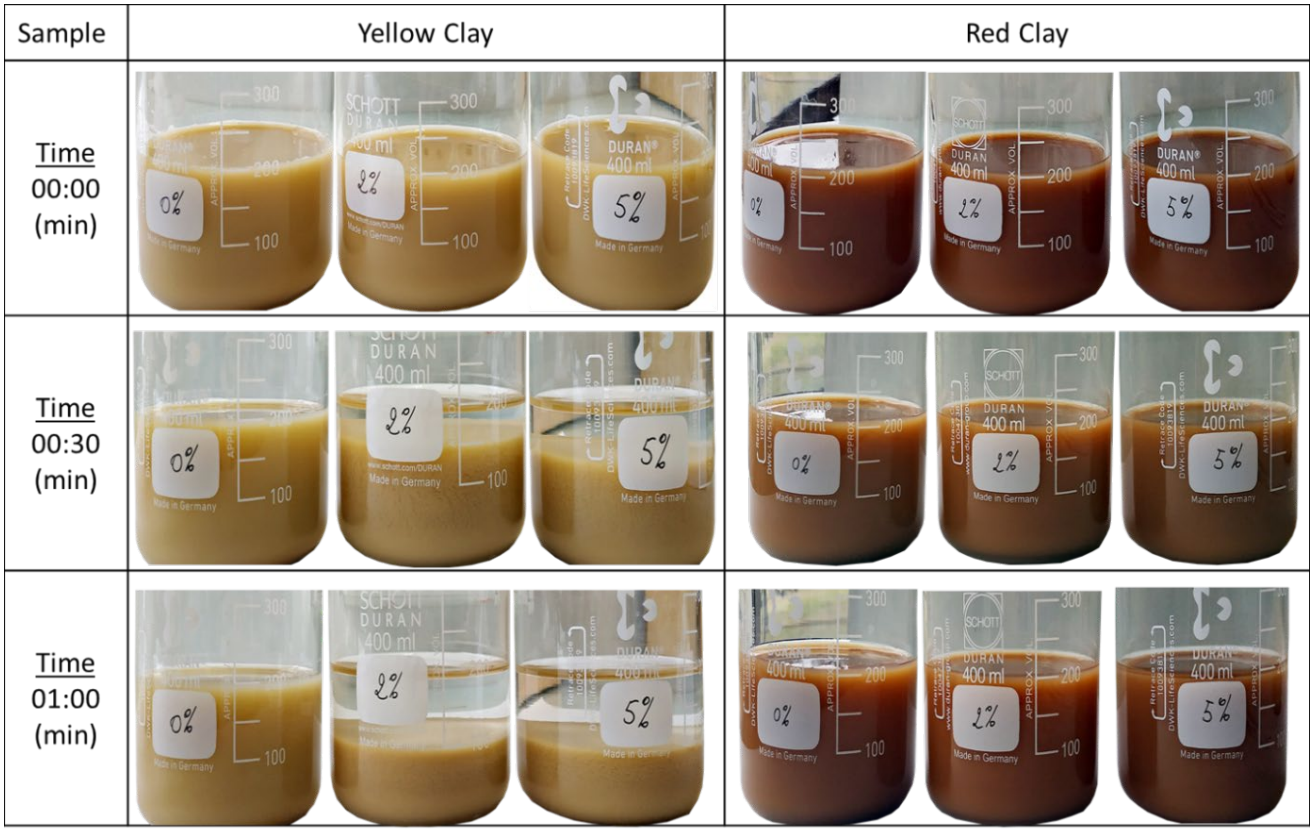

Fig. 39: Laboratory test based on reaction of salt, water and yellow/red clay sediment

The solid particles proved that they are denser than the liquid and sank to the bottom of the beaker, forming sediment. Normally, under constant condition, the rate at which the sediment is settled depends as well on their size: the larger they are, the more rapidly they sink (Worrall, 1982).

It was noticed that the reaction was different for both materials, respectively in the Ca-rich clay (yellow clay sediment) the flocculation stage was reached in a shorter time, while in the Ca-poor clay (red clay sediment) remained in a dispersive stage. It should be considered that a lot of other parameters are playing an important role in the effect of flocculation, such as: the type of clay, the size of the particles, the pH of water, etc.

V.5 Results and discussion – modern sherds

Mineralogical and chemical characterisation of modern potsherds

The initial data regarding the microstructure of the modern sherds were obtained by **petrographic analysis**. The white sherds revealed a significant proportion of inclusions (an estimated 30% by volume) and high quartz content, in which grain diameter ranges from 200 μm and 550 μm (**Fig. 40 a,b**). The presence of iron oxides was also noted, as well as a few lithic fragments (quartz-feldspar) and titanium oxides. The distribution of inclusions is quite homogeneous and rounded, belonging mainly to the fine sand class.
The matrix also presents a dark brown colour with no birefringence. On the other hand, the pink sherds feature a greater density of inclusions (40-50% by volume), among them quartz, iron oxides and biotite are the most notable (**Fig. 40 c,d**). Nonetheless, a large amount of similarities in the mineral composition between the pink sherds and white sherds can be confirmed through this petrographic analysis.
These similarities include the rounded shape of the inclusions and the presence of specific minerals such as quartz and a few feldspars. Although the samples are mineralogically quite similar, the porosity does differ. In this regard, the pink sherds feature more pronounced and abundant pores as compared to the white sherds.
On the **X-Ray patterns**, the presence of potassium feldspars, augite or clinopyroxene, gehlenite, and hematite were noticed in both samples. Nevertheless, the peak of halite has been detected only in the white sherd (**Table 19**). Furthermore, it was noticed that the presence of the amorphous phase is more developed in the white sherd than in its pink counterpart. The proportion of Ca-silicates, formed at high temperature (gehlenite, wollastonite) (Cultrone et al., 2001) is also more significant in the white sherd than in the pink one.

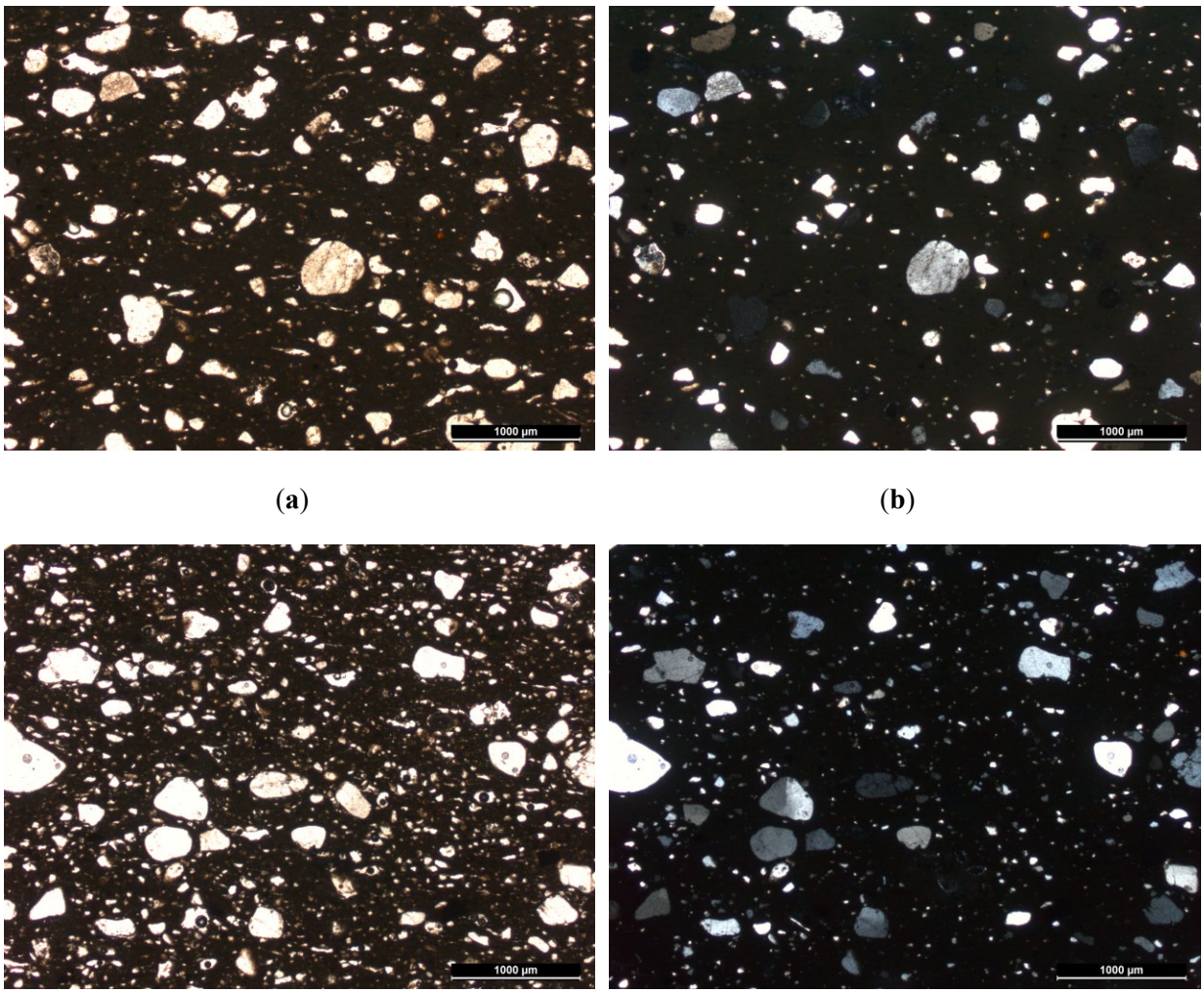

(**a**) (**b**)

(**c**) (**d**)

Fig. 40 Petrographic images: matrix of a white potsherd ((a) plane-polarized light; (b) cross-polarized light); matrix of a pink potsherd ((c) plane-polarized light; (d) cross-polarized light).

Combined, these observations suggest that the sherds were fired under the same conditions (i.e. temperatures), but are yet different due to other factors. For example, the presence of halite is detected in the white sherds and in their case Ca-silicates are also higher than in the pink sherds. In addition, a more developed glassy phase and a higher porosity was also noted. These results (**Table 19**) suggest that more salt had been added to the clay paste of the white sherds than to the pink sherds.

Table 19 Quantification of mineralogical phases of Hebron's modern sherds, using Rietveld method

		illite	quartz	K Feld	Pl Feld	calcite	halite	gehlenite	augite	wollastonite	hematite	spinel	anatase
Modern sherds	White sherd 1	<dl	23,7	0.2	14.9	<dl	0.7	18.2	31.8	9.1	<dl	1.5	1.1
	Pink sherd 1	<dl	30.7	4.3	23.1	<dl	<dl	14.3	20.4	6.1	<dl	<dl	<dl

Finally, the bulk chemical composition of the modern ceramic sherds (pink and white) (**Table 20**) revealed that they have similar chemical composition with high Ca content (20 to 22% CaO) and equivalent percentage of iron (around 6% Fe_2O_3). The two types differ regarding the presence of sodium and chlorine, which is more abundant in the white sherds than in the pink sherds.

Table 20 Chemical composition (wt%), obtained by SEM-EDX on thick sections for the modern sherds (SD – standard deviation)

		Na_2O	MgO	Al_2O_3	SiO_2	SO_3	Cl	K_2O	CaO	TiO_2	Fe_2O_3	K_2O/SiO_2
Modern sherds	White sherd 1	2.3	2.9	14.4	45.5	1.9	1.6	3.0	22.2	0.7	5.6	0.066
	SD	0.1	0.1	0.2	0.5	0.1	0.1	0.1	0.2	0.1	0.1	
	White sherd 2	2.1	2.8	13.7	47.0	1.8	1.4	2.9	21.9	0.8	5.6	0.062
	SD	0.1	0.1	0.5	1.4	0.1	0.1	0.2	0.4	0.1	0.1	
	Pink sherd 1	0.9	3.4	14.1	50.1	0.7	0.2	2.5	20.4	0.8	6.7	0.050
	SD	0.1	0.1	0.2	0.5	0.1	0.1	0.1	0.2	0.1	0.2	
	Pink sherds 2	0.8	3.4	14.0	51.2	0.8	0.2	2.5	19.8	0.9	6.4	0.049
	SD	0.1	0.1	0.4	0.9	0.1	0.1	0.1	0.2	0.1	0.3	

V.6 Results and discussion – experimental bricks

V.6.1 Colorimetry analysis

As presented previously, in order to enlarge our understanding of the whitening effect and the parameters involved in the mechanism of the firing process on Hebron ceramic, experimental samples have been fabricated in the laboratory, using the same clays used by the Palestinian potters. The test on the experimental bricks revealed colour changes that are a result of the differences in preparation protocol as described above (**Table 16**).
The discoloration effect was initiated by the addition of NaCl. Naked eye observations showed that the fired experimental bricks produced from the red clay sediments are universally red in colour and show little variability in this regard. In contrast, the bricks containing yellow clay sediments without added NaCl have a rather orange colour for all firing temperatures and become more yellow as the NaCl content increases (**Fig. 41**).

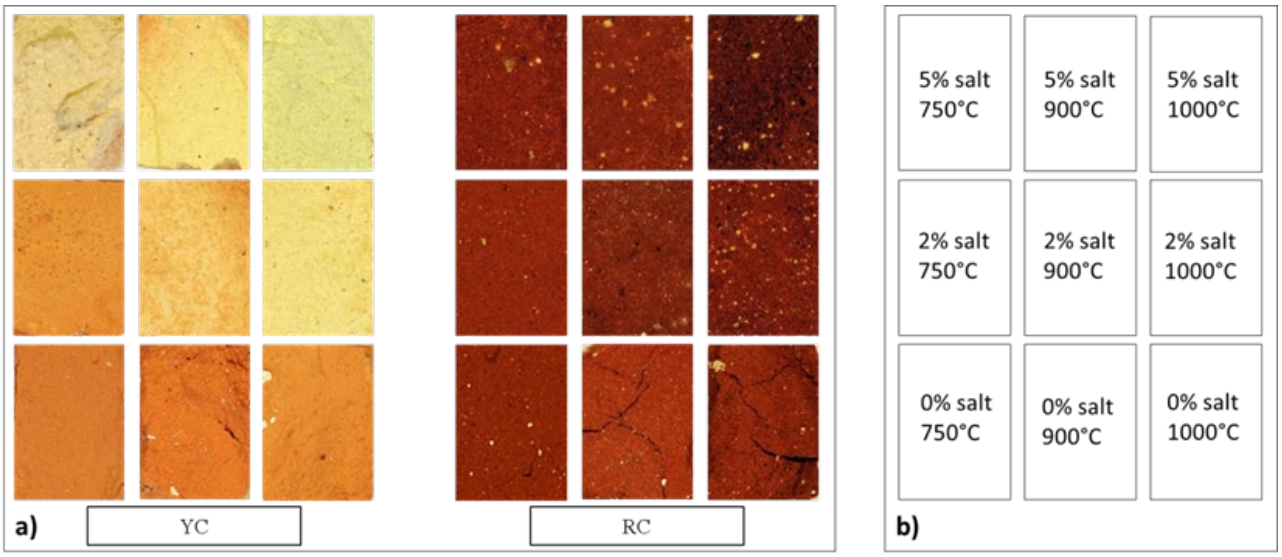

Fig. 41 a) Colour surface of experimental samples made from yellow (YC) and red clay (RC) sediments; (b) the protocol used per sample (salt content and firing temperature)

In order to describe these colour changes in an objective way, it was necessary to carry out colorimetric measurements. Yet this is only necessary for the bricks produced from yellow clay sediments. As the objective of the study is to focus on the whitening effect of salt, which does not appear to effect the coloration of the red clay sediment containing little

amount of calcium (9% CaO), colorimetric measurements for these samples are unnecessary.

When fired at the same temperature, an increase of salt content is associated with a decrease in dominant wavelength. The chromatic coordinates for the sample made with yellow clay, with no salt added and fired at 750°C, are x = 0.41 and y = 0.37 (**Table 21**).

Table 21 Chromatic coordinates of experimental samples in comparison with modern sherds, in the (Yxy) and (L*a*b*) systems, with the associated dominant wavelengths λD and Pe (excitation purity)

		λ_D (nm)	Pe (%)	Y	x	y	L*	a*	b*
Modern sherds	White sherd 1	572.7	17.6	65.5	0.346	0.362	84.7	1.3	15.6
	White sherd 2	573.1	18.3	61.3	0.348	0.362	82.5	1.7	15.8
	Pink sherd 1	577.7	25.6	36.4	0.368	0.368	66.8	6.4	17.9
	Pink sherd 2	577.1	30.2	33.5	0.377	0.376	64.6	6.5	20.8
Experimental bricks	YC 0% 750°C	586.4	38.7	25.4	0.414	0.369	57.5	18.3	22.9
	YC 2% 750°C	585.6	36.0	30.6	0.405	0.367	62.2	17.5	22.6
	YC 5% 750°C	577.0	24.1	47.7	0.364	0.367	74.6	5.9	18.5
	YC 0% 900°C	588.9	42.0	21.7	0.428	0.367	53.7	21.5	23.3
	YC 2% 900°C	581.9	28.5	37.0	0.381	0.365	67.3	11.5	19.3
	YC 5% 900°C	575.9	26.9	49.7	0.368	0.372	75.9	5.4	21.2
	YC 0% 1000°C	586.3	39.2	25.6	0.415	0.369	57.6	18.5	23.3
	YC 2% 1000°C	576.1	21.6	54.6	0.357	0.364	78.8	4.7	17.5
	YC 5% 1000°C	573.1	26.6	48.1	0.363	0.377	74.9	2.2	21.3

This colour is situated in the yellow – orange (585–590 nm) range, where the associated dominant wavelength is equal to 586.4 nm (Kelly and Judd, 1976). This colour is non-saturated with the excitation purity (Pe) of 38.7%, highlighting a relatively dark colour with a Y-clarity of 25.4. By contrast, when a yellow clay is fired at 750°C with 2% NaCl added, the chromatic coordinates are x = 0.40 and y = 0.36. This colour is situated in the orange range (585-600 nm), with the associated dominant wavelength λD = 585.6 nm.

A similar increase can be seen when even more NaCl is added. When the yellow clay sample is fired at 750°C, and 5% NaCl has been added, the λD = 577.0 nm, a value falling within the yellow range (575–580 nm). Simultaneously, a decreasing of excitation purity was noted, indicating a diminution in colour saturation.

Thus, the addition of salt results in the bleaching of the ceramics, as samples to which salt has been added tend to approach the yellow colour (losing the red component). The same observations were made for the other samples produced with yellow clays when fired at 900°C and 1000°C.

According to the **Table 21**, the values of clarity (Y as well as L*) increase universally as temperature increases with the highest values corresponding to the addition of 5% NaCl. Overall, the red component (a* positive) decreases in correlation to higher temperature as well as with the increased addition of salt. The lowest value (2.2) corresponds to the YC sample fired at 1000°C within which 5% NaCl has been added. On the other hand, the yellow component (b* positive) is variable (between 17 and 24) and does not correlate with the variation in firing temperature or the addition of salt.

In sum, these results quantify the whitening effect beyond visual descriptions corresponding with measurements reflective of increases in clarity as well as the suppression of the red component (**Fig. 42a**; **Fig. 42b**).

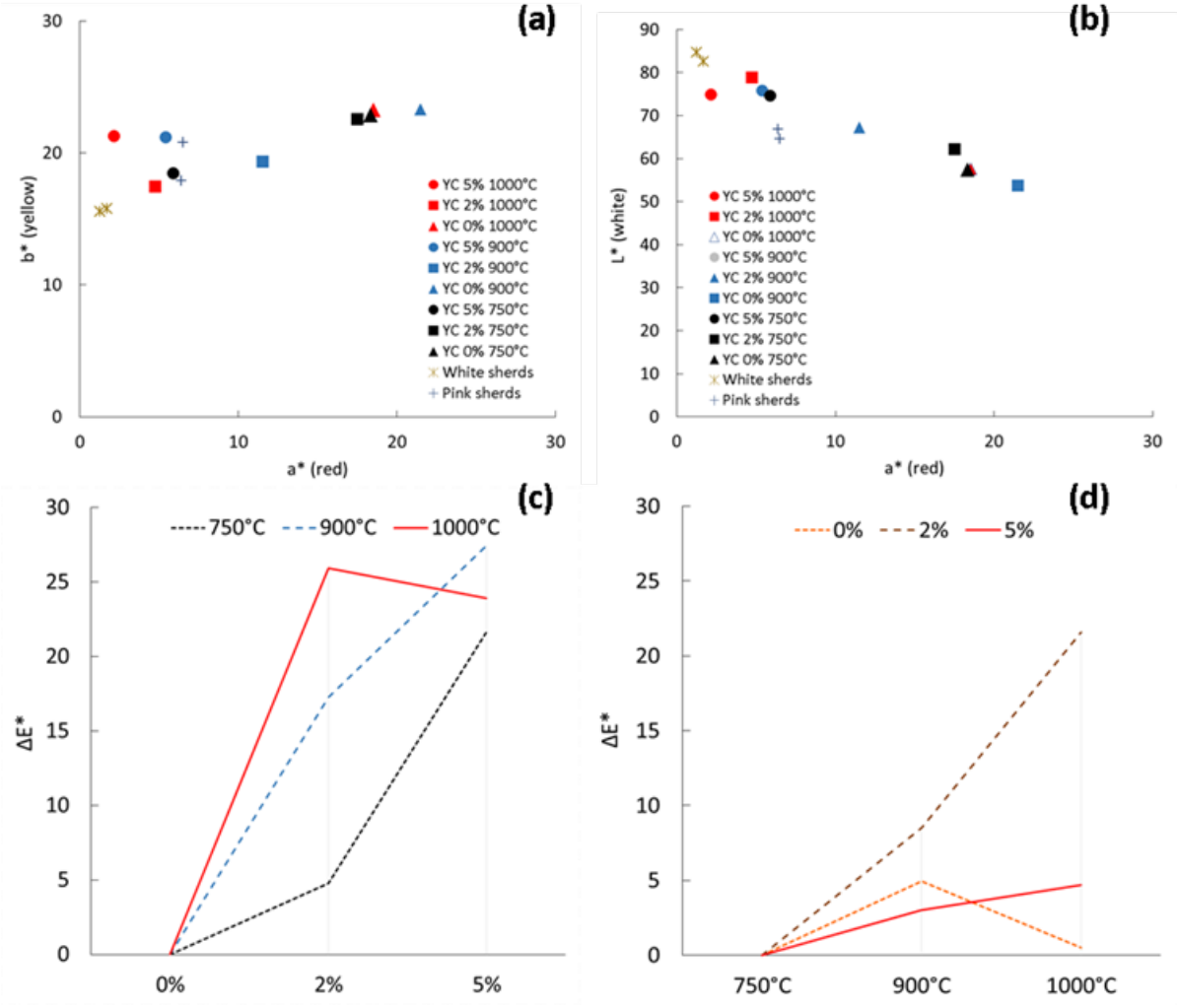

Fig. 42 Chromatic coordinates L*a*b* systems on experimental bricks

Calculating the colour deviation (ΔE*) and comparing to YC 0% samples makes it possible to observe that the colour values rise with the addition of salt, regardless of the temperature at which they have been fired at (**Fig. 42c**). However, in the case of temperature measurements, (ΔE*) when comparing to YC samples fired at 750°C, (**Fig. 42d**) by varying the salt content, no significant changes were noticed, except for 2% salt content between 900°C and 1000°C. For 0 and 5%, the colour deviation is under the value of 5 for all temperatures and therefore imperceptible to the naked eye. As such, the temperature increase appears to have little impact on the colour change.

In contrast, the colour differences are much higher when salt is added. For 5% salt content and 900°C firing temperature, the deviation can reach 27 (**Table 21**). The YC 2% 750°C

sample shows only a weak chromatic deviation imperceptible to the naked eye ($\Delta E^* < 5$). This deviation increases to 22 when salt content is increased to 5% while maintaining a 750°C firing temperature.
Given these results, it appears that the addition of salt to the clay has impacted the ceramic colour much more than the temperature at which it was fired.
As for the sherds from Hebron, it was noticed that the white sherds show a significant difference from the pink sherds, by a higher L* value and a weak red component, b* (**Table 21**).

V.6.2 Mineralogical and chemical composition of experimental bricks

V.6.2.1 Cathodoluminescence

Cathodoluminescence imaging allows for the observation of the variability in luminescence with the experimental bricks at different firing conditions and salt contents. This method highlights the mineralogical transformations.
With the bricks, cathodoluminescence imaging highlights the phase transformations that occurred during the firing process as a function of NaCl content. The calcite ($CaCO_3$) is characterized by the orange luminescence colour (Piponnier et al., 1997; Chapoulie and Daniel, 2007; Chapoulie et al., 2016). It has a high presence at 750°C, though begins to dissipate at 900°C and is totally absent at 1000°C (horizontal view in **Fig. 43**).

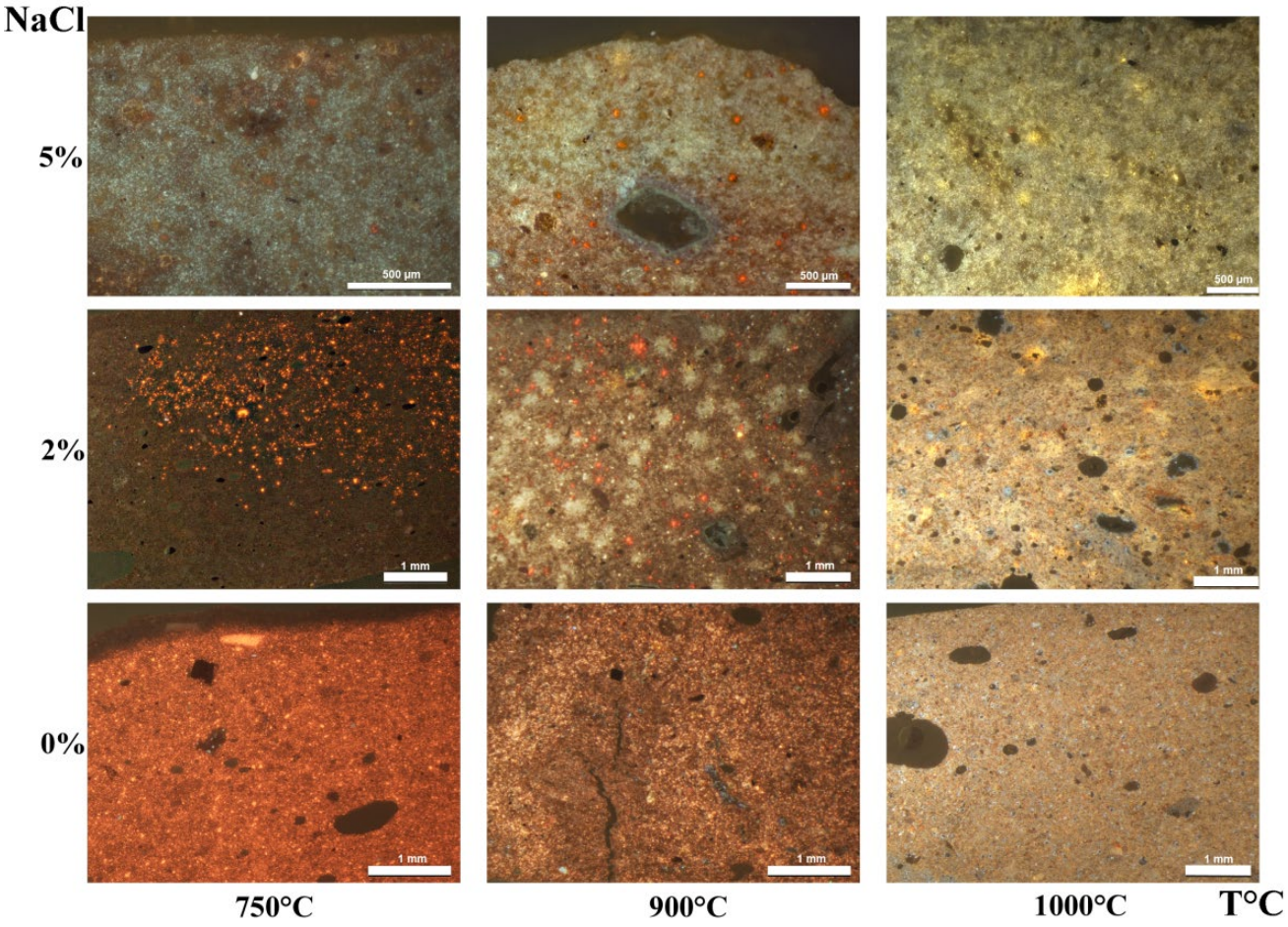

Fig. 43 Cathodoluminescence images of Ca-rich experimental bricks

Previous research has indicated that the calcite grains begin to be converted to fine grained aggregates at a temperature of 550°C. At this point, they are also diffused into the clay matrix (Riccardi et al., 1999).

The presence of calcite is visible on the YC 0 % 750°C sample. While calcite is still present in the YC 2 % 750°C sample, it is not homogeneous. This indicates that the decarbonation has yet to be completed. With 5% salt added to the sample fired 750°C the calcite has indeed totally disappeared.

Moreover, the gehlenite ($Ca_2Al_2SiO_7$) characterized by the blue luminescence colour, is detected in the samples with the highest content of NaCl (5%). This is particularly prominent on the sample with 5% salt fired at 750°C. In this sample, the microcrystals show a very intense blue colour of luminescence. The images acquired for the samples fired at 900°C, also show the decomposition of the carbonates.

The YC 0% 900°C sample presents a weak luminescence with a red-brown matrix colour, while the YC 2% 900°C sample shows some carbonate inclusions present as well as white spots in the matrix. Finally, the samples fired at high temperature (**Fig. 43** (YC 900°C and 1000°C)) show the transition from an orange matrix to a yellow one.
It should be highlighted that the blue luminescence colour can correspond to gehlenite or diopside (Götze et al., 2013).
Furthermore, in concordance with the literature, (Piponnier et al., 1997) the presence of wollastonite should also be mentioned. Wollastonite ($CaSiO_3$) is characterized by a yellow-greenish luminescent colour, and is visible only in samples that have been fired at high temperature.
The YC 5% 1000°C sample, for example, reveals a matrix with this specific colour associated to wollastonite, suggesting that new crystalline phases have been formed. This is confirmed through XRD analysis.

V.6.2.2 X-ray diffraction analysis

The diffraction analysis was made from two points of view: from a qualitative and from a quantitative phase point of view. The diffractograms allowed a schematic view of the crystalline phases, while the quantitative analysis made possible to discriminate better their presence and proportion.
The mineralogical evolution that has occurred during firing (manifested by the successive appearance and disappearance of mineralogical phases) and the salt content of the raw material could be observed through the comparison of the XRD patterns, but also by quantification using the Rietveld method (**Table 22**).

Table 22 Quantification of mineralogical phases of sherds and experimental samples from Hebron by XRD (Rietveld method)

		illite	quartz	K Feld	Pl Feld	calcite	halite	gehlenite	augite	wollastonite	hematite	spinel	anatase
Experimental bricks	YC 0% 750°C	26,6	14.5	23.0	<dl	31.3	<dl	<dl	<dl	<dl	1.9	<dl	1.6
	YC 2% 750°C	18,7	23.0	39.1	<dl	11.7	<dl	<dl	<dl	<dl	5.5	0.1	0.9
	YC 5% 750°C	<dl	5.9	8.1	12.8	<dl	<dl	19.7	38.5	12.9	0.2	1.6	0.3
	YC 0% 900°C	<dl	8.1	11.7	19.7	<dl	<dl	29.5	10.1	10.0	4.2	5.7	<dl
	YC 2% 900°C	<dl	7.3	6.9	22.4	<dl	<dl	23.7	27.4	10.4	0.4	1.1	0.3
	YC 5% 900°C	<dl	7.1	4.6	18.9	<dl	<dl	22.9	31.1	12.7	0.3	2.3	<dl
	YC 0% 1000°C	<dl	6.2	12.4	20.2	<dl	<dl	23.1	19.6	14.9	4.5	1.1	<dl
	YC 2% 1000°C	<dl	6.3	7.1	22.8	<dl	<dl	19.4	27.7	13.7	0.5	2.4	<dl
	YC 5% 1000°C	<dl	5.7	3.6	20.8	<dl	<dl	14.2	38.6	14.1	<dl	2.5	0.3

The main XRD reflections in YC 0% 750°C correspond to quartz and calcite minerals and illite. The increase in the percentage of salt (at 750°C) results in the disappearance of the Ca-carbonate phases. As a reaction of calcite within the clay, the gehlenite thus starts to form according to (Cultrone et al., 2001):

$$2KAl_2(Si_3Al)O_{10}(OH)_2 + 6CaCO_3 \rightarrow 3Ca_2Al_2SiO_7 + 6CO_2 + 2H_2O + K_2O + 3SiO_2$$
(illite) (calcite) (gehlenite)

Besides the clear evidence of the decomposition of calcite (**Fig. 44**), the reflections of illite/muscovite show a decrease as well. With the addition of salt (2% to 5%), traces of newly formed minerals start to appear such as hematite, as well as new calcium silicates: gehlenite, pyroxene such as augite and anorthite. Gehlenite and augite start to form at temperatures between 750°C to 900°C. While gehlenite formation is a result of the reaction between CaO from the carbonates and Al_2O_3 and SiO_2 from the dehydroxylated phyllosilicates (Peters and Iberg, 1978), the presence of phyllosilicates in contact with quartz and calcite allow the formation of new Ca silicates phases that can include Mg and Na (such as augite).
The decomposition of the calcite and the newly formed phases (gehlenite and augite) demonstrated by XRD analysis strengthen the interpretation of CL-images. It also confirms

the conclusion that the presence of salt accelerates and participates in the dissociation of calcite earlier in time than was previously known. Thereby, halite induces the formation of gehlenite, anorthite and augite at low temperature, increasing the reactivity between clays and Ca (Bearat et al., 1989).

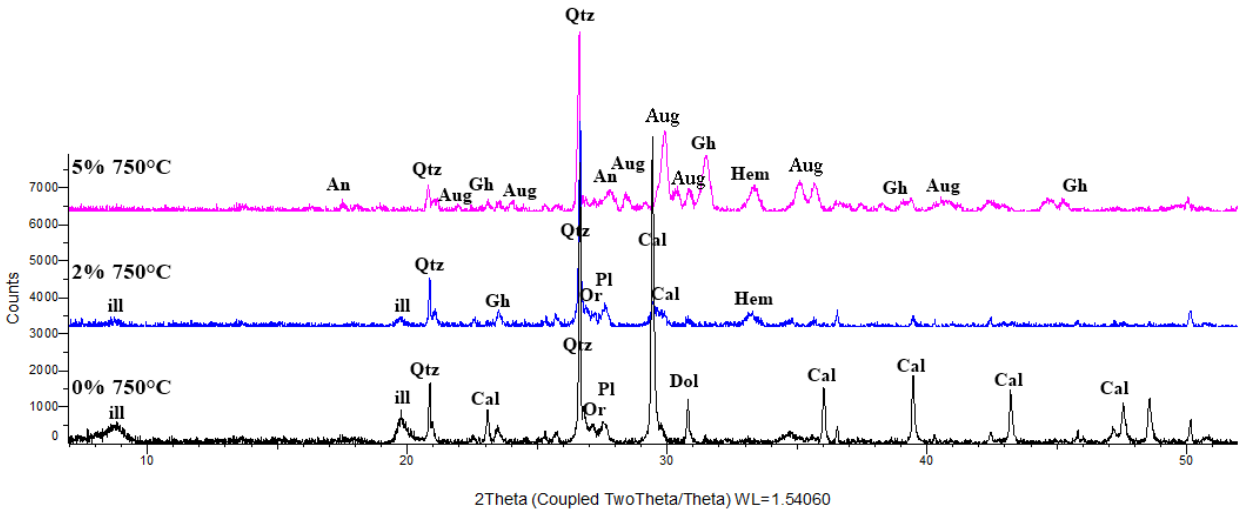

Fig. 44 Evolution of mineralogical phases at 750°C, influenced by the percentage of salt

Hematite formation in Ca-rich ceramics, on the other hand, is limited by the development of the new Ca-silicates, which incorporates Fe^{3+} in their network at temperatures around 900°C to 1000°C. This phenomenon can explain the colour saturation starting at lower temperature due to the addition of salt (De Bonis et al., 2017).

These observations also indicate that the amorphous phase was involved in the melting process, producing a Fe-saturated glass, from which nano-sized hematite crystals precipitated. Low iron diffusion within the glass and short soaking time may have favored the nucleation and inhibited the crystal growth (Nodari et al., 2007). However, in this study, the hematite appears at a lower temperature (beginning at 750°C with 2% NaCl). Gehlenite, anorthite, augite, and hematite were recorded in the pattern obtained from the Ca-rich sample, fired at 900°C (**Fig. 45**). As the quantity of salt increases, the gehlenite content begins to decrease (30% to 23%). This is in contrast with the increases of augite (10 to 31%) and wollastonite (10 to 13%). Despite the addition of salt, anorthite is quite stable, but the K-Feldspars also decrease (12 to 5%) as NaCl amounts increase (**Table 22**).

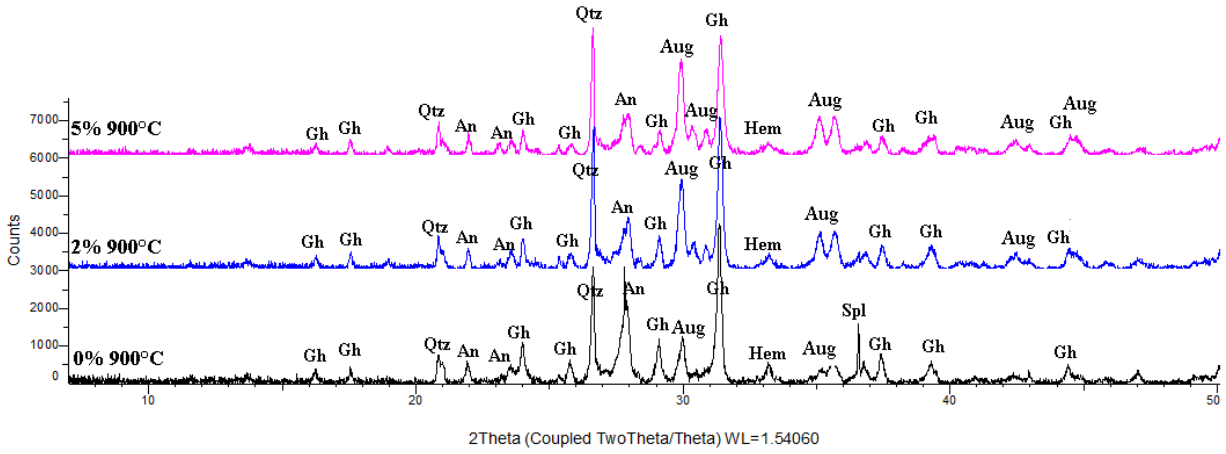

Fig. 45 Evolution of mineralogical phases at 900°C, influenced by the percentage of salt

Moreover, it is noted that if enough Ca is available, anorthite appears either due to the decomposition of the existing gehlenite with the amorphous matrix formed from clay minerals, as dehydroxylation, or only due to the reaction of the decomposed clay minerals and CaO in the rims of the grains (Holakooei et al., 2014). According to previous studies (Piponnier et al., 1997; Traoré et al., 2003; Trindade et al., 2009), wollastonite is an intermediate compound that appears at 800°C to 850°C, and begins formation when the unreacted lime attacks the grains of quartz or, like with anorthite, as a result of the decomposition of gehlenite as follows :

$CaCO_3 + SiO_2 \rightarrow CaSiO_3 + CO_2$
(calcite) (wollastonite) (Traoré et al., 2003)

$Ca_2Al_2SiO_7 + 2SiO_2 \rightarrow CaSiO_3 + CaAl_2Si_2O_8$
(gehlenite) (wollastonite) (anorthite) (Trindade et al., 2009)

At temperatures above 950°C, gehlenite (considered as an intermediate compound) becomes unstable in the presence of SiO_2 and decomposes. This decomposition enables anorthite, and wollastonite to be generated (Tschegg et al., 2009).
At 1000°C, the gehlenite content decreases considerably (23 to 14%) in favor of augite again. The K-feldspars content also collapses, while wollastonite increases little, and plagioclase feldspars are stable. It is also noticeable that the mineralogical phase for anorthite begins to

disappear after the temperature of 1100°C is reached under normal conditions (Traoré et al., 2003).

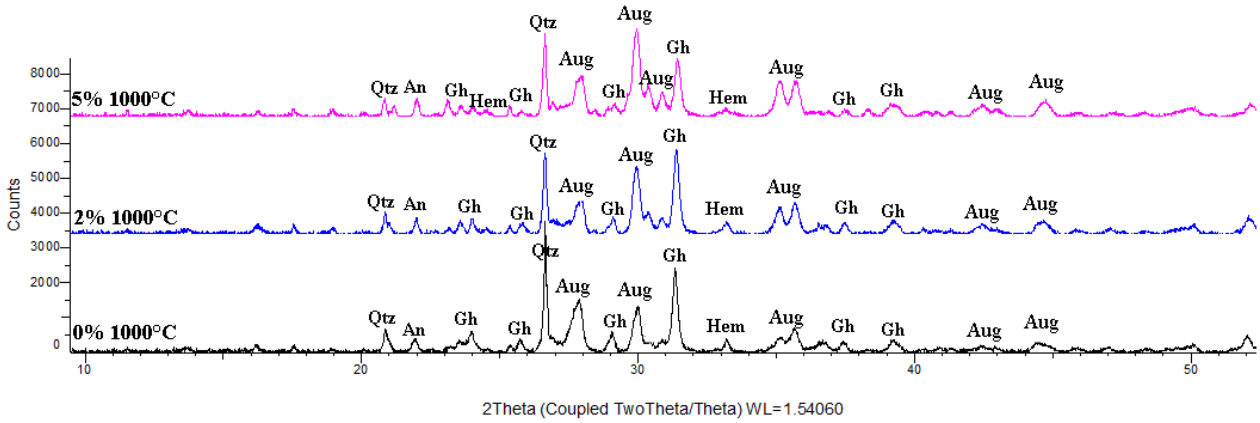

Fig. 46 Evolution of mineralogical phases at 1000°C, influenced by the percentage of salt

The same observation was made for the gehlenite, which starts to decrease concurrent with increasing salt percentages. The hematite reflections do not present any changes, however. Their appearance starts at 750°C within the 2% salt sample, and is similarly present at 1000°C (**Fig. 46**).

In summary, the addition of salt induces mineralogical changes including the disappearance of calcite and the appearance of Ca-silicates from 750°C onwards. The effect of firing at higher temperatures and the salt addition facilitates the decomposition of the carbonates and silicates at lower temperatures than usual, allowing for the formation of new crystallized phases.

All the Ca-rich fired samples, beginning with those with at least 2% added salt and fired at 750°C, contained gehlenite and augite, which have been formed due to the decomposition of calcite. In addition, hematite and anorthite were formed in these samples as well. These newly formed minerals remained present throughout the entire temperature range regardless of the percentage of salt added.

V.6.2.3 SEM-EDX analyses

The SEM observations revealed the microtexture of the carbonate-rich base clay experimental bricks. It also provided information regarding the porosity and the glassy phases. The investigations of the microtexture of the sherds were made on fresh fracture surfaces and on polished thick sections. Normally the development of the crystalline and glassy phase in a ceramic is the result of the temperature of the heating treatments applied. The proportion of

Fe_2O_3 is constant (~6%) in all experimental bricks, regardless of the NaCl level or the temperature applied. The bulk chemical results also reveal that the addition of the salt did not affect the chemical composition, except in the case of the potassic compound (K_2O), which decreases as salt concentration increases (**Table 23**). In fact, the ratio K_2O/SiO_2 decreases from 0.08 to 0.05 for samples fired at 750°C as a result of increasing percentages of salt.

Table 23 Chemical composition (wt%), obtained by SEM-EDX on thick sections of experimental samples (SD – standard deviation, dl – detection limit)

	Na_2O	**MgO**	**Al_2O_3**	**SiO_2**	**SO_3**	**Cl**	**K_2O**	**CaO**	**TiO_2**	**Fe_2O_3**	**K_2O/SiO_2**
YC 0% 750°C	0.2	2.9	20.2	49.1	<dl	0.5	3.8	16.7	0.9	5.8	0.077
SD	0.1	0.1	0.3	0.4		0.1	0.1	0.4	0.1	0.2	
YC 2% 750°C	1.3	2.9	18.0	45.0	0.1	1.2	3.5	21.3	0.8	5.7	0.078
SD	0.4	0.2	0.3	0.6	0.1	0.1	0.2	0.4	0.1	0.2	
YC 5% 750°C	3.1	2.9	17.6	44.1	0.2	2.2	2.0	21.8	0.8	5.1	0.045
SD	0.5	0.1	0.4	0.7	0.1	0.1	0.2	0.8	0.1	0.1	
YC 0% 900°C	0.1	3.0	18.9	44.7	0.1	0.3	3.7	22.4	0.8	5.9	0.083
SD	0.1	0.1	0.3	0.2	0.1	0.1	0.1	0.5	0.1	0.1	
YC 2% 900°C	1.4	3.1	17.9	45.3	<dl	0.4	2.8	22.6	0.8	5.6	0.062
SD	0.5	0.1	0.2	0.8		0.1	0.1	0.5	0.1	0.3	
YC 5% 900°C	2.0	3.2	17.9	45.2	0.1	0.7	2.0	22.4	0.8	5.5	0.044
SD	0.5	0.1	0.2	0.3	0.1	0.0	0.5	0.4	0.0	0.3	
YC 0% 1000°C	0.1	3.3	18.7	47.0	<dl	0.1	3.4	21.3	0.8	5.1	0.072
SD	0.1	0.1	0.1	0.2		0.1	0.1	0.3	0.1	0.1	
YC 2% 1000°C	1.4	3.5	18.0	46.1	<dl	0.2	1.7	22.8	0.8	5.4	0.037
SD	0.6	0.2	0.3	1.4		0.1	0.2	0.8	0.1	0.3	
YC 5% 1000°C	2.8	3.3	18.4	47.3	0.1	0.2	0.8	21.1	0.8	5.1	0.017
SD	0.5	0.1	0.3	0.6	0.1	0.1	0.2	0.8	0.1	0.2	

The same decrease was observed for the other temperatures, until a collapse of the rate for bricks with the highest salt content and highest firing temperature (0.02 for YC 5% 1000°C). On the other hand, the K_2O content of the brick without salt fired at 1000°C is slightly reduced, though still similar to the original one. Thus, the introduction of salt combined with an increase in the firing temperature causes the loss of this element (**Fig. 47**). M. Picon (1991) explained the K-loss phenomenon, due to the alteration within the ceramic and highlighting the importance of different factors that contribute to the availability of silicate materials for structural rearrangements. One important factor is the percentage of lime in the ceramics,

which can allow the development of an unstable glassy or amorphous phase, or even for the evolution of crystalline phases, which are also unstable such as gehlenite.
In addition, Fabbri and Fiori (1985) presented different studies where the reaction between kaolin clays and NaCl led to the complete elimination of chlorine at about 520°C. As for calcareous illitic-chloritic clays, the HCl was volatilized at a higher temperature and stimulated the decomposition of carbonate impurities forming potassium chloride. They observed that the addition of the NaCl caused a significant decrease in the amount of residual potassium and a progressive elimination of residual Cl in samples fired above 750°C.

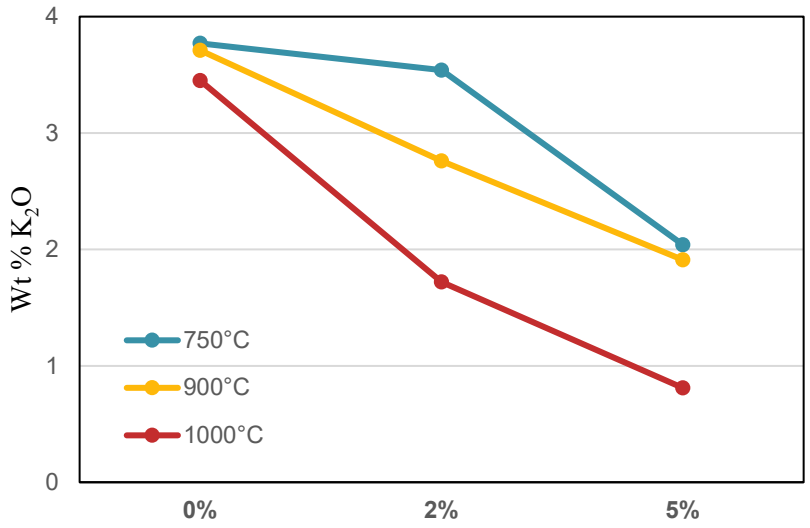

Fig. 47 Evolution of evaporation of K_2O in concordance with the addition of salt

Moreover, Bearat (1990) explained that the eliminated alkalis are in the form of chlorides during the firing process. This means that the formation of calcium silicates promotes the formation of alkaline chlorides, which start to volatilize at temperatures of 700°C - 750°C (Bearat, 1990). However, it is difficult to provide a complete and precise explanation of the phenomenon. The most predominant oxides are SiO_2 and Al_2O_3, which are mainly linked to the clay minerals, although SiO_2 content can often also be associated with the quartz particles. The iron oxide content is normally sensitive during firing. This leads to a certain variety of ceramic colours and textures. (El Boudour El Idrissi et al., 2016). In the present study, the proportion of iron in the samples does not affect the colour change.
In addition, it was studied in the same time the composition of the samples between the core and the exterior (**Fig. 48)**. We did not notice any significant difference that could indicate the migration of elements.

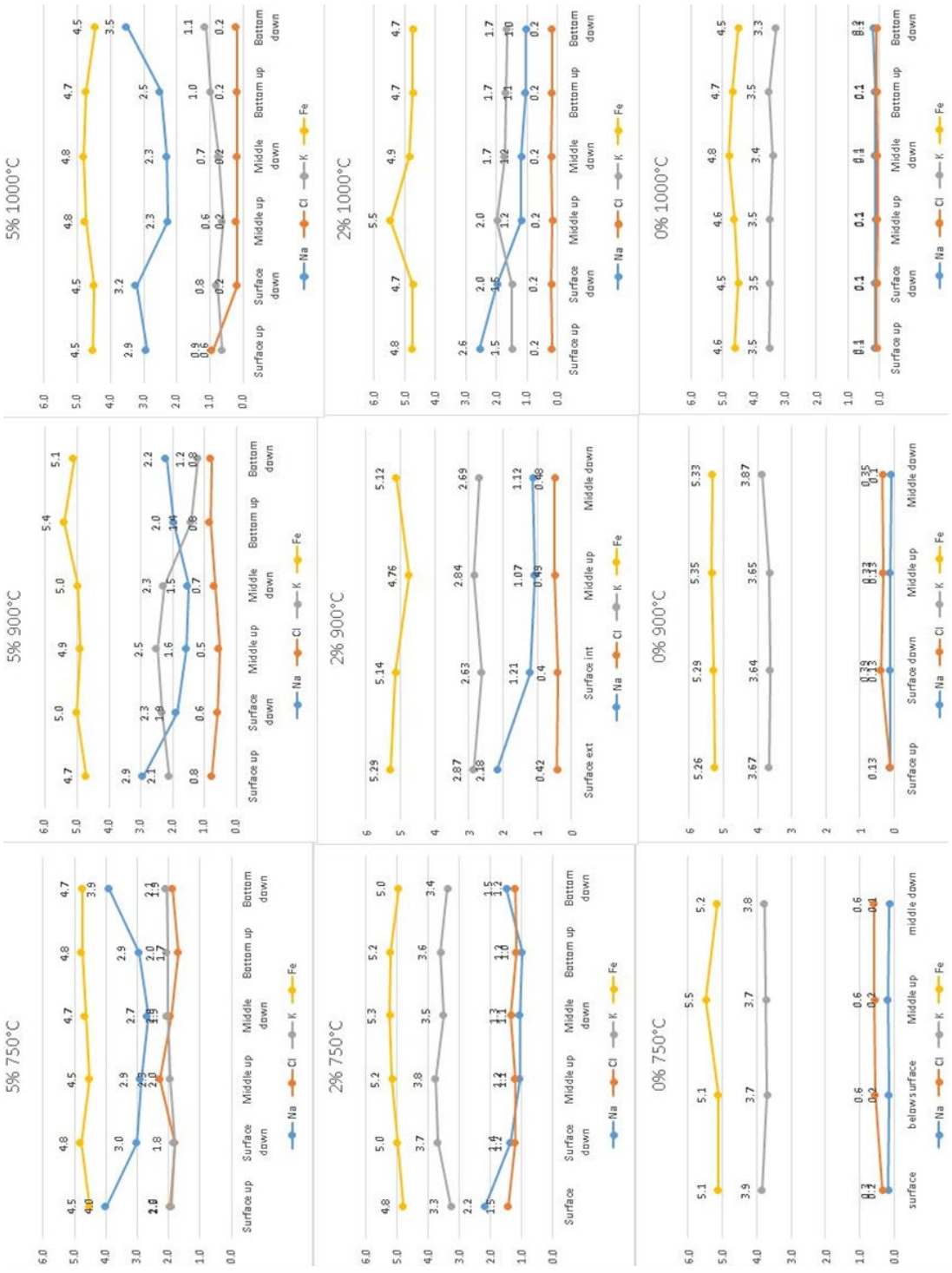

Fig. 48 Evolution of Na, Cl, K and Fe inside of the matrix at 750°C, 900°C and 1000°C

SEM observations also revealed rhombic voids in all the experimental bricks, including those absent salts (**Fig. 49**). At 750°C, *rhombohedral* minerals are yet present but have started to decompose. These forms are attributed to calcite or Mg-calcite minerals. Furthermore, when minerals disappear, their shape is retained with these voids, which are like witnesses of their previous presence before the temperature increase and/or salt addition. Thus, at 1000°C the formation of a new phase can be observed inside the voids.

The core presents a significant Mg enhancement, suggesting that the mineralogical phases of augite have been formed. Further observations in the clay matrix have also been recorded for the samples, including the development of the glassy phase and ellipsoidal vesicles that increase when more salt is added. The same phenomenon is known to occur with increasing temperature.

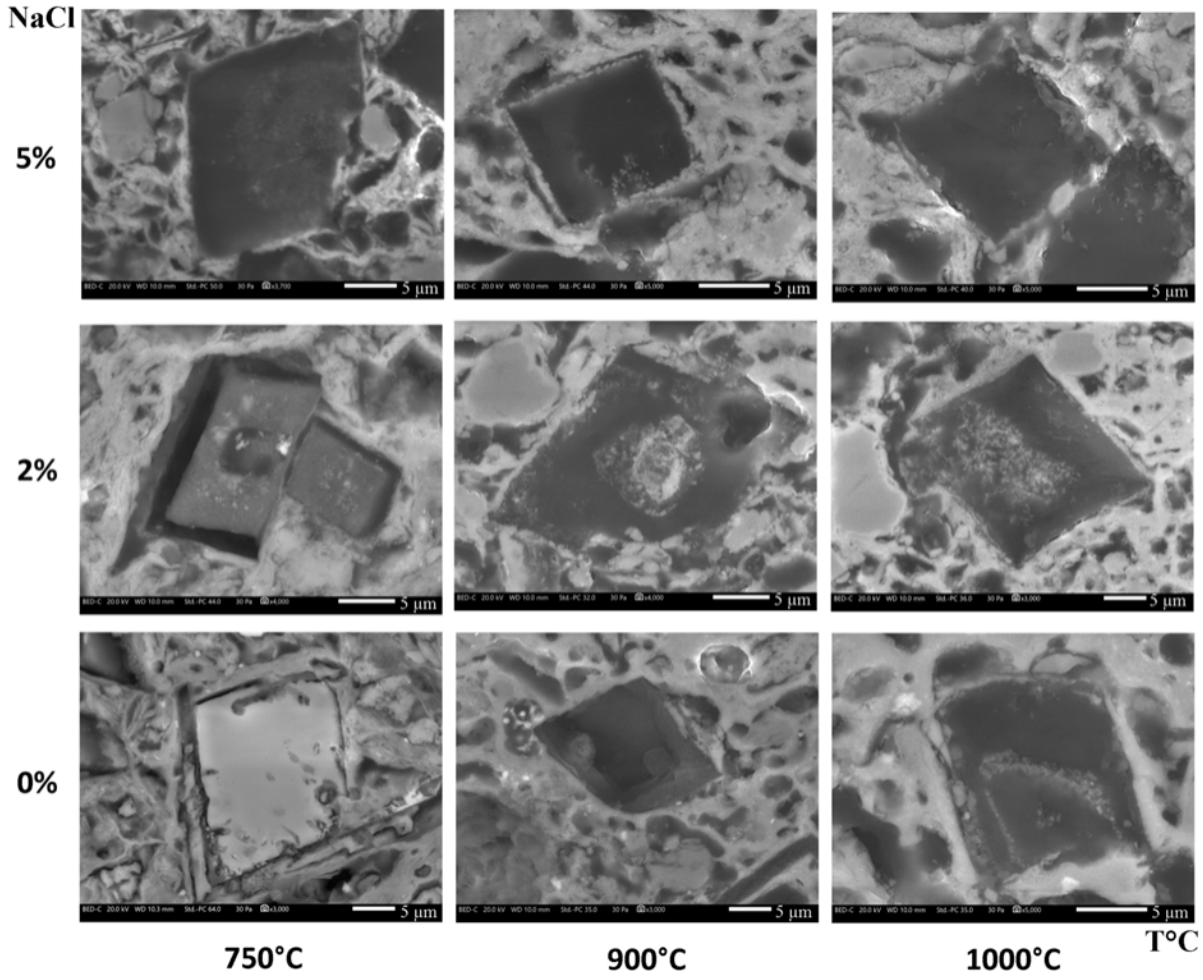

Fig. 49 SEM-BSE images of calcite or rhombohedral voids present in the matrix of the experimental brick

V.7 Concluding remarks

The study confirmed the role of halite in the bleaching of ceramics with a high CaO content. Indeed, colorimetric measurements carried out on experimental bricks with different salt contents, showed a significant loss of the red component as the salt concentration increased, as well as a loss of the yellow component to a lower degree. These colorimetric losses are associated with a decrease of their saturation. At the same time, the clarity has significantly increased. These factors allow for the empirical characterization of the whitening effect observed visually and confirm the main role of salt in this process, beyond the effect of temperature alone.

The mineralogical phase changes recorded in the experimental bricks have also been highlighted by different methods. Cathodoluminescence images showed these changes in the material. Qualitative and quantitative XRD results allowed for the documentation of the evolving proportions for these different phases, relatively to the increases of salt content and firing temperature. In fact, the process of alteration of clay minerals to form new calcium silicates appears to take place at a lower temperature in the presence of salt than has been generally thought. In this regard, significant differences in the microstructure of the calcareous clays with 5% salt are observed with the appearance of Ca-silicates (gehlenite, wollastonite) as early as 750°C.

Furthermore, the colour changes, due to the trapping of Fe ions in the crystal lattice can now be explained (Nodari et al., 2007). Although Mossbauer measurements – which could be the best method to apply in such cases - have not yet been carried out, Chevalier et al. (1976) have shown that gehlenite, anorthite or wollastonite crystals can trap Fe ions in their lattice, by substitution of Al^{3+} and Ca^{2+}. They pointed out that ferric oxide is known to be produced when biotite reaches high temperatures, such as 900°C, and that crystallization improves at 1000°C. In addition, R. Noller and H. Knoll (1983) conducted investigations by making possible the insertion of Fe^{3+} into the lattices of Ca-Mg-Al silicates. They observed that the difference in coloration could be explained for synthetic silicates by a polarized binding of Fe^{3+} ions in a disordered matrix. Therefore, the experimental data presented here provides significant explanatory evidence for the action of NaCl on the whitening of calcareous clays. By lowering the temperature at which calcium silicates are formed, NaCl serves to reduce the necessary temperature at which the bleaching effect commences.

Moreover, the result obtained by the SEM-imagery has made it possible to more accurately describe and assign the presence of rhombohedral voids. Results show that they are due to the dissolution of the carbonates, contrary to what has been put forth previously in the scientific literature where voids were attributed to the dissolution of salts (Rye, 1976).

Regarding the flocculation effect based on the reaction of the salt, red clay sediment and yellow clay we noticed that the reaction was different for both sediments. In the yellow clay

sediment (Ca-rich clay) the flocculation stage was reached faster, while in the red clay sediment (Ca-poor clay) the liquid remained in a dispersive stage. However we should be aware about fact that there are a lot of other parameters that they play an important role in the effect of flocculation (ex: type of clay, size of the particles, pH of water, etc.).

Returning to the Hebron ceramics specifically, it is clear from the experimental results that the two colorations obtained (pink and white) can in fact be explained primarily by a difference in salt concentration in the initial mixture rather than other factors.

Other measurements currently underway will further consider the effect of salt on the porosity of ceramics. These observations will be compared with ceramics produced elsewhere at other sites (notably in India) where similar practices with salt addition, have been reported.

Journal of Archaeological Science: Reports xxx (xxxx) 103303

Contents lists available at ScienceDirect

Journal of Archaeological Science: Reports

journal homepage: www.elsevier.com/locate/jasrep

Mineralogical transformations due to salt whitening agent in modern Hebron ceramics

L. Teodorescu [a, b, *], N. Cantin [a], A. Ben Amara [a], R. Chapoulie [a], V. Roux [c]

[a] IRAMAT-CRP2A, UMR 5060, CNRS, University Bordeaux Montaigne, Maison de l'Archéologie, Domaine Universitaire, Esplanade des Antilles, 33607 Pessac Cedex, France
[b] Department of Materials Science and Engineering, University of Pitesti, Romania
[c] Préhistoire et Technologie, UMR 7055, CNRS, University of Paris Nanterre, 21 Allée de l'Université, 92023 Nanterre Cedex, France

ARTICLE INFO

Keywords:
Ceramic
Hebron
Salt NaCl
Whitening
Firing process
Colorimetry
Petrography
XRD
SEM-EDX

ABSTRACT

The aim of this research is to investigate the influence of NaCl on the colours and chemical composition of Ca-rich ceramic bodies. The addition of salt to ceramics is a practice that has been observed in several potter communities where the addition of salt is explicitly intended to whiten ceramics. In order to conduct this research and characterize the physico-chemical properties induced by the presence of salt, raw clay material and pot sherds were collected from the modern production at Hebron. Experimental bricks were made using two clayed sediments: one with a low CaO content (< 10%) and one with a higher CaO content (20–25%). Different proportions of NaCl were added (up to 5%) to clay pastes which were fired at different temperatures. Mineralogy (petrography, XRD), chemistry (SEM-EDX) and colour analyses were carried out on raw clay materials, pot sherds and experimental (lab-made) bricks. SEM imagery offered the possibility to monitor the evolution of the mineralogical transformations, the pore system with increasing firing temperature and salt content. Results confirm the role of salt as a catalyst in the transformation reaction of calcium silicates during the firing process and its influence on the colour of the finished object.

CHAPTER VI

GENERAL CONCLUSIONS. PERSONAL CONTRIBUTIONS AND PERSPECTIVES

VI.1 Conclusions

The multiscale approach carried out in this thesis research was efficient to investigate the complex and heterogeneous structure of the ceramic materials (archaeological and ethnographic), with the help of three different case studies.

The first case concerned the Dacian ancient ceramics, from La Tène culture, where the main aim was to determine the chemical and mineralogical characteristics of ceramics, making possible to discriminate the ceramic artefacts according to their manufacturing.

The applied methodology made possible the analysis of ten sherds of Dacian pottery discovered in the archaeological site of Ocnița-Buridava, Romania. The study led to the detection of the presence of some non-calcareous ceramic bodies. In addition, we observed a large difference in grain size dimension between the ceramic fragments, such as the hand-made ones being coarser. The research started with petrographic analyses, where we noticed that all ceramic bodies were mostly composed of feldspars, micas (biotite and muscovite), quartz, amphiboles and voids. With the help of cathodoluminescence and SEM images, we observed that the proportion of inclusions was higher in the hand-made ceramic group. In addition, the grain size distribution suggested that these tempers were originally present in the clay and not added by the potter. The XRD analysis highlighted the presence of illite-muscovite in our samples, which we used as a thermal guide (Rodriguez-Navarro et al., 2003). Therefore, the results showed that the firing temperature of the Dacian ceramic sherds was relatively low (below 900°C). Hence, this research made possible to notice the differences in texture, in chemical and mineralogical composition between the ceramics according to their manufacturing technique.

The second case we focused on a provenance study of Adriatic amphorae in the Danube's region, with the help of a new device, which was bought at the beginning of the year 2021 in the laboratory of IRAMAT-CRP2A, a p-XRF VANTA-OLYMPUS (C Series).

Following all the processes for setting parameters and calibration, the methodology was applied on the amphorae samples, on soft polished fractures. With the help of PCA it was possible to create groups and to better observe the distribution of the samples. Moreover, since in our case we had a provenance study with a reference group, we could compare our results with it. We applied the outlier detection method in the multivariate space, using a statistical calculus named Mahalanobis Distance (MD), using R program. Thus, the statistical

approach allowed us to make a hypothesis regarding the provenance of the amphora bodies. Only one sample (BDX 25423) out of thirty-three, could correspond to the Loron production. This study made possible to clarify the reliability of p-XRF, by making the analysis without any special preparation and demonstrating the practicability of this device (without special preparation of the samples).

The last case was focused on the ceramic manufacturing process in Hebron nowadays, by implementing another strategy, which is defined as ethno-archaeometry. This research helped us to understand the role of salt as a bleaching agent and to better understand the transformations of the ceramic material during its manufacture. Furthermore, ceramic analyzes on experimental bricks were made, in order to reconstruct the production processes from the selection of raw materials to the firing of the vessel (Cantin and Mayor, 2018). First we analyzed four modern potsherds and four raw materials (used by the Hebron potters in their manufacture), collected in Hebron. For enlarging our understanding of the whitening effect, eighteen experimental samples were prepared, using the same clays used by Hebron's potters. The study confirmed that the role of salt in the bleaching of ceramics was visible only on the samples with a high CaO content. The mineralogical phase changes in the experimental bricks have been observed and recorded with the help of cathodoluminescence, of qualitative and quantitative XRD analysis and SEM-EDX analysis. The results allowed the observation of the evolving proportions of different phases, relatively to the increases of salt content and firing temperature. We observed that the process of transformation of clay minerals to form new calcium silicates appeared to take place at a lower temperature in the presence of salt than what was been generally expected. Moreover, we managed to accurately describe and assign the presence of rhombohedral voids discovered in the experimental brick with SEM imagery. Results showed that they are due to the dissolution of the carbonates, contrary to what has been put forth previously in the scientific literature where voids were attributed to the dissolution of salts (Rye, 1976).

By studying these three case studies, this thesis achieved to answer to the main challenges such as employing a suitable methodological approach for the study of Dacian potsherds (creating a database which can be used for future projects) and as well in applying different analytical technical methods of materials science which provided an answer to different archaeological and ethnographical questionings.

VI.2 Personal Contributions

These years of research, I could attend many trainings and sessions offered by the laboratories teams. These scientific internships enabled me to implement and finally be autonomous with the use of the techno-analytical methods specific to materials science, required to analyze the ancient ceramic materials, thus contributing to solve archaeological questions.
Furthermore, I achieved to:

1. Understand the archaeologist's questions and contribute to solve its tipping points: identification of raw material and their provenance thanks to physico-chemical characterisation, knowledge of production technics and trading routes
2. Take into account the complex nature of the ancient ceramics:
   2.1. Define and discuss the chronology thanks to the stratigraphic data and the typological information when they are known.
   2.2. Observe and take into account the alteration state of the sherds.
   2.3. Prepare the samples according to the different types of analysis to be performed.
   2.4. Define the best methodology for analyzing ceramics depending on the questioning.
3. Build an archaeometric database of Dacian ceramics from the southern of Carpathians, that will be increased by new incoming data, to enable comparative studies
4. Observe the differences regarding the texture, chemical and mineralogical compositions among ceramics, depending on their manufacturing technique and confirm the role of salt as a bleaching agent in ceramics with a high CaO content.
5. Provide data regarding the provenance of amphora bodies, from the East, making a link between the present countries France, Italy, Croatia and Romania.
6. Demonstrate that portable equipment (pXRF) can be a powerful tool for a preliminary analytical approach (based on elemental composition in this case) that can provide a first classification of ceramics, thus helping for the selection of samples which will undergo further and full laboratory analyses.

VI.3 Perspectives

Since different cases have been investigated and presented in this work, some challenges have inevitably appeared during research and some issues need to be further studied.
For example, in the case of Dacian ceramics it's important for future studies to raise an archaeological/ethno-archaeological question/enquiry in order to be able to select the pottery that can answer the questions posed by archaeologists.

In addition, Dressel 6B amphorae have also been discovered in Romania. It would be interesting to approach the Romanian museums that can provide us the needed samples for study and add the obtained results to the existing database.

Regarding the last case of research, where salt is playing an important role in the manufacturing process in Hebron's ceramic and other ongoing measurements will further investigate the influence of salt on the porosity of ceramics. These observations will be compared to ceramics made in Jodhpur (India) where similar salt addition practices have been reported. In addition, this study will allow to use this implemented methodology and to explore other corpuses where salt was used in the manufacture of ancient archaeological ceramics.

However, in all the case studies above, it should be underlined the fact that the key point in having a successful research, consists in defining archaeological issues or questionings, thus selecting an appropriate corpus of samples to be analyzed. Of course, all these steps require a multidisciplinary collaboration, which begins in the field, continues in the laboratory, and in the end can be valuable for publications and/or museum exhibitions (Gliozzo, 2020).

In addition, possibility to develop intense archaeometric research in Romania in the future are very high since there is a large opportunity to use efficient equipment from several research teams (such as the laboratory from Pitesti, CRC&D AUTO) working on modern materials. It is sufficient to put into practice the skills acquired in the framework of this thesis and to strengthen the links with archaeologists and museum curators.

Thus for the future studies it should be enlarged the number of samples from the present studied corpuses, but also adding other ceramic collections from closed areas (example for the amphorae corpus, samples from Museum Histria – Romania), and to take advantage of the knowledge of the presented methods in this thesis, to use them to other types of materials (such as glass and metals), even if maybe other different methods should then be included (specially for metals).

REFERENCES

Adriaens, R., 2015. Neogene and Quaternary clay minerals in the southern North Sea. University of Leuven, Belgium.

Aimers, J.J., Farthing, D.J., Shugar, A.N., 2012. Handheld XRF analysis of Maya ceramics: a pilot study presenting issues related to quantification and calibration, in: Handheld XRF for Art and Archaeology. Leuven University Press, pp. 423–448.

Aitchison, J., 1982. The Statistical Analysis of Compositional Data. Journal of the Royal Statistical Society. Series B (Methodological) 44, 139–177.

Anghel, D., 2011. Experimente de ardere a ceramicii in cuptoare de tip arhaic. Terra Sebus 3, 339–350.

Anghel, D., 2002. Influenta conditiilor de ardere asupra ceramicii. Revista Terra Sebus 6, 171–173.

Arnold, D.E., Neff, H., Bishop, R.L., 1991. Compositional Analysis and "Sources" of Pottery: An Ethnoarcheological Approach. American Anthropologist 93, 70–90. https://doi.org/10.1525/aa.1991.93.1.02a00040

Artioli, G., 2010. Scientific methods and cultural heritage: an introduction to the application of materials science to archaeometry and conservation science. Oxford University Press, Oxford ; New York.

Bălan, G., Quinn, C., Hodgins, G., 2016. The Wietenberg Culture: Periodization and Chronology. Dacia LX, 67–92.

Barbin, V., Schvoerer, M., 1997. Cathodoluminescence géosciences. Comptes Rendus de l'Académie des Sciences - Series IIA - Earth and Planetary Science 325, 157–169. https://doi.org/10.1016/S1251-8050(97)88284-5

Baxter, M.J., 2001. Statistical Modelling of Artefact Compositional Data. Archaeometry 43, 131–147. https://doi.org/10.1111/1475-4754.00008

Bearat, H., 1990. Etude de quelques alterations physico-chimiques des ceramiques archeologiques. Universite de Caen, France

Bearat, H., Dufournier, D., Nguyen, N., Raveau, B., 1989. Influence de NaCl sur la couleur et la composition chimique des pâtes céramiques calcaires au cours de leur cuisson. arsci 13, 43–53. https://doi.org/10.3406/arsci.1989.871

Beauvoit, E., Cantin, N., Lemasson, Q., Pacheco, C., Pichon, L., Moignard, B., Tessier-Doyen, N., Smith, A., Chapoulie, R., Ben Amara, A., 2019. Industrial production of white earthenware in the Johnston-Vieillard manufactory (19th century): recipes evolution and production strategies, in: XVI ECerS Conference. Torino, Italy.

Beaux, J.-F., Fogelgesang, J.-F., Agard, P., Boutin, V., 2011. Atlas de géologie, pétrologie. Dunod, Paris.

Berciu, D., 1967. Ancient Peoples and Places Series, 1st edition. ed. F.A. Praeger, London.

Berciu, D., Iosifaru, M., 1980. Săpăturile arheologice de la Ocniţa, jud. Vîlcea. Materiale şi cercetări arheologice 14, 183–185. https://doi.org/10.3406/mcarh.1980.1539

Bieber, A.M., Brooks, D.W., Harbottle, G., Sayre, E.V., 1976. Application of multivariate techniques to analytical data on Aegean ceramics. Archaeometry 18, 59–74. https://doi.org/10.1111/j.1475-4754.1976.tb00145.x

Bleininger, A.V., 1915. The use of sodium salts in the purification of clays and in the casting process. Journal of the Franklin Institute 180, 225–227. https://doi.org/10.1016/S0016-0032(15)90442-8

Bohor, B.F., 1963. High-Temperature Phase Development in Illitic Clays. Clays Clay Miner. 12, 233–246. https://doi.org/10.1346/CCMN.1963.0120125

Bouchet, A., Meunier, A., Sardini, P., 2000. Minéraux argileux structure cristalline, identification par diffraction de rayons X = Clay minerals: crystal structure, x-ray diffraction identification. Elf Exploration Production, Pau (Pyrénées-Atlantiques).

Bougard, E., 2011. Les céramiques gravettiennes de Moravie : derniers apports des recherches actuelles. L'Anthropologie 115, 465–504. https://doi.org/10.1016/j.anthro.2011.05.007

Breuer, S., 2012. Pottery vessels have been made for around 18 000 years. But how does clay extracted from the earth become a colourful pot, and what's the chemistry behind the process? The Royal Society of Chemistry Education in Chemistry, 17–20.

Brooks, D., Bieber, A.M., Harbottle, G., Sayre, E.V., 1974. Biblical studies through activation analysis of ancient pottery, in: Archaeological Chemistry, Advances in Chemistry.

AMERICAN CHEMICAL SOCIETY, WASHINGTON, D. C., pp. 8–33. https://doi.org/10.1021/ba-1974-0138

Bugoi, R., Paraschiv-Talmaţchi, C., Haita, C., Ceccato, D., 2019. Archaeometric characterization of Byzantine pottery from Păcuiul lui Soare. Heritage Science 7. https://doi.org/10.1186/s40494-019-0298-2

Bulić, D.; K.U., 2020. Observations on the Architecture and Products of the Figlina in Fažana [Ausonius éd., UBM]. Adriatlas 3.

Buxeda i Garrigós, J., Cau Ontiveros, M., Kilikoglou, V., 2003. Chemical Variability in Clays and Pottery from a Traditional Cooking Pot Production Village: Testing Assumptions in Pereruela. Archaeometry 45, 1–17. https://doi.org/10.1111/1475-4754.00093

Calligaro, T., Castelle, M., Lebon, M., Mauran, G., 2019. Analyse par fluorescence des rayons X portable : quantification, imagerie, où en est-on ? 22.

Cantin, N., Mayor, A., 2018. Ethno-archaeometry in eastern Senegal: The connections between raw materials and finished ceramic products. Journal of Archaeological Science: Reports 21, 1181–1190. https://doi.org/10.1016/j.jasrep.2017.01.015

Carter, C.B., Norton, M.G., 2007. Ceramic Materials. Science and Engineering. Springer-Verlag New York.

Cau Ontiveros, M.Á., Montana, G., Tsantini, E., Randazzo, L., 2015. Ceramic Ethnoarchaeometry in Western Sardinia: Production of Cooking Ware at Pabillonis. Archaeometry 57, 453–475. https://doi.org/10.1111/arcm.12100

Ceccarelli, L., Rossetti, I., Primavesi, L., Stoddart, S., 2016. Non-destructive method for the identification of ceramic production by portable X-rays Fluorescence (pXRF). A case study of amphorae manufacture in central Italy. Journal of Archaeological Science: Reports 10, 253–262. https://doi.org/10.1016/j.jasrep.2016.10.002

Chapoulie, R., Daniel, F., 2007. Cathodoluminescence : recherches sur une méthode d'analyse en archéométrie. British Archaeological Reports (BAR), BAR S1 700 1–16.

Chapoulie, R., Delery, C., Daniel, F., Vendrell-Saz, M., 2005. Cuerda seca ceramics from Al-Andalus, Islamic Spain and Portugal (10th-12th centuries ad): investigation with SEM-EDX and Cathodoluminescence. Archaeometry 47, 519–534. https://doi.org/10.1111/j.1475-4754.2005.00217.x

Chapoulie, R., Robert, B., Casenave, S., 2016. The cathodoluminescence phenomenon used for the study of ancient ceramics and stones. Cities of Memory : International Journal on Culture and Heritage at Risk 1, 53–72.

Chevalier, R., Coey, J.M.D., Bouchez, R., 1976. A study of iron in fired clay : Mössbauer effect and magnetic measurements. J. Phys. Colloques 37, C6-861-C6-865. https://doi.org/10.1051/jphyscol:19766181

Chorom, M., Rengasamy, P., 1995. Dispersion and zeta potential of pure clays as related to net particle charge under varying pH, electrolyte concentration and cation type. European Journal of Soil Science 46, 657–665. https://doi.org/10.1111/j.1365-2389.1995.tb01362.x

Cipriano, S.; M., 2020. Le anfore Dressel 6B prodotte in area nord adriatica [Ausonius éd., UBM]. Adriatlas 3.

Cochrane, S., 2014. The Munsell Color System: A scientific compromise from the world of art. Studies in History and Philosophy of Science Part A 47, 26–41. https://doi.org/10.1016/j.shpsa.2014.03.004

Combès, J.-L., Louis, A., 1967. Les poteries de Djerba. Publication du centre des arts et traditions populaires, Tunis.

Comsa, A., Szücs-Csillik, I., 2013. An archaeoastronomical study regarding some necropolis of the Gumelnita culture. Arheovest 1, 837–846.

Conrey, R.M., Goodman-Elgar, M., Bettencourt, N., Seyfarth, A., Van Hoose, A., Wolff, J.A., 2014. Calibration of a portable X-ray fluorescence spectrometer in the analysis of archaeological samples using influence coefficients. Geochemistry: Exploration, Environment, Analysis 14, 291–301. https://doi.org/10.1144/geochem2013-198

Copoeru, L., Pop, C., 2013. Istoria Pe Intelesul Tuturor. Editura Delfin, Bucuresti.

Crandell, O., Ionescu, C., Giurgiu, A., Simon, V., Trandafir, D., Nagy, J., 2015. Pottery firing technology in the Late Bronze Age & Early Iron Age in NW Romania. Acta Mineralogica-Petrographica 9, 5.

Crişan, I.H., Daicoviciu, C., 1969. Ceramica daco-getică: cu specială privire la Transilvania. Ed. ştiinţifică, Bucureşti.

Cristescu, C., 2011. Contributions to the Study Methodology of Dacian Pottery. Transylvanian Review, XX, Supplement 2:1.

Cultrone, G., Rodriguez-Navarro, C., Sebastian, E., Cazalla, O., De La Torre, M.J., 2001. Carbonate and silicate phase reactions during ceramic firing. Eur. J. Mineral. 13, 621–634. https://doi.org/10.1127/0935-1221/2001/0013-0621

De Bonis, A., Cultrone, G., Grifa, C., Langella, A., Leone, A.P., Mercurio, M., Morra, V., 2017. Different shades of red: The complexity of mineralogical and physico-chemical factors influencing the colour of ceramics. Ceram. Int. 43, 8065–8074. https://doi.org/10.1016/j.ceramint.2017.03.127

Dias, C., Candeias, A., Schiavon, N., Mirao, J., 2014. Basic Aspects of Science applied to Archaeology and Cultural Heritage.

Drob, A., Vasilache, V., Neculai, B., 2021. The Interdisciplinary Approach of Some Middle Bronze Age Pottery from Eastern Romania. Applied Sciences 11, 4885. https://doi.org/10.3390/app11114885

Dufournier, D., 1982. L'utilisation de l'eau de mer dans la préparation des pâtes céramiques calcaires, premières observations sur les conséquences d'un tel traitement. Archeosciences 6, 87–100. https://doi.org/10.3406/arsci.1982.1195

Duminuco, P., Messiga, B., Riccardi, M.P., 1998. Firing process of natural clays. Some microtextures and related phase compositions. Thermochimica Acta 321, 185–190. https://doi.org/10.1016/S0040-6031(98)00458-4

Dupont, D., Steen, D., 2004. Colorimétrie: Mesure des couleurs de surface. Tech. ing., Mes. contrôle RD3, R6442.1-R6442.13.

Edwards, H., Vandenabeele, P., 2016. Analytical Archaeometry: Selected Topics. Royal Society of Chemistry.

El Boudour El Idrissi, H., Daoudi, L., El Ouahabi, M., Fagel, N., 2016. Flaws linked to lime in pottery of Marrakech (Morocco). Journal of Materials and Environmental Science 7, 3738–3745.

El Ouahabi, M., Daoudi, L., Hatert, F., Fagel, N., 2015. Modified Mineral Phases During Clay Ceramic Firing. Clays Clay Miner. 63, 404–413. https://doi.org/10.1346/CCMN.2015.0630506

Eméry, L., 2012. Approches archéométriques des productions faïencières françaises au XVIIIe siècle : le cas de la manufacture Babut à Bergerac (env. 1740 - 1789) (phdthesis). Université Michel de Montaigne - Bordeaux III.

Fabbri, B., Fiori, C., 1985. Influence of Sodium Chloride on Thermal Reactions of Heavy Clays During Firing, in: Proceedings of the International Clay Conference. Clay Minerals Society, Denver.

Fan, D., Jahangiri, N., Kaushik, P., Pielet, H., Jun, H., 2017. Bending Performance Improvement of Dual-Phase Steel With 1000-MPa Tensile Strength.

Fierascu, R.C., Fierascu, I., Baroi, A.M., Brazdis, R.I., Fistos, T., Nicolae, C.A., Raditoiu, V., Inel, I.C., Sava, V., 2020. Characterization of historical ceramics: a case study. Romanian Reports in Physics 72, 14.

Florea, V., 2017. Arta romaneasca de la origini pana in prezent, III. ed. Litera, Bucharest, Romania.

Fonseca, R., Couto, H., 2017. Application of Cathodoluminescence to The Study of Feldspars: Imaging and Spectrometry. IOP Conf. Ser.: Earth Environ. Sci. 95, 032029. https://doi.org/10.1088/1755-1315/95/3/032029

Foucault, A., Raoult, J.-F., 2010. Dictionnaire de Géologie - 7e édition. Dunod.

Frahm, E., 2018. Ceramic studies using portable XRF: From experimental tempered ceramics to imports and imitations at Tell Mozan, Syria. Journal of Archaeological Science 90, 12–38. https://doi.org/10.1016/j.jas.2017.12.002

Frahm, E., Doonan, R.C.P., 2013. The technological versus methodological revolution of portable XRF in archaeology. Journal of Archaeological Science 40, 1425–1434. https://doi.org/10.1016/j.jas.2012.10.013

Frahm, E., Goldstein, S.T., Tryon, C.A., 2017. Late Holocene forager-fisher and pastoralist interactions along the Lake Victoria shores, Kenya: Perspectives from portable XRF of obsidian artifacts. Journal of Archaeological Science: Reports 11, 717–742. https://doi.org/10.1016/j.jasrep.2017.01.001

Frankel, D., Webb, J.M., 2012. Pottery production and distribution in prehistoric Bronze Age Cyprus. An application of pXRF analysis. Journal of Archaeological Science 39, 1380–1387. https://doi.org/10.1016/j.jas.2011.12.032

Frerebeau, N., Amara, A.B., Cantin, N., 2020. Analyse de données de composition et identification des altérations géochimiques des matériaux céramiques : le cas des productions d'un atelier ibérique (Teruel, Espagne ; IIe-Ier siècles avant J.-C.). ArcheoSciences n° 44-1, 33–50.

Gazulla Barreda, M.F., Rodrigo Edo, M., Orduña Cordero, M., Ventura Vaquer, M.J., 2016. Determination of minor and trace elements in geological materials used as raw ceramic materials. Boletín de la Sociedad Española de Cerámica y Vidrio 55, 185–196. https://doi.org/10.1016/j.bsecv.2016.06.003

Giurgiu, A., Ionescu, C., Hoeck, V., Tămaş, T., Roman, C., Crandell, O.N., 2017. Insights into the raw materials and technology used to produce Copper Age ceramics in the Southern Carpathians (Romania). Archaeol Anthropol Sci 9, 1259–1273. https://doi.org/10.1007/s12520-016-0322-3

Gliozzo, E., 2020. Ceramics investigation: research questions and sampling criteria. Archaeol Anthropol Sci 12, 202. https://doi.org/10.1007/s12520-020-01128-9

Goffer, Z., 2007. Clay: Pottery and Other Ceramic Materials, in: Archaeological Chemistry. John Wiley & Sons, Ltd, pp. 231–260. https://doi.org/10.1002/9780471915256.ch7

Gosselain, O.P., 1992. Bonfire of the enquiries. Pottery firing temperatures in archaeology: What for? Journal of Archaeological Science 19, 243–259. https://doi.org/10.1016/0305-4403(92)90014-T

Götze, J., Schertl, H.-P., Neuser, R.D., Kempe, U., Hanchar, J.M., 2013. Optical microscope-cathodoluminescence (OM–CL) imaging as a powerful tool to reveal internal textures of minerals. Mineral. Petrol. 107, 373–392. https://doi.org/10.1007/s00710-012-0256-0

Greene, K., Moore, T., 2010. Archaeology: An Introduction, 5th ed. Routledge, London. https://doi.org/10.4324/9780203835975

Griffiths, D., 1999. The role of interdisciplinary science in the study of ancient pottery. Interdisciplinary Science Reviews 24, 289–300. https://doi.org/10.1179/030801899678957

Hein, A., 2018. Elemental Analysis of Pottery, in: López Varela, S.L. (Ed.), The Encyclopedia of Archaeological Sciences. John Wiley & Sons, Inc., Hoboken, NJ, USA, pp. 1–5. https://doi.org/10.1002/9781119188230.saseas0211

Hogg, R., 2000. Flocculation and dewatering. International Journal of Mineral Processing 58, 223–236. https://doi.org/10.1016/S0301-7516(99)00023-X

Holakooei, P., Tessari, U., Verde, M., Vaccaro, C., 2014. A new look at XRD patterns of archaeological ceramic bodies: An assessment for the firing temperature of 17th century haft rang tiles from Iran. JTHEA 118, 165–176. https://doi.org/10.1007/s10973-014-4012-z

Hunt, A.M.W., Speakman, R.J., 2015. Portable XRF analysis of archaeological sediments and ceramics. Journal of Archaeological Science 53, 626–638. https://doi.org/10.1016/j.jas.2014.11.031

Ignat, T., Luca, A., Dimofte, D., Lazăr, C., Constantin, F., Bugoi, R., 2019. Multidisciplinary study on prehistoric pottery from Southeastern Romania. ArcheoSciences n° 43-2, 165–185.

Institutul Național al Patrimoniului - Cronica cercetărilor arheologice campania 2016, 2016.

Ion, R.-M., Fierascu, R.-C., Teodorescu, S., Fierascu, I., Bunghez, I.-R., Turcanu-Carutiu, D., Ion, M.-L., 2016. Ceramic Materials Based on Clay Minerals in Cultural Heritage Study, in: Do Nascimento, G.M. (Ed.), Clays, Clay Minerals and Ceramic Materials Based on Clay Minerals. InTech. https://doi.org/10.5772/61633

Ionescu, C., Ghergari, L., Horga, M., Rădulescu, G., 2007. Early Medieval ceramics from the Viile Tecii archaeological site (Romania): an optical and XRD study. Studia UBB Geologia 52, 29–35.

Ionescu, C., Hoeck, V., 2011. Firing-induced transformations in Copper Age ceramics from NE Romania. ejm 23, 937–958. https://doi.org/10.1127/0935-1221/2011/0023-2147

Iosifaru, M., 2011. Situri arheologice din oraşul Ocnele Mari, judeţul Vâlcea Buridava IX, 13.

Irigoyen Otamendi, J., 2016. Fabrication and Characterization of Multilayered Assemblies based on Polyelectrolytes and Hybrid Systems with Carbon Nanomaterials for Applications in Nanofiltration and as Smart Surfaces.

Jordán, A., 2014. Lightening the clay (I). Soil System Sciences.

Kilikoglou, V., Maniatis, Y., Grimanis, A.P., 1988. The effect of purification and firing of clays on trace element provenance studies. Archaeometry 30, 37–46. https://doi.org/10.1111/j.1475-4754.1988.tb00433.x

Killick, D., 2015. The awkward adolescence of archaeological science. Journal of Archaeological Science 56. https://doi.org/10.1016/j.jas.2015.01.010

Kirillova, N.P., Grauer-Gray, J., Hartemink, A.E., Sileova, T.M., Artemyeva, Z.S., Burova, E.K., 2018. New perspectives to use Munsell color charts with electronic devices. Computers and Electronics in Agriculture 155, 378–385. https://doi.org/10.1016/j.compag.2018.10.028

Konert, M., Vandenberghe, J., 1997. Comparison of laser grain size analysis with pipette and sieve analysis: a solution for the underestimation of the clay fraction. Sedimentology 44, 523–535. https://doi.org/10.1046/j.1365-3091.1997.d01-38.x

Kretz, R., 1983. Symbols for rock-forming minerals. American Mineralogist 68, 277–279.

Kumari, N., Mohan, C., 2021. Basics of Clay Minerals and Their Characteristic Properties. IntechOpen. https://doi.org/10.5772/intechopen.97672

Lajarte, S., 1979. Les verres colorés, in: Actualité Chimique. Société Chimique de France (SCF).

Leahy, K., Geake, H., 2019. Pottery Recording Guide.

Levcovici, S., Boiciuc, S., Alexandru, P., 2006. Indrumar de lucrari de laborator - Stiinta si Ingineria Materialelor.

Livingstone Smith, A., 2001. Bonfire II: The Return of Pottery Firing Temperatures. Journal of Archaeological Science 28, 991–1003. https://doi.org/10.1006/jasc.2001.0713

Machut, P., 2013. Amphores de Loron: Recherche de provenance des matieres premieres (Mémoire de stage). Universite Bordeaux Montaigne, Pessac Cedex, France.

Machut, P., Ben Amara, A., Cantin, N., Chapoulie, R., Frèrebeau, N., Le Bourdonnec, F.-X., Marion, Y., Tassaux, F., 2015. Towards high resolution ceramic series for production site studies: the case of Loron amphorae (Croatia, 1st–3rd c. A.D.). Herit Sci 3, 21. https://doi.org/10.1186/s40494-015-0050-5

Machut, P., Ben Amara, A., Cantin, N., Chapoulie, R., Le Bourdonnec, F.-X., Marion, Y., Tassaux, F., 2017. Production strategies in Istrian oil amphorae workshops 1st-3rd c. AD.

Machut, P., Marion, Y., Ben Amara, A., Tassaux, F., 2020. AdriAtlas 3. Recherches pluridisciplinaires recentes sur les amphores nord-adriatiques a l'epoque romaine. Ausonius éditions, Bordeaux, France.

Maggetti, M., Neururer, C., Ramseyer, D., 2011. Temperature evolution inside a pot during experimental surface (bonfire) firing. Applied Clay Science 53, 500–508.

Marion, Y., Tassaux, F., 2020. Les amphores d'Istrie septentrionale et centrale : ateliers et typochronologie, in: AdriAtlas 3. Recherches pluridisciplinaires recentes sur les amphores nord-adriatiques a l'epoque romaine. Ausonius Editions, UBM, Bordeaux, France.

Maritan, L., 2004. Archaeometric study of Etruscan-Padan type pottery from the Veneto region: petrographic, mineralogical and geochemical-physical characterisation. ejm 16, 297–307. https://doi.org/10.1127/0935-1221/2004/0016-0297

Maritan, L., Nodari, L., Mazzoli, C., Milano, A., Russo, U., 2006. Influence of firing conditions on ceramic products: Experimental study on clay rich in organic matter. Applied Clay Science 31, 1–15. https://doi.org/10.1016/j.clay.2005.08.007

McCormick, D.R., Wells, E.C. (Eds.), 2014. Pottery, People, and pXRF: Toward the Development of Composition Profiles for Southeast Mesoamerican Ceramics, in: Social Dynamics of Ceramic Analysis: New Techniques and Interpretations: Papers in Honour of Charles C. Kolb:, Bar International Series. University of Michigan Press, Ann Arbor, MI, pp. 22–35. https://doi.org/10.30861/9781407313290

Menne, J., Holzheid, A., Heilmann, C., 2020. Multi-Scale Measurements of Neolithic Ceramics—A Methodological Comparison of Portable Energy-Dispersive XRF, Wavelength-Dispersive XRF, and Microcomputer Tomography. Minerals 10, 931. https://doi.org/10.3390/min10100931

Miller, R.S., 1958. The Munsell System of Color Notation. Journal of Mammalogy 39, 278–286. https://doi.org/10.2307/1376204

Montana, G., 2016. Ceramic Raw Materials, in: The Oxford Handbook of Archaeological Ceramic Analysis. Oxford Handbooks. https://doi.org/10.1093/oxfordhb/9780199681532.013.7

Montana, G., Cau Ontiveros, M., Polito, M., Azzaro, E., 2011. Characterisation of clayey raw materials for ceramic manufacture in ancient Sicily. Applied Clay Science - APPL CLAY SCI 53, 476–488. https://doi.org/10.1016/j.clay.2010.09.005

Nakamura, H., 2021. Colloidal Crystals -Self-Assembly of Monodispersed Colloidal Particles.

Nassau, K., 1998. Color for science, art and technology. Elsevier, Amsterdam; New York.

Nodari, L., Marcuz, E., Maritan, L., Mazzoli, C., Russo, U., 2007. Hematite nucleation and growth in the firing of carbonate-rich clay for pottery production. Journal of the European Ceramic Society 27, 4665–4673. https://doi.org/10.1016/j.jeurceramsoc.2007.03.031

Nöller, R., Knoll, H., 1983. Magnetic properties of calcium-silicates (diopside and gehlenite) doped with iron (III). Solid State Commun. 47, 237–239. https://doi.org/10.1016/0038-1098(83)90552-5

Opris, V., 2018. Arheometria intre necesitate si “trend” metodologic.

Orton, C., Tyers, P., Vince, A., 1993. Pottery in Archaeology, No. 1. ed, Cambridge Manuals in Archaeology. Cambridge University Press, New York, USA.

Pacheco, C., Chapoulie, R., Dooryhee, E., Goudeau, P., 2015. Gold leaf decoration on medieval islamic glazed ceramics – in search of technological features with XRD, in: Gold Leaf Decoration on Medieval Islamic Glazed Ceramics – in Search of Technological Features with XRD. Oldenbourg Wissenschaftsverlag, pp. 317–324. https://doi.org/10.1524/9783486992540-050

Peters, T., Iberg, R., 1978. Mineralogical Changes During Firing of Calcium-Rich Brick Clay. Am. Ceram. Soc. Bull. 57, 503–506.

Pettijohn, F.J., Potter, P.E., Siever, R., 2012. Sand and sandstone. Springer Science & Business Media.

Picon, M., 1991. Quelques observations complémentaires sur les altérations de composition des céramiques au cours du temps : cas de quelques alcalins et alcalino-terreux. Archeosciences 15, 117–122. https://doi.org/10.3406/arsci.1991.1263

Piponnier, D., Bechtel, F., Florin, D., Molera, J., Schvoerer, M., Vendrell, M., 1997. Apport de la Cathodoluminescence à l'Etude des Transformations de Phases Cristallines dans des Céramiques Kaolinitiques Carbonatées. Key Eng. Mater. 132–136, 1470–1473. https://doi.org/10.4028/www.scientific.net/KEM.132-136.1470

Potts, P.J., West, M. (Eds.), 2008. Portable x-ray fluorescence spectrometry: capabilities for in situ analysis. RSC Pub, Cambridge, UK.

Price, T.D., Burton, J.H., 2011. An Introduction to Archaeological Chemistry. Springer New York, New York, NY. https://doi.org/10.1007/978-1-4419-6376-5

Quinn, P.S., 2013. Ceramic Petrography: The Interpretation of Archaeological Pottery and Related Artefacts in Thin Section. Archaeopress, Oxford.

R. Core Team, 2013. R: A language and environment for statistical computing 16.

Rapp, G., 2009. Archaeomineralogy, Natural Science in Archaeology. Springer Berlin Heidelberg, Berlin, Heidelberg. https://doi.org/10.1007/978-3-540-78594-1

Reedy, C.L., 2008. Thin Section Petrography of Stone and Ceramic Cultural Materials. Archetype Publications, London.

Regert, M., Guerra, M.F. (Eds.), 2016. Physico-chimie des matériaux archéologiques et culturels. Editions des archives contemporaines. https://doi.org/10.17184/eac.9782813001924

Renfrew, C., Bahn, P.G., 2016. Archaeology: Theories, Methods, and Practice, Seventh edition revised&updated. ed. Thames & Hudson, London.

Riccardi, M.P., Messiga, B., Duminuco, P., 1999. An approach to the dynamics of clay firing. Appl. Clay Sci. 15, 393–409. https://doi.org/10.1016/S0169-1317(99)00032-0

Ricci, G., 2016. Archaeometric studies of historical ceramic materials (Scienze Chimiche). Universita Ca'Foscari Venezia.

Roux, V., 2019. Ceramics and Society: A Technological Approach to Archaeological Assemblages. Springer International Publishing, Cham. https://doi.org/10.1007/978-3-030-03973-8

Roux, V., 2018. Traditional knowledge of the Hebron's potters and Heritage Resilience (Palestinian Territories).

Roux, V., 2015. The white matka: ethnography of a water jar. Rupayan Sansthan, Jodhpur.

Rye, O.S., 1976. Keeping Your Temper under Control: Materials and the Manufacture of Papuan Pottery. Archaeol. Oceania 11, 106–137.

Sanjurjo-Sánchez, J., Montero Fenollós, J.-L., Prudêncio, M.I., Barrientos, V., Marques, R., Dias, M.I., 2016. Geochemical study of beveled rim bowls from the Middle Syrian Euphrates sites. Journal of Archaeological Science: Reports 7, 808–818. https://doi.org/10.1016/j.jasrep.2016.02.018

Santos, J.O. dos, Munita, C.S., Soares, E.A.A., 2013. Outlier detection by robust Mahalanobis distance in geological data obtained by INAA to provenance studies. Presented at the INAC 2013: international nuclear atlantic conference, Brazil.

Schindelholz, E., 2001. A simple guide for archaeological materials characterization (Senior Reseacr Paper). University of Minnesota, USA.

Schindler, K., E., 2009. Contributo alla questione cronologica : l'apporto delle anfore del Magdalensberg. In Pesavento Mattioli and Carre (2009).

Sciau, P., Goudeau, P., 2015. Ceramics in art and archaeology: a review of the materials science aspects. Eur. Phys. J. B 88, 132. https://doi.org/10.1140/epjb/e2015-60253-8

Shackley, M.S., 2011. An Introduction to X-Ray Fluorescence (XRF) Analysis in Archaeology, in: Shackley, M.S. (Ed.), X-Ray Fluorescence Spectrometry (XRF) in Geoarchaeology. Springer New York, New York, NY, pp. 7–44. https://doi.org/10.1007/978-1-4419-6886-9_2

Shepard, A.O., 1985. Ceramics for the archaeologist, Repr. ed, Publication / Carnegie Institution of Washington. Carnegie Inst, Washington, DC.

Speakman, R.J., Little, N.C., Creel, D., Miller, M.R., Iñañez, J.G., 2011. Sourcing ceramics with portable XRF spectrometers? A comparison with INAA using Mimbres pottery from the American Southwest. Journal of Archaeological Science 38, 3483–3496. https://doi.org/10.1016/j.jas.2011.08.011

Speakman, R.J., Shackley, M.S., 2013. Silo science and portable XRF in archaeology: a response to Frahm. Journal of Archaeological Science 40, 1435–1443. https://doi.org/10.1016/j.jas.2012.09.033

Stan, E., 2017. Ceramica – Trecut, Prezent si Viitor. Liceul Tehnologic "Dimitrie Paciurea."

Stefan, A., Mazare, P., 2001. Metode de prelevare a materialelor ceramice pe santerele arheologice. Arheologie-Istorie-Muzeologie 7, 259–276.

Stiles, D., 1977. Ethnoarchaeology: A Discussion of Methods and Applications. Man 12, 87–103. https://doi.org/10.2307/2800996

Szakmány, G., 2020. Fažana amphorae: geological context and new petrographic and chemical results [Ausonius éd., UBM]. Adriatlas 3.

Tassaux, F., 2004. Les Importations de l'Adriatique et de l'Italie du Nord vers les provinces danubiennes de César aux Sévères. Edizioni ETS, Pisa, pp. 165–205.

Tassaux, F., 2001. Production et diffusion des amphores à huile istriennes. Antichità Altoadriatiche 46, 501–543.

Tassaux, F., Jean-Courret, E., Tassaux, Y., Ausonius-Institut de recherche sur l'Antiquité et le Moyen âge (Pessac, G., 2010. Les milliardaires de l'Adriatique romaine: [exposition présentée à l'Archéopôle d'Aquitaine, du 19 mars au 18 juin 2010. Ausonius, Pessac.

Tassaux, F., Matijašić, R., Kovačić, V., 2001. Loron (Croatie), un grand centre de production d'amphores à huile istrienne (Ier-IVe s. ap. J.-C.), Mémoires. Ausonius Editions.

Teodorescu, L., Ben Amara, A., Cantin, N., Chapoulie, R., Ducu, C., Ciucă, S., Tulugea, C., Terteci, C., Abrudeanu, M., 2021. Characterization of Archaeological Artefacts Using Methods Specific to Materials Science: The Case Study of Dacian Ceramics from 2nd c. BC to 1st c. AD. Materials 14, 3908. https://doi.org/10.3390/ma14143908

Teodorescu, L., Cantin, N., Ben Amara, A., Chapoulie, R., Roux, V., 2022. Mineralogical transformations due to salt whitening agent in modern Hebron ceramics. Journal of Archaeological Science: Reports 41, 103303. https://doi.org/10.1016/j.jasrep.2021.103303

Thér, R., 2020. Ceramic technology. How to reconstruct and describe pottery-forming practices. Archaeol Anthropol Sci 12, 172. https://doi.org/10.1007/s12520-020-01131-0

Tian, W., 2016. A Multi-scale Study of Ancient Ceramics Using a Series of Analytical Techniques. Universite de Toulouse, Institut National des Sciences Appliquees de Toulouse.

Tite, M. s, 2008. Ceramic production, provenance and use - A review. Archaeometry 50, 216–231. https://doi.org/10.1111/j.1475-4754.2008.00391.x

Tite, M.S., 1999. Pottery Production, Distribution, and Consumption—The Contribution of the Physical Sciences 53.

Traoré, K., Kabré, T.S., Blanchart, P., 2003. Gehlenite and anorthite crystallisation from kaolinite and calcite mix. Ceram. Int. 29, 377–383. https://doi.org/10.1016/S0272-8842(02)00148-7

Trindade, M.J., Dias, M.I., Coroado, J., Rocha, F., 2009. Mineralogical transformations of calcareous rich clays with firing: A comparative study between calcite and dolomite rich clays from Algarve, Portugal. Appl. Clay Sci. 42, 345–355. https://doi.org/10.1016/j.clay.2008.02.008

Tschegg, C., Ntaflos, T., Hein, I., 2009. Thermally triggered two-stage reaction of carbonates and clay during ceramic firing — A case study on Bronze Age Cypriot ceramics. Appl. Clay Sci. 43, 69–78. https://doi.org/10.1016/j.clay.2008.07.029

Tsetlin, Y., 2003. Organic tempers in ancient pottery. Ceramic in Society: Proceedings of the 6th European Meeting on Ancient Ceramics, Fribourg 289–306.

Tuţulescu, I., Schuster, C., Dumitrescu, I., 2012. “Zum Salz im Nordosten Olteniens (Rumänien) in der Vorgeschichte bis ins Mittelalter. Eine Einführung” ‘Salt and Gold:The Role of Salt in Prehistoric Europe.’ Provadia - Veliko Tarnovo 201–212.

Tykot, R.H., 2004. Scientific methods and applications to archaeological provenance studies. Physics Methods in Archaeometry 407–432. https://doi.org/10.3254/978-1-61499-010-9-407

Vandiver, P.B., Soffer, O., Klima, B., Svoboda, J., 1989. The origins of ceramic technology at dolni vecaronstonice, czechoslovakia. Science 246, 1002–1008. https://doi.org/10.1126/science.246.4933.1002

Velde, B., Druc, I.C., 1999. Archaeological Ceramic Materials, Natural Science in Archaeology. Springer Berlin Heidelberg, Berlin, Heidelberg. https://doi.org/10.1007/978-3-642-59905-7

von der Crone, M.J., Maggetti, M., 1998. Experimental firing of clays using salt water. Presented at the Archaeometry 98, BAR International Series, Oxford, pp. 249–255.

Worrall, W.E., 1982. Ceramic raw materials. Pergamon Press, New York.

ANNEXES

Figure 1A Selected ceramics sherds for analysis, from the archaeological site Câmpulung – Jidova (samples provided by Museum of Argeş district, Piteşti, lot 1)

Figure 2A Selected ceramics sherds for analysis, from the archaeological site Câmpulung – Jidova (samples provided by Museum of Argeş district, Piteşti, lot 2)

Figure 3A Selected ceramics sherds for analysis, from the archaeological site Cetăţeni (samples provided by Museum of Argeş district, Piteşti

Figure 4A Selected ceramics sherds for analysis, from the archaeological site Valea Stânii (samples provided by Museum of Argeş district, Piteşti)

N° Sample	Laboratory	Analysis Type	SiO2	Al2O3	Fe2O3	TiO2	CaO	MgO	K2O	MnO	Sr	Zr	Rb	Y	Cr	Zn	Ni	V	Ba	Ce
BDX 15773	Caen	ICP-AES	57.4	14.0	6.4	0.9	17.0	1.9	2.2	0.2	342	148	124	29	0	0	0	127	414	0
BDX 15784	Caen	ICP-AES	62.6	14.9	6.9	0.9	9.4	2.2	2.7	0.2	240	158	136	30	0	0	0	142	453	0
BDX 17740	Caen	ICP-AES	68.0	16.9	9.5	1.1	0.6	0.9	2.4	0.4	60	966	121	116	0	0	0	96	280	0
BDX 17732	Caen	ICP-AES	64.0	19.2	10.4	1.2	0.9	1.1	2.6	0.5	72	904	123	75	0	0	0	113	441	0
BDX 24955	Lyon	WDXRF	62.4	18.2	5.7	0.7	7.4	1.9	3.4	0.1	310	317	204	34	89	104	41	103	541	131
BDX 24952	Lyon	WDXRF	66.5	16.6	6.5	0.7	4.1	2.3	2.9	0.2	197	135	140	22	133	111	71	128	363	79
BDX 19621	Caen	ICP-AES	71.3	25.8	0.7	0.7	0.8	0.2	0.5	0.1	30	141	31	19	41	27	33	42	84	21
BDX 19627	Caen	ICP-AES	73.7	22.9	0.6	0.3	0.6	0.2	1.7	0.1	85	27	165	15	40	53	47	63	192	46
Min			57.4	14.0	0.6	0.3	0.6	0.2	0.5	0.1	30	27	31	15	40	27	33	42	84	21
Max			73.7	25.8	10.4	1.2	17.0	2.3	3.4	0.5	342	966	204	116	133	111	71	142	541	131

Table 1A Chemical composition of 8 internal standards (archaeological ceramics) analyzed previously in other French partners laboratory by liquid ICP-AES (Caen) and WD-XRF (Lyon)

Table 2A SARM69 - Certified property values and confidence limits (all values relate to the dried (110°) material.

CERTIFIED PROPERTY VALUES AND CONFIDENCE LIMITS

SARM 69	95 % Confidence Limits		
Constituent	Certified value %	Low	High
SiO_2	66,6	66,1	67,1
Al_2O_3	14,4	14,2	14,5
Total Fe as Fe_2O_3	7,18	7,10	7,25
CaO	2,37	2,33	2,41
K_2O	1,96	1,92	2,00
MgO	1,85	1,83	1,88
MnO	0,129	0,127	0,132
TiO_2	0,777	0,769	0,785
	Certified value mg/kg		
Ba	518	499	537
Cr	223	215	230
Zn	68	65	70
Ni	53	51	54
Cu	46	43	48
Co	28	27	29
Sc	20	19	21

Figure 5A: Differences using and without using the collimator, for each chemical element, of sample section BDX 16854.

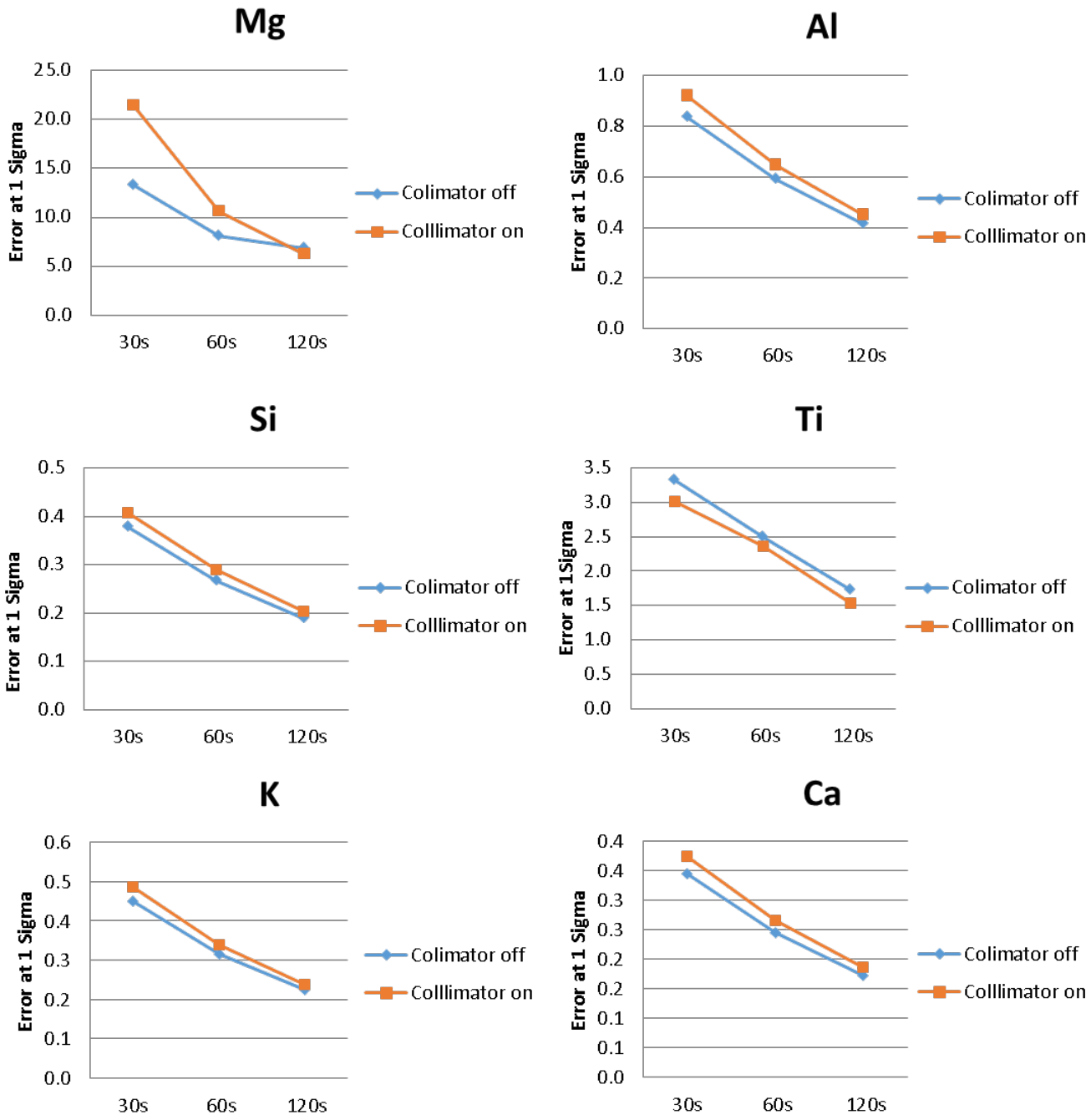

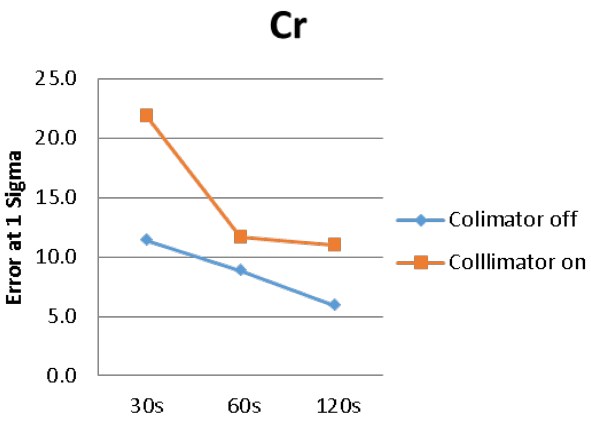
Cr
Error at 1 Sigma
25.0
20.0
15.0
10.0
5.0
0.0
30s
60s
120s
Colimator off
Colllimator on

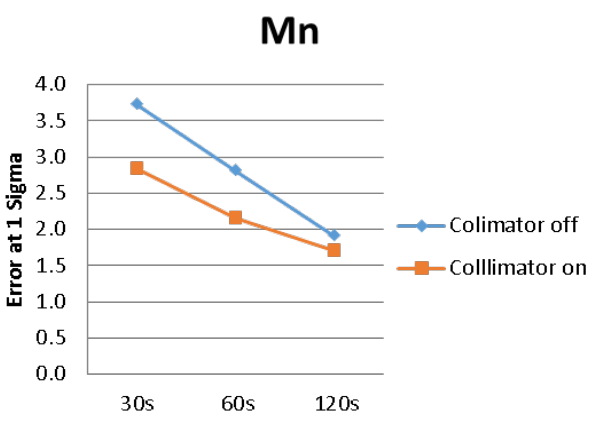
Mn
Error at 1 Sigma
4.0
3.5
3.0
2.5
2.0
1.5
1.0
0.5
0.0
30s
60s
120s
Colimator off
Colllimator on

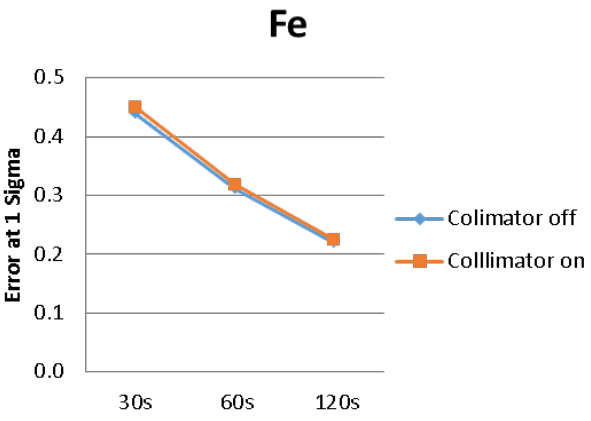
Fe
Error at 1 Sigma
0.5
0.4
0.3
0.2
0.1
0.0
30s
60s
120s
Colimator off
Colllimator on

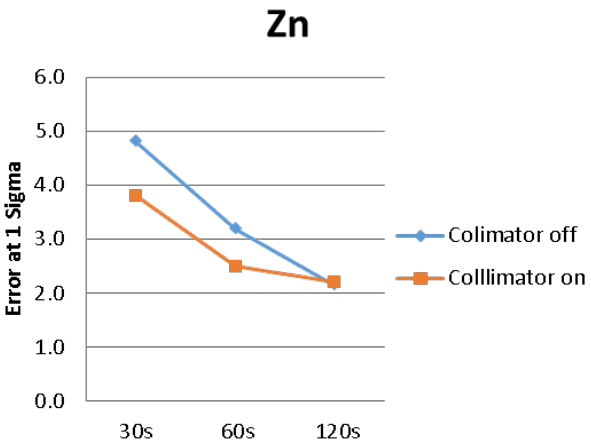
Zn
Error at 1 Sigma
6.0
5.0
4.0
3.0
2.0
1.0
0.0
30s
60s
120s
Colimator off
Colllimator on

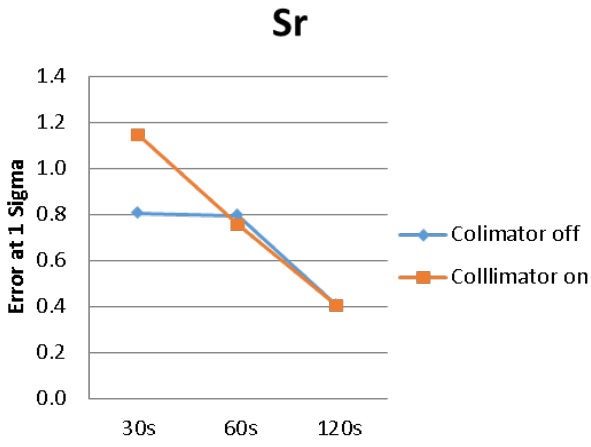
Sr
Error at 1 Sigma
1.4
1.2
1.0
0.8
0.6
0.4
0.2
0.0
30s
60s
120s
Colimator off
Colllimator on

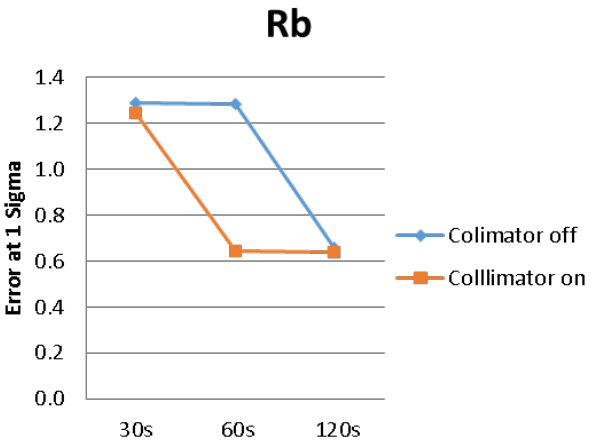
Rb
Error at 1 Sigma
1.4
1.2
1.0
0.8
0.6
0.4
0.2
0.0
30s
60s
120s
Colimator off
Colllimator on

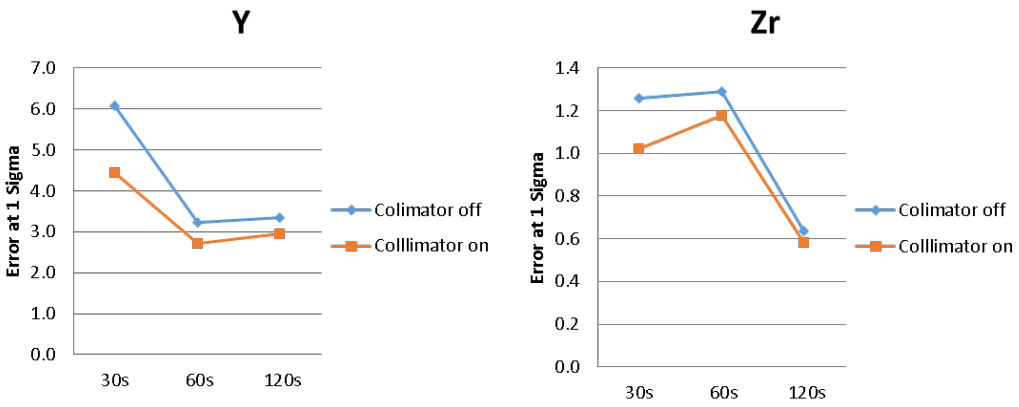
Y
Error at 1 Sigma
7.0
6.0
5.0
4.0
3.0
2.0
1.0
0.0
30s
60s
120s
Colimator off
Colllimator on
Zr
Error at 1 Sigma
1.4
1.2
1.0
0.8
0.6
0.4
0.2
0.0
30s
60s
120s
Colimator off
Colllimator on

Table 2A: Analyses made with the “Geochem” mode and factor correction (Geochem_corr), and their deviation compared to the reference.

BDX16854	Geochem	Geochem_cor	Reference	Dev. Geochem	Dev. Geochem_corr
Si	58.2	57.3	60.5	2.3	3.2
Al	16.3	15.8	15.4	-0.9	-0.4
Fe	7.1	8.2	7.0	-0.1	-1.1
Ti	0.9	1.0	0.9	0.1	0.1
Ca	12.1	11.9	9.8	-2.3	-2.1
Mg	2.3	2.2	2.4	0.1	0.2
K	2.8	3.3	2.8	0.1	-0.5
Mn	0.16	0.2	0.2	0.1	0.1
Sr	258	289	246	-11.6	-42.6
Zr	161	169	145	-16.5	-23.9
Rb	154	168	148	-5.8	-19.9
Y	32	33	28	-3.7	-4.9
Zn	106	104	n.d	-105.6	-103.7
Cr	219	238	n.d	-219.3	-237.6

BDX17729	Geochem	Geochem_cor	Reference	Dev. Geochem	Dev. Geochem_corr
Si	65.9	65.2	65.8	-0.1	0.6
Al	19.2	18.5	18.1	-1.0	-0.3
Fe	10.1	11.4	10.6	0.5	-0.8
Ti	1.0	1.1	1.0	0.1	0.1
Ca	0.5	0.8	0.6	0.1	-0.2
Mg	1.1	1.1	0.9	-0.2	-0.2
K	1.8	2.2	2.4	0.6	0.3
Mn	0.3	0.3	0.4	0.1	0.1
Sr	46.7	52.1	56.0	9.3	3.9
Zr	1103	1015	1171	67.9	156.3
Rb	95	103	112	17.2	9.1
Y	107	108	115	7.7	7.4
Zn	201	231	n.d	-201.0	-230.8
Cr	165	189	n.d	-165.0	-189.5

BDX21063	Geochem	Geochem_cor	Reference	Dev. Geochem	Dev. Geochem_corr
Si	69.8	69.2	70.6	0.9	1.5
Al	27.5	26.3	26.3	-1.2	0.0
Fe	0.7	1.2	0.8	0.1	-0.5
Ti	0.4	0.4	0.4	0.1	-0.1
Ca	0.4	0.7	0.6	0.2	-0.1
Mg	0.2	0.3	0.2	0.1	-0.1
K	0.8	1.0	0.9	0.1	-0.1
Mn	0.1	0.1	0.1	0.1	0.1
Sr	63.8	71.3	65.0	1.2	-6.3
Zr	55	74	42	-13.3	-31.6
Rb	101	109	114	13.2	4.6
Y	15	16	33	17.9	16.6
Zn	137	145	103	-33.5	-41.9
Cr	24	64	88	64.4	23.6

SARM69	Geochem	Geochem_cor	Reference	Dev. Geochem	Dev. Geochem_corr
Si	69.1	68.5	69.9	0.8	1.4
Al	17.1	16.5	15.1	-2.0	-1.4
Fe	6.5	7.5	7.5	1.0	0.1
Ti	0.7	0.8	0.8	0.1	0.1
Ca	2.4	2.6	2.5	0.1	-0.1
Mg	2.2	2.0	1.9	-0.2	-0.1
K	1.8	2.2	2.1	0.3	-0.1
Mn	0.1	0.1	0.1	0.1	0.1
Sr	102	114	114	12.2	0.1
Zr	257	255	284	27.1	29.4
Rb	57	61	69	12.2	7.9
Y	29	30	30	1.1	-0.1
Zn	68	54	71	3.3	17.7
Cr	257	271	234	-23.1	-37.0

materials

MDPI

Article

Characterization of Archaeological Artefacts Using Methods Specific to Materials Science: The Case Study of Dacian Ceramics from 2nd c. BC to 1st c. AD

Laura Teodorescu [1,2,*], Ayed Ben Amara [1], Nadia Cantin [1], Rémy Chapoulie [1], Cătălin Ducu [2], Sorin Ciucă [3], Claudiu Tulugea [4], Carol Terteci [4] and Mărioara Abrudeanu [2,5]

1 Institut de Recherche sur les Archéomatériaux—Centre de Recherche en Physique Appliquée à L'archéologie, IRAMAT-CRP2A, UMR5060 CNRS—Université Bordeaux Montaigne, CEDEX 33607 Pessac, France; ayed.ben-amara@u-bordeaux-montaigne.fr (A.B.A.); ncantin@u-bordeaux-montaigne.fr (N.C.); chapouli@u-bordeaux-montaigne.fr (R.C.)
2 Department of Materials Science and Engineering, University of Pitesti, 110040 Pitesti, Romania; catalinducu@yahoo.com (C.D.); abrudeanu@gmail.com (M.A.)
3 Department of Materials Science and Engineering, University Politehnica of Bucharest, 060042 Bucharest, Romania; sorin.ciuca@upb.ro
4 "Aurelian Sacerdoțeanu" Vâlcea County Museum, 240096 Râmnicu Vâlcea, Romania; claudiu.tulugea@yahoo.com (C.T.); terteci.carol@gmail.com (C.T.)
5 Department of Materials Science and Engineering, Technical Sciences Academy of Romania, 030167 Bucharest, Romania
* Correspondence: laura.teodorescu93@gmail.com

Abstract: Combined analysis methods such as optical microscopy (OM), cathodoluminescence (CL) microscopy, X-ray diffraction (XRD), and scanning electron microscopy–energy dispersive X-ray spectrometry (SEM–EDX) have made it possible to obtain the first physico-chemical data of Dacian potsherds, exhumed at the archeological site of Ocnița-Buridava, Romania; the samples were provided by the "Aurelian Sacerdoțeanu" County Museum Vâlcea, dating from the 2nd century BC to the 1st century AD. The mineralogical and petrographic analyses revealed two types of ceramic pastes, taking into account the granulometry of the inclusions and highlighting the choice of the potter for fabricating the ceramic either by wheel or by hand. All samples showed an abundance in quartz, mica (muscovite and biotite), and feldspars. These observations were confirmed by cathodoluminescence imagery, revealing heterogeneous pastes with varied granulometric distributions. The XRD patterns indicated the presence of the mineral phases, indicating a firing temperature below 900 °C. The wheel-made ceramics have a fine, compact matrix with very fine inclusions (<40 μm). On the other hand, the hand-made ceramics present a coarse matrix, with inclusions whose granulometry reaches approximately 2 mm. The difference between these two types of ceramics is also confirmed by the mineralogical and chemical analysis. The wheel-made potsherds are more abundant in MgO, Al_2O_3, and CaO contents.

Keywords: Dacian archaeological ceramic; materials science; mineralogy; petrography; cathodoluminescence; XRD; SEM–EDX

Citation: Teodorescu, L.; Ben Amara, A.; Cantin, N.; Chapoulie, R.; Ducu, C.; Ciucă, S.; Tulugea, C.; Terteci, C.; Abrudeanu, M. Characterization of Archaeological Artefacts Using Methods Specific to Materials Science: The Case Study of Dacian Ceramics from 2nd c. BC to 1st c. AD. *Materials* **2021**, *14*, 3908. https://doi.org/10.3390/ma14143908

Academic Editor: Cornel Samoilă

Received: 7 June 2021
Accepted: 8 July 2021
Published: 13 July 2021

1. Introduction

Pottery and, more precisely, ceramic artefacts are one some of the most studied objects by archeologists, since they can be found in large amounts in the majority of archeological sites, dating from the Neolithic period onwards. Therefore, the study of these objects has been essential to the archeological interpretation of a site, region and period. The analytical techniques that have been developed in the field of materials science are widely applied to the study of the ancient objects of art and archaeology, in order to obtain information about the composition and structure of the material used [1–3].

One of the main aspects in approaching the study of archaeological materials is to properly identify the type of material that is being investigated, which is the first step in interpreting how it was made, its field of use, its origin, and other cultural information related to the human community. Archaeometric methods involve the integration of exact sciences, especially physics, chemistry, and materials science, in the study of artifacts. It should be taken into account the fact that each analytical technique offers advantages but also limitations, so a broad vision is needed to understand the obtained results [4].

The main aim of this ongoing research is to determine the chemical and mineralogical characteristics of ceramics and to see if it is possible to discriminate ceramics according to their manufacturing technique [5]. These datasets allow the formulation of hypotheses on the nature of the raw materials used and the heat treatments applied. The first aspect focuses on the petrographic analysis (imagery-data) of ceramic fragments. These analyses provide information such as the mineralogical composition of the clay sediment used in the formation of ceramics. The images are then be correlated with the images acquired by the cathodoluminescence. The second aspect focuses on X-ray diffraction in order to determine the mineral content of the potsherds. The results are then compared with petrographic observations to confirm the presence of certain minerals/phases. Finally, the third aspect focuses on the analysis with SEM–EDX. It provides information about the chemical composition of major and minor elements, as well as information about the micro-texture of the ceramics.

2. Materials and Methods

2.1. Archaeological Context and Potsherd Descriptions

In 1973, excavations were carried out by D. Berciu's team from the Institute of Archaeology in Bucharest in the area of the archeological site of Ocnița; fragments of ceramic, metal, and glass objects were discovered [6–8]. The Dacian city was of great importance to the region; however, after the Roman conquest, the Dacian city began to lose its prestige [9]. Archaeological discoveries have highlighted the role and status of the Dacian settlement in trade with the Roman world, as well as the existence of a possible center of dynastic power. The area is well known for its richness in salt since prehistory. The Latin inscriptions, the numerous Roman artifacts, and the chronology give Buridava a special status, even during the 1st century BC [10–12].

In this study, 10 different ceramic fragments were selected (Table 1). They come from incomplete vessels, discovered during the excavations, dating from the La Tène culture. The archeologists provided five wheel-made potsherds Figure A1) and five hand-made potsherds (Figure A2) for our research. They selected the samples based on macroscopic observations (morphology and topography of the surface and fresh-fractures), the color of the ceramic body, granulometry, and the proportion of inclusions corresponding to their manufacturing technique. The samples were indexed at Bordeaux laboratory (IRAMAT-CRP2A), from BDX 24414 to BDX 24423. Two types of samplings were made per ceramic fragment in order to prepare on one hand powder and on the other, thick and thin sections.

2.2. Petrographic Analysis on Thin Sections

Petrographic analysis (OM) was used to characterize non-plastic inclusions in ceramic paste, especially minerals and rocks [13,14]. The inclusions were identified, as well as the shape and particle size distribution. The repartition and shape of the pores were also taken into account. The study was performed on thin sections orientated perpendicular to the vessel wall (thickness 30 µm) using a polarizing microscope (Leica Microsystems, Wetzlar, Germany) coupled to a LEICA DM2500 camera (Leica Microsystems, Wetzlar, Germany). LEICA Application Suite V3 software was used to acquire and record the images. The images were transmitted in parallel and cross-polarized light. For the description of thin ceramic sections, F.J Pettijohn's diagrams were used to assess the particle size distribution and pore shape [15].

Table 1. Detailed context and features of potsherds studied in this research (YD—year of discovery, Tr.—trench number).

Technology Group	Sample ID	Archaeological Context	Category	Object Type
Wheel-made	BDX 24414	YD. 1975, Tr. XXVE	Fine	Pitcher
	BDX 24415	YD. 1976, Tr. XXIX		Fruit bowl
	BDX 24416	YD. 1975, Tr. XXVF		Fruit bowl
	BDX 24417	YD. 1968, Tr. Xa		Bowl
	BDX 24418	YD. 1974, Tr. XXVD		Bowl
Hand-made	BDX 24419	YD. 1975, Tr. XXVF	Coarse	Bowl
	BDX 24420	YD. 1974, Tr. XXVD		Bowl
	BDX 24421	YD. 1968, Tr. Xa		Bowl
	BDX 24422	YD. 1974, Tr. XXVD		Bowl
	BDX 24423	YD. 1975, Tr. XXVF		Bowl

2.3. Cathodoluminescence (CL) on Thick Sections

Cathodoluminescence (CL) (i.e., the emission of photons in the visible wavelength range of the electromagnetic spectra under cathode excitation) is a very helpful method used for the study of ceramics [16]. When the surface of a material is bombarded by the beam of electrons, the result is a photon emission in the spectrum (near UV-IR visible) [17–19]. For analysis, the Cathodyne OPEA equipment updated (Microvision Instruments, Evry, France) has a cold cathode cathodoluminescence system, paired with a Leica M125 binocular magnifier and a Leica DFC4500 digital camera (Leica Microsystems, Wetzlar, Germany) to capture images (using LAS software). The electron beam was fixed and positioned at 45° to the surface of the part. The exposure time for CL images was about 15 s with a current density of 10 µA. It is a non-destructive analysis regarding the integrity of the ceramic material.

2.4. X-ray Diffraction (XRD) on Powder

The XRD measurements were performed on powder to identify the minerals in the ceramic body, using a diffractometer (D8-Advance, set in Bragg–Brentano reflection mode, Bruker AXS, Karlsruhe, Germany) and an X-ray tube with Cu Kα radiations operating at 40 kV and 40 mA. The measurements were recorded from 3° to 60°, with a scan step size of 0.01° and an acquisition time step of 1 s. Qualitative analysis of the obtained diffractograms was realized with EVA software using the PDF-2004 database from ICDD. In addition, a Rietveld refinement was applied by using TOPAS software, in order to quantify the mineral phases.

2.5. SEM–EDX on Pellets and Thick Sections

SEM imagery (JEOL-IT500 HR, JEOL Ltd., Tokyo, Japan) made it possible to observe the micro-texture of the samples on thick polished sections. The microscope was used in low-vacuum mode with a pressure of 30 Pa. The parameters used for the analysis of the samples were an acceleration voltage of 20 kV and a probe current from 10^{-10} to 5×10^{-9} A. Micrographs were recorded in back-scattered electron mode (BSE). The acquisition of the spectra (performed with a double EDX, Oxford Instruments UltimMax 100, Oxford Instruments, Oxford, UK) was done on the clay matrix and powder pellets. The chemical composition was obtained by quantification from the average of 4 areas of 0.58 mm^2 each. All results were expressed in wt.% oxides. Data obtained in low-vacuum mode offer results equivalent to those acquired in high-vacuum mode [20]. Quantification was determined using the ϕ (ρz) correction procedure for the AZtec NanoAnalysis (Oxford Instrument, Oxford, UK). This analysis made it possible to quantify major and minor elements such as Na_2O, MgO, Al_2O_3, SiO_2, SO_3, K_2O, CaO, TiO_2, MnO, and Fe_2O_3. Standard corrections were performed using the software's internal standard. Contents were calculated from

standards consisting of synthetic compounds and natural minerals. The detection limit for most elements was about 0.1 wt.%. It addition, the composition data were converted into a log ratio analysis, which made it possible to explore the interdependent relationships in the case of a multivariate dataset and to focus on the covariance and correlation between the variables [21,22].

3. Results

3.1. Petrographic Analysis

Information about the microstructure of ceramics is first obtained by analysis under a polarizing microscope. Petrographic analyses were performed on all 10 thin sections.

The petrographic analysis made it possible to observe the granulometry and the distribution of the inclusions, allowing us to make initial assumptions about the manufacturing techniques. Microscopically, all the ceramic bodies are mainly composed of quartz, feldspars, micas (biotite and muscovite), amphiboles, and voids (pores).

The wheel-made samples (from BDX 24414 to BDX 24418) show a fine and compact matrix. All these samples are very rich in very fine inclusions, which do not exceed 40 µm in size (Figure 1a,b). The size distribution of the non-plastic components presents a unimodal texture. It can be assumed that the clay raw material has been specially purified or selected. The presence of voids is low, demonstrating the compactness of the ceramic. The porosity seen under the microscope indicates a controlled and slow burning in special furnaces, such as the two-chamber furnace discovered at Buridava Dacică [23,24].

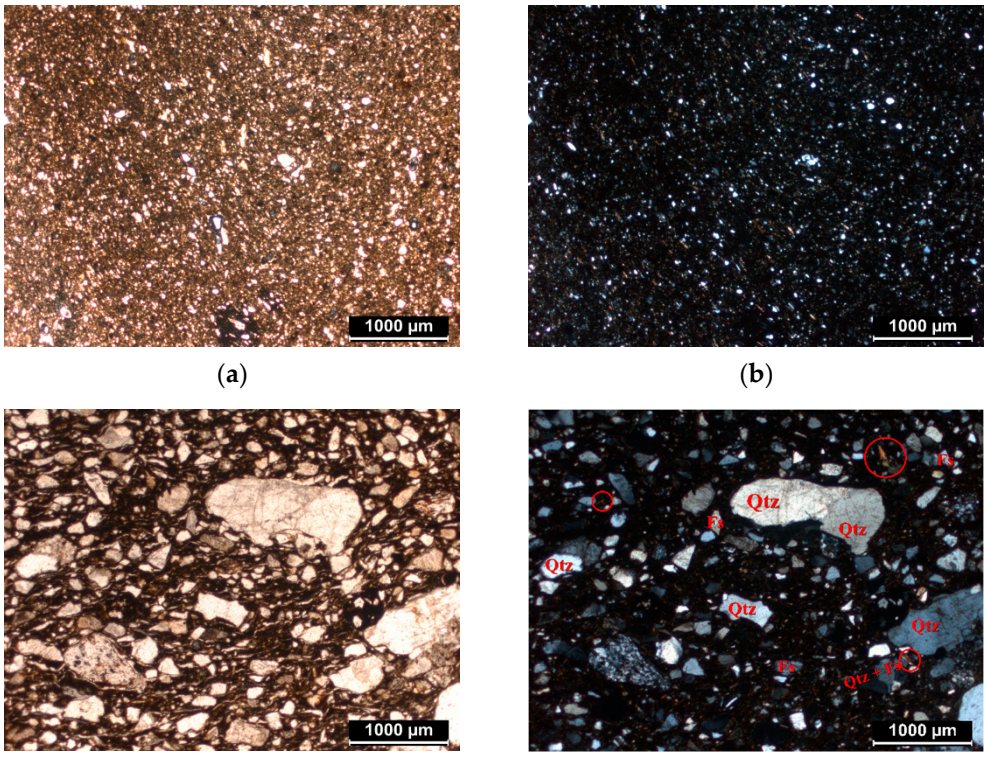

Figure 1. Petrographic observations: observation on matrix of BDX 24418 ((**a**) plane-polarized light, (**b**) cross-polarized light); observation of matrix of BDX 24419 ((**c**) plane-polarized light, (**d**) cross-polarized light). The identified minerals are mainly quartz (Qtz), altered feldspars (Fs) and mica (indicated by the circle).

In contrast, the hand-made samples also contain metamorphic rocks and acid plutonic rocks. They present a coarse matrix, with inclusions whose granulometry reaches approximately 2 mm (Figure 1c,d). The size distribution of the present inclusions present

a trimodal texture and the porosity observed is mainly represented by elongated voids. Usually, these voids are the primary pores, randomly distributed in the ceramic body. They are formed during the modelling process, when thin layers of water and/or air are trapped between the layers of clay. Then, after the drying and burning of the ceramic, the pore size primarily increases.

The difference in porosity typology between the samples produced by wheel and by hand may be the result of the variation of the molding technique.

Figure 1 shows images acquired with the polarizing microscope, highlighting the difference between a very fine matrix and a coarse one (with the same scale—1 mm).

3.2. Cathodoluminescence Imaging

The first results from cathodoluminescence made it possible to formulate hypotheses regarding the nature of the minerals in the clay matrix.

In the wheel-made samples, a compact ceramic body was observed, with low luminescent inclusions with yellow-green and blue color. As noticed in the petrography, the presence of the very fine and few inclusions provided evidence for the purified clay used for manufacture by wheel, which reflects the choice of the potter for obtaining a plastic clay.

For the hand-made samples, the CL images (Figure 2) show the presence of large angular inclusions (from approximately 1 mm to 2 mm) distributed in the matrix. Porosity was observed and identified in the CL images as dark green areas.

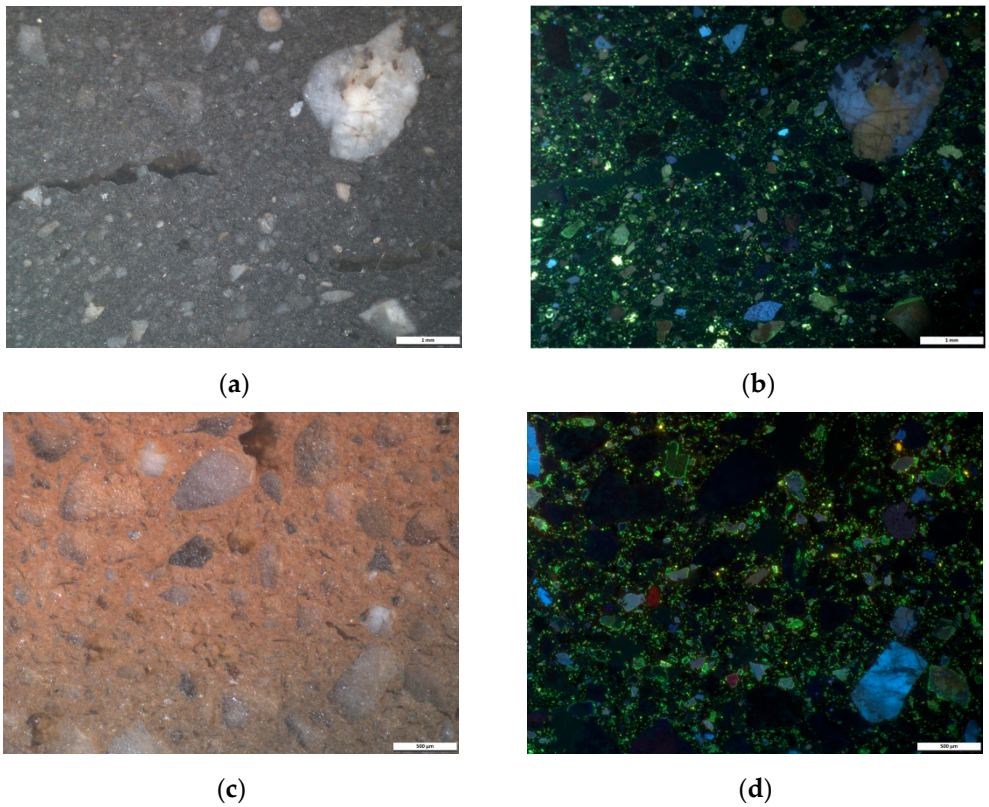

Figure 2. Observations in CL-imagery for ceramic fragments made by hand: sample BDX 24419 ((**a**) white light reflectance, (**b**) cathodoluminescence emission); and sample BDX 24420 ((**c**) white light reflectance, (**d**) cathodoluminescence emission).

As in the wheel-made samples, the main colors seen in CL were a blue luminescent color highlighting the presence of potassium feldspars, the yellow-green luminescence representing plagioclases, and a brownish luminescent color combined with non-luminescent minerals, which represent the quartz inclusions (Figure 2) [25].

In addition, since no inclusions with orange or red luminescent colors where observed in any of the samples, inclusions that are usually characterized as calcium carbonates [26] allowed us to make initial assumptions, such as the clay used by potters being a Ca-poor clay.

3.3. XRD Analysis

The X-ray diffraction analysis presented some differences considering the abundance or deficiency of the mineralogical phases (Table 2).

Table 2. Mineralogical composition (wt.%) according to X-ray diffraction analysis by Rietveld method. Hematite detected with a value of <1%.

Technology Group	Sample ID	Illite-Muscovite	Biotite	Quartz	Microcline	Orthoclase	Albite	Anorthite	Hornblende
Wheel-made	BDX 24414	22	3	36	6	5	18	9	1
	BDX 24415	11	4	35	20	1	35	14	3
	BDX 24416	11	3	32	16	5	32	14	5
	BDX 24417	31	8	23	9	5	23	12	5
	BDX 24418	21	7	29	17	1	29	11	4
Hand-made	BDX 24419	19	6	43	3	5	13	7	4
	BDX 24420	14	4	55	7	1	9	7	2
	BDX 24421	16	5	43	2	6	20	6	3
	BDX 24422	25	5	37	14	1	6	7	4
	BDX 24423	20	8	35	8	3	13	10	4

Initially, we noted a certain variability in each manufacturing-technique group, which can be seen in the high values of the standard deviation. In addition, we noted mineralogical differences between wheel-made and hand-made ceramics, in agreement with the petrographic analyses.

In all the samples, reflections of muscovite/illite were detected, although two samples from the wheel-made sample set (BDX 24415 and BDX 24416) showed lower values than the others. The quartz content is globally higher in the hand-made ceramics. In the wheel-made samples, higher values of microcline and anorthite were noted compared with the hand-made samples (Table 2).

It should be noted that illite-muscovite can be used as a thermal guide. Based on previous studies, Rodriguez-Navarro [27] explained that the muscovite crystals can face a significant change from heating at temperatures above 350 °C. Furthermore, previous studies have demonstrated the fact that illite (muscovite) is completely decomposed at about 900 °C [28,29]. In addition, the anorthite detected in all the samples did not result from a transformation at a high temperature during newly formed Ca phases, but rather, from a natural presence in the clayey sediments used for the manufacture of the ceramics. To summarize, in all the samples, the firing temperature was relatively low (below 900 °C), which is in agreement with their porosity aspects.

3.4. SEM–EDX Analysis

The SEM observations revealed the microtexture of the potsherds made by wheel and by hand. In addition, SEM–EDX analyses were performed on both the ceramic powder and thick sections.

The SEM images revealed a compact matrix and the presence of fine inclusions present in the potsherds made by wheel, confirming the observations by petrography and cathodoluminescence. In addition, regarding the size of the inclusions, a clear difference was observed corresponding to the two manufacturing-technique groups (Figure 3).

Due to SEM–EDX, the values obtained for the powder samples were expressed in oxide percentages, choosing the average value of the spectra (Table 3).

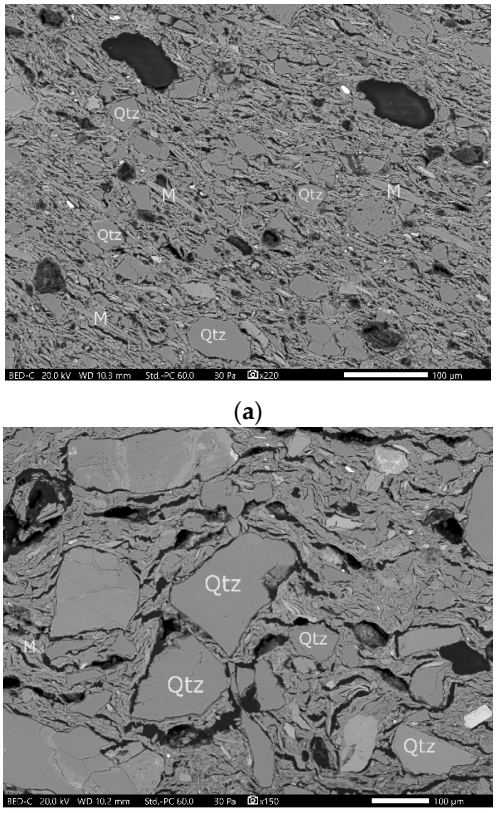

Figure 3. BSE SEM images showing quartz (Qtz) and mica (M) inclusions: (**a**) sample BDX 24414, scale 100 μm; (**b**) sample BDX 24421, scale 100 μm.

Table 3. Chemical composition (wt.%) of potsherds obtained by SEM–EDX (SD—standard deviations, number of measurements: n = 4).

Technology Group	Sample ID	Na_2O	MgO	Al_2O_3	SiO_2	P_2O_5	K_2O	CaO	TiO_2	MnO	Fe_2O_3
Wheel-made	BDX 24414	1.1	2.4	19.4	61.8	1.0	3.3	2.7	0.9	0.1	7.2
	BDX 24415	1.4	3.5	19.1	57.8	0.8	3.5	5.2	0.9	0.1	7.6
	BDX 24416	1.3	3.6	19.2	58.7	0.5	3.6	4.1	1.0	0.1	7.9
	BDX 24417	1.1	3.2	21.1	58.4	2.1	3.6	1.8	1.0	0.1	7.7
	BDX 24418	1.1	3.2	20.1	58.7	1.5	3.6	2.7	1.0	0.1	8.0
	Average	1.2	3.2	19.8	59.1	1.2	3.5	3.3	1.0	0.1	7.7
	SD	0.1	0.5	0.8	1.6	0.6	0.1	1.3	0.1	0.1	0.3
Hand-made	BDX 24419	1.7	1.4	17.4	67.1	1.5	2.5	1.6	0.7	0.2	5.9
	BDX 24420	1.6	1.4	17.4	67.1	1.6	2.5	1.6	0.7	0.2	6.0
	BDX 24421	1.5	1.7	15.7	69.7	0.7	2.6	1.2	0.8	0.1	6.1
	BDX 24422	0.9	1.8	18.5	64.3	1.4	3.5	1.3	0.8	0.2	7.1
	BDX 24423	1.6	1.9	17.7	66.2	0.8	2.7	1.5	0.8	0.1	6.6
	Average	1.5	1.6	17.3	66.9	1.2	2.8	1.4	0.8	0.2	6.3
	SD	0.3	0.2	1.0	1.9	0.4	0.4	0.2	0.1	0.1	0.5

The matrix of all the samples indicates the following composition: 58–70% SiO_2, 16–21% Al_2O_3, 1–5% CaO, 6–8% Fe_2O_3, 3–4% K_2O, and 1–4% MgO. Therefore, the clay presents as a Ca-poor one, with a dominant alumino-silicate matrix, as observed by petrography and CL. The high calcium content (in comparison to the CaO content from the hand-made ceramics) in the wheel-made ceramics is likely correlated to the anorthite content.

Furthermore, it was noted that two groups of chemical composition can be distinguished by the Al_2O_3, SiO_2, CaO, and MgO content (Table 3), in concordance with the manufacture-type groups. The group represented by the potsherds made by wheel is

more abundant in MgO, Al_2O_3, and CaO contents, with less SiO_2 content. In order to achieve a better visualization of these two groups, binary diagrams using log-ratios on Al_2SiO_3/SiO_2-MgO/SiO_2 and CaO/SiO_2-MgO/SiO_2 were made (Figure 4). The differences observed between the two groups for microtexture and mineralogy are reinforced by the chemical data. Based on these results, it is most likely that the clay sediments employed are different and were chosen to adapt to the manufacturing technique (more inclusions for the hand-made ceramics).

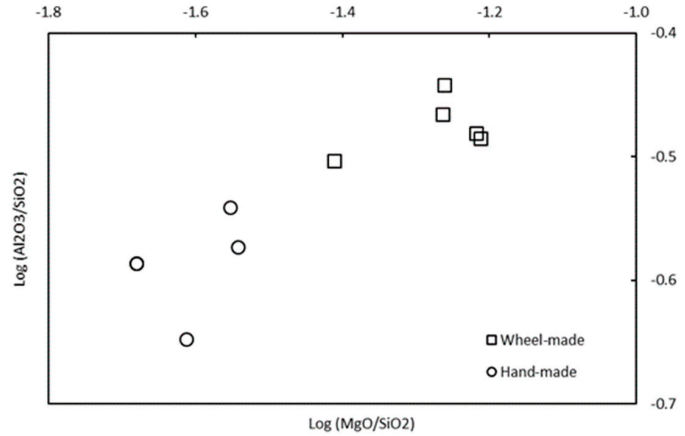

(**a**)

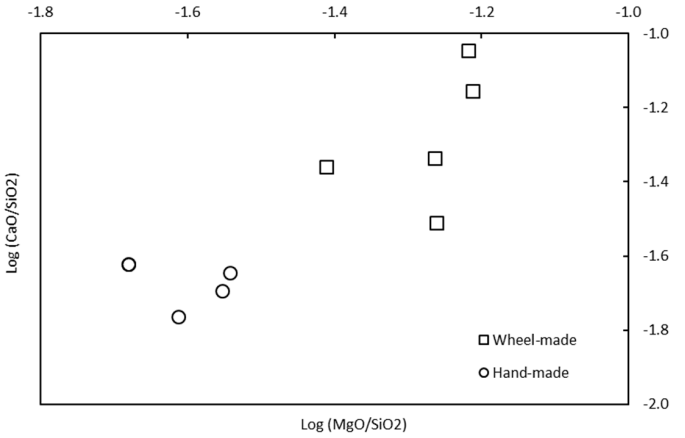

(**b**)

Figure 4. Binary diagrams of potsherds (square-shape potsherds made by hand; circle-shape potsherds made by wheel) expressed in log Al_2O_2/Si-log MgO/SiO_2 (**a**) and log CaO/SiO_2-log MgO/SiO_2 (**b**). Hand-made samples BDX 24419 and BDX 24421 present very close values, so their points are overlapping.

4. Conclusions

Combined analysis methods made it possible to distinguish two types of ceramic manufacturing techniques for ten Dacian potsherds, exhumed at the archeological site of Ocnița-Buridava, Romania, dating from the 2nd century BC to the 1st century AD.

Non-calcareous clay sediments were used to make all the ceramics. We observed a major difference in grain size between the ceramic sherds. Those made by hand are coarser. Petrographic analysis, cathodoluminescence and SEM images show that the proportion of inclusions (mostly quartz, muscovite, and albite) is higher in this group. The granulometric distribution suggests that these non-plastic inclusions were initially present in the clay sediment rather than temper added by the potter. The presence of these inclusions reduces the plasticity of the clays and provides a more suitable raw material for the manufacture of hand-made ceramics.

At this stage of the study, and from the limited number of samples, we have noted differences in terms of texture and chemical and mineralogical compositions between the ceramics according to their manufacturing technique. Fine clay sediments (eventually obtained by removing a large part of the inclusions) were chosen to make the ceramics by wheel, and coarse clay sediments to make the ceramics by hand. For all the ceramics, the firing temperature was relatively below 900 °C, in agreement with their porosity aspects. It is necessary to extend this study to a larger number of samples and to other nearby sites to confirm these initial results; nevertheless, these initial investigations have allowed the generation of archaeometric data that will enable the creation of an initial database for future comparisons when additional data are recorded.

Author Contributions: Data curation, L.T.; Funding acquisition, C.D.; Investigation, L.T., A.B.A. and N.C.; Methodology, L.T., A.B.A. and N.C.; Project administration, R.C., C.D. and M.A.; Resources, C.T. (Claudiu Tulugea) and C.T. (Carol Terteci); Supervision, A.B.A., N.C., R.C., C.D., S.C. and M.A.; Validation, R.C., C.D., S.C., C.T. (Claudiu Tulugea), C.T. (Carol Terteci) and M.A.; Visualization, A.B.A. and N.C.; Writing—original draft, L.T.; Writing—review & editing, A.B.A., N.C., R.C. and C.T (Carol Terteci). All authors have read and agreed to the published version of the manuscript.

Funding: We gratefully acknowledge financial support from the University of Pitesti and the Research Group CRC&D-Auto (Romania).

Institutional Review Board Statement: Not applicable.

Informed Consent Statement: Not applicable.

Data Availability Statement: The data presented in this study are available on request from the corresponding author.

Acknowledgments: We thank the Institut de recherche sur les Archéomatériaux–Centre de recherche en physique appliquée à l'archéologie (IRAMAT-CRP2A UMR 5060) of the Bordeaux Montaigne University-CNRS, for allowing to use their OM, Cathodoluminescence, XRD, and SEM–EDX facilities. We are thankful to the three anonymous referees for their critical reading and sugestions, which helped to improve the paper.

Conflicts of Interest: The authors declare no conflict of interest.

Appendix A

Figure A1. Description of ceramic fragments made by wheel, donated by the museum of Rm. V âlcea "Aurelian Sacerdoțeanu", Vâlcea County History Museum. The wheel was used at all stages of the manufacturing process.

Figure A2. Description of ceramic fragments made by hand, donated by the museum of Rm. Vâlcea "Aurelian Sacerdoțeanu", Vâlcea County History Museum.

References

1. Tite, M. Ceramic production, provenance and use—A review. *Archaeometry* **2008**, *50*, 216–231. [CrossRef]
2. Sciau, P.; Goudeau, P. Ceramics in art and archaeology: A review of the materials science aspects. *Eur. Phys. J. B* **2015**, *88*, 132. [CrossRef]
3. Montana, G.; Cau Ontiveros, M.Á.; Polito, A.M.; Azzaro, E. Characterisation of clayey raw materials for ceramic manufacture in ancient Sicily. *Appl. Clay Sci.* **2011**, *53*, 476–488. [CrossRef]
4. Vandenabeele, P.; Edwards, H. *Analytical Archaeometry: Selected Topics*, 1st ed.; Royal Society of Chemistry: Cambridge, UK, 2012.
5. Thér, R. Ceramic technology. How to reconstruct and describe pottery-forming practices. *Archaeol. Anthropol. Sci.* **2020**, *12*, 172. [CrossRef]
6. Iosifaru, M. Situri Arheologice din Oraşul Ocnele Mari, Judeţul Vâlcea Buridava IX, 13. 2011. Available online: http://www.muzee-valcea.ro/buridava/B9_07.iosifaru.pdf (accessed on 5 February 2021).
7. Institutul Național al Patrimoniului. *Cronica Cercetărilor Arheologice Campania 2016*; Institutul Național al Patrimoniului: Bucharest, Romania, 2016.
8. Tuţulescu, I.; Schuster, C.; Dumitrescu, I. Zum Salz im Nordosten Olteniens (Rumänien) in der Vorgeschichte bis ins Mittelalter. Eine Einführung. In *Salt and Gold: The Role of Salt in Prehistoric Europe; Proceedings of the International Symposium, Provadia, Bulgaria, 30 September–4 October 2010*; Verlag Faber: Veliko Tarnovo, Bulgaria, 2012; pp. 201–212.
9. Crisan, I.H. *Civilizatia Geto-Dacilor*; Editura Meridiane: Bucarest, Romania, 1993.
10. Berciu, D. *Buridava Dacica*; Editura Academiei Republicii Socialiste: Bucuresti, Romania, 1981.
11. Berciu, D. *Ancient Peoples and Places Series*, 1st ed.; F.A. Praeger: London, UK, 1967.
12. Berciu, D.; Iosifaru, M. Săpăturile arheologice de la Ocniţa, jud. Vîlcea. *Materiale şi Cercetări Arheologice* **1980**, *14*, 183–185. [CrossRef]
13. Foucault, A.; Raoult, J.-F. *Dictionnaire de Géologie*, 7th ed.; Dunod: Bucharest, France, 2010.
14. Regert, M.; Guerra, M.-F.; Reiche, I. Physico-chimie des matériaux du patrimoine culturel—Partie 2. In *Techniques de l'Ingenieur*; Éditions des archives contemporaines: Paris, France, 2006; pp. 1–21.
15. Pettijohn, F.J.; Potter, P.E.; Siever, R. *Sand and Sandstone*; Springer Science & Business Media: New York, NY, USA, 2012.
16. Chapoulie, R.; Robert, B.; Casenave, S. The cathodoluminescence phenomenon used for the study of ancient ceramics and stones. *Cities Mem. Int. J. Cult. Herit. Risk* **2016**, *1*, 53–72.
17. Chapoulie, R.; Daniel, F. *Cathodoluminescence: Recherches sur une Méthode d'analyse en Archéométrie*; British Archaeological Reports, BAR S1700; British Archaeological Reports: Oxford, UK, 2007; pp. 1–16.
18. Chapoulie, R.; Delery, C.; Daniel, F.; Vendrell-Saz, M. Cuerda Seca Ceramics from Al-Andalus, Islamic Spain and Portugal (10th–12th Centuries Ad): Investigation with Sem–Edx and Cathodoluminescence. *Archaeometry* **2005**, *47*, 519–534. [CrossRef]
19. Dudley, R.J. The Use of Cathodoluminescence in the Identification of Soil Minerals. *J. Soil Sci.* **1976**, *27*, 487–494. [CrossRef]
20. Emery, L. Approches Archéométriques des Productions Faïencières Françaises du XVIIIe Siècle. Le cas de la Manufacture Babut à Bergerac (env. 1740–1789). Ph.D. Thesis, Université Michel de Montaigne Bordeaux 3, Bordeaux, France, 2012.

21. Aitchison, J. *The Statistical Analysis of Compositional Data. Monographs on Statistics and Applied Probability*; Chapman and Hall: London, UK; New York, NY, USA, 1986.
22. Frerebeau, N.; Ben Amara, A.; Cantin, N. Analyse de données de composition et identification des altérations géochimiques des matériaux céramiques: Le cas des productions d'un atelier ibérique (Teruel, Espagne; iie-ier siècles avant J.-C.). *ArchéoSciences* **2020**, *44-1*, 33–50. [CrossRef]
23. Anghel, D. Experimente de ardere a ceramicii in cuptoare de tip arhaic. *Terra Sebus* **2011**, *3*, 339–350.
24. Anghel, D. Influenta conditiilor de ardere asupra ceramicii. *Revista Terra Sebus* **2002**, *6*, 171–173.
25. Fonseca, R.; Couto, H. Application of Cathodoluminescence to the Study of Feldspars: Imaging and Spectrometry. *IOP Conf. Ser. Earth Environ. Sci.* **2017**, *95*, 032029. [CrossRef]
26. Piponnier, D.; Bechtel, F.; Florin, D.; Molera, J.; Schvoerer, M.; Vendrell, M. Apport de la Cathodoluminescence à l'Etude des Transformations de Phases Cristallines dans des Céramiques Kaolinitiques Carbonatées. *Key Eng. Mater.* **1997**, *132–136*, 1470–1473. [CrossRef]
27. Rodriguez-Navarro, C.; Cultrone, G.; Sanchez-Navas, A.; Sebastian, E. TEM study of mullite growth after muscovite breakdown. *Am. Mineral.* **2003**, *88*, 713–724. [CrossRef]
28. Bohor, B.F. High-Temperature Phase Development in Illitic Clays. *Clays Clay Miner.* **1963**, *12*, 233–246. [CrossRef]
29. Holakooei, P.; Tessari, U.; Verde, M.; Vaccaro, C. A new look at XRD patterns of archaeological ceramic bodies: An assessment for the firing temperature of 17th century haft rang tiles from Iran. *J. Therm. Anal. Calorim.* **2014**, *118*, 165–176. [CrossRef]

Journal of Archaeological Science: Reports 41 (2022) 103303

Contents lists available at ScienceDirect

Journal of Archaeological Science: Reports

journal homepage: www.elsevier.com/locate/jasrep

Mineralogical transformations due to salt whitening agent in modern Hebron ceramics

L. Teodorescu [a,b,*], N. Cantin [a], A. Ben Amara [a], R. Chapoulie [a], V. Roux [c]

[a] IRAMAT-CRP2A, UMR 5060, CNRS, University Bordeaux Montaigne, Maison de l'Archéologie, Domaine Universitaire, Esplanade des Antilles, 33607 Pessac Cedex, France

[b] Department of Materials Science and Engineering, University of Pitesti, Romania

[c] Préhistoire et Technologie, UMR 7055, CNRS, University of Paris Nanterre, 21 Allée de l'Université, 92023 Nanterre Cedex, France

ARTICLE INFO

Keywords:
Ceramic
Hebron
Salt NaCl
Whitening
Firing process
Colorimetry
Petrography
XRD
SEM-EDX

ABSTRACT

The aim of this research is to investigate the influence of NaCl on the colours and chemical composition of Ca-rich ceramic bodies. The addition of salt to ceramics is a practice that has been observed in several potter communities where the addition of salt is explicitly intended to whiten ceramics. In order to conduct this research and characterize the physico-chemical properties induced by the presence of salt, raw clay material and pot sherds were collected from the modern production at Hebron. Experimental bricks were made using two clayed sediments: one with a low CaO content (<10%) and one with a higher CaO content (20–25%). Different proportions of NaCl were added (up to 5%) to clay pastes which were fired at different temperatures. Mineralogy (petrography, XRD), chemistry (SEM-EDX) and colour analyses were carried out on raw clay materials, pot sherds and experimental (lab-made) bricks. SEM imagery offered the possibility to monitor the evolution of the mineralogical transformations, the pore system with increasing firing temperature and salt content. Results confirm the role of salt as a catalyst in the transformation reaction of calcium silicates during the firing process and its influence on the colour of the finished object.

1. Introduction

Salt has long been used by potters in various forms because they knew the different effects produced on their ceramics, especially a whitening effect (Brooks et al., 1974). Indeed, the use of salt to obtain white pottery, in the form of salted clay (salted water or added salt), is noted in Mesopotamia and can still currently be found in a diversity of countries, from Central America to the Indian subcontinent (Rye, 1976; von der Crone and Maggetti, 1998). The question of the physico-chemical properties induced by the presence of salt continue to intrigue, as several scientific studies have been conducted to better understand the effect of halite in ceramic production, from an analytical point of view. For example, Rye (1976) highlighted conspicuous cubic voids in thin sections, which were interpreted as pseudomorphs of salt crystals.

The effects produced during firing by the presence of sodium chloride in a Ca-rich ceramic body (obtained from a carbonate-rich clayey material) are numerous and wide-ranging (Bearat et al., 1989; Combès and Louis, 1967). In various studies, it has been pointed out that the use of salt in addition to raw clay material prevents the hydration of the CaO grains after firing (Rye, 1976). The presence of chlorides, such NaCl, also accelerates and participates in the dissociation reaction of calcite. The resultant decarbonation of the $CaCO_3$ increases the porosity of the paste (Bearat, 1990). Furthermore, salt can be considered as a discoloration agent in ceramic pastes produced from these carbonate-rich clays (Dufournier, 1982). Finally, the use of salt can also cause a partial disappearance of potassium in Ca-rich pastes during firing (Fabbri & Fiori, 1985). According to previous works, it was observed that the maximum addition of salt to the clay material was 5% (Rye, 1976). As for the firing temperature range, Fabbri and Fiori (1985) noticed that with 2% of salt addition, crystalline phases such as gehlenite and diopside start to appear at 700 °C. In addition, Bearat (Bearat et al., 1989) specified that the alkalin chlorures will typically start to volatize with the addition of NaCl at temperatures of 700–750 °C.

The aim of this research was to develop a multi-approach methodology in order to better understand the effects of salt NaCl in terms of

* Corresponding author at: IRAMAT-CRP2A, UMR 5060, CNRS, University Bordeaux Montaigne, Maison de l'Archéologie, Domaine Universitaire, Esplanade des Antilles, 33607 Pessac Cedex, France.

E-mail address: laura.teodorescu93@gmail.com (L. Teodorescu).

https://doi.org/10.1016/j.jasrep.2021.103303
Received 31 May 2021; Received in revised form 10 November 2021; Accepted 29 November 2021
Available online 17 December 2021

whitening and the physico-chemical changes which occur in the ceramic body. Furthermore, elaborated experimental bricks were manufactured by varying the salt content and the firing temperatures, with the same raw materials as those used by the Hebron potters for their production.

2. Materials and methods

2.1. Ethnographic context

An ethnographic survey was recently conducted in Hebron (Palestinian territories) by V. Roux. In her study, she found that potters used four different types of raw materials for producing utilitarian vessels: yellow clay sediment (noted as YC), red clay sediment (terra rossa) (noted as RC), sand and salt (Fig. 1). The volumic proportion between YC and RC is 2:1. Meanwhile, sand accounts for 1/6 of the total paste volume. The red clay sediment is said to give its yellow counterpart more plasticity. This serves to prevent rapid shrinkage when drying, and to avoid accidents during the firing process (bloating). The yellow clay material is brought from construction sites located in the region of Hebron. The YC is most likely from the Moza Formation (upper Cenomanian stage). The Moza Formation extends throughout the southern central hills of the southern Levant, from north of Jerusalem to south of Hebron. On the other hand, the red clay is acquired from neighboring lands and is a type of agricultural soil. The terra rossa (RC) can come from any place, but more probably on the more leached soil (without carbonates) that develops on hard limestone and dolomite.

The sand is collected from local mountains and added to the clay. Since the early 1970's, fires used in ceramic production have largely been fueled with tires, resulting in firing temperatures rapidly rising to approximately 1000 °C. Subsequently, thermal shock and breakage while firing is a critical consideration. The addition of sand thus helps prevent cracking of the vessel while it is being fired. The sand is added to the yellow and red clay material in a mixing tank. The salt, taken from local shops, is then added during the wedging process (Fig. 1 right).

It is said by potters that the salt is added for the pots to become white and for the clay to "better behave". Overall, the clay preparation includes the following main steps: a) drying the clay materials; b) mixing the yellow and red clay material with the sand in water mixing tanks; c) pouring the liquid clay material in a soaking tank through a nylon screen; d) following the complete wetting of the clay material, one then pours the liquid material in a drying tank; and e) after the solidification of the clay, it is wedged with a pug mill. During this final stage, the salt is added in amounts up to 0.5% of the quantity of clay paste to be wedged according to the potters.

2.2. Materials

In this study, the sampling consists in four modern potsherds and four raw materials (which are used by the Hebron potters in their manufacture), collected in Hebron. The modern sherds were selected by visual aspects, representing two types of ceramic bodies: a white and a pink ceramic sherd. The raw clay materials included both yellow (YC) and red (RC) clayey sediments, the sand temper, and the salt used for achieving a whitening effect.

Fig. 1. Raw materials: yellow clay, red clay, and sand (left image). Wedging the clay with a pug mill. It is at this stage that the salt is added to the clay paste (right image). (photographs by V. Roux). (For interpretation of the references to color in this figure legend, the reader is referred to the web version of this article).

In addition, for enlarging our understanding of the whitening effect and the parameters involved in the mechanism of the firing process on Hebron ceramic, 18 experimental bricks have been manufactured in the laboratory of IRAMAT-CRP2A (Bordeaux), using the same clays used by the Hebron potters (Table 1). The preparation of the briquettes consisted in using 20 g of each clay sediment (previously desegregated), to which salt was added in different proportions: 0%, 2% and 5% of total clay by weight. Due to the absorption effect, the red sediment was mixed with 10 ml of water, and the yellow sediment, with 15 ml. After, they were placed on an aluminum container and allowed to air-dry at room temperature for 48 h. The experimental bricks were fired in an electric kiln at 750 °C, 900 °C and 1000 °C, in an oxidizing atmosphere. The temperature was raised at a heating rate of 100 °C/h, with a soaking time of three hours and cooling down to room temperature (Fig. 2).

2.3. Methods

The methodological protocol encompasses a multitude of analytical techniques (petrographic, cathodoluminescence, SEM-EDX, XRD, colorimetry) to ensure representativeness and complementarity of observations.

Before analyzing the potsherds and the experimental bricks, the grain size distribution of the raw materials was first performed using a Laser Diffraction particle size analyser Horiba LA-950 device in order to characterize their properties and evaluate clay plasticity. The raw material - samples were treated with oxygenated water (H_2O_2) and sodium hexametaphosphate ($Na_6O_{18}P_6$). They were diluted before pipetting to 300 ml, and placed in the grain size sampler. Grain sizes were then reported as broader classes according to Konert and Vandenberghe (1997) classification system: clays [<7 μm], silts [7–63 μm], and sands [63 μm–2 mm]. Color of the material studied were monitored using a Konica Minolta CM-2600D portable spectrophotometer (360–740 nm) with a spectral resolution of 10 nm and a diameter area of 8 mm. The standard illuminator was D65 using CIE 1964 10° standard observer. The calibration was performed with a black and white reference set to SCI (spectral reflection included) mode. Cathodoluminescence (CL) was then utilized mainly to follow the evolution of mineralogical phase changes in the experimental bricks. The device employed was a Cathodyne Microvision instrument coupled with a Leica M125 binocular lens and a Leica DFC4500 digital camera to capture images with the LAS software. The electron gun was fixed and positioned at 45° to the surface

Table 1
Procedure for the preparation of the 18 experimental bricks.

Salt NaCl	Clay type	Firing Temperature (°C)	Sample ID Name
0 %	YC	750	YC 0% 750 °C
		900	YC 0% 900 °C
		1000	YC 0% 1000 °C
	RC	750	RC 0% 750 °C
		900	RC 0% 900 °C
		1000	RC 0% 1000 °C
2 %	YC	750	YC 2% 750 °C
		900	YC 2% 900 °C
		1000	YC 2% 1000 °C
	RC	750	RC 2% 750 °C
		900	RC 2% 900 °C
		1000	RC 2% 1000 °C
5 %	YC	750	YC 5% 750 °C
		900	YC 5% 900 °C
		1000	YC 5% 1000 °C
	RC	750	RC 5% 750 °C
		900	RC 5% 900 °C
		1000	RC 5% 1000 °C

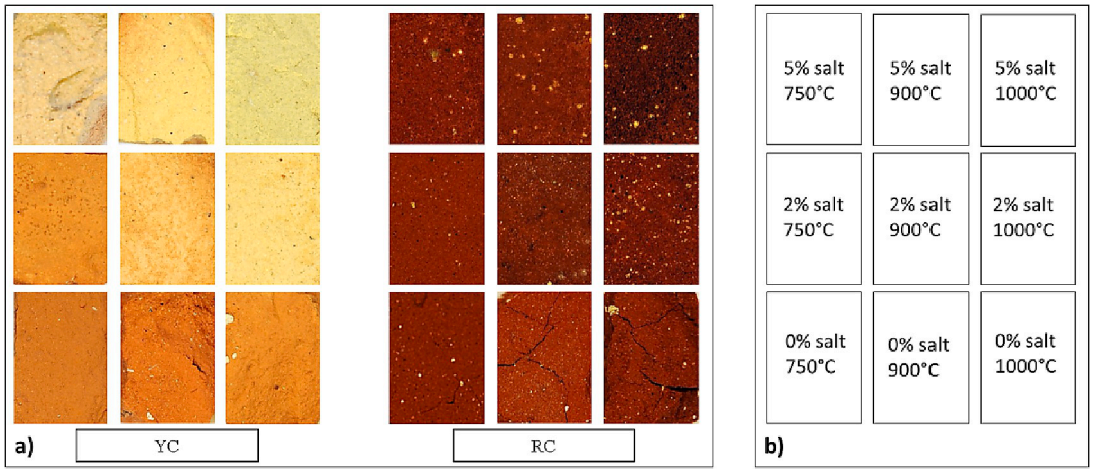

Fig. 2. (a) Colour surface of experimental samples made from yellow (YC) and red clay (RC) sediments; (b) the protocol used per sample (salt content and firing temperature). (For interpretation of the references to color in this figure legend, the reader is referred to the web version of this article.)

of the sample. The exposure time for the CL images was 15 s with a current intensity of 10 μA. Petrography allowed for the characterisation of the minerals and rocks present in the ceramic body, where identifiable. For this, a Leica DM2500 polarizing microscope was used with objectives from 2.5 to 40.

The XRD powder measurements were performed to identify the mineral constituents of both raw materials and experimental bricks, and for the orientation of deposits to discriminate the clay mineral species. This was completed using a Bruker diffractometer (D8-Advance, set in Bragg-Brentano reflection mode) a X-ray tube with Cu Kα radiations operating at 40 kV and 40 mA. The measurements were recorded from 3° to 60°, with a scan step size of 0.01° and an acquisition time/step of 1 s. Qualitative analysis of the obtained diffractograms was realized with the EVA software using the PDF − 2008 database from ICDD. In addition, a Rietveld refinement was applied by using TOPAS software, to quantify the mineral phases. For analyzing clay minerals on oriented slides, it was first necessary to eliminate the carbonates without attacking the clay phases. For this, a weak acid solution with a buffer at pH 5 was used. The oriented slides were then submitted to ethylene glycol and heat treatments (at 350 °C and 550 °C) according to Bouchet et al. (2000).

SEM imagery (JEOL – IT500 HR) facilitated the observations of the micro-texture of the modern potsherds and briquettes in thick sections, as well as the progress of the mineral transformations upon firing. The microscope was used in Low Vacuum mode with a pressure of 30 Pa. The parameters used for the analysis of the samples included the acceleration voltage of 20 kV, with the probe current from 10^{-10} to 5.10^{-9} A and about 4 000 000 counts per second. The acquisition of the spectra (performed with a double EDX, Oxford Instruments UltimMax 100) was done on the thick polished sections of the ceramic bodies and on pressed pellets. Finally, the analyse was performed using Oxford Instruments AZtec NanoAnalysis. The standard corrections were calculated using the software's internal standard. The quantification of chemical composition was obtained from the average of 4 areas of 0.58 mm^2 each. All results were expressed in wt% oxides (normalized to 100%), thus making it possible to quantify the major and minor elements (Na_2O, MgO, Al_2O_3, SiO_2, SO_3, K_2O, CaO, TiO_2 and Fe_2O_3), while Cl was expressed in simple wt.

3. Results and discussion

3.1. Mineralogical and chemical characterisation of raw materials

Results concerning grain size distribution revealed that the yellow clay sediment (YC) has a higher concentration of particles smaller than 7 μm compared to the red clay sediment (RC) (Table 2). Furthermore, approximately 26% of the particles in the red clay sediment are larger than 16 μm and are distributed between coarse silt (17%) and fine sand (9%). In contrast, the yellow clay sediment is mainly composed of particles smaller than 16 μm, ranging from fine silt (37%) to clay particles (58%). The sand used as temper consists of 75% fine sand and 16% coarse sand. Regarding the salt, it contains approximately 79% coarse particles, with sizes between 16 and 500 μm.

X-ray diffraction analysis showed that the two clay sediments used by the Hebron potters have a similar mineralogical composition, composed of clay minerals, calcite, quartz, iron oxides (for RC) and iron hydroxides (for YC), potassium feldspars and plagioclases. However, YC is richer in potassium feldspar and calcite. Finally, the analysis of the oriented slides allows the precise identification of the clay minerals detected during the powder analysis. The yellow clay sediment consists of a large quantity of kaolinite, a smaller proportion of a mixed layer clay around 11.3 Å (Illite/Vermiculite), illite and a small proportion of chlorite. The RC sediment has a similar clay mineral composition but the proportions differ. The proportion of kaolinite is lower in this sediment and the ratio of the others minerals (I/V, Ch, I) are therefore higher, giving this raw clay material more plasticity.

The chemical analysis by SEM-EDX indicates that the both clayey sediments are rich in calcium (Table 3), the yellow sediment being more calcium-rich with 23% CaO. The potassium content is also higher (3.5% K_2O), which may be related to the presence of the orthoclases detected

Table 2
Grain size distribution of raw materials of Hebron.

Sample	% coarse sand (500–2000 μm)	% fine sand (63–500 μm)	% coarse silt (16–63 μm)	% fine silt (7–16 μm)	Clay (<7 μm)
Red Clay Sediment (RC)	0	9	17	27	46
Yellow Clay Sediment (YC)	0	1	4	37	58
Salt	0	41	28	21	11
Sand temper	16	75	2	3	4

Table 3
Chemical composition (wt%), obtained by SEM-EDX (powders pellets for raw materials and thick sections for sherds and experimental samples (SD – standard deviation, dl – detection limit).

		Na_2O	MgO	Al_2O_3	SiO_2	SO_3	Cl	K_2O	CaO	TiO_2	Fe_2O_3	K_2O/SiO_2
Raw Materials	Sand	0.1	0.2	1.9	95.0	0.2	<dl	<dl	1.2	0.5	0.9	
	SD	0.1	0.1	0.1	0.3	0.1			0.1	0.1	0.1	
	Salt	46.2	0.1	0.2	0.7	1.8	49.2	0.2	1.6	<dl	0.2	
	SD	0.1	0.1	0.1	0.1	0.2	0.1	0.1	0.1		0.1	
	YC	0.2	2.3	18.7	42.6	0.2	<dl	3.5	23.3	0.8	8.3	
	SD	0.1	0.1	0.3	0.7	0.1		0.1	0.5	0.1	0.7	
	RC	0.4	2.2	18.5	57.3	0.1	<dl	1.5	8.9	1.4	9.8	
	SD	0.1	0.1	0.1	0.1	0.1		0.1	0.2	0.1	0.1	
Modern sherds	White sherd 1	2.3	2.9	14.4	45.5	1.9	1.6	3.0	22.2	0.7	5.6	0.066
	SD	0.1	0.1	0.2	0.5	0.1	0.1	0.1	0.2	0.1	0.1	
	White sherd 2	2.1	2.8	13.7	47.0	1.8	1.4	2.9	21.9	0.8	5.6	0.062
	SD	0.1	0.1	0.5	1.4	0.1	0.1	0.2	0.4	0.1	0.1	
	Pink sherd 1	0.9	3.4	14.1	50.1	0.7	0.2	2.5	20.4	0.8	6.7	0.050
	SD	0.1	0.1	0.2	0.5	0.1	0.1	0.1	0.2	0.1	0.2	
	Pink sherds 2	0.8	3.4	14.0	51.2	0.8	0.2	2.5	19.8	0.9	6.4	0.049
	SD	0.1	0.1	0.4	0.9	0.1	0.1	0.1	0.2	0.1	0.3	
Experimental bricks	YC 0% 750 °C	0.2	2.9	20.2	49.1	<dl	0.5	3.8	16.7	0.9	5.8	0.077
	SD	0.1	0.1	0.3	0.4		0.1	0.1	0.4	0.1	0.2	
	YC 2% 750 °C	1.3	2.9	18.0	45.0	0.1	1.2	3.5	21.3	0.8	5.7	0.078
	SD	0.4	0.2	0.3	0.6	0.1	0.1	0.2	0.4	0.1	0.2	
	YC 5% 750 °C	3.1	2.9	17.6	44.1	0.2	2.2	2.0	21.8	0.8	5.1	0.045
	SD	0.5	0.1	0.4	0.7	0.1	0.1	0.2	0.8	0.1	0.1	
	YC 0% 900 °C	0.1	3.0	18.9	44.7	0.1	0.3	3.7	22.4	0.8	5.9	0.083
	SD	0.1	0.1	0.3	0.2	0.1	0.1	0.1	0.5	0.1	0.1	
	YC 2% 900 °C	1.4	3.1	17.9	45.3	<dl	0.4	2.8	22.6	0.8	5.6	0.062
	SD	0.5	0.1	0.2	0.8		0.1	0.1	0.5	0.1	0.3	
	YC 5% 900 °C	2.0	3.2	17.9	45.2	0.1	0.7	2.0	22.4	0.8	5.5	0.044
	SD	0.5	0.1	0.2	0.3	0.1	0.0	0.5	0.4	0.0	0.3	
	YC 0% 1000 °C	0.1	3.3	18.7	47.0	<dl	0.1	3.4	21.3	0.8	5.1	0.072
	SD	0.1	0.1	0.1	0.2		0.1	0.1	0.3	0.1	0.1	
	YC 2% 1000 °C	1.4	3.5	18.0	46.1	<dl	0.2	1.7	22.8	0.8	5.4	0.037
	SD	0.6	0.2	0.3	1.4		0.1	0.2	0.8	0.1	0.3	
	YC 5% 1000 °C	2.8	3.3	18.4	47.3	0.1	0.2	0.8	21.1	0.8	5.1	0.017
	SD	0.5	0.1	0.3	0.6	0.1	0.1	0.2	0.8	0.1	0.2	

by X-Ray diffraction. Iron and magnesium contents are relatively similar between the two clayey sediments. Therefore, the colour difference between the two clays it is not related to differences in iron content, but rather to its crystallographic form: hematite for the red clay sediment and goethite for the yellow clay sediment according to XRD results. The salt has a high Cl and Na_2O content, which is specific for halite (Table 3). The sand used consists mainly of silica (95%), containing a small proportion of clay minerals, detected by XRD, as impurities.

3.2. Mineralogical and chemical characterisation of modern potsherds

The initial data regarding the microstructure of the modern sherds were obtained by petrographic analysis. The white sherds revealed a significant proportion of inclusions (an estimated 30% by volume) and high quartz content, in which grain diameter ranges from 200 μm and 550 μm. The presence of iron oxides was also noted, as well as a few lithic fragments (quartz-feldspar) and titan oxides. The distribution of inclusions is quite homogeneous and rounded, belonging mainly to the fine sand class. The matrix also presents a dark brown colour with no birefringence. On the other hand, the pink sherds feature a greater density of inclusions (40–50% by volume), among them quartz, iron oxides and biotite are the most notable. Nonetheless, a large amount of similarities in the mineral composition between the pink sherds and white sherds can be confirmed through this petrographic analysis. These similarities include the rounded shape of the inclusions and the presence of specific minerals such as quartz and a few feldspars. Although the samples are mineralogically quite similar, the porosity does differ. In this regard, the pink sherds feature more pronounced and abundant pores as compared to the white sherds.

On the X-Ray patterns, the presence of potassium feldspars, augite or clinopyroxene, gehlenite, and hematite were noticed in both samples. Nevertheless, the peak of halite has been detected only in the white

Table 4
Quantification of mineralogical phases of sherds and experimental samples from Hebron by XRD (Rietveld method).

		illite	quartz	K Feld	Pl Feld	calcite	halite	gehlenite	augite	wollastonite	hematite	spinel	anatase
Modern sherds	White sherd 1	<dl	23,7	0.2	14.9	<dl	0.7	18.2	31.8	9.1	<dl	1.5	1.1
	Pink sherd 1	<dl	30.7	4.3	23.1	<dl	<dl	14.3	20.4	6.1	<dl	<dl	<dl
Experimental bricks	YC 0% 750 °C	26,6	14.5	23.0	<dl	31.3	<dl	<dl	<dl	<dl	1.9	<dl	1.6
	YC 2% 750 °C	18,7	23.0	39.1	<dl	11.7	<dl	<dl	<dl	<dl	5.5	0.1	0.9
	YC 5% 750 °C	<dl	5.9	8.1	12.8	<dl	<dl	19.7	38.5	12.9	0.2	1.6	0.3
	YC 0% 900 °C	<dl	8.1	11.7	19.7	<dl	<dl	29.5	10.1	10.0	4.2	5.7	<dl
	YC 2% 900 °C	<dl	7.3	6.9	22.4	<dl	<dl	23.7	27.4	10.4	0.4	1.1	0.3
	YC 5% 900 °C	<dl	7.1	4.6	18.9	<dl	<dl	22.9	31.1	12.7	0.3	2.3	<dl
	YC 0% 1000 °C	<dl	6.2	12.4	20.2	<dl	<dl	23.1	19.6	14.9	4.5	1.1	<dl
	YC 2% 1000 °C	<dl	6.3	7.1	22.8	<dl	<dl	19.4	27.7	13.7	0.5	2.4	<dl
	YC 5% 1000 °C	<dl	5.7	3.6	20.8	<dl	<dl	14.2	38.6	14.1	<dl	2.5	0.3

sherd (Table 4). Furthermore, it was noticed that the presence of the amorphous phase is more developed in the white sherd than in its pink counterpart. The proportion of Ca-silicates, formed at high temperature (gehlenite, wollastonite) (Cultrone et al., 2001) is also more significant in the white sherd than in the pink one.

Combined, these observations suggest that the sherds were fired under the same conditions (i.e. temperatures), but are yet different due to other factors. For example, the presence of halite is detected in the white sherds and in them Ca-silicates are also higher than in the pink sherds. In addition, a more developed glassy phase and a higher porosity was also noted. These results suggest that more salt had been added to the clay paste of the white sherds than had been added to the pink sherds.

Finally, the bulk chemical composition of the modern ceramic sherds (pink and white), (Table 3) revealed that they have similar chemical composition with high Ca content (20 to 22% CaO) and equivalent percentage of iron (around 6% Fe_2O_3). The two types differ in that the presence of sodium and chlorine, which is more abundant in the white sherds than in the pink sherds.

3.3. Experimental bricks

3.3.1. Colorimetry

The test on the experimental bricks revealed colour changes that are a result of the differences in preparation protocol as described above (see section 2.2). The whitening effect occurred only in the calcium-rich bricks (CaO ~ 23%), prepared with yellow clay (YC). The discoloration effect was initiated by the addition of NaCl. Naked eye observations showed that the fired experimental bricks produced from the red clay sediments are universally red in colour and show little variability in this regard. In contrast, the bricks containing yellow clay sediments without added NaCl have a rather orange colour for all firing temperatures and become more yellow as the NaCl content increases (Fig. 2). In order to describe these colour changes in an objective way, it was necessary to carry out colorimetric measurements. Yet this is only necessary for the bricks produced from yellow clay sediments. As the objective of the study is to focus on the whitening effect of salt, which does not appear to effect the coloration of the red clay sediment containing little amount of calcium (9% CaO), colorimetric measurements for these samples are unnecessary.

When fired at the same temperature, an increase of salt content is associated with a decrease in dominant wavelength. The chromatic coordinates for the sample made with yellow clay, with no salt added and fired at 750 °C, are × = 0.41 and y = 0.37 (Table 5). This colour is situated in the yellow – orange (585–590 nm) range, where the associated dominant wavelength is equal to 586.4 nm (Kelly and Judd, 1976). This colour is non-saturated with the excitation purity (Pe) of 38.7%, highlighting a relatively dark colour with a Y-clarity of 25.4. By contrast, when a yellow clay is fired at 750 °C with 2% NaCl added, the chromatic coordinates are × = 0.40 and y = 0.36. This colour is situated in the orange range (585–600 nm), with the associated dominant wavelength λD = 585.6 nm. A similar increase can be seen when even more NaCl is added. When the yellow clay sample is fired at 750 °C, and 5% NaCl has been added, the λD = 577.0 nm, a value falling within the yellow range (575–580 nm). Simultaneously, a decreasing of excitation purity was noted, indicating a diminution in colour saturation.

Thus, the addition of salt results in the bleaching of the ceramics, as samples to which salt has been added tend to approach the yellow colour (losing the red component). The same observations were made for the other samples produced with yellow clays when fired at 900 °C and 1000 °C. According to the table, the values of clarity (Y as well as L*) increase universally as temperature increases with the highest values corresponding to the addition of 5% NaCl. Overall, the red component (a* positive) decreases in correlation to higher temperature as well as with the increased addition of salt. The lowest value (2.2) corresponds to the YC sample fired at 1000 °C within which 5% NaCl has been added. On the other hand, the yellow component (b* positive) is variable (between 17 and 24) and does not correlate with the variation in firing temperature or the addition of salt. In sum, these results quantify the whitening effect beyond visual descriptions corresponding with measurements reflective of increases in clarity as well as the suppression of the red component (Fig. 3a, b).

Calculating the colour deviation (ΔE*) and comparing to YC 0% samples makes it possible to observe that the colour values rise with the

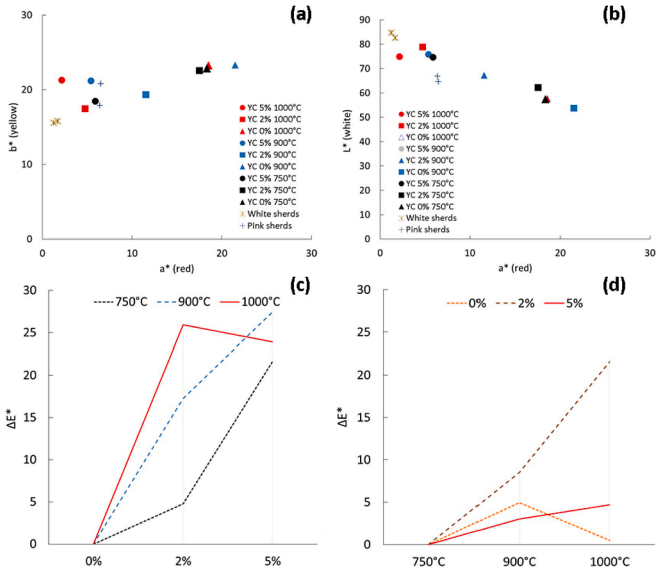

Fig. 3. Chromatic coordinates L*a*b* systems on experimental bricks.

Table 5
Chromatic coordinates of experimental samples, in the (Yxy) and (L*a*b*) systems, with the associated dominant wavelengths λD and P_e (excitation purity).

		λ_D (nm)	Pe (%)	Y	x	y	L*	a*	b*
Modern sherds	White sherd 1	572.7	17.6	65.5	0.346	0.362	84.7	1.3	15.6
	White sherd 2	573.1	18.3	61.3	0.348	0.362	82.5	1.7	15.8
	Pink sherd 1	577.7	25.6	36.4	0.368	0.368	66.8	6.4	17.9
	Pink sherd 2	577.1	30.2	33.5	0.377	0.376	64.6	6.5	20.8
Experimental bricks	YC 0% 750 °C	586.4	38.7	25.4	0.414	0.369	57.5	18.3	22.9
	YC 2% 750 °C	585.6	36.0	30.6	0.405	0.367	62.2	17.5	22.6
	YC 5% 750 °C	577.0	24.1	47.7	0.364	0.367	74.6	5.9	18.5
	YC 0% 900 °C	588.9	42.0	21.7	0.428	0.367	53.7	21.5	23.3
	YC 2% 900 °C	581.9	28.5	37.0	0.381	0.365	67.3	11.5	19.3
	YC 5% 900 °C	575.9	26.9	49.7	0.368	0.372	75.9	5.4	21.2
	YC 0% 1000 °C	586.3	39.2	25.6	0.415	0.369	57.6	18.5	23.3
	YC 2% 1000 °C	576.1	21.6	54.6	0.357	0.364	78.8	4.7	17.5
	YC 5% 1000 °C	573.1	26.6	48.1	0.363	0.377	74.9	2.2	21.3

addition of salt, regardless of the temperature at which they have been fired at (Fig. 3c). However, in the case of temperature measurements, (ΔE*) when comparing to YC samples fired at 750 °C, (Fig. 3d) by varying the salt content, no significant changes were noticed, except for 2% salt content between 900 °C and 1000 °C. For 0 and 5%, the colour deviation is under the value of 5 for all temperatures and therefore imperceptible to the naked eye. As such, the temperature increase appears to have little impact on the colour change.

In contrast, the colour differences are much higher when salt is added. For 5% salt content and 900 °C firing temperature, the deviation can reach 27 (Fig. 3). The YC 2% 750 °C sample shows only a weak chromatic deviation imperceptible to the naked eye (ΔE*<5). This deviation increases to 22 when salt content is increased to 5% while maintaining a 750 °C firing temperature. Given these results, it appears that the addition of salt to the clay has impacted the ceramic colour much more than the temperature at which it was fired.

As for the sherds from Hebron, it was noticed that the white sherds show a significant difference from the pink sherds, by a higher L* value and a weak red component, b* (Table 5).

3.3.2. *Cathodoluminescence*

Cathodoluminescence imaging allows for the observation of the variability in luminescence with the experimental bricks at different firing conditions and salt contents. This method highlights the mineralogical transformations.

With the bricks, cathodoluminescence imaging highlights the phase transformations that occurred during the firing process as a function of NaCl content. The calcite ($CaCO_3$) is characterized by the orange luminescence colour (Piponnier et al., 1997; Chapoulie et al. 2016, Chapoulie & Daniel 2007). It has a high presence at 750 °C, though begins to dissipate at 900 °C and is totally absent at 1000 °C (horizontal view in Fig. 4. Previous research has indicated that the calcite grains begin to be converted to fine grained aggregates at a temperature of 550 °C. At this point, they are also diffused into the clay matrix (Riccardi et al., 1999). The presence of calcite is visible on the YC 0 % 750 °C sample. While calcite is also still present in the YC 2 % 750 °C sample, it is not homogeneous. This indicates that the decarbonation has yet to be completed. With 5% salt added to the sample fired 750 °C the calcite has indeed totally disappeared. Moreover, the gehlenite ($Ca_2Al_2SiO_7$) characterized by the blue luminescence colour, is detected in the samples with the highest content of NaCl (5%). This is particularly prominent on the sample with 5% salt fired at 750 °C. In this sample, the microcrystals show a very intense blue colour of luminescence. The images acquired for the samples fired at 900 °C, also show the decomposition of the carbonates. The YC 0% 900 °C sample presents a weak luminescence with a red-brown matrix colour, while the YC 2% 900 °C sample shows some carbonate inclusions are present as well as white spots in the matrix. Finally, the samples fired at high temperature (Fig. 4 (YC 900 °C and 1000 °C)) show the transition from an orange matrix to a yellow matrix.

It should be highlighted that the blue luminescence colour can correspond to gehlenite or diopside (Götze et al., 2013). Furthermore, in concordance with the literature, (Piponnier et al., 1997) the presence of wollastonite should also be mentioned. Wollastonite ($CaSiO_3$) is characterized by a yellow-greenish luminescent colour, and is visible only in samples that have been fired at high temperature. The YC 5% 1000 °C sample, for example, reveals a matrix with this specific colour associated to wollastonite, suggesting new crystalline phases have been formed. This is confirmed through XRD analysis (see section 3.3.3).

3.3.2.1. X-ray diffraction. The mineralogical evolution that has occurred during firing (manifested by the successive appearance and disappearance of mineralogical phases), and the salt content of the raw material could be observed through the comparison of the XRD patterns but also by quantification using the Rietveld method (Table 4). The main XRD reflections in YC 0% 750 °C corresponds to quartz and calcite minerals and illite. The increase in the percentage of salt (at 750 °C) results in the disappearance of the Ca-carbonate phases. As a reaction of calcite within the clay, the gehlenite thus starts to form. Besides the clear evidence of the decomposition of calcite, the reflections of illite/muscovite show a decrease as well. With the addition of salt (2% to 5%), traces of newly formed minerals start to appear such as hematite, as well

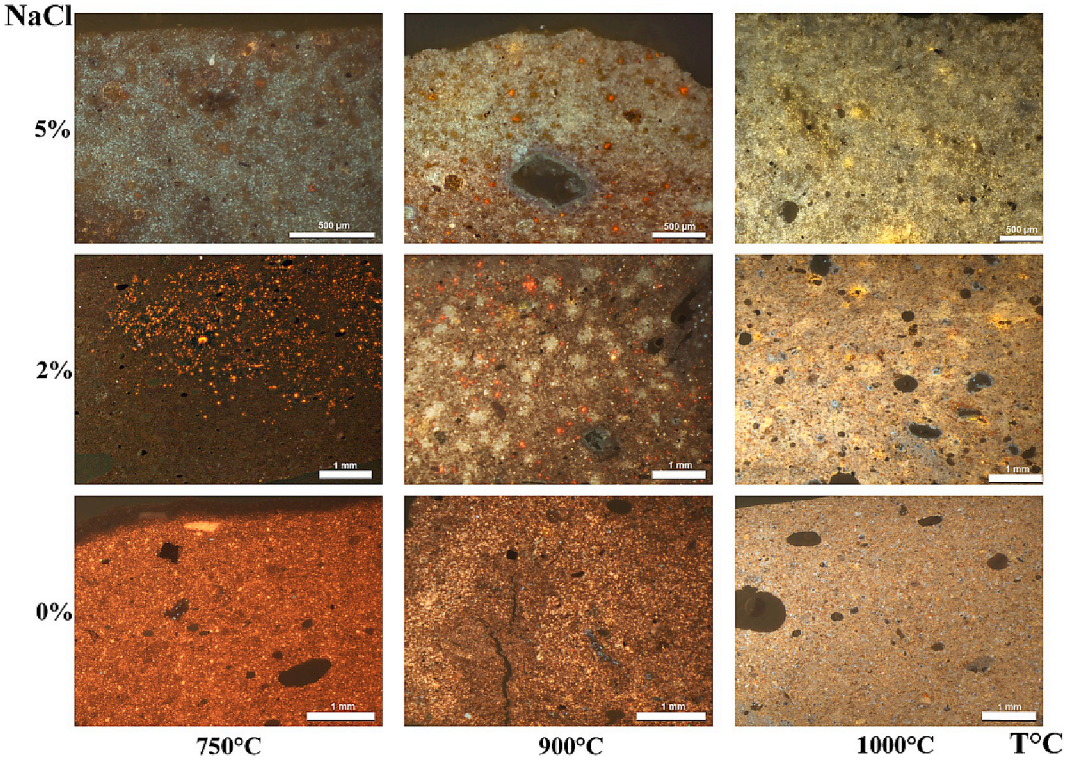

Fig. 4. Cathodoluminescence images of Ca-rich experimental bricks.

as new calcium silicates: gehlenite, pyroxene such as augite and anorthite. Gehlenite and augite start to form at temperatures between 750 °C and 900 °C. While, gehlenite formation is a result of the reaction between CaO from the carbonates and Al_2O_3 and SiO_2 from the dehydroxylated phyllosilicates (Duminuco et al., 1998; Peters and Iberg, 1978), the presence of phyllosilicates in contact with quartz and calcite allow the formation of new Ca silicates phases that can include released Mg and Na (such as augite).

The decomposition of the calcite and the newly formed phases (gehlenite and augite) demonstrated by XRD analysis strengthen the interpretation of CL-images. It also confirms the conclusion that the presence of salt accelerates and participates in the dissociation of calcite earlier in time than was previously known. Thereby, halite induces the formation of gehlenite, anorthite and augite at low temperature, increasing the reactivity between clays and Ca (Bearat et al., 1989).

Hematite formation in Ca-rich ceramics, on the other hand, is limited by the development of the new Ca-silicates, which incorporates Fe^{3+} in their network at temperatures around 900 °C to 1000 °C. This phenomenon can explain the colour saturation starting at lower temperature due to the addition of salt (De Bonis et al., 2017). These observations also indicate that the amorphous phase was involved in the melting process, producing a Fe-saturated glass, from which nano-sized hematite crystals precipitated. Low iron diffusion within the glass and short soaking time may have favored the nucleation and inhibited the crystal growth (Nodari et al., 2007). However, in this study, the hematite appears at a lower temperature (beginning at 750 °C with 2% NaCl). Gehlenite, anorthite, augite, and hematite were recorded in the pattern obtained from the Ca-rich sample, fired at 900 °C. As the quantity of salt increases, the gehlenite content begins to decrease (30% to 23%). This is in contrast with increases in augite (10% to 31%) and wollastonite (10% to 13%). Despite the addition of salt, anorthite is quite stable, but the K-Feldspars also decrease (12% to 5%) as NaCl amounts increase. Moreover, it is noted that if enough Ca is available, anorthite appears either due to the decomposition of the existing gehlenite with the amorphous matrix formed from clay minerals, dehydroxylation, or only due to the reaction of the decomposed clay minerals and CaO in the rims of the grains (Holakooei et al., 2014). According to previous studies (Piponnier et al., 1997; Traoré et al., 2000; Trindade et al., 2009), wollastonite is an intermediate compound that appears at 800 °C to 850 °C, and begins formation when the unreacted lime attacks the grains of quartz or, like with anorthite, as a result of the decomposition of gehlenite. At temperatures above 950 °C, gehlenite (considered as an intermediate compound) becomes unstable in the presence of SiO_2 and decomposes. This decomposition enables anorthite, and wollastonite to be generated (Tschegg et al., 2009). At 1000 °C, the gehlenite content decreases considerably (23% to 14%) in favor of augite again. The K-feldspars content also collapses, while wollastonite increases little, and plagioclase feldspars are stable. It is also noticeable that the mineralogical phase for anorthite begins to disappear after a temperature of 1100 °C is reached under normal conditions (Traoré et al., 2003).

The same observation was made for the gehlenite, which starts to decrease concurrent with increasing salt percentages. The hematite reflections do not present any changes, however. Their appearance starts at 750 °C within the 2% salt sample, and is similarly present at 1000 °C, with 5% salt added.

In summary, the addition of salt induces mineralogical changes including the disappearance of calcite and the appearance of Ca-silicates from 750 °C onwards. The effect of firing at higher temperatures and the salt addition facilitates the decomposition of the carbonates and silicates at lower temperatures than usual, allowing for the formation of new crystallized phases. All the Ca-rich fired samples, beginning with those with at least 2% added salt and fired at 750 °C, contained gehlenite and augite, which have been formed due to the decomposition of calcite. In addition, hematite and anorthite were formed in these samples as well. These newly formed minerals remained present throughout the entire temperature range regardless of the percentage of salt added.

3.3.2.2. SEM-EDX analyses. The SEM observations revealed the microtexture of the carbonate-rich base clay experimental bricks. It also provided information regarding the porosity and the glassy phases. The investigations of the microtexture of the sherds were made on fresh fracture surfaces and on polished thick sections. Normally the development of the crystalline and glassy phases in a ceramic is the result of the temperature of the heating treatments applied. The proportion of Fe_2O_3 is constant (~5%) in all experimental bricks, regardless of the NaCl level or the temperature applied. The bulk chemical results also reveal that the addition of the salt did not affect the chemical composition, except in the case of the potassic compound (K_2O), which decreases as salt concentration increases (Table 3). In fact, the ratio K_2O/SiO_2 decreases from 0.08 to 0.05 for samples fired at 750 °C as a result of increasing percentages of salt (Table 3). The same decrease was observed for the other temperatures, until a collapse of the rate for bricks with the highest salt content and highest firing temperature (0.02 for YC 5% 1000 °C). On the other hand, the K_2O content of the brick without salt fired at 1000 °C is slightly reduced, though still similar to the origin alone. Thus, the introduction of salt combined with an increase in the firing temperature causes the loss of this element. Picon (1991) explained the K-loss phenomenon, due to the alteration within the ceramic and highlighting the importance of different factors that contribute to the availability of silicate materials for structural rearrangements. One proposed factor is the percentages of lime in the ceramics, which can allow the development of an unstable glassy or amorphous phase, or even for the evolution of crystalline phases, which are also unstable such as gehlenite. In addition, Fabbri and Fiori (1985) presented different studies where the reaction between kaolin clays and NaCl led to the complete elimination of chlorine at about 520 °C. As for calcareous illitic-chloritic clays, the HCl was volatilized at a higher temperature and stimulated the decomposition of carbonate impurities forming potassium chloride. They observed that the addition of the NaCl caused a significant decrease in the amount of residual potassium and a progressive elimination of residual Cl in samples fired above 750 °C.

In addition, Bearat explained that the eliminated alkalis are in the form of chlorides during the firing process (1990). This means that the formation of calcium silicates promotes the formation of alkaline chlorides, which start to volatilize at temperatures of 700 °C–750 °C (Bearat, 1990). However, it is difficult to provide a complete and precise explanation of the phenomenon. The most abundant oxides are SiO_2 and Al_2O_3, which are mainly associated with the clay minerals, although often the SiO_2 content may also be associated with the quartz particles. The content of iron oxide is normally sensitive during firing. This results in variable colour and texture of the ceramic (El Ouahabi et al., 2015; El Boudour El Idrissi, 2016). In the present study, the proportion of iron in the samples does not affect the colour change.

SEM observations also revealed rhombic voids in all the experimental bricks, including those absent salts (Fig. 5). At 750 °C, rhombohedral minerals are yet present but have started to decompose. These forms are attributed to calcite or Mg-calcite minerals. With the addition of salt and/or with the increasing of firing temperature, voids are then created replacing the minerals. Furthermore, at 1000 °C the formation of a new phase can be observed inside the voids. The core presents a significant Mg enhancement, suggesting that the mineralogical phases of augite have been formed. Further observations in the clay matrix have also been recorded for the samples, including the development of the glassy phase and ellipsoidal vesicles that increase with added the salt content. The same phenomenon is known to occur with increasing temperature. The specific role of salt in promoting the development of pores in the material is currently being investigated further and will be the subject of a future publication.

4. Conclusion

The study confirmed the role of halite in the bleaching of ceramics with a high CaO content. Indeed, colorimetric measurements carried out

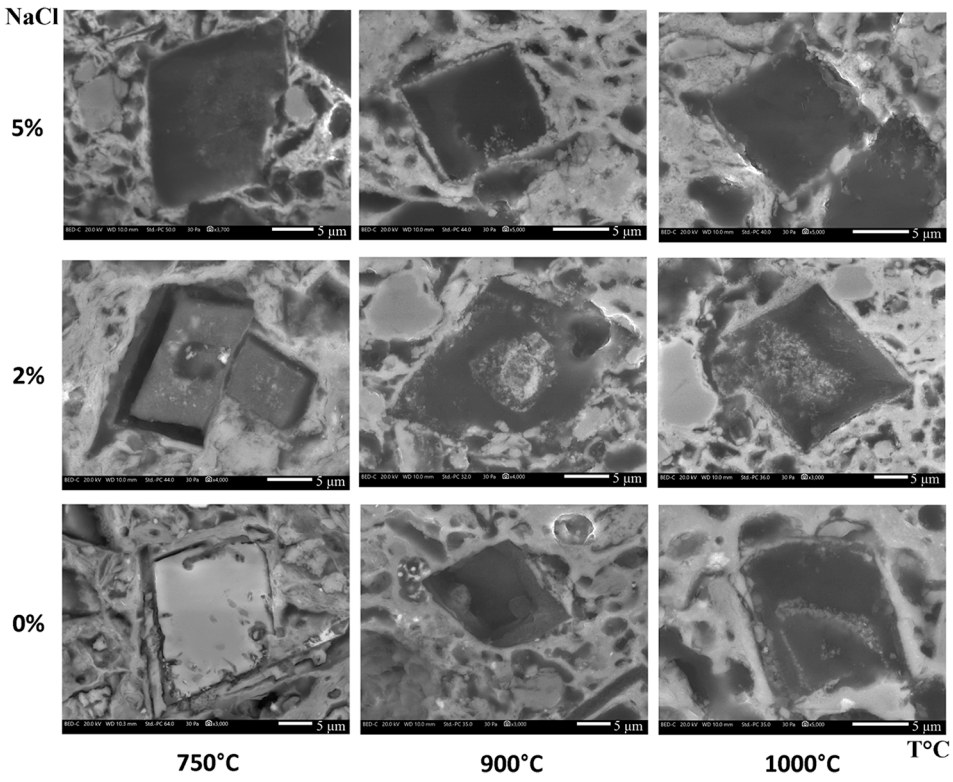

Fig. 5. SEM-BSE images of calcite or rhombohedral voids present in the matrix of the experimental bricks.

on experimental bricks with different salt contents, showed a significant loss of the red component as the salt concentration increased, as well as a loss of the yellow component to a lesser degree. These colorimetric losses are associated with a decrease of their saturation. At the same time, the clarity has significantly increased. These factors allow for the empirical characterisation of the whitening effect observed visually and confirm the main role of salt in this process, beyond the effect of temperature alone.

The mineralogical phase changes recorded in the experimental bricks manufactured in the laboratory have also been highlighted by different methods. Cathodoluminescence images showed these changes in the material. Qualitative and quantitative XRD results allowed for the documentation of the evolving proportions for these different phases, coincident with increases of salt content and firing temperature. In fact, the process of alteration of clay minerals to form new calcium silicates, appears to take place at a lower temperature in the presence of salt than has been generally thought. In this regard, significant differences in the microstructure of the calcareous clays with 5% salt are observed with the appearance of Ca-silicates (gehlenite, wollastonite) as early as 750 °C.

Furthermore, the colour changes, due to the trapping of Fe ions in the crystal lattice can now be explained (Nodari et al., 2007). Although Mossbauer measurements have not yet been carried out, Chevalier et al. (1976) have shown that gehlenite, anorthite or wollastonite crystals can trap Fe ions in their lattice, by substitution of Al^{3+} and Ca^{2+}. They pointed out that ferric oxide is known to be produced when biotite reaches high temperatures, such as 900 °C, and that crystallization improves at 1000 °C. In addition, Nöller and Knoll (1983) conducted investigations by making possible the insertion of Fe^{3+} into the lattices of Ca-Mg-Al silicates. They observed that the difference in coloration could be explained for synthetic silicates by a polarized binding of Fe^{3+} ions in a disordered matrix. Therefore, the experimental data presented here provides significant explanatory evidence for the action of NaCl on the whitening of calcareous clays. By lowering the temperature at which calcium silicates are formed, NaCl serves to reduce the necessary temperature at which the bleaching effect starts.

Moreover, the result obtained by the SEM-imagery has made it possible to more accurately describe and assign the presence of rhombohedral voids. Results show that they are due to the dissolution of the carbonates, contrary to what has been put forth previously in the scientific literature where voids had been attributed to the dissolution of salts (Rye, 1976).

Returning to the Hebron ceramics specifically, it is clear from the experimental results that the two colorations obtained (pink and white) can in fact be explained primarily by a difference in salt concentration in the initial mixture rather than other factors.

Other measurements currently underway will further consider the effect of salt on the porosity of ceramics. These observations will be compared with ceramics produced elsewhere at other sites (notably in India) where similar practices with salt addition, have been reported.

CRediT authorship contribution statement

L. Teodorescu: Conceptualization, Investigation, Writing – original draft, Writing – review & editing. **N. Cantin:** Conceptualization, Methodology, Investigation, Writing – review & editing, Validation, Visualization, Supervision, Data curation. **A. Ben Amara:** Investigation, Methodology, Writing – review & editing, Validation, Visualization, Data curation. **R. Chapoulie:** Validation, Resources, Visualization. **V. Roux:** Validation, Resources, Visualization, Supervision, Project administration.

Acknowledgements

The authors would like to thank the internal collaborators of the IRAMAT-CRP2A laboratory (especially D. Pierce for his English review and remarks, and Y. Lefrais for SEM-EDS expertise) as well as the external collaborators who contributed to this study, particularly by A. Queffelec for performing grain size analysis at PACEA Laboratory (University of Bordeaux) and A. Bocquet-Lienard CRAHAM Laboratory

(University of Caen) for providing us documentation. The sampling and study of the clay material and ceramics from Hebron is part of the project "Traditional knowledge of the Hebron's potters and Heritage Resilience (Palestinian Territories)", National Geographic Society- NGS-398R-18 (PI, V. Roux). We are thankful to the two anonymous referees for their critical reading and suggestions, which helped improving the paper.

References

Bearat, H., 1990. Etude de Quelques Altérations Physico-Chimiques des Céramiques Archéologiques. Université de Caen, France, Thèse de doctorat.

Bearat, H., Dufournier, D., Nguyen, N., Raveau, B., 1989. Influence de NaCl sur la couleur et la composition chimique des pâtes céramiques calcaires au cours de leur cuisson. Archeosciences 13, 43–53. https://doi.org/10.3406/arsci.1989.871.

Bouchet, A., Meunier, A., Sardini, P., 2000. Minéraux Argileux Structure Cristalline, Identification par Diffraction de rayons X = Clay Minerals: Crystal Structure. X-ray diffraction identification, Elf Exploration Production, Pau (Pyrénées-Atlantiques).

Brooks, D., Bieber, A.M., Harbottle, G., Sayre, E.V., 1974. Biblical studies through activation analysis of ancient pottery, in: Archaeological Chemistry, Advances in Chemistry. AMERICAN CHEMICAL SOCIETY, WASHINGTON, D. C., pp. 8–33. 10.1021/ba-1974-0138.

Chapoulie, R., Robert, B., Casenave, S., 2016. The cathodoluminescence phenomenon used for the study of ancient ceramics and stones. International Journal on Culture and Heritage at Risk – cities of memory, Edifir Florence, 1.1, 53-72.

Chapoulie, R., Daniel, F., 2007. Cathodoluminescence: recherches sur une méthode d'analyse en archéométrie. British Archaeological Reports, BAR S1700, 1-16.

Chevalier, R., Coey, J.M.D., Bouchez, R., 1976. A study of iron in fired clay : Mössbauer effect and magnetic measurements. J. Phys. Colloques 37, C6-861-C6-865. Doi: 10.1051/jphyscol:19766181.

Combès, J.-L., Louis, A., 1967. Les poteries de Djerba. Publication du centre des arts et traditions populaires, Tunis.

Cultrone, G., Rodriguez-Navarro, C., Sebastian, E., Cazalla, O., De La Torre, M.J., 2001. Carbonate and silicate phase reactions during ceramic firing. Eur. J. Mineral. 13, 621–634. https://doi.org/10.1127/0935-1221/2001/0013-0621.

De Bonis, A., Cultrone, G., Grifa, C., Langella, A., Leone, A.P., Mercurio, M., Morra, V., 2017. Different shades of red: The complexity of mineralogical and physico-chemical factors influencing the colour of ceramics. Ceram. Int. 43, 8065–8074. https://doi.org/10.1016/j.ceramint.2017.03.127.

Dufournier, D., 1982. L'utilisation de l'eau de mer dans la préparation des pâtes céramiques calcaires, premières observations sur les conséquences d'un tel traitement. Archeosciences 6, 87–100. https://doi.org/10.3406/arsci.1982.1195.

Duminuco, P., Messiga, B., Riccardi, M.P., 1998. Firing process of natural clays. Some microtextures and related phase compositions. Thermochim. Acta 321, 185–190. https://doi.org/10.1016/S0040-6031(98)00458-4.

El Boudour El Idrissi, H., Daoudi, L., El Ouahabi, M., Fagel, N., 2016. Flaws linked to lime in pottery of Marrakech (Morocco). J. Mater. Environ. Sci. 7, 3738–3745.

El Ouahabi, M., Daoudi, L., Hatert, F., Fagel, N., 2015. Modified mineral phases during clay ceramic firing. Clays Clay Miner. 63, 404–413. https://doi.org/10.1346/CCMN.2015.0630506.

Fabbri, B., Fiori, C., 1985. Influence of Sodium Chloride on Thermal Reactions of Heavy Clays During Firing, in. Clay Minerals Society, Denver.

Götze, J., Schertl, H.-P., Neuser, R.D., Kempe, U., Hanchar, J.M., 2013. Optical microscope-cathodoluminescence (OM–CL) imaging as a powerful tool to reveal internal textures of minerals. Mineral. Petrol. 107, 373–392. https://doi.org/10.1007/s00710-012-0256-0.

Holakooei, P., Tessari, U., Verde, M., Vaccaro, C., 2014. A new look at XRD patterns of archaeological ceramic bodies: An assessment for the firing temperature of 17th century haft rang tiles from Iran. JTHEA 118, 165–176. https://doi.org/10.1007/s10973-014-4012-z.

Kelly, K.L., Judd, D.B., 1976. Color : Universal Language and Dictionary of Names. National Bureau of Standards, New York, Special Publication, U.S. Dept. of Commerce, p. 440.

Konert, M., Vandenberghe, J., 1997. Comparison of laser grain size analysis with pipette and sieve analysis: a solution for the underestimation of the clay fraction. Sedimentology 44, 523–535. https://doi.org/10.1046/j.1365-3091.1997.d01-38.x.

Nodari, L., Marcuz, E., Maritan, L., Mazzoli, C., Russo, U., 2007. Hematite nucleation and growth in the firing of carbonate-rich clay for pottery production. J. Eur. Ceram. Soc. 27, 4665–4673. https://doi.org/10.1016/j.jeurceramsoc.2007.03.031.

Nöller, R., Knoll, H., 1983. Magnetic properties of calcium-silicates (diopside and gehlenite) doped with iron (III). Solid State Commun. 47, 237–239. https://doi.org/10.1016/0038-1098(83)90552-5.

Peters, T., Iberg, R., 1978. Mineralogical changes during firing of calcium-rich brick clay. Am. Ceram. Soc. Bull. 57, 503–506.

Picon, M., 1991. Quelques observations complémentaires sur les altérations de composition des céramiques au cours du temps : cas de quelques alcalins et alcalino-terreux. Archeosciences 15, 117–122. https://doi.org/10.3406/arsci.1991.1263.

Piponnier, D., Bechtel, F., Florin, D., Molera, J., Schvoerer, M., Vendrell, M., 1997. Apport de la cathodoluminescence à l'etude des transformations de phases cristallines dans des céramiques kaolinitiques carbonatées. Key Eng. Mater. 132–136, 1470–1473. https://doi.org/10.4028/www.scientific.net/KEM.132-136.1470.

Riccardi, M.P., Messiga, B., Duminuco, P., 1999. An approach to the dynamics of clay firing. Appl. Clay Sci. 15, 393–409. https://doi.org/10.1016/S0169-1317(99)00032-0.

Rye, O.S., 1976. Keeping your temper under control: materials and the manufacture of papuan pottery. Archaeol. Oceania 11, 106–137.

Traoré, K., Kabré, T.S., Blanchart, P., 2003. Gehlenite and anorthite crystallisation from kaolinite and calcite mix. Ceram. Int. 29, 377–383. https://doi.org/10.1016/S0272-8842(02)00148-7.

Traoré, K., Siméon Kabré, T., Blanchart, P., 2000. Low temperature sintering of a pottery clay from Burkina Faso. Appl. Clay Sci. 17, 279–292. https://doi.org/10.1016/S0169-1317(00)00020-X.

Trindade, M.J., Dias, M.I., Coroado, J., Rocha, F., 2009. Mineralogical transformations of calcareous rich clays with firing: a comparative study between calcite and dolomite rich clays from Algarve, Portugal. Appl. Clay Sci. 42, 345–355. https://doi.org/10.1016/j.clay.2008.02.008.

Tschegg, C., Ntaflos, T., Hein, I., 2009. Thermally triggered two-stage reaction of carbonates and clay during ceramic firing — A case study on bronze age cypriot ceramics. Appl. Clay Sci. 43, 69–78. https://doi.org/10.1016/j.clay.2008.07.029.

von der Crone, M.J., Maggetti, M., 1998. Experimental firing of clays using salt water. Presented at the Archaeometry 98, BAR International Series, Oxford, 249–255.